Golder Associates Ltd.
CONSULTING ENGINEERS

REPORT TO CANMET

CROWN PILLAR STABILITY BACK-ANALYSIS

Supported by the Canada Centre for Mineral
and Energy Technology (CANMET)
Department of Energy Mines and Resources

DSS Contract No. 23440-8-9074/01-SQ
DSS File No. 098Q.23440-8-9074

CONTRACT SERIAL NO. 89074-01-SQ
CONTRACT REQUISITION NO. 23440-8-9074
CONTRACTOR: GOLDER ASSOCIATES

Distribution:

8 copies - CANMET, Ottawa, Ontario
7 copies - Golder Associates Ltd.
Mississauga, Ontario

MICROMEDIA

259 pp + figs

April, 1990

881-1739

GOLDER ASSOCIATES LTD. • 2180 MEADOWVALE BLVD., MISSISSAUGA, ONTARIO, CANADA L5N 5S3 • TELEPHONE (416) 567-4444 • TELEX 06-218812 • FACSIMILE (416) 567-6561

OFFICES IN CANADA • UNITED STATES • UNITED KINGDOM • SWEDEN • AUSTRALIA

91-04676/

Golder Associates Ltd.
CONSULTING ENGINEERS

May 24, 1990

881-1739

Energy Mines and Resources
CANMET - MRL Division
555 Booth Street
Ottawa, Ontario
K1A 0G1

Dear Sirs:

RE: BACK ANALYSIS OF SURFACE CROWN PILLAR STABILITY
CONTRACT #23440-8-9074/01-SQ
DSS FILE #009SQ.23440-9-9074

This report was compiled as part of the CANMET initiative to examine methods for design of surface crown pillars. The document was prepared to address the issue of surface crown pillar stability specifically by back-analysis examination of failed and stable case records.

In Part 1 of the report an evaluation of 70 case records comprising 237 crown pillars is presented to define classes of instability, failure mechanisms, and parameters critical to stability. A review of currently available design methods is presented in Part 2 and in Part 3 an empirical design procedure along the lines of the NGI and CSIR geomechanics classifications is developed for assessing surface crown pillar stability.

Yours truly,

GOLDER ASSOCIATES LTD.

T.G. Carter, P.Eng.

TGC:se

GOLDER ASSOCIATES LTD. • 2180 MEADOWVALE BLVD., MISSISSAUGA, ONTARIO, CANADA L5N 5S3 • TELEPHONE (416) 567-4444 • TELEX 06-218812 • FACSIMILE (416) 567-6561

OFFICES IN CANADA • UNITED STATES • UNITED KINGDOM • SWEDEN • AUSTRALIA

TABLE OF CONTENTS

Page No.

Covering Letter

1.0 INTRODUCTION & EXECUTIVE SUMMARY 1
- 1.1 Background 1
- 1.2 Scope of the Problem 1
- 1.3 Objectives 2
- 1.4 Case Study Records 2
- 1.5 Failure Situations 3
- 1.6 Methods of Evaluation 4
- 1.7 Summary Conclusions 5
- 1.8 Acknowledgements 6

PART 1 CLASSIFICATION AND EVALUATION OF CASE RECORDS

2.0 CROWN PILLAR CHARACTERIZATION 7
- 2.1 Key Components of Pillar Characterization 7
- 2.2 Availability of Key Data 8
- 2.3 Classification of Surface Crown Pillars 9
- 2.4 Development of Surface Crown Pillar Data Base 10
- 2.5 Applicability of Existing Rock Mass Classifications 11
  - 2.5.1 NGI - Q System 12
  - 2.5.2 CSIR - RMR Geomechanics Classification 14
  - 2.5.3 Empirical Assessment of Rock Strength and Deformability 15

3.0 REVIEW OF CASE RECORDS 20
- 3.1 Overburden Considerations 20
- 3.2 Case Examples - Failure Situations 21
  - 3.2.1 Crown Pillar Type A - Tabular Ore Zones 23
  - 3.2.2 Crown Pillar Type B - Blocky Rock Mass Conditions 26
  - 3.2.3 Crown Pillar Type C - Foliated Environments 28
  - 3.2.4 Crown Pillar Type D - Disseminated Ore Zones, with Slabby HW/FW Conditions Largely in Competent Rock 30
  - 3.2.5 Crown Pillar Type E - Fault Controlled Situations 32
- 3.3 Case Examples - Non-failed Situations 33

PART 2 ANALYSIS OF PILLAR STABILITY

4.0 REVIEW OF DESIGN METHODS 35
- 4.1 Empirical Methods 35
  - 4.1.1 Rules of Thumb 35
  - 4.1.2 Rock Mass Classifications 36
- 4.2 Analytical Approximations 38
  - 4.2.1 Bending of Beams 38
  - 4.2.2 Arch Analysis 40
  - 4.2.3 Plate Analysis 41
  - 4.2.4 Voussoir Beams 42
  - 4.2.5 Gravity and Structurally Controlled Failures 43
  - 4.2.6 Chimney Failure Analyses 45
  - 4.2.7 Block Caving Analogies 47
  - 4.2.8 Analytical Methods Summary 50
- 4.3 Numerical Procedures 52
  - 4.3.1 Boundary Element Method 53
  - 4.3.2 Finite Element and Finite Difference Methods 55
  - 4.3.3 Distinct Element Method 59
  - 4.3.4 Three-Dimensional Stress Analysis 61
  - 4.3.5 Block Theory Applications 63
- 4.4 Failure Probability Appraisal 63

5.0 APPLICATION OF EVALUATION PROCEDURES 66
- 5.1 Category A Crown Pillars 66
- 5.2 Category B Crown Pillars 73
- 5.3 Category C Crown Pillars 73
- 5.4 Category D and E Crown Pillars 78

PART 3 EMPIRICAL DEVELOPMENT OF DESIGN PROCEDURE

6.0 EMPIRICAL EVALUATION OF CROWN PILLAR STABILITY 79
- 6.1 Review of Controlling Parameters 79
- 6.2 Stability Graph Development 79
- 6.3 Assessment of Crown Pillar Stability Scaling Factors 81
- 6.4 Development of Crown Pillar Geometry Number 82
  - 6.4.1 Crown Pillar Weight Factor 82

6.4.2 Span to Thickness Ratio 83
6.4.3 Stope Span to Strike Length Ratio 83
6.4.4 Influence of Foliation Dip 84
6.4.5 Crown Geometry Number 85
6.5 Proposed Scaled Span and Critical Span Expressions 85
6.6 Example Application of the Scaled Crown Span Plot to Derive Required Crown Pillar Thickness 86

7.0 CONCLUSIONS AND RECOMMENDATIONS 88

BIBLIOGRAPHY following page 90

APPENDIX A - Summary Tabulation of Surface Crown Pillar Characteristics for 70 Case Records

Note: Tables and Figures are presented following each Section of the Text.

LIST OF TABLES

SECTION 2

2.1 Key Data Required for Characterization of Surface Crown Pillar Stability Conditions
2.2 Summary Mine Site List Outlining Character Type & Rock Conditions
2.3 Summary of Stable and Failed Crown Pillar Cases by Category
2.4 Descriptive Assessment of Rock Mass Quality
2.5 Representative Rock Mass Classifications and Shear Strength Parameters for Various Rock Qualities
2.6 Representative Deformation Properties for Various Rock Qualities

SECTION 4

4.1 Summary of Post Failure Analysis Results (Wright-Hargreaves - Mine 42)
4.2 Generic Analysis of Stopes Using MUDEC
4.3 Summary of MUDEC Analysis for Schistose Rock Conditions (Poor Rock Quality, Q = 0.1, RMR = 23)
4.4 Summary of MUDEC Analysis for Competent, Slabby and Blocky Rock Conditions (Good Rock Quality, Q = 10, RMR = 65)
4.5 Comparison of Advantages and Disadvantages of Various Available Numerical Methods

SECTION 5

5.1 Summary of Numerical Analyses Undertaken for Crown Pillar Evaluation Project
5.2 Input Parameters for Beam, Plate & Voussoir Beam Analyses
5.3 Input Data for FLAC and MUDEC Analyses

SECTION 6

6.1 Required Crown Pillar Thickness and Thickness: Span Ratios for Two Spans in Two Rock Masses

LIST OF FIGURES

SECTION 2

2.1 Major Subclassifications of Surface Crown Pillar Geometries
2.2 Empirical Stope Design Charts for Open Stoping at Depth
2.3 NGI Rock Mass Classification System Parameter Evaluation
2.4 Suggested NGI Design Limits for Maximum Spans for Unsupported Excavations (From Barton, 1974)
2.5 CSIR Geomechanics Classification for Jointed Rock Masses
2.6 Correlations Between CSIR-RMR and Q-System Classifications and Hoek-Brown Failure Criterion Constants m and s
2.7 Relationship Between Rock Mass Quality and In situ Modulus of Deformation and Relationships for Shear and Bulk Modulus
2.8 Joint Normal and Shear Stiffness (Empirical and Theoretical Derivations)

SECTION 3

3.1 North-South Cross-Sections of Main and South Breaks Mine #36 and Mine #11
3.2 Detailed Sections of Near Surface Stope (Mine #11)
3.3 Mine #11 Detailed Drilling Data for Assessment of Crown Pillar Conditions
3.4 Geometrical Details of Crown Pillar Configuration Adjacent to Cave-In Area (Mine #38)
3.5 Contrast in Stope Geometry Between Failure Area at Mine #46A and Stable Area at Mine #46B in the Same Rock Conditions
3.6 Generalized Geological Cross-Section of Mine #53
3.7 Plan and Sections of Mine #53 Showing Location of Open Stope and Slides
3.8 Geometrical Details of Stopes at Mine #57
3.9 Logitudinal Section Showing Crown Pillar Collapse and Remedial Capping at Mine #64
3.10 Cross-Section of Crown Pillar Collapse Zone (Mine #12)
3.11 Surface and Composite Plan of Crown Pillar Failure Area (Mine #12)
3.12 Generalized Geological Cross-Section and Detailed Sections of Typical Cave-In Zones (Mine #29)
3.13 Detailed Geotechnical Section at 20 025 E. Showing Crown Pillar Geometry (Mine #29)
3.14 Geometry of Intact and Collapsed Crown Pillars (Mine #59)
3.15 Detailed Ore - Zone Cross - Section (Mine #14)
3.16 Mine #14 Summary Geotechnical Information
3.17 Mine #22 Cave Zone Geometry, After Crown Pillar Collapse
3.18 Dimensions and Location Details for Stope Cave-Ins at Mine #25

3.19 Overall Configuration of Crown Pillar Failure Geometry (Mine #35)
3.20 Longitudinal Section of Crown Pillar Failure at Mine #50
3.21 Crown Pillar Geometry and Cave - Zone Configuration (Mine #41)
3.22 Details of Pillar Collapse Areas (Mine #67)
3.23 Mine #27 Summary Geotechnical Information
3.24 East - West Section Through Mine #28 Showing Caving Stopes
3.25 Geometrical Arrangement of Crown Failure of Stope 2-15, Mine #62
3.26 Cross Section Showing Instrumentation Arrays and Geology of Area of Sloughing Hangingwall (Mine #45)
3.27 Mine #45 Detailed Crown Pillar Drill Array for Instrumentation Installations
3.28 Mine #26 Detailed Geotechnical X-Section of Stoping in Vicinity of Private Dwellings

SECTION 4

4.1 Typical Thickness to Span Correlations for Various Crown Pillars (After Bétournay, 1987)
4.2 CSIR Geomechanics (RMR) and NGI Q-System Correlations to Unsupported Spans and Stand-Up Time
4.3 Comparison Charts for Evaluation of Stable Spans Using Published Rock Mass Classification Procedures
4.4 Generic Beam Theory Design Curves Illustrating Maximum Tensile Stress for Various Overburden Depths
4.5 Comparative Shear and Bending Moment Diagrams for Flat and Arched Crown Analogies
4.6 Generic Relationships for Crown Pillars Analysed as Two-Way Spanning Plates
4.7 Concept of Arch Action of Voussoir Beams for Crown Pillar Analysis
4.8 Results of Voussoir Beam Analyses for Various Rock Quality and Beam Geometries
4.9 Mechanisms of Kinematic Failure of Crown Pillars and Methods of Geological Data Presentation for Kinematic Stability Evaluation
4.10 Typical Geometry for Crown Chimney Caving Analysis
4.11 Transition From Caving to Stoping Conditions for Various Rock Mass Qualities
4.12 Geometrical Characteristics for Various Caving Situations
4.13 Drawing Patterns for Caved Rock
4.14 Critical Stope Heights for Limitation of Caving (Assuming Complete Stope Filling by Caved Rock)
4.15 Mine #26 - Case 1 Stress Input 2-D Boundary Element Analysis Results
4.16 Mine #26 - Case 2 Stress Input 2-D Boundary Element Analysis Results
4.17 Mine #22 - Case 1 Stress Input 2-D Boundary Element Analysis Results
4.18 Mine #22 - Case 2 Stress Input 2-D Boundary Element Analysis Results

4.19 Results of Flac Analysis Plot of Principal Stress Trajectories and Tension Zone for Mine #42 (Elastic Model)
4.20 Results of Flac Modelling for Mine #42 Using Mohr-Coulomb Model (No Tension : No Cohesion)
4.21 Results of Flac Modelling for Mine #42 Using Mohr-Coulomb Model with $c' = 1.25$ MPa, ϕ', $= 63°$, $\sigma_t = 0$
4.22 Results of Flac Modelling for Mine #42 Using Mohr-Coulomb Model with $c' = 1.25$ MPa, $\phi' = 63°$, $\sigma_t = 1.0$ MPa
4.23 Geometrical Layout for Parametric Series of Mudec Analyses
4.24 Representative Results from Mudec Analyses for Overall Range of Crown Pillars Examined
4.25 Model Results for Stope Geometry Showing Crown Stress Conditions
4.26 Geometrical Configurations for Solid Model and Finite Element Mesh for Mine #29 Crown Pillar and Stope Layout
4.27 Stress Configurations on Upper Surface and Within Rock Mass 3-D Model - Mine #29
4.28 Stress Configurations - Undersides of Stope Crown Pillars and Within Strike Pillar Region - Mine #29
4.29 Comparison Between Mesh Arrangements for 2-D Flac Model and 3-D I-Deas Geometry (Mine #29)
4.30 Modelling Configurations for 2-D Boundary Element and P-Frame Structural Solution Approaches (Mine #29)
4.31 Results of Chimney Failure Analyses for Two Different Rock Qualities

SECTION 5

5.1 Generalized Geological Cross-Sections and Plan (Mine #44)
5.2 Typical P-Frame Output For Beam Analysis Deflection, Shear and Bending Moment Plots for Crown Pillar at Mine #44
5.3 Appraisal of Crown Pillar at Mine #44 Using Elastic Beam Theory (P-Frame)
5.4 Influence of Lateral Confining Stresses on Stability of Crown Pillar (Mine #44)
5.5 Crown Pillar Thickness Parametric Evaluation (Mine #29)
5.6 Evaluation of Crown Pillar at Mine #42 Analysed as Beam with Fixed Ends
5.7 Isometric Diagram of #1 and #2 Shaft Areas (Mine #25)
5.8 Appraisal of Crown Pillar Stability for Mine #26 Using Plate Analysis Methods (Assuming Plates with Fixed Ends)
5.9 Overall Geology and Geometry of #3, #5 and #7 Vein Areas at Mine #33
5.10 Results of Flac Analysis Showing Plot of Principal Stress Trajectories and Tension Zone for Mine #33 (Elastic Model)
5.11 Results of Post-Failure Analysis Using Flac Displacement and Stress Trajectory Plots (Mine #15)

5.12 Results of Post - Failure Analysis Using Flac Displacement and Stress Trajectory Plots (Mine #14)
5.13 Conceptual Sketch of Mine #22 After Original Crown Pillar Failure
5.14 Results of Mudec Analysis Plot of Principal Stress Trajectories (Mine #22)
5.15 Output Plots From Mudec Analysis for Mine #22 Showing Crown Pillar Failure Sequence
5.16 Idealized Stope Geometry for Stability Analysis of Crown Pillar and Hangingwall Zone for Dewatering of Mine #45
5.17 Stability Assessment - 1st Level Stope (Mine #45)

SECTION 6

6.1 Summary of Crown Pillar Case Records (Thickness to Span Ratios Vs Rock Quality)
6.2 Terzaghi Rock Load Concept Used for Dimensionally Scaling Effective Induced Loading/Crown Pillar Weight Effects
6.3 Various Derating Factors Proposed to Account for Dip of Geological Structure with Respect to Excavation Geometry
6.4 Summary of Crown Pillar Case Records (Scaled Critical Crown Sapn $[C_s]$ Vs Rock Quality)

Section 1
Introduction and Executive Summary

Golder Associates

1.0 INTRODUCTION AND EXECUTIVE SUMMARY

The Department of Energy, Mines and Resources (CANMET, MRL Division), under the unsolicited proposal scheme, awarded D.S.S. Contract #23440-8-9074/01-SQ to Golder Associates to undertake back-analysis stability examinations of failed and stable surface crown pillars. This report presents the results of the studies completed to address these issues. The report also examines the more general problem of realistically assessing surface crown pillar stability and design. The report is divided into three sections:

- Part 1 contains an evaluation of case records used to define classes of instability, failure mechanisms, and parameters critical to stability;
- Part 2 presents a review of currently available design methods in order to determine whether there is an appropriate design methodology or combination of approaches, reliable enough to be used as a standard design tool for crown pillar assessment; and,
- Part 3 outlines the development of an empirical design procedure along the lines of the NGI and CSIR geomechanics classifications to allow geological parameters to be incorporated together with details of the geometry of the crown pillar and underlying stope to assess likely pillar stability.

1.1 Background

Our present understanding of the behaviour of rock crown pillars during failure is limited. Existing methods of laying out crown pillars still rely heavily on *rules of thumb*. Although far from rigorous, this traditional approach has considerable validity where much experience in a particular rock mass has been accumulated. The fact that such approaches are still widely used reflects the lack of a more valid procedure, rather than any desire on the part of the mines to short-circuit more rigorous design approaches. The lack of a proven relationship between theoretical prediction and reality is the crux of the problem. Addressing this credibility issue therefore forms a major focus for the present study.

1.2 Scope of the Problem

Although much has been accomplished in recent years in documenting procedures used by various mines for defining their surface crown pillars, there has been only limited acceptance of the need for formalizing crown pillar design in the industry. This problem has been compounded by the fact that existing design approaches are generally limited in scope (Bétournay, 1989).

Furthermore, because of perceived reliability problems, it is also recognized that existing analytical methods need to be verified and extended by reference to actual failure mechanisms. Unfortunately, only limited data on the geometry of known failures and virtually no data on the cause of such failures exists in the literature. Thus, although some attempts have been made to review and document design approaches for crown pillar layout, (CANMET 1984, 1985, and Bétournay 1986a), it is clear that there still remain significant gaps in current knowledge.

1.3 Objectives

The primary objective of this study has therefore been to establish whether available design approaches could be improved by appraisal of past surface crown pillar failures. Clearly, successful design methods must be able to identify and incorporate solutions to the problems that can lead to failure. In consequence, available methods have been tested as a guide to developing valid approaches for the assessment and design of future surface crown pillars.

This report does not purport to form a design manual. However, through back-analysis, it examines current methods of design; and provides comments on the limitations of current methodology to realistically design crown pillars. The influence on crown pillar stability analyses of variations in geometrical, geological and geomechanical parameters for different quality rock masses is addressed by comparison of failed and stable surface crown pillars. Such variations are wide and include differences in pillar geometry, failure mode, in situ stress and groundwater conditions, as well as with mining method and sequencing.

Much of the thrust of the work discussed in this report has been directed towards developing an empirically based relationship between the geometry of stable crown pillars and the controlling rock mass properties expressed in terms of an NGI-Q or CSIR-RMR rating (Barton, 1974, Bieniawski, 1[illegible]73). This approach has been followed not only as a means of quantifying the vast array of data collected on stable and failed crown pillar cases but also as a means for assessing the reliability of available analytical techniques.

1.4 Case Study Records

In order to accomplish these aims, modelling and generic rock mass classification methods have been used to evaluate a variety of case study records. In total, 70 mine sites encompassing over 200 individual crown pillar case records have been evaluated. The data from this examination is summarized in Appendix A and reviewed in detail in later sections of this report. As much of this data has been compiled from confidential information, individual mine case records discussed in this report are referenced by code numbers only.

For many of the larger scale failures which occurred over the last few decades, and usually involved some loss of life, information on the geometry and geology of the failures can be drawn from the popular press and also from extensive testimonies presented to the Commissions of Enquiry which followed the disasters. Such information is not so readily available for most of the older failures which occurred in the early years of the Century. Unfortunately, even for the well known failure cases, little, if any, rigorous, geotechnically based documentation is available. Specifically, data on the properties of the rock materials forming the sidewalls and crowns of the failed openings is often sparse or completely non-existent. Information about the behaviour of the pillars during actual failures is also usually absent. Design data used for the original layout of the pillars is also hard to find. In fact, the design of some of the crown pillars that failed may well have been compromised by later mining events (such as adjacent stoping development causing destabilization of abutments). In some cases, no specific crown pillar design was undertaken in the first place.

For collapses which did not involve loss of life or property damage, the availability of reliable data is even worse. Generally, only word-of-mouth information remains for most of these failures.

1.5 Failure Situations

The correct use of any analytical method of evaluation or back-analysis pre-supposes a knowledge of the likely failure mechanism so that the correct method of analysis can be used and representative controlling parameters can be modelled. Progressive failures are particularly intractable analytically since each component of the failing geometry has to be known in sufficient detail so that it can be modelled either discretely or statistically. Nevertheless, use of deterministic analytical methods can provide some insight into the likelihood of failure initiation.

Throughout the case history review several distinctly different failure mechanisms have been recognized. While proximity to surface, and extracted stope volume both have an influence on stability, for a given crown geometrical configuration it is geological structure that dominates failure behaviour. Sometimes, it is individual geological weaknesses that are important. In other cases, it is a more pervasive structural fabric such as schistosity that controls failure development.

Individual major weakness planes, such as faults or cross-cutting dykes, are not often the major cause of failure. Perhaps this is because they are more easily recognizable to the mine operators as potential problems and therefore taken into consideration in the original crown pillar design.

In blocky rock masses, failures occur where the intersection of several adversely oriented discontinuities occur, or where a particular suite of major joints provides a release mechanism for gravity collapse. Several narrow vein crown pillars have failed on such a block controlled basis defined by the geometry of individual master cross joints. Similarly, in failure situations which are more extensive in area than the narrow vein collapses just described, the geometry is also frequently controlled by the orientations of major individual cross-cutting discontinuities. In both cases, carefully constructed stereonet diagrams that clearly identify such discontinuities can be of immense value in defining possible failure geometries.

In cases where ubiquitous fabrics are the cause of failure, uncontrollable slabbing and sloughing is often resposible for inducing progressive or chimney-type crown failures. In such cases, it is important to consider not only the structural fabric of the crown pillar itself, but also the implied weakness that such a fabric creates on the hangingwall side of the stope where the geological structure, in conjunction with the overall stresses, can initiate a form of progressive failure that leads first to enlargement of the stope width and ultimately to destabilization of the crown.

For all rock masses, therefore, attention to detail with respect to accurate documentation of fabric characteristics is essential. Data must be collected on spacing, continuity and orientation of all major discontinuities as well as on pervasive rock fabrics in order to fully assess the potential for stope failure.

1.6 Methods of Evaluation

As indicated in Section 1.5 above, structural geology, as well as excavation geometry, plays a significant role in crown pillar stability and together they both define the mechanism of likely failure. In undertaking the back-analyses of the case records, therefore, because of lack of precise geotechnical data for many of the cases, the mode of failure (and hence, the selection of the method of analysis) has often had to be based solely on descriptions in the literature or from knowledge of the geological conditions at the site. Much the same situation exists with regard to the availability of hard data on geotechnical properties. Available measurements are sparse and in the case of in situ stresses are essentially non-existent. Thus, in the analyses, controlling geotechnical parameters (such as shear strength, etc.) have often had to be based on data and experience with other similar rocks elsewhere, guided by generic classifications of the rock mass at the site being analysed. In each case, though, an attempt has been made to validate the model by comparing the derived conclusions with observations or records of the actual failures.

1.7 Summary Conclusions

Based on analyses of several of the better documented failures and parametric evaluation of numerous other typical geometries, the study results confirm that, for a given rock mass characterized by either discrete discontinuities or ubiquitous geological fabric, the dominant control on crown pillar stability is the geometry of the excavation and the thickness of the rock crown. In consequence, for many situations, specific stable pillar dimensions can be inferred based on accurately characterizing controlling geological elements within the rock mass. Other broad reaching conclusions are that:

- The stability of most crown pillars is controlled by the geometry of the originally mined excavations, rather than by subsequent changes arising from adjacent mining.
- The mode of failure for rock crowns varies with the competence of the crown material. Arch buckling and beam bending type failures are unique to the good to very good quality rock mass environments where crown pillars of thin aspect ratio can be created. For poor quality rock masses, failure tends to be either of the purely chimney type, or by progressive caving and ongoing ravelling through to surface.
- Thin stable crown pillars are possible in hard competent rock material that readily arches or forms a distinct beam, but thick crown pillars of limited width are generally needed for low strength, schistose rock of small block size in order to prevent progressive caving or ravelling to surface. (It should be noted that this latter generality may not be universally applicable for some very weak rock masses where control of ravelling is impossible without positive support.)
- Rock mass characteristics and particularly those of the weakest discontinuity surfaces are of prime importance to defining crown pillar stability. Identifying the individual discontinuity surface or part of the rock fabric that will control failure is difficult. With ore bodies that vary from weak schistose horizons through to competent silicified units, it is not always the ore zone that dominates rock mass behaviour.
- Rock mass classification methods using the NGI-Q and CSIR-RMR systems allow ready understanding and categorization of rock conditions within a specific failure or stable crown pillar situation. They also provide a means of reliably transferring site specific rock quality information from one site to another. Routine procedures described in the literature for characterizing the NGI-Q index and the CSIR-RMR ratings for a given rock mass must be applied with caution in order to avoid over-compensating for groundwater and/or stress effects in the rock mass ratings, particularly where analytical solutions are later to be employed which incorporate such terms within their formulations.
- Crown pillar failure conditions cannot be described uniquely by any one theoretical failure model. Rather, a whole range of different failure mechanisms are evident and currently different models are required to evaluate each of these mechanisms. Further, a governing potential failure-mode needs to be assigned for any crown pillar situation before any current design method can be used.

- Many numerical modelling approaches have application to crown pillar design, but most are severely limited when there is a need to deal with the geometries of real crown pillars. All of the models have some application, but no one method of analysis is sufficiently representative of crown pillar behaviour to be considered for use as a unique design tool.

- Of all the available numerical procedures that are routinely applied in rock mechanics evaluation (boundary element, finite element, finite difference and distinct element methods), only the distinct element approach seems to possess the necessary flexibility for modelling the essentially gravity-controlled failure mechanisms which characterize crown pillar behaviour. Finite difference codes, which allow post-failure analysis, can have validity, but the choice of input parameters is critical to producing rational results.

- Simple limit equilibrium models ranging from simple beams and plates through to voussoir arches have limited applicability and display wide disparity in calculated results.

- Discrete block codes are appropriate for many situations, and provide considerable assistance in visualizing the failure mechanisms that develop for differing crown pillar geometries.

- Current three dimensional models have potential application, but require too sophisticated a database of information and are generally too time-consuming for routine application. In consequence, they are of limited practical usefulness. Furthermore, they seem severely limited in their ability to improve our understanding of the complexities in three dimensions of realistic crown pillar failures.

- The role of in situ stress within the crown pillar zone is still not clearly understood. In certain situations, lateral clamping stresses are significant and in other cases they seem to be ineffective or completely absent. Theoretically, the presence of clamping stresses and the development of a compression arch within a crown pillar will significantly enhance the stability of the pillar. Determination of the in situ stress state in stable crown pillars therefore would provide invaluable data to further current understandings of crown pillar behaviour.

1.8 Acknowledgements

The information collected to compile the database included as Appendix A has formed the framework for the back-analysis work carried out in this study. The data was obtained from CANMET, from various Provincial Ministry archives, from Golder Associates files and from the confidential records of numerous mining companies. The contribution of these organizations, is acknowledged, and in fulfillment of the confidentiality agreements made with the many contributors, no record of property names or locations is included in this document.

Part 1
Classification and Evaluation of Case Records

Golder Associates

Section 2
Crown Pillar Characterization

Golder Associates

2.0 CROWN PILLAR CHARACTERIZATION

Assessing the stability of the many widely varying geometrical configurations that occur in surface crown pillars is complex. Rock types vary, geological structures vary, groundwater conditions differ and in almost all cases, mining sequencing and extraction ratios are different from location to location even within the same mine site. Considerable experience in applied rock engineering is required in order to interpret these factors for the purpose of assessing the risk of collapse. A detailed understanding of rock mass properties and pillar geometry is therefore essential to increasing the level of confidence in any analytical prediction of short-term or long-term stability of a surface crown pillar.

Obviously, where crown pillars exist under areas of municipal infrastructure (i.e. highways, houses, schools and such like) and the risk to the general public of failure is great, factors of safety against collapse must be higher than might be tolerable in a mine-site environment. This makes the tacit assumption that all mining areas will never be developed, a situation known to be erroneous, as towns such as Timmins, Malartic, Kirkland Lake and Cobalt visibly demonstrate. The emphasis therefore in crown pillar design must be to ensure stability both during and subsequent to mining. This requires a detailed understanding of rock mass behaviour and of crown pillar failure mechanisms.

2.1 Key Components of Pillar Characterization

Whatever the required risk level, for analysis of any crown pillar situation the same basic suite of data need to be collected. Unfortunately, it is apparent that such data are often incomplete or lacking.

Ideally, for each crown pillar situation, data are required on all of the aspects outlined on Table 2.1. As the table indicates, rock mass conditions are only one of a number of factors which affect stability. As a minimum, in order to evaluate ongoing crown pillar stability or back-analyze existing stability or failure conditions, sufficient data should be available to:

- define the geometry of the problem;
- determine groundwater conditions in situ at the outset of mining (and, if mining is active, over the course of the proposed mine development sequence);
- assess rock mass characteristics and relevant geomechanical strength parameters for each recognizable material type; and
- evaluate in situ and induced stress conditions around the stope and in the planned or existing surface crown pillar and abutments, especially with respect to ongoing mining sequencing or infrastructure development.

For the back-analysis studies discussed in this report, in addition to adequate details of the geometry and geology of the crown pillar, information on original surface configuration, overburden characteristics, and on the rock mass conditions and geology of the failure zone are important guides to rational evaluation and back-analysis.

2.2 Availability of Key Data

Prior to the start of the CANMET programme on Crown Pillar Characterization, culminating in compilation of the extensive list of case records presented in Appendix A and summarized on Table 2.2, little, if any, collected geotechnical or geological data was available on crown pillar conditions. In fact, published detailed geomechanical data pre-dating the mid 1980's on rock mass characteristics associated with surface crown pillar failures, is virtually non-existent, particularly with respect to information on rock conditions in and adjacent to the actual failure zones. In many cases, though, information is available from unpublished mining records on the geometry of the mining block and/or on its generalized geology. As a result, it has been possible to at least undertake some generic categorization of failure behaviour. Also, in most cases, some data has been found on groundwater conditions and likely overburden thicknesses and material characteristics, thus assessment of the influence of these factors has also been feasible within this study.

For many of the old failures, information on the geometry of the workings is often incomplete or conflicting. In other situations, only data on the geology of the area are available with no indications being found of actual stoping geometry. Of necessity, information on underground layouts in some cases has had to be interpolated between the various drift sections shown on the geological drawings.

Despite careful review of available data sources, relevant information on the timing, sequencing and characteristics of most of the old failures, and documentation relating to their absolute causes is virtually non-existent. Even in the case of the Belmoral tragedy which occurred in May, 1980, and for which several detailed reports were produced from the evidence given to the enquiries, it is surprising that almost no detailed geomechanical data was documented relating to overall rock mass characteristics, or even to the specific geology or geometry of the ore zone/hangingwall and/or the ore zone/footwall contact areas where the failure developed. Some data on RQD's of the various rock units was compiled, and in this case, some information on overburden characteristics was collected and evaluated, but often such data are also lacking.

In consequence, wherever only partial information was available for that given case record, strength and material properties were estimated for both rock mass conditions and for overburden deposits. Such estimates of rock and soil properties for use in the analytical evaluations were not arbitrarily made. Rather, they were carefully based on information provided from discussions with mining or exploration personnel familiar with the property, guided by unpublished and published information pertaining to the properties of similar materials at other sites.

2.3 Classification of Surface Crown Pillars

Seventy case records of various Canadian hard rock mines encompassing 237 thin or problematic crown pillar geometries have been evaluated. Geologically and geometrically five main sub-classifications can be recognized (refer to Figure 2.1):

- **tabular, narrow vein ore body situations**, usually, but not always, comprising weaker sheared ore zone rocks bounded by competent, hard, wall-rock units (Figure 2.1, Category A);
- **complex, blocky rock mass conditions** often with structurally controlled weaknesses cross-cutting both the large scale ore body geometry and the adjacent country rock mass (Figure 2.1, Category B);
- **foliated rock environments** with strongly anisotropic weak structure generally parallel to the strike and dip of the ore body. Slaty rock masses, wide shear zones and ubiquitously schistose rock masses are characteristic of this type of situation (Figure 2.1, Category C);
- **disseminated ore zone situations**, usually within an overall competent but frequently slabby rock mass which exhibits at least one predominant subplanar discontinuity set parallel to the ore zone dissemination (Figure 2.1, Category D); and,
- **faulted or structurally dominated situations** where a weak or adversely oriented major structure (other than the ore zone itself) either cross-cuts or parallels the direction of stope excavation (Figure 2.1, Category E).

For each of these situations, specific examples can be cited for both failed and currently stable crown pillar geometries. The mine sites evaluated are listed on Table 2.2 together with information on the rock types forming the footwall, ore zone and hangingwall at each site. The dip of the ore body is also given as well as an assessment of which of the rock structure categories listed above most appropriately describes the surface crown pillars documented. Mines at which failures of a surface crown pillar have occurred are highlighted by an asterisk adjacent to the code for crown pillar type. When these are summarized, by crown pillar category, as shown on Table 2.3, it is of interest to note that typically more than one failure situation is recorded for each category, often with more than one failed crown pillar per mine site. In total, of the 237 case records evaluated, failure cases only account for 30 (ie. approximately 13% of the total database).

While the list of crown pillar locations included in Table 2.2 is not exhaustive, the trends summarized on Table 2.3 are indicative of the dominant modes of failure. The data suggests that most failures occur in situations where weak, adversely oriented geological structural fabric dominates the geometry of the crown pillar zone.

Although these statistics are helpful in focusing attention on the mode of potential failure, not all of the failure cases are sufficiently well documented that they can be examined in detail. Comprehensive geological, geomechanical and geometric data is lacking for most cases. However, for some specific examples, available data has permitted geotechnical assessment and back-analysis. The cases for which reasonable data are available are discussed further in Sections 3, 4 and 5 of this report.

For most of the failed cases, where data is available, and for those in similar conditions where failure has not occurred, some inference can be made regarding the geotechnical parameters which controlled failure. However, not all failure cases have been examined in detail. Individual mines were eliminated from consideration where the mode of failure appeared similar to other better defined situations or where, on detailed examination, it was found that the data was inadequate for definitive back-analysis purposes. Similarly, mines for which data were being evaluated elsewhere under other facets of the overall CANMET crown pillar programme were also omitted from detailed review.

2.4 Development of Surface Crown Pillar Data Base

Compilation of the case records included in Appendix A and summarized on Tables 2.2 and 2.3 involved several field visits to mine sites to complement an extensive review of published literature and unpublished, frequently confidential information from mine plans and other records obtained from mine archives, from Provincial and Federal Government agencies and from the extensive report documentation and in-house files of Golder Associates. The list of sites in the database includes the original 24 case records collected under CANMET Contracts 26SQ23440-5-9014 and 26SQ23440-3-9005 (Bétournay, 1987 and Bétournay, Nantel et al, 1987), plus two near-surface stope situations from the case records compiled under CANMET Contract No. 17SQ.23440-0-9020 (Golder Associates, 1981). For each of the documented case records, the site and its geometry has been classified according to its overall hangingwall, ore-zone and footwall geological characteristics, and, where possible, an assessment has been made of geotechnical characteristics and rock quality conditions based on rock mass classification approaches.

2.5 Applicability of Existing Rock Mass Classifications

To date there have been at least a dozen different rock mass classifications developed, each aimed at characterizing rock from the viewpoint of constructing excavations within it. The earliest methods merely transferred analytical approaches used in soil mechanics to rock characterization; (e.g., Terzaghi's rock load concept). The more recent and, in many ways, more versatile approaches, including those primarily used in this study for assessing crown pillar conditions, have been based more on observational procedures within a framework of appraisal of hundreds of case histories. Numerous papers have been written on the topic, so it is unnecessary to repeat here all the details of the many viable classifications that have been expounded over the last few decades. The following list provides a chronology of the publications of the more widely referenced classification approaches. Full references are included in the bibliography at the end of this report.

Terzaghi, 1946	Rock Load Concept
Lauffer, 1958	Stand-up Time
Deere, 1964	Rock Quality Designation (RQD)
Deere & Miller, 1966	Intact Rock Strength
Wickham et al., 1972	RSR Concept
Bieniawski, 1973	Rock Mass Rating (RMR)
Barton et al., 1974	Q-System Index
Franklin, 1975	Strength/Block Size Concept
ISRM, 1981	Basic Geotechnical Classification

Although each of these systems was designed to be used by itself, when considering complex situations such as surface crown pillars, it has been found much more effective to employ two or more classification systems in order to allow comparative ranking of rock mass conditions.

One of the primary purposes of rock mass classifications is to allow support designs of new excavations to be accomplished based on the experience gained from past behaviour. Since most of the design guidelines formulated from rock mass classifications have been developed on the basis of civil engineering case histories, which, themselves, reflect previous precedent practise, they tend to err on the safe side. Further, most of the classifications were developed from appraisal of conditions within tunnels in civil engineering projects, thus support and span recommendations tend to be more conservative overall than would be used normally in the mining industry. They also have generally not been specifically developed for application to irregularly shaped openings of large sizes such as are typical in many mining situations.

In consequence, various attempts have been made to extend the applicability of the civil engineering based classification approaches to mining practice. The adjustments to the CSIR system, proposed by Laubscher (1975, 1976) and the approaches to modify the Q-system as developed by Golder Associates (1981) and extended by Potvin et al (1988) (Figure 2.2) are attempts to extend such civil engineering based classifications to routine mining design.

As it is important that stable stopes exist beneath a surface crown pillar, these approaches also have some merit as a means for deriving stope dimensions for near surface stopes. They are not, however, directly applicable to crown pillar design as the thickness of the crown is not considered explicitly. It is important to note also that although all of these classifications can be used for establishing preliminary estimates of stable spans, for mining purposes, the more comprehensive rock quality classifications, such as the NGI-Q and the CSIR-RMR systems, can be of considerably more use as a quantifiable guide for assessing the character of the rock mass. However, it should be appreciated that classifications, *per se*, are not a substitute for good engineering design, in fact they are really only aids towards optimizing the overall design approach. As such, they should be applied intelligently and used in conjunction with observational methods and analytical studies to formulate an overall design rationale compatible with the site geology. It is in this context that classifications have been of most use in this study, as they have provided a method of rigorously assessing rock mass conditions within the crown pillars where insufficient data was available from other sources.

For this study extensive use has been made of the NGI-Q system and the CSIR (RMR) approach as these two classifications are the most versatile and best calibrated.

2.5.1 NGI - Q System

The Q system was developed in 1974 by Barton, Lien and Lunde of the Norwegian Geotechnical Institute (NGI), as a quantitative rock mass classification method. It was originally based on the analysis of approximately 200 tunnel case histories from Scandinavia, but has since been applied to numerous projects around the world in a wide variety of rock types and geological environments.

The Q system provides a numerical assessment of rock mass quality based on six parameters which are as follows:

RQD - rock quality designation,% (Deere, 1964)
J_n - joint set number
J_r - joint roughness number
J_a - joint alteration number
J_w - joint water reduction number
SRF - stress reduction factor

The overall rock mass quality, Q, is a function of these six parameters which are combined to form three (3) quotients as follows:

$$Q = \frac{RQD}{J_n} \times \frac{J_r}{J_a} \times \frac{J_w}{SRF} \qquad (2.1)$$

The first quotient (RQD/J_n) is a crude measure of relative block size of material that would fall from the roof of a tunnel or underground opening or would constitute weakness controlled discrete elements within the rock mass fabric. The second quotient (J_r/J_a) is a rough measure of inter-block shear strength. The final term (J_w/SRF) involves a water pressure parameter and a 'total stress' parameter, the quotient of which is a measure of in situ 'active stress' conditions. Numerical values for the six parameters for various rock mass conditions are presented in summary on Figure 2.3.

One of the prime purposes of the Q-system was the estimation of support requirements for underground civil engineering structures, particularly tunnels. As it was originally developed, based on both stable and failed case records, it can also be used for estimating the maximum span of an underground opening that can be expected to remain unsupported. As a first estimate for a limiting, maximum span, Barton in 1974 proposed the relationship:

$$\text{Span} = 2Q^{0.66} \quad \text{(metres)} \qquad (2.2)$$

This was subsequently modified to account for the desired use of the excavation, by determining the equivalent dimension (D_e) for the underground excavation of concern, which is a function of both the size and purpose of the opening and is defined as follows:

$$D_e = \frac{S}{ESR} \qquad (2.3)$$

> where D_e is the equivalent dimension of the opening as defined above, S is the span, diameter or height of the opening, and ESR is the excavation support ratio as defined on Figure 2.4.

As the effects of stress and water pressure are, in many cases, accounted for in the analytical techniques used to assess rock masses, the J_w/SRF quotient is frequently set to unity. This also removes the only non-rock material or fabric term from the parameter groupings, thus making the deduced value of Q more generically applicable and transferable from site to site. In many surface crown pillar situations, this quotient is unity anyway, as water-pressures are not usually high and stresses are also not sufficiently high to cause rock-burst types of problem. This modified Q index has been termed Q' (Golder Associates, 1981).

2.5.2 CSIR - RMR Geomechanics Classification

The geomechanics classification or rock mass rating (RMR) system provides an alternative quantitive method for assessing rock mass quality and required tunnel support. The RMR system was developed by Bieniawski of the South African Council for Scientific and Industrial Research (CSIR) in 1973, based largely on experience from tunnel construction. Since its initial development, however, the RMR system has, like the Q-System, been used in a variety of applications including rock slopes, foundations, underground caverns and hard rock and coal mining situations.

The RMR classification system is based on assigning a weighted value or rating to the following six parameters:

- uniaxial compressive strength (of an intact specimen of the rock material)
- rock quality designation (RQD, %)
- spacing of discontinuities
- condition of discontinuities
- groundwater conditions
- orientation of discontinuities

The rating values for each parameter are presented in Figure 2.5. The basic rock mass rating is determined by summing the individual ratings for the first five parameters. The rating for the sixth parameter is a correction factor which is subtracted from the basic RMR value in order to account for the orientation of controlling discontinuities with respect to the direction of excavation of the underground opening. This correction is applied separately because it is dependent on the engineering purpose of the underground opening. Arguably, therefore, it should not be included in the assessment of the rock mass quality as it is really an excavation geometry correction term.

In consequence, many workers choose to set this adjustment correction to zero corresponding to a favourable orientation for all cases (ref. Figure 2.5). Whether this correction is included or not, the overall RMR value, so calculated, gives an indication of rock mass quality. For convenience, the RMR values have been grouped into five classes representing rock mass conditions ranging from very poor to very good rock, (see Figure 2.5).

The CSIR rock mass ratings have been correlated in a number of papers to those determined using the Q-index. Perhaps the best verified correlation is that given by Bieniawski, (1976):

$$RMR = 9\text{Log}_e Q + 44 \qquad (2.4)$$

Unfortunately, because of the differences in terminology used in the two classifications to describe rock classes, there is a lack of correspondence in the descriptions of rock groups at the very poor and very good ends of the scale (see Figure 2.6). This leads to some confusion as to the interpretation of rock mass quality based simply on the summary descriptions given by the two classifications. Although, some correspondence of descriptors occurs for the *good rock* category, because of the differences at the two ends of the descriptive scale, for the purposes of this report, the RMR terminology will be used, as these descriptors encompass 90% of the rock qualities seen in most mining situations.

2.5.3 Empirical Assessment of Rock Strength and Deformability

One of the great benefits of the application of effective rock mass classifications is that they provide a means to quantitatively categorize rock masses. Now that repeatable correlations between the commonly used NGI-Q system and the RMR system are available (see upper graph on Figure 2.6 for example), joint application of these two approaches provides a useful starting point to empirically evaluate most other required design parameters.

For the back-analysis of some of the old crown pillar failures, where the descriptions of geological conditions are often the only available information, this ability to define representative rock mass parameters is of immense value. It also provides a means to assign realistic ranges of input parameters for parametric modelling approaches. Fortunately, the geological descriptions provided in the older mining geological references, are often in very quantifiable engineering terminology. Therefore, with reference to summary tabulations, such as presented on Table 2.4 or by reference to the individual codes within the NGI and CSIR classifications (Figures 2.3 and 2.5), it is possible to assign realistic Q and RMR values to the rock units in the crown and abutments of a given surface crown pillar for a particular mine site.

As many of the surface crown pillar case records are also devoid of any reliable rock mass and/or material property information, often it has also been necessary to develop realistic strength, modulus and stiffness values for use in parameter back-analysis. Use of such classifications allows appropriate values to be deduced.

- Rock Mass Compressive Strength

Prediction of global rock-mass strength, based on rock-mass classifications, can be fairly effectively accomplished by first assigning a representative intact strength using available test data or, where no data is available, by reference either to the upper tabulations on Figure 2.5 or to available published data on intact strengths of similar rock material. With an appropriate value of σ_c known, it is then possible to derive the Hoek-Brown m and s constants appropriate to the rock mass. This can be accomplished graphically from the lower graph on Figure 2.6 or from relationships published by Hoek and Brown in 1988, which define the two sets of rock mass quality ranges - undisturbed and disturbed rock, the curves for which are shown on Figure 2.6. For most surface crown pillar situations, even with surface weathering, blasting, stress cracking or caving effects, the crown rock mass usually fits within the definition of "undisturbed" rock and thus will be best represented by:

$$m = m_i e^{\frac{(RMR - 100)}{28}} \quad \text{and} \quad s = e^{\frac{(RMR - 100)}{9}} \qquad (2.5)$$

where m_i is the value of the constant m for intact material (Hoek, 1983, 1988).

It should be appreciated that the m and s parameters deduced from these relationships are relatively consistent with parameters established for the low to medium stress range in the laboratory. In such situations, which are analagous to many surface crown pillar locations, derived rock mass strengths tend to be very sensitive to the chosen m and s parameters reflecting the increased sensitivity of the rock mass to failure at low confining stresses. Nevertheless, when properly chosen and calibrated, m and s parameters derived from the above relationships are appropriate for use in analysis of surface crown pillar situations where the rock mass is within a low stress environment. For situations where the rock mass is under high confining stresses, the shape of the non-linear failure envelope is much flatter, thus derived rock mass strengths are less sensitive to the choice of m and s parameters.

Once values of m and s for the rock mass have been determined from Q and/or RMR, it becomes possible to deduce most of the other shear strength parameters required for analysis purposes by substitution into the Hoek-Brown failure criterion:

$$\sigma_1' = \sigma_3' + \sqrt{m\sigma_c\sigma_3' + s\sigma_c^2} \qquad (2.6)$$

where σ_1' is the maximum principal stress that the rock mass can sustain under a confining minor principal stress of σ_3',

σ_c is the uniaxial compressive strength of the intact rock (usually measured from core samples or can be ascribed from the individual sub-groups to the CSIR ratings or by reference to published data).

and m and s are parameters relating to rock material fabric and rock mass fabric respectively; where m for intact rock samples ranges from values of the order of 5 for rocks with highly ordered crystalline microfabrics to 25 for rocks with polyminerallic interlocking crystal micro-structures; and s ranges from 1 for intact rock samples to 0 for completely disintegrated rock masses with a gravel, rockfill or soil-like composition.

An estimate of an overall compressive strength for the rock mass under no confinement can then be obtained by substituting $\sigma_3' = 0$ into the general Hoek-Brown failure criterion, thus:

$$\sigma_{cmass} = \sqrt{s}\,\sigma_c \tag{2.7}$$

Similarly, substituting $\sigma_1' = 0$ and solving the resulting quadratic equation gives the uniaxial tensile strength of the rock mass as:

$$\sigma_t = \frac{\sigma_c}{2}\left(m - \sqrt{m^2 + 4s}\right) \tag{2.8}$$

o Rock Mass Shear Strength

Applications of the Hoek-Brown failure criterion can be further extended to allow definition of a non-linear failure envelope for any particular rock mass type. Mohr failure shear strength parameters can then be directly derived as tangents to the failure envelope for the global rock mass knowing the uniaxial compressive strength of intact samples and with the rock fabric parameters m and s, established from NGI-Q or CSIR-RMR quality assessments. The governing equation relating the Mohr-Coulomb failure envelope to the Hoek-Brown m and s parameters in a form that can be used for such assessment is:

$$\tau = \frac{(\mathrm{Cot}\,\phi' - \mathrm{Cos}\,\phi')\,m\sigma_c}{8} \tag{2.9}$$

with the instantaneous friction angle ϕ' given by:

$$\phi' = \mathrm{Arctan}\,\frac{1}{\sqrt{4h\mathrm{Cos}^2\Theta - 1}} \tag{2.10}$$

$$\text{where } h = 1 + \frac{16\,(m\sigma_n' + s\sigma_c)}{3m^2\sigma_c}$$

$$\text{and } \Theta = 1/3\ \left[\ 90^\circ + \mathrm{Arctan}\left(\frac{1}{\sqrt{h^3 - 1}}\right)\right]$$

and with the corresponding instantaneous cohesion value c' calculated from:

$$c' = \tau - \sigma_n' \tan\phi' \tag{2.11}$$

where σ_n' is the effective normal stress acting on the shear plane.

In addition to specifically defining parameters for individual case records, this approach has also been followed in order to compile a set of representative shear strength parameters for characterizing a complete range of rock qualities from very poor to very good rock (Table 2.5). For this study, the purpose of this compilation has primarily been to allow realistic values to be developed for use in the parametric evaluations discussed in Sections 4 and 5 of this report.

Although reasonable estimates, such as those in Table 2.5, can be readily generated, when undertaking detailed stability evaluations, it is also worthwhile checking such derived values against other published data, as assessment of representative values of shear strength parameters for the principal controlling discontinuities in a given crown pillar situation can be particularly difficult. For the typical non-linear failure behaviour of most rock discontinuities, the most representative parameters depend on accurately assessing the normal stress that acts on the discontinuity surface at the time of shearing. This normal stress is particularly difficult to determine realistically. Barton (1974) however provides some generalized relationships that can be of assistance in ascribing realistic shear strength parameters, namely:

(a) at low normal stresses ϕ' tends towards 70°

(b) for most other stress ranges of interest

$$\phi' = [\, 20 \log_{10}(\sigma_c/\sigma_n') + \phi_b']\,^\circ \qquad (2.12)$$

where $\phi_b' = 15^\circ$ for chlorite/sericite coated surfaces, and between 25 and 30° for most other natural surfaces.

o Rock Mass Deformability and Joint Stiffness Parameters

Estimates of the elastic, shear and bulk moduli of the rock mass and determination of the shear and normal stiffnesses for the controlling discontinuities within the rock mass have also been completed (Table 2.6). These parameters are required for defining joint and rock mass properties when undertaking detailed numerical or analytical appraisal of rock mass responses to excavation effects. Again, these can be generically estimated by reference to the rock mass classifications, or by using published empirical correlation graphs (Figure 2.7) or explicitly from the following relationships:

Modulus of deformation, $$E = 10^{((RMR - 10)/40)} \text{ GPa} \qquad (2.13)$$

Shear modulus, $$G = \frac{E}{2(1+\nu)} \qquad (2.14)$$

Bulk modulus, $$K = \frac{E}{3(1-2\nu)} \qquad (2.15)$$

For modelling purposes, in which jointing is explicitly examined, information is also needed on the normal and shear stiffnesses of the controlling discontinuities, particularly where the models treat a jointed rock mass as an equivalent transversely isotropic material.

Information on realistic normal and shear stiffnesses for a wide range of rock materials is not readily available, however, some data has been published by Barton, in 1977 and 1981 (Figure 2.8), by Kulhawy in 1985 and by Goodman, in 1988 and some data is also presented in the various program manuals for the finite difference code (FLAC) and for the distinct element code (MUDEC).

Some estimate of shear and normal stiffnesses can also be determined explicitly if information is available on the spacing and character of the joints and on the elastic modulus of the intact rock and rock mass. The governing relationships for this type of approach are given by Goodman (1988) as:

Joint Normal Stiffness:
$$J_{kn} = \frac{E_{rm}.E_i}{S(E_i - E_{rm})} \tag{2.16}$$

Joint Shear Stiffness:
$$J_{ks} = \frac{G_{rm}.G_i}{S(G_i - G_{rm})} \tag{2.17}$$

where E_i and E_{rm} = elastic moduli for the intact rock and rock mass
G_i and G_{rm} = shear moduli for the intact rock and rock mass
and S = controlling joint spacing

As with shear strengths, these joint stiffness parameters are extremely difficult to define realistically. Of necessity, therefore, because reliable laboratory data is limited, any estimates deduced from the above approach must be thoroughly cross-checked. One means to achieve this is to empirically derive appropriate values by using Barton's joint roughness coefficient and overall strength relationships as given on Figure 2.8. Comparison of theoretical predictions based on the E_i and E_{rm} values, derived for various rock masses, as given on Table 2.6, suggests that for the joint spacings given on Table 2.5, the equivalent length of shear displacement on the plot on Figure 2.8 is of the order of 1 mm. for most of the calculated cases. This however needs further refinement before it can be reliably used universally for assessing actual joint properties within rock masses present in surface crown pillar situations.

TABLE 2.1 - Key Data Required for Characterization of Surface Crown Pillar Stability Conditions

Surface Conditions	- Topography - Presence or Absence of Water Body
Overburden Characteristics	- Thickness, Material Properties and Stratigraphy - Groundwater Regime - Bedrock/Overburden Interface Conditions

Rock Mass Characteristics	- General Geological Regime
	- Ore Zone Dip
	- Rock Types and Classification* Characteristics:
	  - Hangingwall
	  - Footwall
	  - Ore Zone in Crown Pillar
	- Structural Controls:
	  - Jointing
	  - Faulting
	  - Cleavage
	- Geometry of Crown Pillar and Upper Openings:
	  - Width
	  - Thickness
	  - Stope Spans
	  - Fill Height
	  - Support Methods
	- Other Factors:
	  - Available data on Stresses
	  - Complicating Geometry (ie Multiple Ore Zones)
	  - Extent of weathered zone within upper bedrock
	  - Details of contact zone with overburden

* Full NGI(Q) and CSIR(RMR) classifications based on core data, laboratory tests, field assesment of discontinuity characteristics, etc.

TABLE 2.2 - Summary Mine Site List Outlining Character Type & Rock Conditions

Mine No.	Category (* Indicates Failure Case)	CHARACTERISTICS			
		HW	Ore Zone	FW	DIP°
1	A	Gneiss, Slate	Sulphides	Diorite, Gabbro	70°
2	D	Chlorite Schist	Multiple Sulphides	Gneissic Volcanics	70°
3	C	Gneiss, Schist	Schist/Amphibolite	Gneiss	65°
4	D	Tuffs, Schists	Sphalerite	Metasediments, gneiss	45°
5	D	Rhyolite, dacite	Sulphides	Rhyolite, andesite	75°
6	A	Andesite, rhyolite	Schists	Andesite, rhyolite	65°
7	A	Diorite, andesite	Quartz-carbonate Veins	Diorite, andesite	80°
8	C	Periodotite, greenstone	Brecciated Sulphides	Sheared peridotite	80°
9	B	Norite, peridotite	Brecciated Sulphides	Granitized Metasediments	45°
10	B	Porphyritic rhyolite	Siderite, Quartz	Chert, banded siderite	65°
11	A	Syenite porphyry	Quartz/Chlorite/Sericite	Syenite, conglomerate	80°
12	B*	Andesite, peridotite	Rhyolite, sulphides	Volcanics, gabbro	65°
13	C	Anorthosite	Sericitized schist	Anorthosite	45°
14	C*	Greywacke, tuffs	Schists, tuffs	Mafic sericitized schist	85°
15	C	Sheared andesites	Graphitic schist	Andesite, tuffs	80°
16	D	Argillitic metasediments	Gossen Iron-formation	Metaseds, quartz-schist	75°
17	C	Sericitized, biotite schist	Quartz-stibnite	Sericite, biotite schist.	33°
18	D	Rhyolite, serpentinized	Chalcopyrite, breccia	Rhyolite, andesite	75°
19	A	Anorthosite, porphyry dyke	Sulphide, porphyry	Altered Anorthosite	55°
20	A	Epidiorite, shears	Quartz-Chalcopyrite, gabbro	Altered gabbro, porphyry	65°
21	E	Tuffs, breccias	Carbonized, kaolinized shears	Chlorite/Pyritic Volcanics	55°
22	C*	Volcanics, conglomerate	Conglomerate, greywacke	Slates, greywackes	75°
23	D	Altered peridotite	Peridotite	Altered peridotite, basalt	35°
24	C	Peridotite	Serpentinized peridotite	Peridotites, shears	40°
25	C	Porphyry	Quartz-carbonate shears	Greywacke	85°
26	A	Sheared greywacke	Schist, greywacke	Quartzite, greywacke	55°
27	E*	Porphyry/schist	Foliated porphyry	Talc chlorite schist	75°
28	E*	Sheared porphyry, peridotite	Schist, porphyry	Talc chlorite schist	70°
29	B*	Conglomerate	Sheared conglomerate	Conglomerate	65°
30	A	Porphyry, volcanics	Quartz-carbonate-chalcopyrite	Porphyrys	80°
31	A	Gabbro, volcanics	Quartz infilled shears	Volcanics, Gabbro	85°
32	A	Gabbro, foliated	Altered chalcopyrite	Gabbro, blocky	70°
33	A	Basalt, Greenstone Porphyry	Quartz veins, porphyry	Porphyry	80°
34	A	Granodiorite	Silicified granodiorite	Granodiorite	80°
35	C*	Sheared granodiorite	Sheared, foliated granodiorite	Foliated granodiorite	70°
36	A*	Syenite, Porphyry	Splay fault, dykes	Syenite Porphyry	87°
37	A	Argillite, conglomerate	Quartz-carbonate shears	Conglomerates	85°
38	A*	Conglomerate, argillite	Quartz-carbonate shears	Conglomerates	85°
39	B*	Gabbro, volcanics	Quartz, cross-cutting shears	Mafic volcanics	80°
40	A	Conglomerate	Conglomerate, Greywacke	Syenite Porphyry	80°
41	D*	Serpentinite, meta-dolomite	Dolomitic Magnesite	Limestone, dolo. magnesite	65°
42	A	Syenite Porphyry	Diabase, quartz-carbonate	Syenite, Conglomerate	80°
43	A	Syenites, tuffs	Quartz-carbonate fractures	Metasediments, tuffs	85°
44	A	Chlorite schist, basalt	Carbonate-quartz veins	Carbonate schist, porphyry	80°
45	C	Ultramafic, schists	Quartz-carbonate porphyry	Mafic Volcanics	80°
46	A*	Volcanics, conglomerates	Greywacke, conglomerate	Greywacke, slates	80°
47	D	Norite, tonalite	Sheared, altered diorite	Diorite, Tonalite	36°
48	B	Limestone	Altered carbonate	Carbonate	0°
49	A	Chlorite basalt, shear zone	Massive basalt	Graphic schist	70°
50	C*	Dacite/Andesites	Serpentinized Peridotite	Basalt/Andesite	80°
51	C	Andesites, chlorite schist	Sheared altered rhyolites	Rhyolite, basalts	45°
52	D*	Gneiss	Serpentinite	Gneiss	70°
53	A*	Syenite, sheared altered porphyry	Brecciated Syenite Porphyry	Tuff and andesites	80°
54	B*	Andesite	Brecciated Quartz Vein Andesite	Andesite Breccia	80°
55	C	Altered felsic schists, tuff	Silicified Agglomerates, schist	Schistose agglomerate	80°
56	B	Altered porphyry	Monzonite porphyry	Greywackes, metasediments	55°
57	A*	Amygdaloidal andesite	Brecciated Andesite, tuffs	Leucocratic Andesite	75°
58	A	Volcanics, Metasediments	Quartz-Carbonate veins	Sheared schistose metaseds	80°
59	B*	Sheared diabase	Quartz-Carbonate veins	Diabase	80°
60	A	Granodiorite	Agglomerates, tuff, quartz veins	Granodiorite Porphyry	65°
61	B	Norite	Breccia	Greenstone/Schist	75°
62	E*	Biotite Schists	Sheared & brecciated schists	Schists, greywackes	80°
63	A	Ultramafics, basalts, tuffs	Diorite porphyry, shears	Porphyry + agglomerates	70°
64	A*	Argillite, conglomerate	Conglomerate, calcite veins	Conglomerate	90°
65	A	Argillite, conglomerate	Conglomerate, calcite veins	Conglmerate	90°
66	A	Conglomerates, metasediments	Quartz conglomerate	Conglomerates + metaseds	35°
67	D*	Wollastonite, diopside hornfels	Porcellanite, skarn	Porcel.,Wollastonite,Hornfels	30°
68	D	Quartz mica schist	Banded schist	Quartz mica schist	15°
69	D	Quartz biotite schist	Massive Sulphides	Sericite Schist	85°
70	D	Quartz Porphyry	Massive Sulphides	Chlorite Tuff	85°

TABLE 2.3 - Summary of Stable and Failed Crown Pillar Cases by Category

Category	A (Tabular Ore Zone Situations)	B (Blocky Rock Mass Conditions)	C (Foliated Environments)	D (Disseminated Ore Zones in Competent but Slabby Rock)	E (Fault Controlled Situations)	Totals
Number of Crown Pillars Listed	103	31	66	28	9	237
Number of Failed Pillar Cases	8	6	10	3	4	30
Failure Percent	8%	20%	16%	11%	44%	13%
Mine Sites with Failure Cases	#26,#36,#38,#46, #53,#57,#64	#12,#29,#39, #54,#59	#14,#22,#25, #35,#50	#41,#52,#67	#21,#27,328,#62	

TABLE 2.4 - Descriptive Assessment of Rock Mass Quality

Rock Mass Quality	CSIR RMR	NGI Q	Characteristics Using Terzaghi, (1946) Terminology*	Typical Rock Condition
Exceptionally Good Quality	100	500	Massive, intact "sound" rock	Virtually non-jointed high strength rock mass free from significant rock defects.
Very Good Quality	85	100	Massive to moderately jointed	Tightly interlocking, jointed, undisturbed rock with unweathered joints spaced at ± 3 metres. Block sizes range from several metres to tens of metres in dimension. RQD usually above 85%. Joint surfaces usually rough.
Good Quality	65	10	Moderately blocky and seamy	Fresh to slightly weathered rock, often with stained discontinuities, spaced at 1-3 metres. Controlling block size in the 1.0 - 5.0 metre range. RQD's typically 75-85%.
Fair Quality	44	1	Moderately block and seamy	Several sets of weathered or low strength discontinuities, spaced at 0.3 - 1 m. Block sizes typically about 0.5 m. RQD's typically 40-60%.
Poor Quality	23	0.1	Very block and seamy	Numerous sets of weathered or low strength discontinuities spaced at 30 mm to 500 mm. Some with gouge filling. Rock material often showing penetrative staining and alteration. RQD's typically 25-40%.
Very Poor Quality Exceptionally Poor Quality	3 0	0.01 0.001	Very blocky and seamy to completely crushed	Closely jointed, or foliated, with controlling block size in the mm. to cm. range. RQD's typically 0-25%. Sugar cube jointing or paper thin foliation. In near surface environments more competent parent rock materials may exhibit extensive weathering and closely spaced, heavily weathered discontinuities.

* Ref: Terzaghi K. (1946): "Rock Defects and Loads on Tunnel Support", Rock Tunnelling with Steel Supports, eds. R.V. Proctor and T.L. White, Commercial Shearing and Stamping Company, Youngstown, Ohio, 15-99.

TABLE 2.5 - Representative Rock Mass Classification and Shear Strength Parameters for Various Rock Qualities

Rock Conditions	NGI Q	CSIR RMR	γ (T/m^3)	UCS (MPa)	Selected Mi Value	RQD %	Joint Spacing (mm)	Contact Stress (MPa)	"Undisturbed" Rock Mass Parameters		Equivalent Discontinuity Shear Strength	
									m	s	c' (MPa)	ϕ' (MPa)
Very Poor Quality	0.01	3	2.8	30	9	≤ 20	25 *	0.20	0.30	0.00002	0.04	15
Poor Quality	0.1	23	2.7	90	12	35	80	1.60	0.80	0.0002	0.40	20
Fair Quality	1.0	44	2.6	120	13	50	160	3.60	2.00	0.002	1.00	30
Good Quality	10.0	65	2.6	180	14	75	350	7.70	4.00	0.02	3.50	40
Very Good Quality	100.0	85	2.6	210	25	100	625	5.10	15.00	0.2	8.00	60

* Irrelevant for gouge-filled zones, within weak schists or in weak altered soil-like rock masses.

TABLE 2.6 - Representative Deformation Properties for Various Rock Qualities

Rock Conditions	NGI Q	CSIR RMR	Poisson's Ratio for Intact Rock and Rock Masses		Intact Rock and Rock Mass Moduli						Rock Mass and Joint Stiffnesses *			
					Deformation		Bulk		Shear					
			ν_i	ν_{rm}	E_i (GPa)	E_{rm} (GPa)	K_i (GPa)	K_{rm} (GPa)	G_i (GPa)	G_{rm} (GPa)	K_n (GPa)	K_s (GPa)	J_{kn} (GPa/m)	J_{ks} (GPa/m)
Very Poor Quality †	0.01	3	0.30	0.04	5.5	0.7	4.5	0.2	2.1	0.3	0.1	0.05	30.0	15.0
Poor Quality	0.1	23	0.30	0.10	6.3	2.1	5.1	0.9	2.4	1.0	0.4	0.2	42.0	21.0
Fair Quality	1.0	44	0.29	0.16	13.1	7.5	10.2	3.7	5.1	3.2	1.8	0.9	115.0	56.0
Good Quality	10.0	65	0.26	0.22	28.7	23.7	20.2	14.0	11.3	9.7	14.0	7.0	400.0	200.0
Very Good Quality	100.0	85	0.20	0.19	76.3	75.0	41.7	40.5	31.9	31.5	430.0	220.0	7000.0	3500.0

* Stiffness based on assessment of Figure 2.8; values very sensitive to assumed critical joint lengths.

† Single values for parameters provided as guidelines only, significantly lower values may occur within extremely poor quality rock masses.

MAJOR SUBCLASSIFICATIONS OF SURFACE CROWN PILLAR GEOMETRIES

FIGURE 2.1

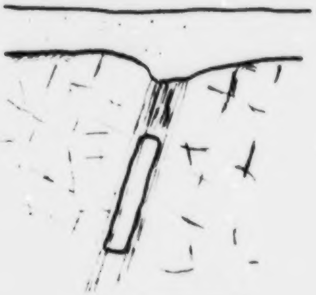

CATEGORY A GEOMETRY

TABULAR , NARROW VEIN SITUATIONS (EITHER WEAKER SHEARED ORE ZONE WITH COMPETENT WALL ROCKS OR STRONG ORE ZONE WITH WEAK MARGINS AND WALL ROCKS).

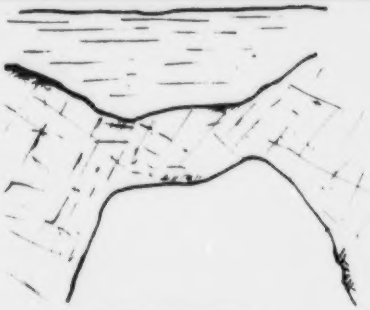

CATEGORY B GEOMETRY

COMPLEX , BLOCKY CONDITIONS WITH STRUCTURALLY CONTROLLED DISCONTINUITY WEAKNESSES. MASTER JOINTS DOMINATE WITH FEW AREAS OF SHEARED OR DISTURBED ROCK.

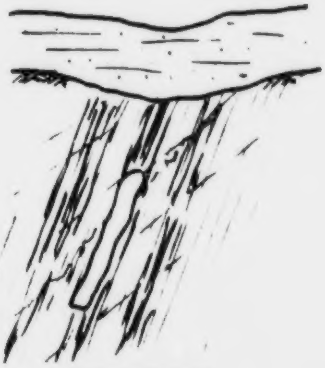

CATEGORY C GEOMETRY

FOILIATED ENVIRONMENTS , UBIQUITOUS ANISOTROPIC WEAK STRUCTURE, OFTEN SCHISTOSE OR SLATY.

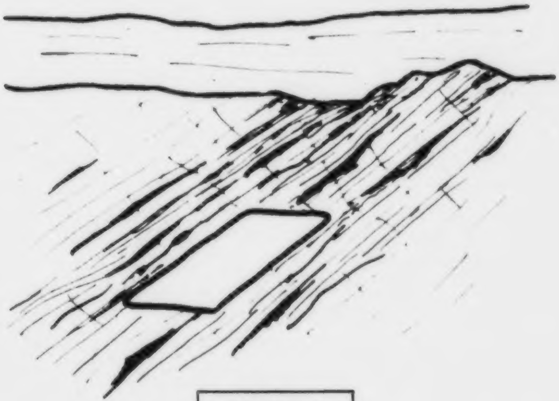

CATEGORY D GEOMETRY

DISSEMINATED ORE ZONE SITUATION . USUALLY IN COMPETENT ROCK MASS. OFTEN WITH WELL DEVELOPED PRIMARY JOINTING PARALLELLING ORE DISSEMINATION.

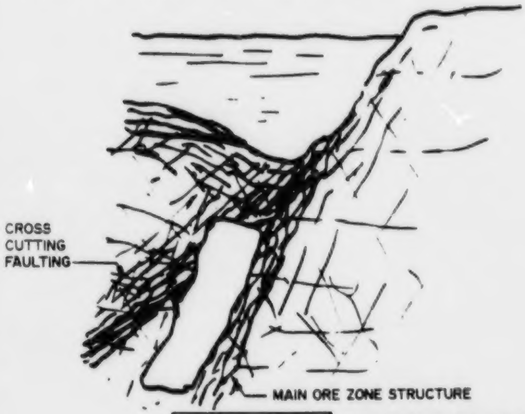

CATEGORY E GEOMETRY

FAULTED OR STRUCTURALLY DOMINATED SITUATION, ADVERSELY ORIENTED OR WEAK MAJOR STRUCTURAL CONTROL

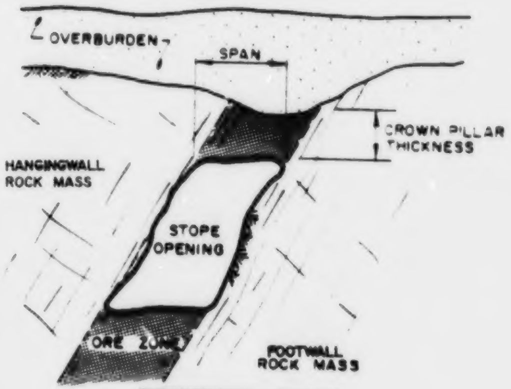

DEFINITION SKETCH

Date FEBRUARY 1, 1990.
Project 881-1739

Golder Associates

Drawn R.B.C.
Chkd. 14c

EMPIRICAL STOPE DESIGN CHARTS FOR OPEN STOPING AT DEPTH

FIGURE 2.2

GOLDER ASSOCIATES (1981)

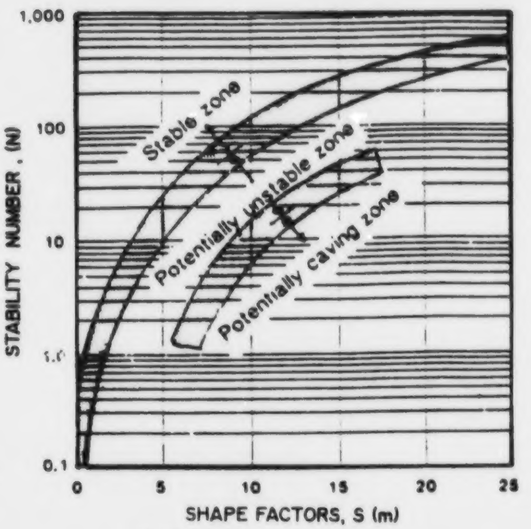

$N = Q' \times A \times B \times C$

WHERE A = ROCK STRESS FACTOR

B = ROCK DEFECT ORIENTATION FACTOR

C = DESIGN SURFACE ORIENTATION FACTOR

Q' = NGI-Q WITH $\frac{J_w}{SRF} = 1$

POTVIN et al (1988)

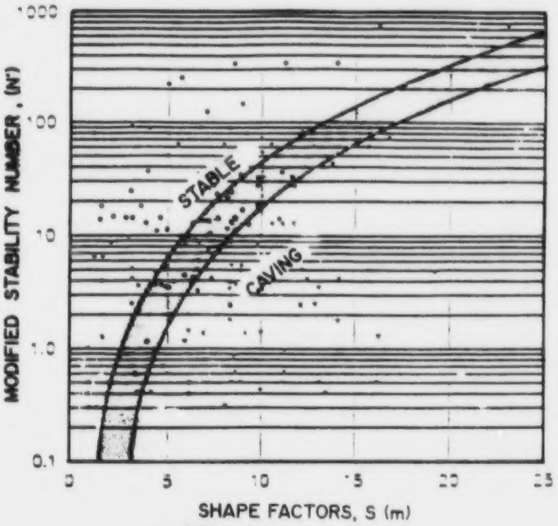

$N' = \frac{RQD}{J_n} A \cdot B \cdot G$

RQD = ROCK QUALITY DESIGNATION %

J_n = NUMBER OF JOINT SETS

G = GRAVITY FACTOR

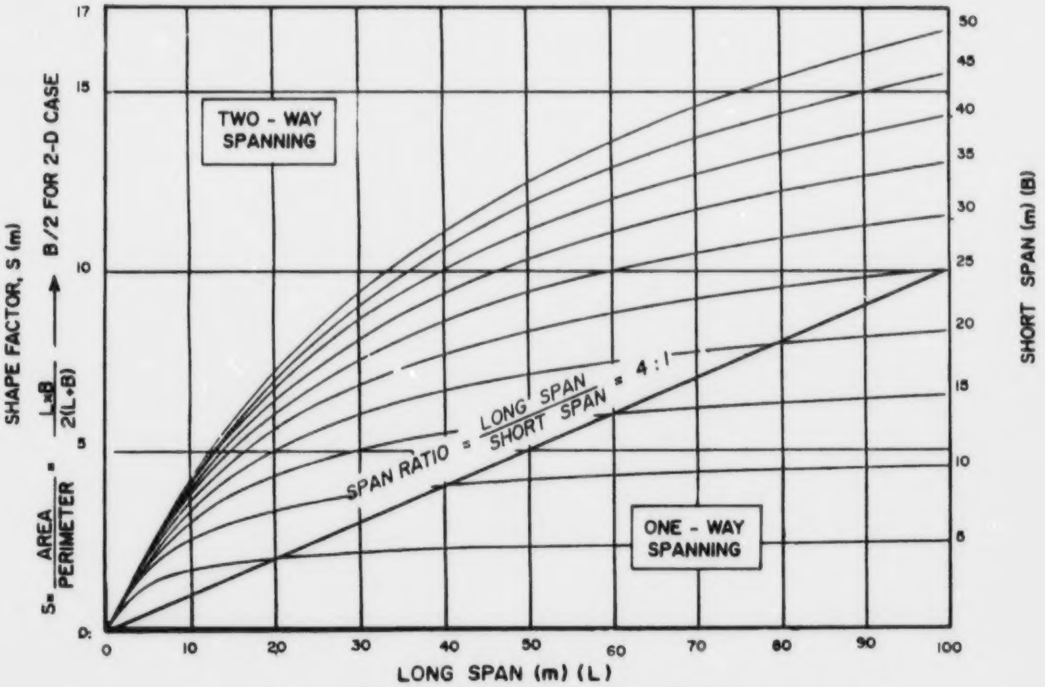

RELATION OF SHAPE FACTOR TO PILLAR WIDTH AND STRIKE LENGTH

Date FEBRUARY 1, 1990.

Project 881-1739

Golder Associates

Drawn R.B.C.

Chkd. 1ql

NGI ROCK MASS CLASSIFICATION SYSTEM
PARAMETER EVALUATION

FIGURE 2.3

Item and Description	Parameter	Value
Number of Sets of Discontinuities	J_n	
Massive		0.5
One set		2.0
Two sets		4.0
Three sets		9.0
Four or more sets		15.0
Crushed rock		20.0
Roughness of Discontinuities	J_r	
Noncontinuous joints		4.0*
Rough and wavy		3.0*
Smooth and wavy		2.0*
Rough and planar		1.5*
Smooth and planar		1.0*
Slick and planar		0.5*
Filled discontinuities		1.0*
Filling and Wall-Rock Alteration, Essentially Unfilled	J_a	
Healed		0.75
Staining only; no alteration		1.0
Silty or sandy coatings		3.0
Clay coatings		4.0
Filling and Wall-Rock Alteration, Filled	J_a	
Sand or crushed rock filling		4.0
Stiff clay filling less than 5 mm thick		6.0
Soft clay filling less than 5 mm thick		8.0
Swelling clay filling less than 5 mm thick		12.0
Stiff clay filling more than 5 mm thick		10.0
Soft clay filling more than 5 mm thick		15.0
Swelling clay filling more than 5 mm thick		20.0
Water Conditions	J_w	
Dry		1.0
Medium water inflow		0.66
Large inflow, unfilled joints		0.5
Large inflow; filled joints with washout		0.33
Large inflow; filled joints; high transient inflow		0.2 to 0.1
Large inflow; filled joints; high continuous inflow		0.1 to 0.05
Stress Reduction Class	SRF	
Loose rock with clay-filled discontinuities		10.0
Loose rock with open discontinuities		5.0
Shallow depth (50 m or less) rock with clay-filled discontinuities		2.5
Rock with tight unfilled discontinuties; medium stress		1.0
Rock-Mass Quality for Tunneling	Q	
Exceptionally poor		Less than 0.01
Extremely poor		0.01 to 0.10
Very poor		0.10 to 1.00
Poor		1.00 to 4.00
Fair		4.00 to 10.0
Good		10.0 to 40.0
Very good		40.0 to 100.0
Extremely good		100.0 to 400.0
Exceptionally good		400.0 to 1000.0

Adapted from: Barton, N., Lien, R., and Lunde, J., 1974.

* Add 1.0 if the mean joint spacing exceeds 3.0 m.

Date FEBRUARY 5, 1990.

Project 881-1739-3

Golder Associates

Drawn R.B.C.

Chkd

SUGGESTED NGI DESIGN LIMITS FOR MAXIMUM SPANS FOR UNSUPPORTED EXCAVATIONS (FROM BARTON, 1974)

FIGURE 2.4

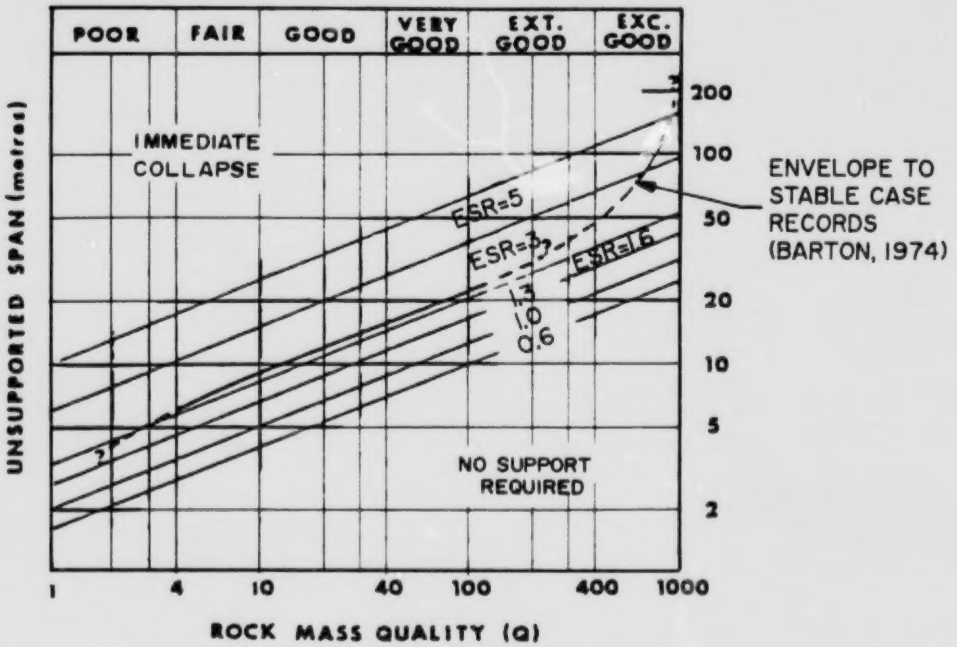

SUGGESTED DESIGN SPAN LIMITS FOR VARIOUS EXCAVATION TYPES IN DIFFERENT QUALITY ROCK MASSES

Excavation Support Ratio (ESR) Appropriate to a Variety of Underground Excavations

Type of Excavation	*ESR*	No.
A. Temporary mine openings, etc.	ca. 3–5?	(2)
B. Vertical shafts: (1) circular section	ca. 2.5?	(0)
(2) rectangular/square section	ca. 2.0?	(0)
C. Permanent mine openings, water tunnels for hydro power (exclude high pressure penstocks), pilot tunnels, drifts and headings for large excavations, etc.	1.6	(83)
D. Storage rooms, water treatment plants, minor road and railway tunnels, surge chambers, access tunnels, etc. (hemispherical caverns?)	1.3	(25)
E. Power stations, major road and railway tunnels, civil defense chambers, portals, intersections etc.	1.0	(79)
F. Underground nuclear power stations, railway stations, sports and public facilities, factories, etc.,	ca. 0.8?	(2)

* No. OF CASE RECORDS AVAILABLE

REFERENCE : BARTON, N., LIEN, R., & LUNDE, J., 1974.

Date JANUARY 31, 1990.
Project 881-1739

Golder Associates

Drawn R.B.C.
Chkd.

CSIR GEOMECHANICS CLASSIFICATION FOR JOINTED ROCK MASSES

FIGURE 2.5

Classification Parameters and Their Ratings

Strength of intact rock material	Point-load strength index	>8 MPa	4–8 MPa	2–4 MPa	1–2 MPa	Use of uniaxial compressive test preferred		
	Uniaxial compressive strength	<200 MPa	100–200 MPa	50–100 MPa	25–50 MPa	10–25 MPa	3–10 MPa	1–3 MPa
Rating		15	12	7	4	2	1	0
Drill core quality-RQD		90–100%	75–90%	50–75%	25–50%	25%		
Rating		20	17	13	8	3		
Spacing of joints		>3 m	1–3 m	0.3–1 m	50–300 mm	<50 mm		
Rating		30	25	20	10	5		
Condition of joints		Very rough surfaces; not continuous; no separation; hard joint wall rock	Slightly rough surfaces; separation <1 mm; hard joint wall rock	Slightly rough surfaces; separation <1 mm; soft joint wall rock	Slickensided surfaces or gouge <5 mm thick or joints open 1–5 mm; continuous joints	Soft gouge >5 mm thick or joints open >5 mm; continuous joints		
Rating		25	20	12	6	0		
Ground Water	Inflow per 10 m tunnel length	None		25 L/min.	25–125 L/min	>125 L/min		
	Ratio: Joint water pressure / Major principal stress	0		0.0–0.2	0.2–0.5	>0.5		
	General conditions	Completely dry		Moist only	Water under moderate pressure	Severe water problems		
	Rating	10		7	4	0		

Adjustments For Joint Orientation

Strike and dip orientations of joints		Very favorable	Favorable	Fair	Unfavorable	Very unfavorable
Ratings	Tunnels	0	−2	−5	−10	−12
	Foundations	0	−2	−7	−15	−25
	Slopes	0	−5	−25	−50	−60

Rock Mass Classes And Their Ratings

Class No.	I	II	III	IV	V
Description	V.Good rock	Good rock	Fair rock	Poor rock	V. Poor rock
Rating	90–100	70–90	50–70	25–50	25

Meaning of Rock Mass Classes

Class No.	I	II	III	IV	V
Average stand-up time	10 years for 5 m span	6 months for 4 m span	1 week for 3 m span	5 hr for 1.5 m span	10 min for 0.5 m span
Cohesion of the rock mass	300 kPa	200–300 kPa	150–200 kPa	100–150 kPa	100 kPa
Rock mass friction angle	45°	40–45°	35–40°	30–35°	30°
Caveability of ore	Very poor	Will not cave readily; large fragments	Fair	Will cave readily; good fragmentation	Very good

Date FEBRUARY 5, 1990.

Project 881-1739-3

Golder Associates

Drawn R.B.C.

Chkd. TG

CORRELATIONS BETWEEN CSIR-RMR AND Q-SYSTEM CLASSIFICATIONS AND HOEK-BROWN FAILURE CRITERION CONSTANTS m AND s .

FIGURE 2.6

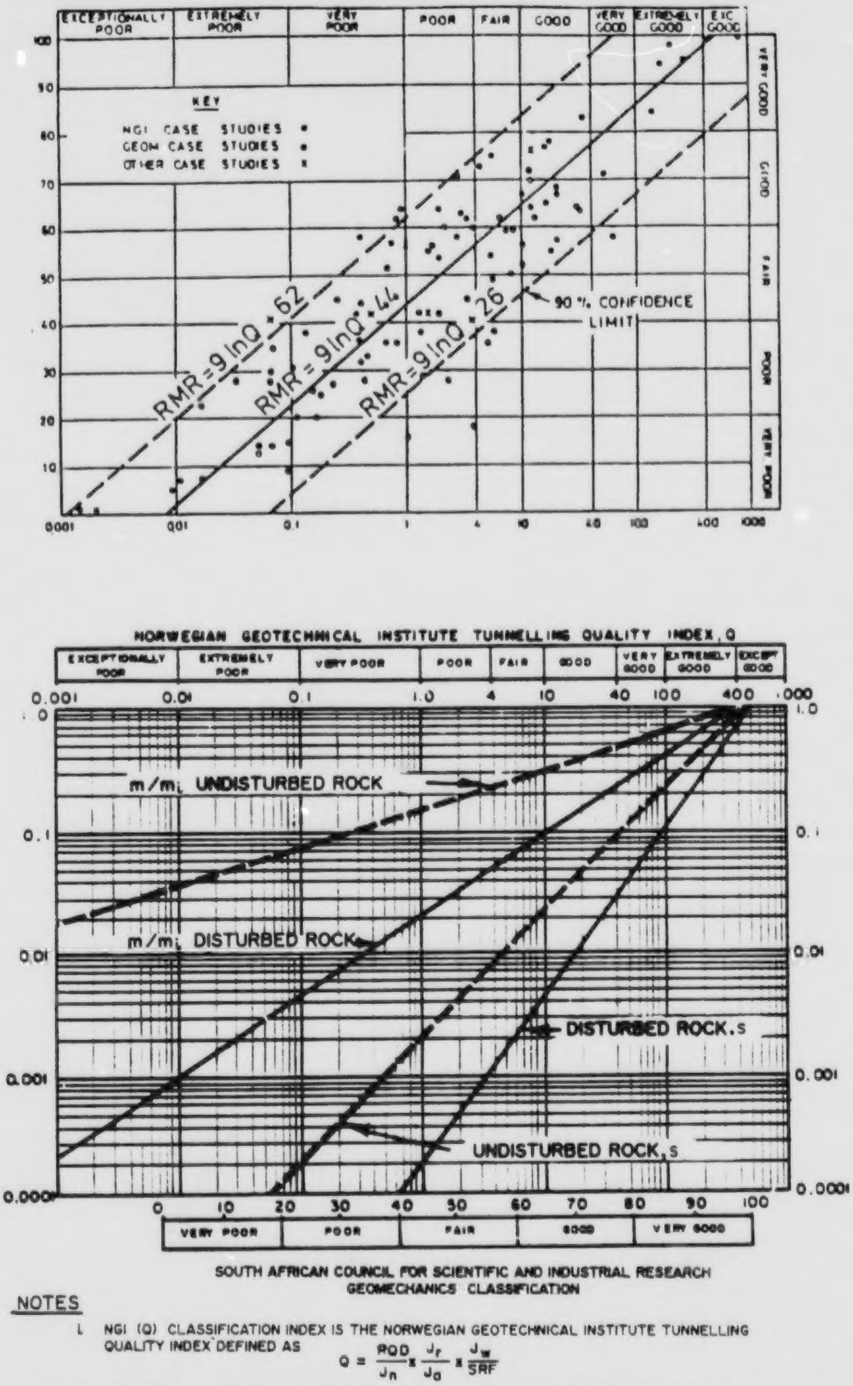

NOTES

1. NGI (Q) CLASSIFICATION INDEX IS THE NORWEGIAN GEOTECHNICAL INSTITUTE TUNNELLING QUALITY INDEX DEFINED AS

$$Q = \frac{RQD}{J_n} x \frac{J_r}{J_a} x \frac{J_w}{SRF}$$

2. CSIR (RMR) CLASSIFICATION VALUE IS THE SOUTH AFRICAN COUNCIL FOR SCIENTIFIC AND INDUSTRIAL RESEARCH GEOMECHANICS ROCK MASS RATING

3. m_i / m_i AND S GRAPH LINES DERIVED FROM HOEK AND BROWN "UNDERGROUND EXCAVATIONS IN ROCK"

4. GRAPHS ADAPTED FROM HOEK, 1983, 1988.

Date FEBRUARY 1, 1990.
Project 881-1739

Golder Associates

Drawn R.B.C.
Chkd. TGL

RELATIONSHIP BETWEEN ROCK MASS QUALITY AND INSITU MODULUS OF DEFORMATION AND RELATIONSHIPS FOR SHEAR AND BULK MODULUS

FIGURE 2.7

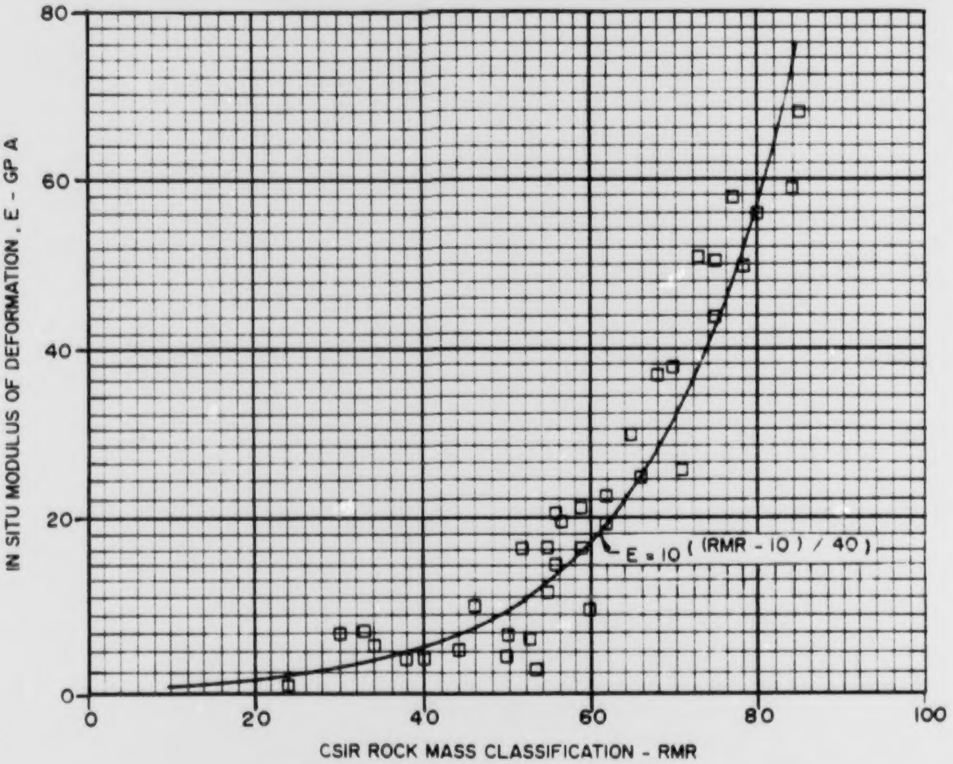

(RELATIONSHIP AFTER SERAFIM AND PERIERA, 1983.)

SHEAR AND BULK MODULUS RELATIONSHIPS

$$\text{SHEAR MODULUS, } G = \frac{E}{2(1+\nu)}$$

$$\text{BULK MODULUS, } K = \frac{E}{3(1-2\nu)}$$

Date FEBRUARY 7, 1990.
Project 881-1739-3

Golder Associates

Drawn R.B.C.
Chkd TGL

JOINT NORMAL AND SHEAR STIFFNESS (EMPIRICAL AND THEORETICAL DERIVATIONS)

FIGURE 2.8

EMPIRICAL CORRELATIONS:

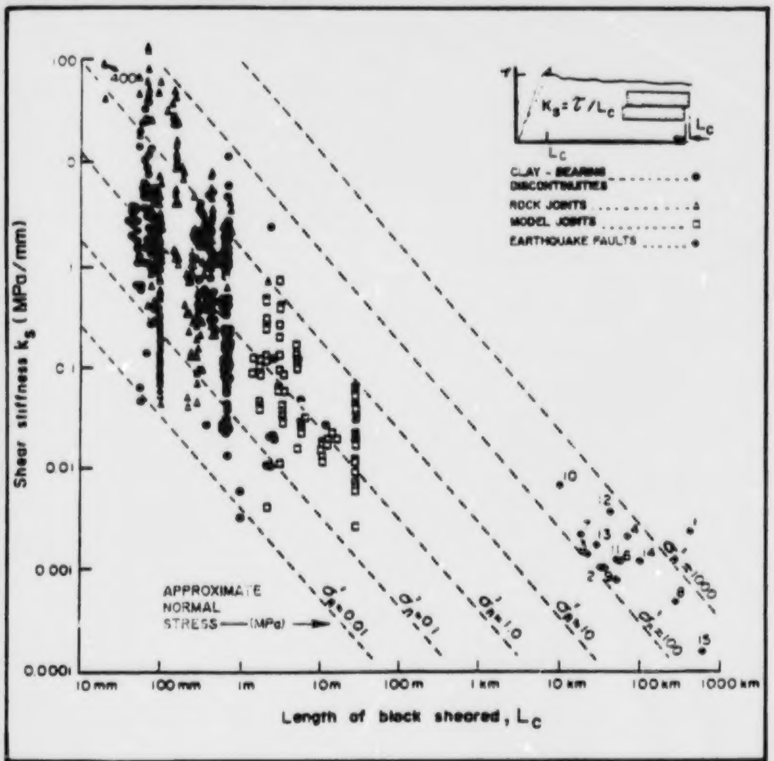

SHEAR STIFFNESS (J_{ks}) VERSUS SHEAR MOVEMENT

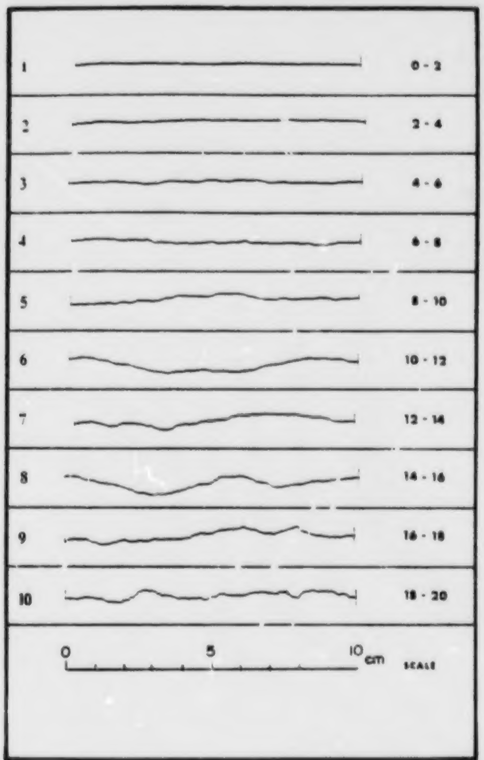

SURFACE ROUGHNESS PROFILES AND VALUES OF JOINT ROUGHNESS COEFFICIENT (JRC)

JOINT SHEAR STIFFNESS

$$J_{ks} = \frac{100}{L_c} \sigma_n' \tan \left[JRC \log_{10}\left(\frac{JCS}{\sigma_n'}\right) + \phi_r \right]$$

WHERE :
JRC = JOINT WALL ROUGHNESS
σ_n' = EFFECTIVE NORMAL STRESS
JCS = JOINT WALL COMPRESSION STRENGTH
ϕ_r = RESIDUAL FRICTION ANGLE
L_c = SHEAR DISPLACEMENT LENGTH (CROSS-JOINT SPACING)

JRC AND JCS CAN BE RELATED TO ϕ BY: $\phi = \phi_r + i$ WHERE $i = JRC \log(JCS/\sigma_n)$

THEORETICAL RELATIONSHIPS:

JOINT NORMAL STIFFNESS :

$$J_{kn} = \frac{E_{rm} \cdot E_i}{S(E_i - E_{rm})}$$

JOINT SHEAR STIFFNESS :

$$J_{ks} = \frac{G_{rm} \cdot G_i}{S(G_i - G_{rm})}$$

WHERE:
E_i AND E_{rm} = ELASTIC MODULI FOR INTACT ROCK AND ROCK MASS
G_i AND G_{rm} = SHEAR MODULI
S = CONTROLLING JOINT SPACING (EQUIVALENT TO L_c)

Date FEBRUARY 9, 1990.
Project 881-1739-3

Golder Associates

Drawn R.B.C.
Chkd. TGL

Section 3
Review of Case Records

Golder Associates

3.0 REVIEW OF CASE RECORDS

Of the 237 crown pillar cases examined, twenty four failure cases are sufficiently well documented that they provide useful insight into failure mechanisms. Several case records for marginally stable surface crown pillars that have been extensively drilled and in some instances heavily instrumented, are also examined in more detail as these provide some of the most quantifiable data on crown pillar rock mass conditions. As most of the discussion in the remainder of this report relates to failure behaviour of the rock mass, and as in many cases, the most tragic consequences of such crown failures have been overburden related, a brief generic review of overburden behaviour related to crown failure is presented as an introduction to the detailed case studies.

3.1 Overburden Considerations

The response of overburden materials in the event of a failure of the crown pillar depends on the shear strength and flow characteristics of the overburden materials and on the prevailing groundwater conditions within the overburden.

If rock crown failure occurs, an instantaneous loss of support to the base of the soils occurs which will initiate a redistribution of stresses within the soils allowing associated deformations to develop. The nature of the stress redistribution and the magnitude of the soil deformation will depend on the geometry of the opening created beneath the overburden and, typically, for conditions applicable to crown pillar failures, will result in a decrease of loading over the void and an increase in loading around the circumference of the opening. This load transfer mechanism, or arching of the soil, can well sustain the stability of the overburden above a small underground opening, for example when failure of a small section of the crown pillar occurs. However, for arching to be maintained, it requires that the strength of the overburden soils at large strains remain sufficient to sustain the arch and, to a lesser extent, that the load induced by the arching mechanism on the rock surrounding the void does not initiate progressive failure of the pillar, leading to further breakdown of the soil arch mechanism.

Soils which exhibit a tendency to flow after failure and which therefore would have a potential to infiltrate the mine workings as a consequence of a crown rock collapse, include highly sensitive clays and uniform sands in the presence of water, although, under certain conditions of rapid drainage, such sands can even develop arching due to the effects of induced negative pore pressures.

Certain clayey soils including some of the varved clays of Northern Ontario and Quebec (the Champlain Sea Clays) are very sensitive and exhibit significant strain softening during failure. In the event of a failure of a crown pillar causing loss of support to the overburden, and thereby ultimately leading to failure of any arching in the soil, these materials would lose much of their shear strength and would flow into the workings. The susceptibility of a plastic (clayey) soil to flow after failure is related to the sensitivity of the material, (S_t), which is defined as the ratio of the undisturbed to the remoulded undrained shear strength of the material. Classes of sensitivity may be defined, as per the Canadian Foundation Engineering Manual, as follows:

- low sensitivity $S_t < 10$
- medium sensitivity $10 < S_t < 40$
- high sensitivity $40 < S_t$

This problem of flow susceptibility increases with the sensitivity of the clay; clays with high sensitivity can be anticipated to present substantial problems while medium sensitive clays could also present problems in certain situations.

For granular (sandy) soils, high susceptibility to flow only occurs with loose uniform saturated fine sands and silts under the influence of large hydraulic gradients. A common characteristic of such sands, which become involved in flow slides, is uniform gradation. Given the right gradation and hydraulic conditions, loose uniform sand can flow when triggered by relatively minor stress changes. Most of the sands involved in flow slides contain less than 10 per cent fines (silt and clay sizes). They usually have a D_{50} grain size of between 0.2 and 1.0 mm, and a uniformity coefficient (D_{60}/D_{10}) of between 2 and 5.

In several of the following case records, where overburden materials subject to these types of flow behaviour exist, the failures of the rock crowns have lead to severe overburden instability problems.

3.2 Case Examples - Failure Situations

Although many surface crown pillar failures, both large and small, are well remembered in the mining industry it should be realized that failures are the exception not the rule. In fact, it is both encouraging and noteworthy that so few failures of surface crown pillars have occurred; only 30 individual pillars out of 237 cases are documented in Appendix A.

In this section of the report, the best documented failure cases, as summarized on Table 2.3 from the list given on Table 2.2, are discussed by reference to the categories shown on Figure 2.1; namely:

A - tabular, narrow vein ore zone situations,
B - complex, blocky rock mass conditions
C - foliated rock environments
D - disseminated ore zones, usually in slabby, competent rock
E - fault-controlled situations

For each of these categories, specific failure examples can be cited where sufficient data has been collected to allow evaluation of failure mechanisms. Based on these evaluations it is evident that there are some distinct differences in failure behaviour between crown pillars within rock masses of each of the various categories. In some of the narrow vein, type A situations, both where overburden cover is present and where it is absent, 80 year old unsupported crown pillars of less than 1 m. thickness still remain intact over 5 to 7 m. wide open stopes. In many cases, the stopes were mined very close to surface using hand mining methods. That many still stand today may be due to the fact that the crown and sidewalls of the stopes are competent and free from significant foliation weaknesses but it may also relate to the differences in the degree of blasting-induced damage produced by black powder versus that possible with indiscriminate use of modern gel explosives. In all of the well-documented cases of failure in such competent rock conditions, either considerable blast disturbance is evident or an adverse geometry of the surface topography is present. Most commonly, failure can be traced to the presence of particularly weak discontinuity surfaces which now delineate the collapsed area.

The characteristics of the failures that have occurred in schistose, slabby or faulted rock (Types C, D and E) are different. They tend to be chimney or progressive caving collapses on a large scale, rather than the block-controlled failure mode of crown pillars of categories A and B.

These differences are well demonstrated by review of the following case histories which illustrate some of the similarities or differences between actual failures. It should be appreciated, while reading through these case records, that in almost all cases, the failures of the crowns have occurred through unsupported ground. Seldom has a significant level of support been recorded to have been installed in any of the known collapse situations.

3.2.1 Crown Pillar Type A - Tabular Ore Zones

o Mines #11 and #36

Various minor sill and crown pillar problems have been experienced associated with mining through the "Main Break" fault in the area of Mine #36 (Figure 3.1). These failures are inferred to be related to the fact that the rock is schistose along the "Main Break", but composed of relatively competent porphyries on both sides of the fault. Several existing glory holes which exist on the property are thought to have initially developed as minor crown failures probably brought about by progressive sloughing of the sidewalls up and into the crown.

Often during mining at this property, it was found that the central ore zone section was self-caving. Unfortunately, though, very little data are available on the history of the progressive caving failures that developed, the most notable of which occurred right in front of the mine office and necessitated moving all of the surface infrastructure in the area. However comparative data is available on the characteristics of the remaining rock crowns at Mine #36 and at the adjacent Mine #11 property. Several crowns are still in place at Mine #11, and in a couple of instances, detailed mapping and drilling of these crown pillars has been undertaken (see Figures 3.2 and 3.3). It is of note that these crowns are still in place while other similarly dimensioned crowns at Mine #36, possibly in slightly less competent rock, or perhaps in a zone where clamping crown stresses were lower, have failed. The examples shown on Figures 3.2 and 3.3, together with several other cases along the same zone at Mine #42, further along strike are thus of immense value as they provide several upper bound case records of crown pillars known to be of marginal stability, and therefore eminently suitable for detailed back-analysis, as discussed in Sections 4 and 5 of this report.

o Mine #38

Failure of several remnant portions of thin crown pillars over narrow vein stopes at Mine #38 have occurred in the past few years. Although most have been associated with thin rock crown sections where wooden stull supports have given way or decayed, a few examples of failure of poorer quality ore zone material have also been documented. Failure and destabilization of adjacent cantilevered sections of the remnant rock mass generally have occurred by central key-block destabilization on sub-vertical or steeply inclined discontinuities, or by kinematic instability of abutment blocks on weak planar discontinuities bounding the hangingwall and/or footwall of the stoped zone.

The classic geometry of the narrow vein stopes at Mine #38 is illustrated on the upper diagram on Figure 3.4, while the lower drawing shows an intersection area of two stopes where a section of crown pillar collapsed. The failure in this case was bounded on the ore zone contacts on either side and by major cross joints at each end. The contacts are mainly calcite coated shear features, while the cross joints are typically planar to uneven clean surfaces, characteristic of brittle tensile fractures.

- Mine #46

A number of surface pillar caves are known to have occurred at Mine #46A, in the area of a contact zone from volcanic lavas at surface to sediments at a depth of about one hundred metres. The surface rock crown pillar of one stope, 3-5 m. in width collapsed during the mining stage, when the stope was still 20 metres below the bedrock surface. Mining in the stope was being undertaken using timber square sets to maintain the walls. The stope became filled with caved rock and overburden, and subsequently the subsidence area was back-filled to average ground level. In contrast, at the adjacent Mine #46B (Figure 3.5) one vertical open stope, which is over 3 metres wide and 90 metres long still exists with a 3 metre thick surface crown pillar (Figure 3.5). This stope crown is located within the same mixed sequence of volcanic and sedimentary rocks and in the same vein system as the series of adjacent stopes on the Mine #46A property where crown pillar collapse and surface subsidence has occurred. This pair of case records again provides an excellent example for comparative assessment purposes.

- Mine #53

Mining of the breccia ore body at Mine #53 was undertaken both from underground and by open glory hole methods. In 1943, a large remnant section of the main crown / rib pillar, separating the underground mine from an area of surface open cut workings, caved, triggering major earthflows into the open workings from the deep varved clay overburden on either side.

Although some data are available on the overall pre-failure geology and on the surface post-failure geometry in the area of the open cut and transverse pillar that collapsed (Figures 3.6 and 3.7) virtually no data are available on the geometry of the original rock pillar. Failure, however, seems most likely to have been controlled by shearing on the hangingwall side (see Figure 3.7).

- Mine #57

The classic 1963 collapse of the placed fill within the #1-2 stope at Mine #57, which caused subsidence of an entire parking area and loss of 5 school buses, took place in an area where extensive mining had previously been completed. Based on inspection of numerous photographs of the collapse, it appears that the rock mass adjacent to the collapse, initially remained in place but some minor toppling of the hangingwall developed soon after the time of failure. The surface subsidence effects, in this case, were therefore entirely controlled by movement of the sand fill within the old stope. This fill, which had probably arched previously, gave way, possible due to piping. This removed any passive support to the walls and crown of the stope, thus initiating some minor destabilization of the stope hangingwall.

Although there are some detailed records available outlining the geometry and geology of the rock mass in the vicinity of the stope, (Figure 3.8), little detailed information is available from which to establish whether the crown pillar became destabilized during original mining. The mine records, which date back to the early 1940's, suggest that some of the stoping in this area was by narrow vein shrinkage, which mostly remained unfilled. The stope where the 1963 fill collapse occurred was a glory hole that reportedly was mined through to surface after depleting the subsurface section of the vein by shrinkage. The glory hole was subsequently backfilled to approximately the existing ground surface elevation and at some later date, the workings were allowed to flood.

The plan and longitudinal section shown on Figure 3.8 shows that Stope 1-2 is open at surface and sand-filled. By contrast, adjacent stopes extend for some considerable distance along strike and for some 50 m. along the length of Stope 1-1, a relatively thin crown geometry still remains. These stopes are all steeply dipping with hangingwall and footwall rocks comprising competent basalts, although experience in the area indicates that zones of vertical schistosity are present. Drilling of the crown pillar of Stope 1-1 however, has proved relatively good quality, tuffaceous units with relatively high RQD's and compressive strengths (105 MPa). Assessed NGI-Q index values are also relatively high (ranging between 14-20) thus providing some confidence in the stability of these remnant thin crowns.

- Mine #64

Detailed diamond drilling and ultrasonic profiling of the geometry of the still standing section of the #8 stope of Mine #64 indicates that crown rock conditions, dominated by slickensided shearing on the margin of the ore-vein, controlled the two failures of the crown pillar at this site (Figure 3.9). Both failures apparently involved shear release on the ore vein on one side and cantilevering of the rock mass from joints on the other side of the stope crown. In general, the wall rocks, as exposed, are competent and, like the failure at Mine #38, these collapse situations seem to have been significantly affected by degradation and weathering of the ore margins in the very near surface region of the crown pillar.

3.2.2 Crown Pillar Type B - Blocky Rock Mass Conditions

- Mine #12

The circumstances leading up to the failure of the crown pillar at Mine #12 are complex, as is the geometry of the actual failure. Mining of the sulphide ore zone in stope block P34 was ongoing at the time failure occurred of the crown zone of block P35 (Figures 3.10 and 3.11). The extent of the failure and the effect of the failure on the remaining crown rock mass and on overburden stability appears to have been governed by pre-existing shears criss-crossing the main ore block. Actual failure geometries are well documented, (see Figure 3.10), as are details of the geological units through which the failure passed. This essentially followed break lines within and adjacent to rhyolite porphyry units that transect the rhyolitic cap rock which hosts the massive sulphide ore body.

In plan (Figure 3.11), the area of collapse/subsidence is located on the edge of several mining blocks within a blocky peridotite unit on the margin of more competent andesite. From data collected on the failure sequence, surface subsidence effects initially developed fifteen days or so after mining of Block P34. The rock mass in this block (under some 50 ft. of soft clay overburden) was described from drill core and underground data as weak, moderately blocky ground.

As only a section of the ore body had been extracted and surface subsidence could be controlled by sand fill placement into the stope voids, mining was continued using progressive sand filling of the various stopes as a control on subsidence rates. Mine production was completed without further major complication.

- Mine #29

The geometry and geology of the very complex crown pillar situation at Mine #29 has been well documented following detailed core drilling, underground surveying, geophysical investigations and review of the old mining records. Several crown pillar areas at the site may have caved, others were known to have been mined through to surface by raises from underground or by glory holes from surface. Most of the identifiable failure areas are essentially wedge and block type ravelling failures that have developed adjacent to some of the glory hole zones. One somewhat larger failure area, however, that is not close to any raise locations, occurs where one stope failed under an area of thin, relatively stoney overburden (Figure 3.12 lower right diagram).

All of these failures are of considerable interest because they are of such limited areal extent, yet the magnitude of the spans of the stopes (>30 metres) and the limited (<2 metres) thickness of the crowns at the site are remarkable, (ref. Figure 3.13). This mine-site has therefore been examined more closely by both 3-D and 2-D numerical modelling methods as described in Sections 4 and 5 of this report.

- Mine #39

The absolute dimensions of the original break-throughs that developed at this mine site are unknown. However, there currently exist two large glory holes which have been opened up both from surface and from underground. The dimensions of these glory holes appear to have been controlled by planar schistose rock units on the footwall side and by blocky gabbroic rock units on the hangingwall side.

Based on the results of an underground inspection of the property and of available records, it appears that initial failure of the crown zone at the property likely occurred by large scale rock movements in the blocky hangingwall area, with possibly some release mechanism on the footwall. In some ways, this case is analagous to other documented failure cases. However, it illustrates one of the most unfavourable types of crown pillar geometry, i.e. a blocky or slabby, competent hangingwall and ore zone and a weak or low strength schistose or slabby footwall or footwall / ore zone contact. This sort of layered structure seems very prone to allowing block fall-out of the hangingwall and ready shear failure of the footwall, due to rotational movements within the crown zone.

- Mine #54

This case record is of particular interest in that no natural collapse of the crown pillar occurred even when the stope area beneath the crown zone had been control blasted to within 2.5 metres of surface over about a 20 metres span. In a second case, at the same mine site, where a crown was designed to be only 1 metre thick over much the same span dimensions, crown failure did occur by central cracking and cantilever collapse at the abutments and shoulders of the crown arch. For the 2.5 m. thick crown though, a drop-ball had to be used to break the crown arch and induce failure.

The rock mass at this site is a massive andesite with few persistent throughgoing adversely oriented discontinuities. Natural block size within the rock mass is of the same order or larger than stope span dimensions, thus, natural failure was unlikely under most normal mining situations. This case record thus provides an upper member to cases within blocky types of rock mass, and, in conjunction with situations like Mine #29 permits rational delimitation of failure likelihood for good quality rock conditions.

o Mine #59

The crown pillar area at Mine #59 is known to have collapsed in the 1890's. Failure apparently took place by simple gravity sliding of a section of the 10 metres thick rock crown pillar over a 12 metres wide stope. The failure is thought to have occurred on slickensided sheet joints as a release surface, and probably developed either due to removal of some form of rib pillar or due to excessive development of stope strike length.

The failure, which is illustrated on Figure 3.14, extended over a hundred metres of strike length and caused the closure of one part of the mining operation. From the available published data and the old records of the mining company, the failure of the crown led to collapse of several sill and rib pillars down to a level where the geometry of the stope narrowed appreciably (see longitudinal section on Figure 3.14).

Although available geometric data make it possible to recreate the geometry of excavation to a certain point in the mine sequencing, no detailed data are available on the geology and geometry of the actual failure zone. The only currently published or available information is that presented on Figure 3.14.

3.2.3 Crown Pillar Type C - Foliated Environments

o Mine #14

Failure of a section of ground above the #1 and #3 Vein ore zones occurred in 1988, apparently by classic chimney failure following a period of quiescence after mining. The crown appears to have been destabilized first on the schistose hangingwall side, south of the main ore zones, where the initial surface failure depression occurred. Although some of the upper levels had been mined by open stoping methods, mining of most of the ground adjacent to the failure had been by sublevel caving. The stopes were subsequently used to transmit backfill, introduced on surface for filling of the deeper Avoca-style stopes. The crown areas of the stopes at the time of failure were open, and as good data are available on the geometry of the failure (Figures 3.15 and 3.16) as well as on geotechnical properties, detailed back-analysis of this situation has been possible, as discussed in Section 5.

o Mine #22

The extensive crown failure of the surface pillar at Mine #22 (Figure 3.17) is known to have broken back to the slaty greywacke of the footwall. Based on field observations and discussions with mine personnel, failure of the crown zone seems to have occurred almost monolithically, possibly initiated by sliding, developing by progressive shear on the footwall side. This then led to wedge and toppling-type destabilization of the crown and catastrophic overturning failure of the blocky hangingwall volcanics and conglomerates. Fortunately, because of subsequent planning for open pit development and for ongoing underground mining, considerable geometric and geological data are available on the area of this failure. This old failure has therefore also been analyzed in some detail in Section 5.

- Mine #25

Several surface collapses have occurred on this property as shown on Figure 3.18

Caving in the area of stopes 22-2 and 22-3 occurred initially during 1970 and gave rise to surface subsidence over the stopes. Further subsidence occurred above these stopes in the spring of 1981. Caving and associated surface subsidence related to stope 21-2 commenced shortly after mining had terminated in the stope between 1943 and 1945.

The area of these stopes is structurally complex in that the stopes lie at the junction between two extensive fault zones. To the north of the area of stoping, the country rock is schistose. To the south, the country rock is a silicified greywaoke. Considerable cross faulting, which probably contributed to the caving, also occurs in the vicinity of the two stopes.

The ore mineralization, which is almost vertical, occurs as lenticular or irregular sheet-like bodies contained within schist, diorite and silicified porphyry intrusives. Stopes have thus been developed as vertical tabular slots with strike extents of approximately 60 to 150 metres, crown spans of between 8 to 20 metres and heights of between 50 and 150 metres.

The sheared metavolcanic rocks comprising the stope crowns and hangingwall areas are frequently found to have been altered to talc chlorite schists by the proximity of major faulting. Such alteration has likely promoted the instability seen in some of the stopes, due to foliation weaknesses. The development of caving in such situations is, therefore, directly attributable to the rate of ravelling feasible in such rock. Comparison of the behaviour of adjacent, more stable, stopes in more brittle rock (e.g. in the silicified greywacke) suggests that more bulking occurs on failure in such rocks than in rock of a more plastic character (e.g. the schists of the 22-2/22-3 stope areas).

Caving in the schistose rock of the hangingwall of these stopes appears to have been progressive, slower, and more extensive than tends to occur in a more competent rock. These fundamental characteristics probably also help to explain the progressive caving between 1964 and 1968 of the schistose ground in Mine #27 located to the northwest of this site. The rate of caving of the stopes at this site, as well as at Mine #27, also appears to have been influenced by inflow of groundwater, which possibly weakened the rock mass fabric thereby generating accelerated rates of caving.

o Mine #35

The well documented catastrophic collapse of the crown pillar at Mine #35 is characteristic of the failure behaviour of stopes in weak schistose rocks. Instability is thought to have developed by progressive sloughing of the hangingwall which seems then to have led to upward caving of the stope crown through to the base of the overburden. The inrush of mud from the saturated soils and the resultant loss of life are well documented. Unfortunately, the extent of detailed documentation on rock mass properties is limited. There is, however, sufficient good data on layouts (Figure 3.19) and on rock types and overburden characteristics that some examination by back-analysis has been feasible (see Sections 4 and 5 of this report).

o Mine #50

The failure geometry at this mine site is reasonably well documented, due to the fact that mining at the site was ongoing, at least through the early 1970's (Figure 3.20).

The actual events leading up to the failure are not known in detail, however, from appraisal of available data, failure of the stope crown occurred monolithically. A sizeable depression was created which has become a lake since mining operations ceased and the workings were allowed to flood. Based on appraisal of the geometric and geological data for the site, it would appear that this failure occurred by block chimney collapse probably on discrete geological discontinuities bounding all major failure surfaces.

3.2.4 Crown Pillar Type D - Disseminated Ore Zones, with Slabby HW/FW Conditions Largely in Competent Rock

o Mine #41

Progressive slabbing and delamination of a section of the hangingwall and crown pillar of an old stoping area at Mine #41 occurred sequentially over the period between 1950, when stoping was completed, and 1975. As a result, a significant area of the near surface rock mass adjacent to the shaft headframe and adjacent buildings, began to show settlement effects.

Stoping had been completed to just above the 300 ft. level in the early 1950's, and soon after excavation, the back was noted to have caved such that the crown of the stope was approximately 5 metres above the original mining level. The stope was noted to have also partly infilled with broken rock. Caving of the stope continued naturally from the early 1950's right through to the 1970's. This caving was noticed at the 250 ft. level by October 1974 and intersected the 110 level by May 1975. The extent of the cave at this time was determined by drilling from the 110 level (Figure 3.21).

Subsequent observations indicated that the stope walls and back were progressively ravelling and that caving was developing along an apparent weak zone paralleling the footwall. Because of concerns with regard to the stability of the headframe and adjacent buildings, a backfilling programme was initiated to tight fill the stope with granular material placed through an existing escape raise and two 280 mm. diameter holes which were drilled from the surface to the crown of the cave zone. Approximately 110,000 tons of fill were placed in the upper caved portion of the stope, however, significant subsidence (in the order of 0.6 to 1 metre) still continued adjacent to the shaft headframe.

Permanent stabilization measures were therefore immediately implemented to attempt to consolidate the caving zone in the back and hangingwall of the stope. Consolidation grouting of the disturbed and broken rock mass was successfully conducted with the result that settlements were stopped and caving halted.

o Mine #52

Failure of the crown pillar at Mine #52 occurred in about 1976, at least a year after cessation of mining operations. Mining by open stoping had progressed into a serpentinized ultramafic ore zone sandwiched between hangingwall and footwall gneisses. At the time of failure the crown had been mined to within about 10 metres of the bedrock surface beneath an approximately 60 metres thick overburden cover. Most of the mining had been by tight cut and fill methods. However, the section that collapsed had been developed using experimental open stoping.

Based on information that could be pieced together after the failure, the collapse is thought to have developed as a classic chimney failure, from 300 metres depth (6th level) to surface. Unfortunately, like so many of the other known failures, little detailed geometrical or geological data are available on the actual collapse configuration for use as the basis for analytical evaluation. However, the fact that a lake some 100 metres across was created by the depression provides some indication of the scale of the failure.

o Mine #67

A major failure occurred in 1981 at Mine #67. The failure apparently developed as a chimney plug collapse some 60 metres in diameter and over 250 metres high. Based on exposures of the margins of the collapse area, the geometry of the failure was controlled by extensive slabby joint surfaces. In total, the plug dropped about 1.5 metres, completely crushing the room and pillar workings beneath the plug as shown on Figure 3.22. Failure of adjacent pillars in the mine then occurred by domino effects over a period of 3 to 6 months after the main cave-in.

3.2.5 Crown Pillar Type E - Fault Controlled Situations

o Mine #21

A detailed discussion and back-analysis of a small crown failure that occurred of a stope at Mine #21 is presented in CANMET contract report 15SQ 23440-5-9017. In consequence, a description of this failure has not been repeated here.

o Mines #27 and #28

The sizeable failure of the crown pillar at Mine #27 and the failure of several smaller areas at Mine #28 appear to have been directly related to the highly sheared, faulted and schistose nature of many parts of the ore zones at these properties. The rocks mined at these two sites were prone to slabbing and spalling even during initial mining. The stability of the stopes and crowns, therefore, was controlled only by the extent to which it was possible to limit the rock's natural propensity to undergo progressive slabbing failure and footwall and hangingwall sloughing. Typically, where this could not be controlled, it led to progressive increase in the span or height of a stope and eventually to crown pillar failure if bulking of the ravelling rock did not first completely fill the stope void.

The failure of the crown pillar at Mine #27 is recorded to have taken place initially as a small cave-zone on one side of the main porphyry dyke forming the ore zone. Several adjacent small holes then developed, and slime and water inflows were noted entering the mine workings. Within hours this situation had deteriorated and progressively the whole area some 250 metres deep and of nearly 200 metres strike length collapsed. It is not known whether the last section dropped as a chimney plug, or whether the entire area caved through to surface by ravelling.

The mining that was being carried out had been using retreat sublevel caving from drawpoints created along strike. 6 m of porphyry was being left on the footwall adjacent to the main schistose fault zone rocks, while the hangingwall contact was being developed along a porphyry / diorite contact zone. The failure eventually crossed between both of these geological weakness zones.

Similar, but somewhat smaller, cave-ins developed at Mine #28. The largest cave-in was subsequently mined as a glory hole. By research of the mine records, some data on geometries have been collected. The Mine #27 situation is illustrated on Figure 3.23 and the geometry of the caving stopes at Mine #28 are illustrated on Figure 3.24.

From the available data, these stopes all lie on and are parallel with the main fault zone that transects both mine sites. The country rock on either side of the mineralized fault zone area is comprised of massive to schistose peridotite. In the proximity of the fault zone, the peridotite has been altered to chlorite schist. Breccias re-cemented with quartz-carbonate, and gouge-filled fissures occur within this zone of deformation and these thus provide release mechanisms for caving development.

o Mine #62

Dewatering of old mine workings in the vicinity of a major fault zone at Mine #62 initiated the failure of a section of the rock crown pillar. This rock crown collapse promoted development of flow failures of the sensitive glacial lake silts and clays overlying the crown pillar (Figure 3.25). The data collected from drilling of the crown and hangingwall area indicated that hangingwall caving of the stope possibly developed due to water pressure effects creating buckling delamination of the schistose hangingwall rocks during dewatering. This was a particular concern also for the dewatering programme carried out at Mine #45 which, in places, exhibits similarly schistose hangingwall conditions. This is discussed further in the following section. The comparison, however provides useful indications on the vulnerability of schistose crowns to pore-pressure induced delamination type failures.

3.3 Case Examples - Non-failed Situations

For the vast majority of the mines listed on Table 2.2 and, in many cases, even where crown pillar geometries are known to be thin, no failure has developed. As some pillars have failed alongside others which have remained in place in much the same rock conditions, several good sets of comparative cases are available for analysis, (see Sections 4 and 5 of this report).

Specific pillars, because of concern with regard to their stability, have been extensively drilled. Some contain comprehensive arrays of installed instrumentation: eg. Mine #45 - see Figures 3.26 and 3.27, Mine #29 - see Figures 3.12 and 3.13; and a whole group of other sites where crown pillars occur under buildings (Figure 3.28), under highways (Figure 3.4) or in other critical locations. The fact that few of these instrumented pillars show any significant movement, even under severe stress changes (such as are imposed by dewatering old workings in schistose ground), suggests that given the right conditions, it is possible to mine very close to surface and yet still retain a stable pillar geometry.

Situations, such as that at Mine #11, where the crown pillar over an extensively stoped area of deep workings was removed by underhand mining methods using concrete fill to stabilize the overcuts, indicate that even in very blocky, heavily fractured ground with RQD values usually less than 20% (see detailed crown section shown on Figure 3.3), stability of the crown could still be maintained. For such situations, clamping stress from the abutments through the crown must play a significant role.

For most of the other crown geometries documented in Appendix A, it has been impossible to assess the current factor of safety. This is because conditions are non-critical, possibly because of a modicum of installed support, or because stopes have been filled as they were excavated.

A slightly different situation exists for some marginally stable stopes at Mine #18, adjacent to areas where collapses are known to have occurred. All the stopes at this mine site are typical of marginally controllable caving ground conditions. In almost all cases, ravelling and rat-hole caving is the classic failure mode with caving of the crowns slowly progressing upwards through weak shear-zones, complemented by block release controlled by dipping discontinuities. In the particular situation illustrated on Figure 3.28, introduction of significant quantities of surface water into the stope crown area had compromised the stability of the crown shear zone, thereby leading to some hangingwall spalling but not to complete crown failure. Although overall crown pillar stability of this stope and some of the other stopes that remain at the site, are likely marginal, no actual breakthroughs occurred. This contrast to other stopes at the property, which failed through to surface aids immensely in defining the extent to which mining is feasible without surface disruption. This is not to say that the type of geometry illustrated on Figure 3.28 should be deliberately developed in a new crown pillar, only that such examples provide excellent back-analysis case records.

NORTH-SOUTH CROSS-SECTIONS OF MAIN AND SOUTH BREAKS MINE #36 AND MINE #11

FIGURE 3.1

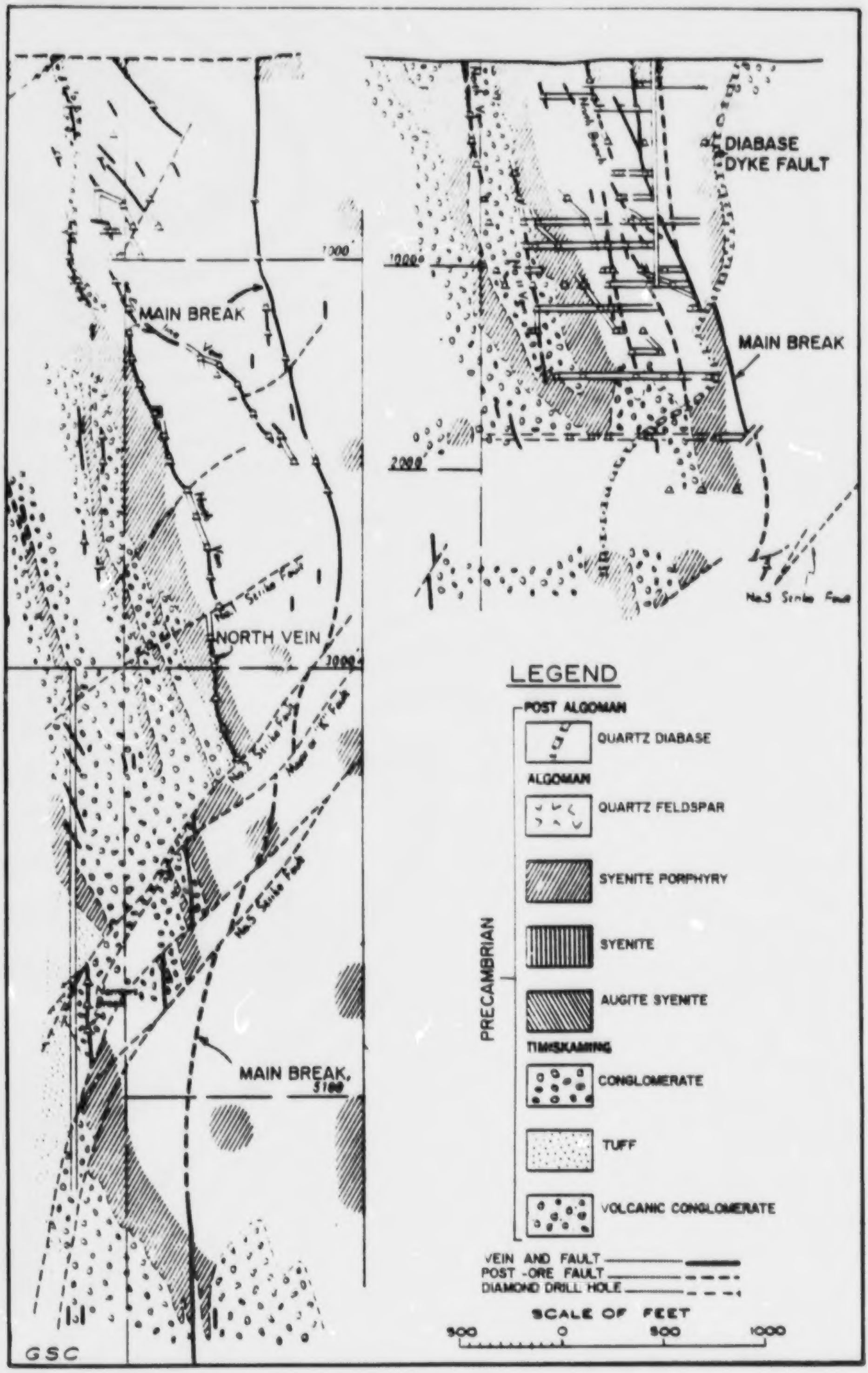

Date FEBRUARY 2, 1990.

Project 881-1739-3

Golder Associates

Drawn R.B.C.

Chkd.

DETAILED SECTIONS OF NEAR SURFACE STOPE (MINE #11)

FIGURE 3.2

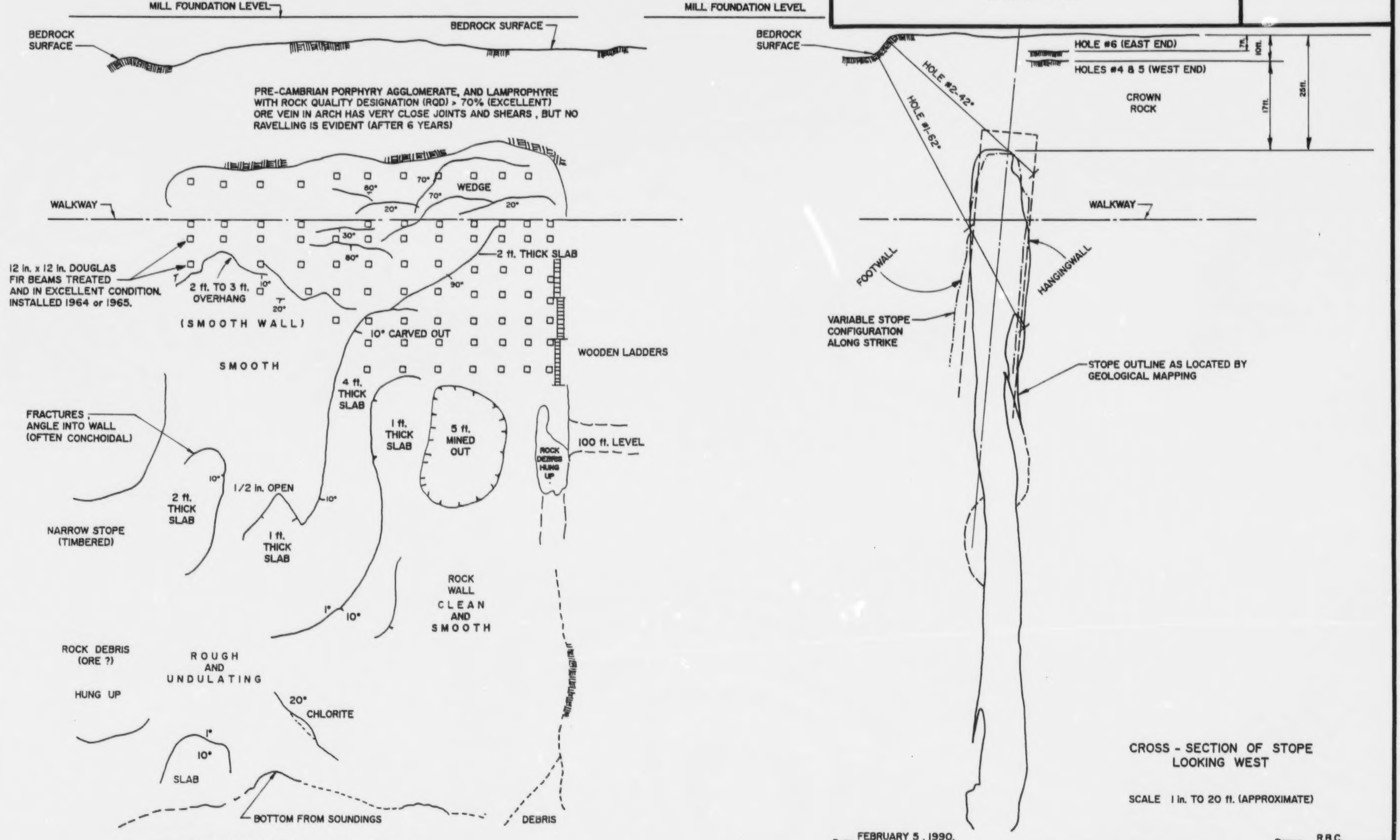

LONGITUDINAL SECTION OF NORTH WALL

CROSS - SECTION OF STOPE
LOOKING WEST

SCALE 1 in. TO 20 ft. (APPROXIMATE)

Date FEBRUARY 5, 1990.
Project 881-1739-3

Golder Associates

Drawn R.B.C.
Chkd

GEOMETRICAL DETAILS OF CROWN PILLAR CONFIGURATION ADJACENT TO CAVE-IN AREA (MINE #38)

FIGURE 3.4

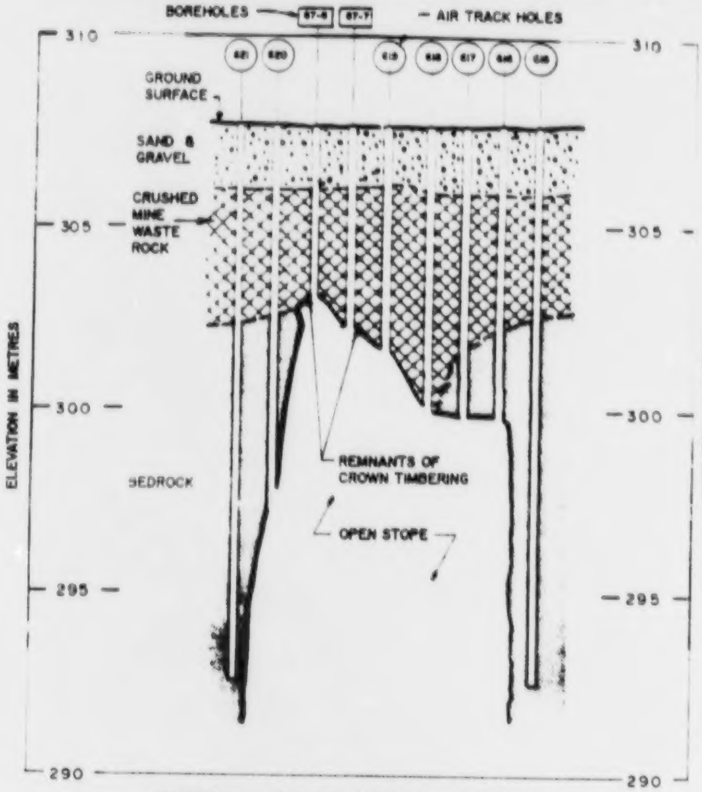

TYPICAL STOPE CROSS-SECTION

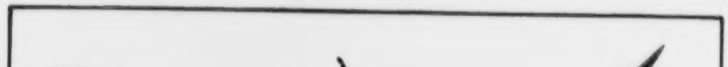
CROWN FRACTURED AND BROKEN BENEATH : SOME 1 - 2 mm OPEN CRACKS
80°
70°
75°
STOPE SIDEWALL UNDERCUTS LEDGE AT 85°
BROKEN AND SHATTERED BENEATH
OVERHANGING
BASELINE
- 0+25
- 0+20
0+10
ROCK BOLTS 35 mm LONG AT 45°
ORIGINAL VOIDS THROUGH CROWN PILLAR
0
5
10
15 metres

DETAILED PLAN OF CAVE-IN ZONE

Date FEBRUARY 2, 1990.

Project 881-1739-3

Golder Associates

Drawn R.B.C.

Chkd. TGL

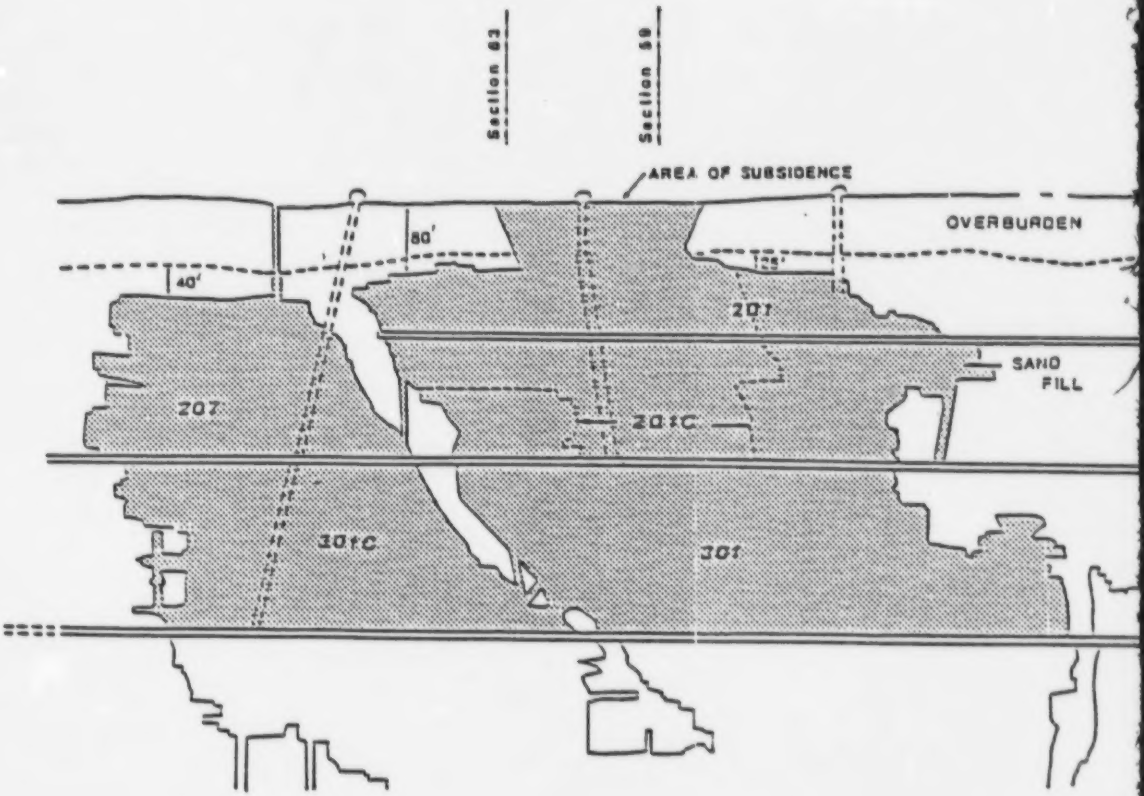
Section 63
Section 59
AREA OF SUBSIDENCE
OVERBURDEN
SAND FILL

MINE #46A

CONTRAST IN STOPE GEOMETRY BETWEEN FAILURE AREA
AT MINE #46A AND STABLE AREA
AT MINE #46B IN THE SAME ROCK CONDITIONS

FIGURE 3.5

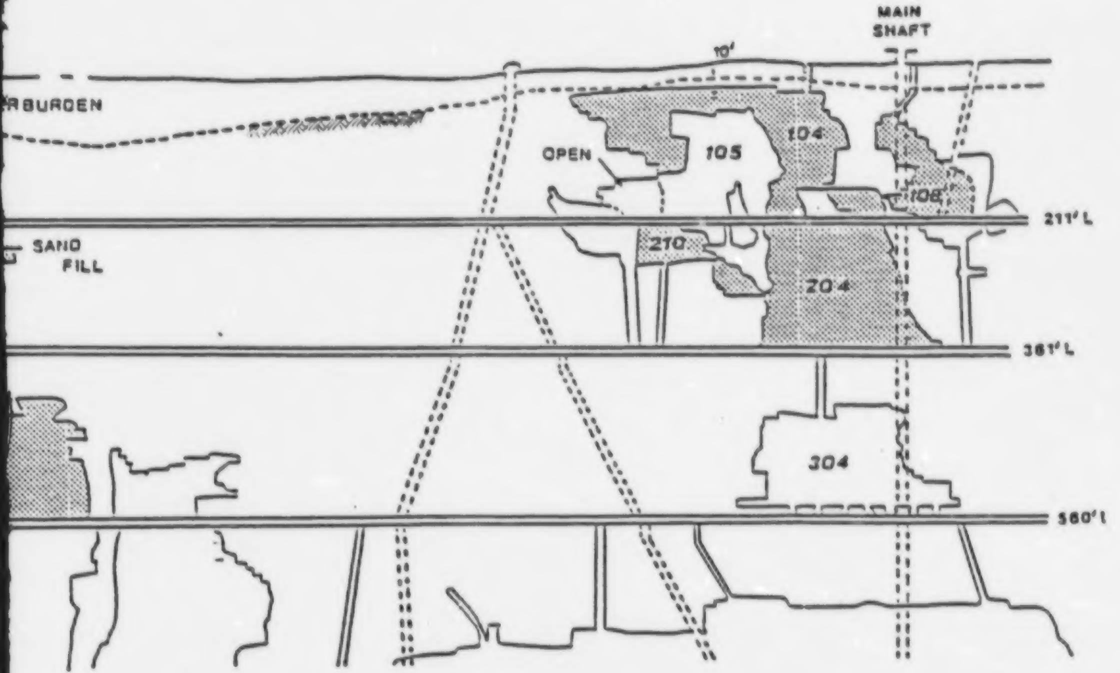

MINE #46B

LEGEND

▨ BACKFILLED STOPES

Date FEBRUARY 12, 1990.
Project 881-1739-3

Golder Associates

Drawn R.B.C.
Chkd Tu

GENERALIZED GEOLOGICAL CROSS-SECTION OF MINE # 53

FIGURE 3.6

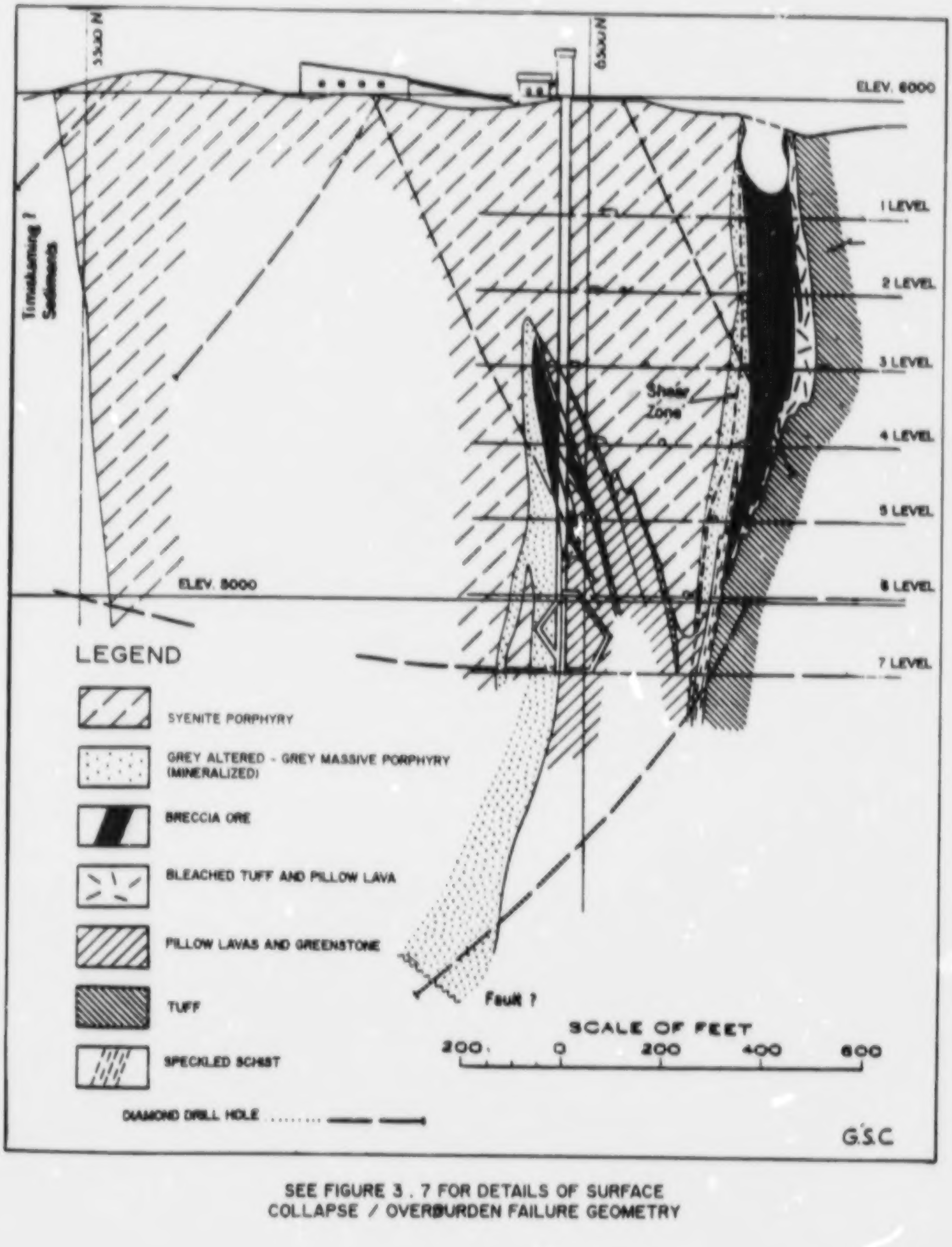

SEE FIGURE 3.7 FOR DETAILS OF SURFACE COLLAPSE / OVERBURDEN FAILURE GEOMETRY

Date FEBRUARY 2, 1990.

Project 881-1739-3

Golder Associates

Drawn R.B.C.

Chkd. TGL

PLAN AND SECTIONS OF MINE #53 SHOWING LOCATION OF OPEN STOPE AND SLIDES

FIGURE 3.7

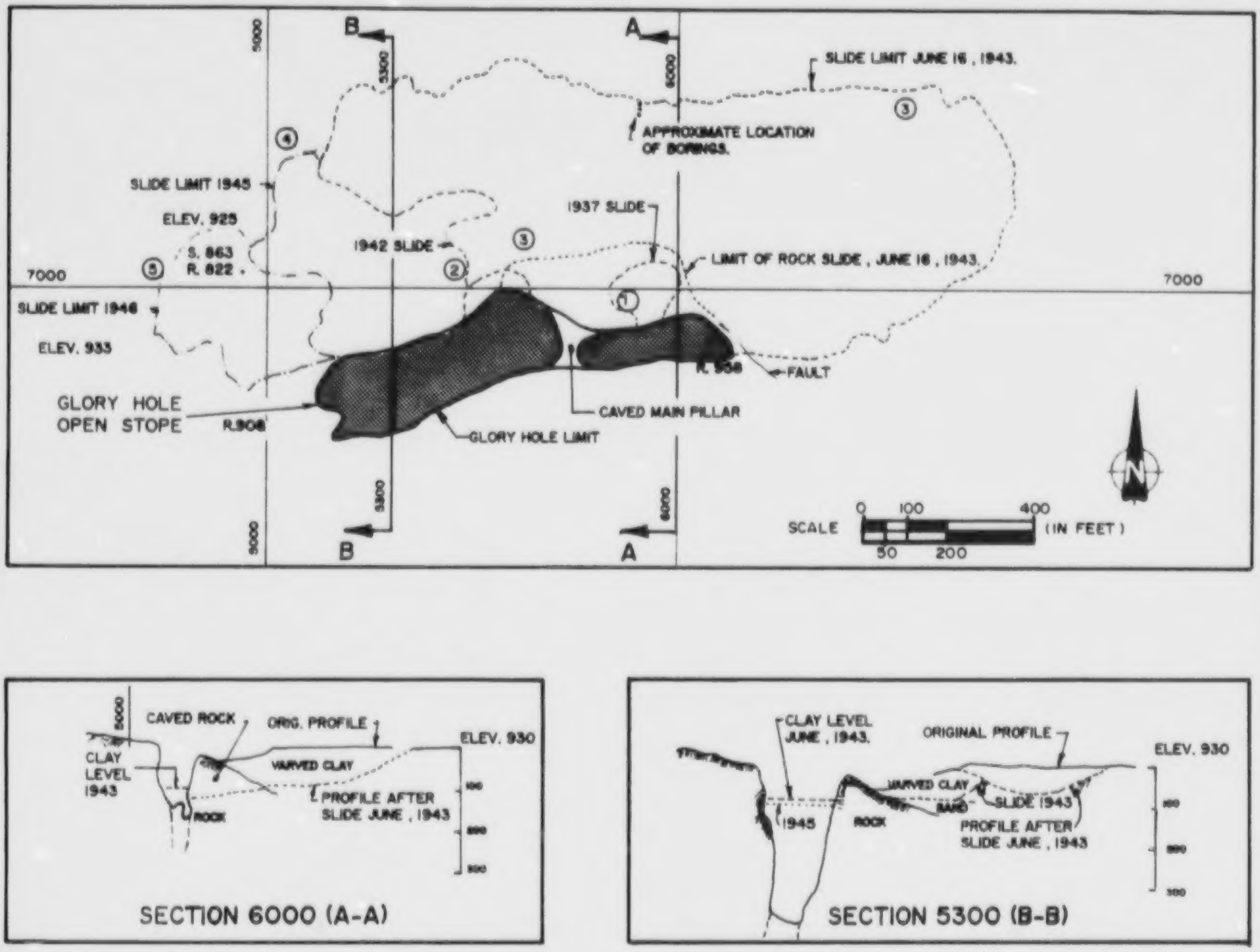

SECTION 6000 (A-A)

SECTION 5300 (B-B)

① 1937 ⎫ LOCAL SLIDES IN OVERBURDEN
② 1942 ⎭

③ JUNE 16, 1943 - CROWN RIB PILLAR FAILURE ROCK SLIDE TRIGGERS VARVED CLAY SLIDE

④ 1945 CLAY SLIDE

⑤ 1946 CLAY SLIDE

SEE FIGURE 3.6 FOR FULL DEPTH SECTION SHOWING MINE GEOLOGY

Date FEBRUARY 2, 1990.
Project 881-1739-3

Golder Associates

Drawn R.B.C.
Chkd. TGC

GEOMETRICAL DETAILS OF STOPES AT MINE #57

FIGURE 3.8

DIAGRAM MODIFIED FROM HUNT ET AL , 1989.

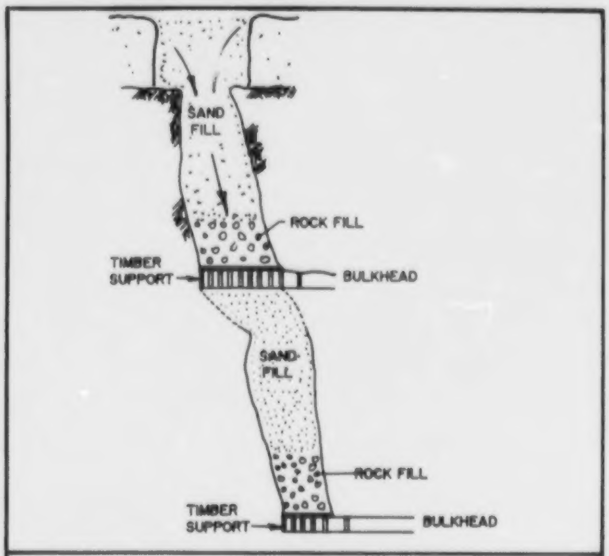

TYPICAL CROSS-SECTION , A - A THROUGH 1-2 STOPE

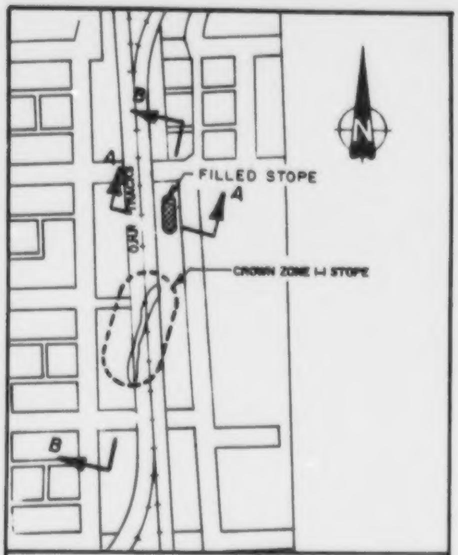

KEY PLAN
(NOT TO SCALE)

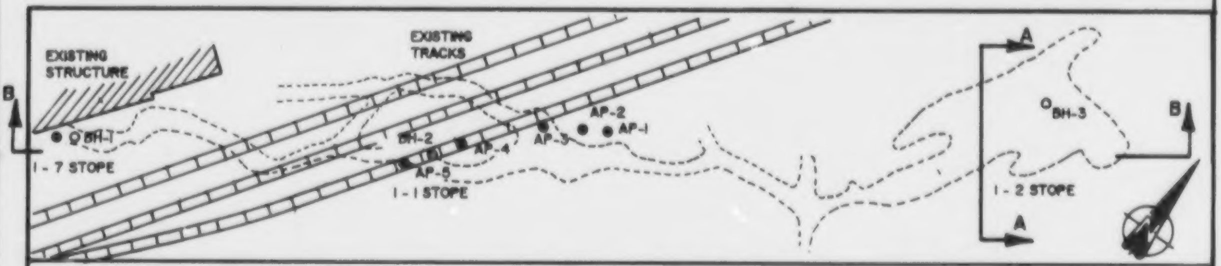

PLAN VIEW - 150ft. LEVEL
(NOT TO SCALE)

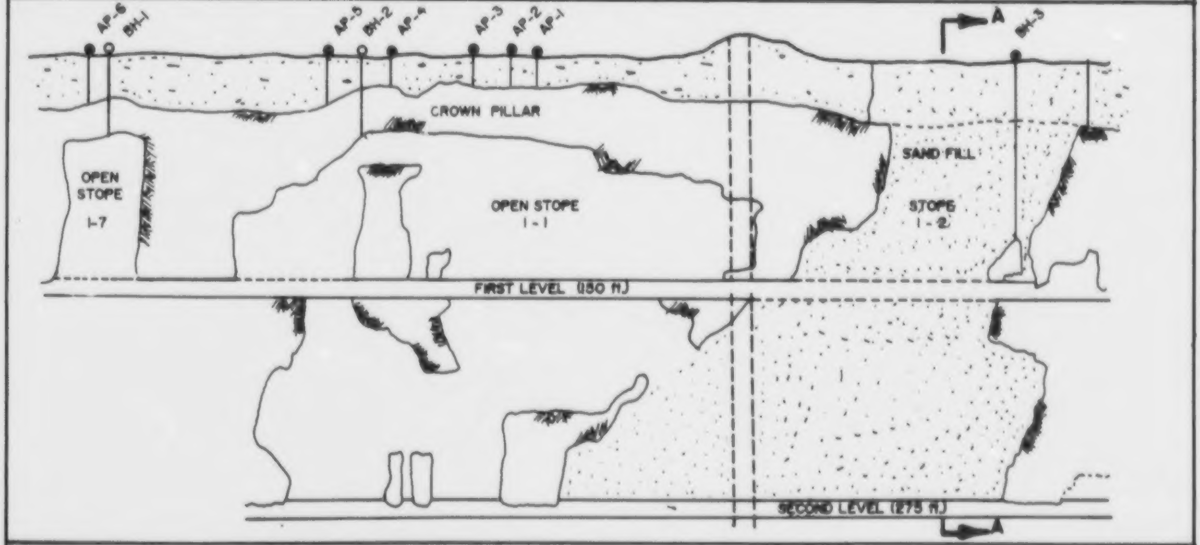

LONGITUDINAL SECTION B-B

Date FEBRUARY 6 , 1990

Project 881-1739-3

Golder Associates

Drawn R.B.C

Chkd. TGC

LOGITUDINAL SECTION SHOWING
CROWN PILLAR COLLAPSE AND
REMEDIAL CAPPING AT MINE #64

FIGURE 3.9

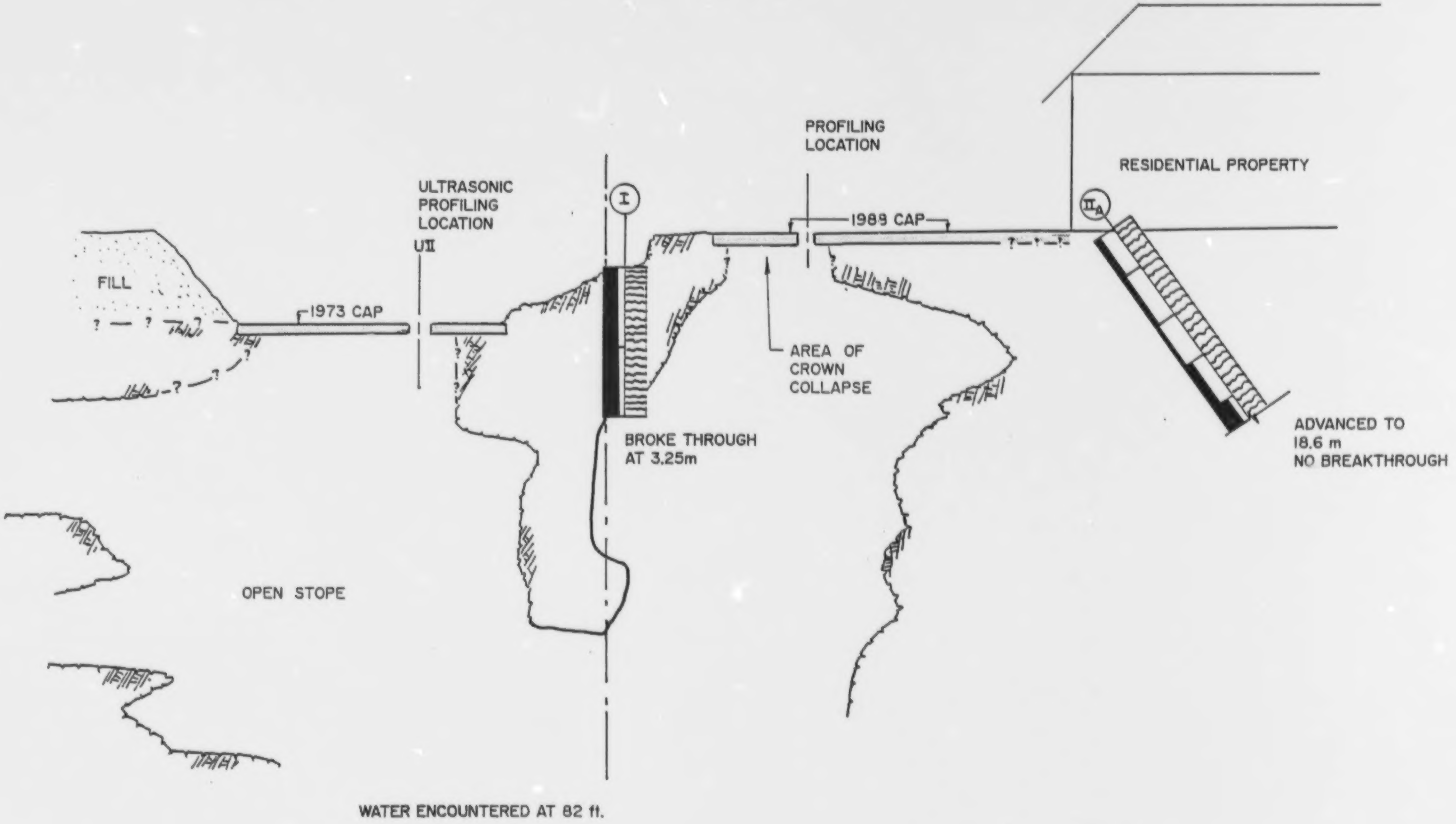

SCALE: 1" = 10'

Date FEB. 9, 1990
Project 881-1739-3

Golder Associates

Drawn D.J.R
Chkd TGL

CROSS-SECTION OF CROWN PILLAR COLLAPSE ZONE
(MINE #12)

FIGURE 3.10

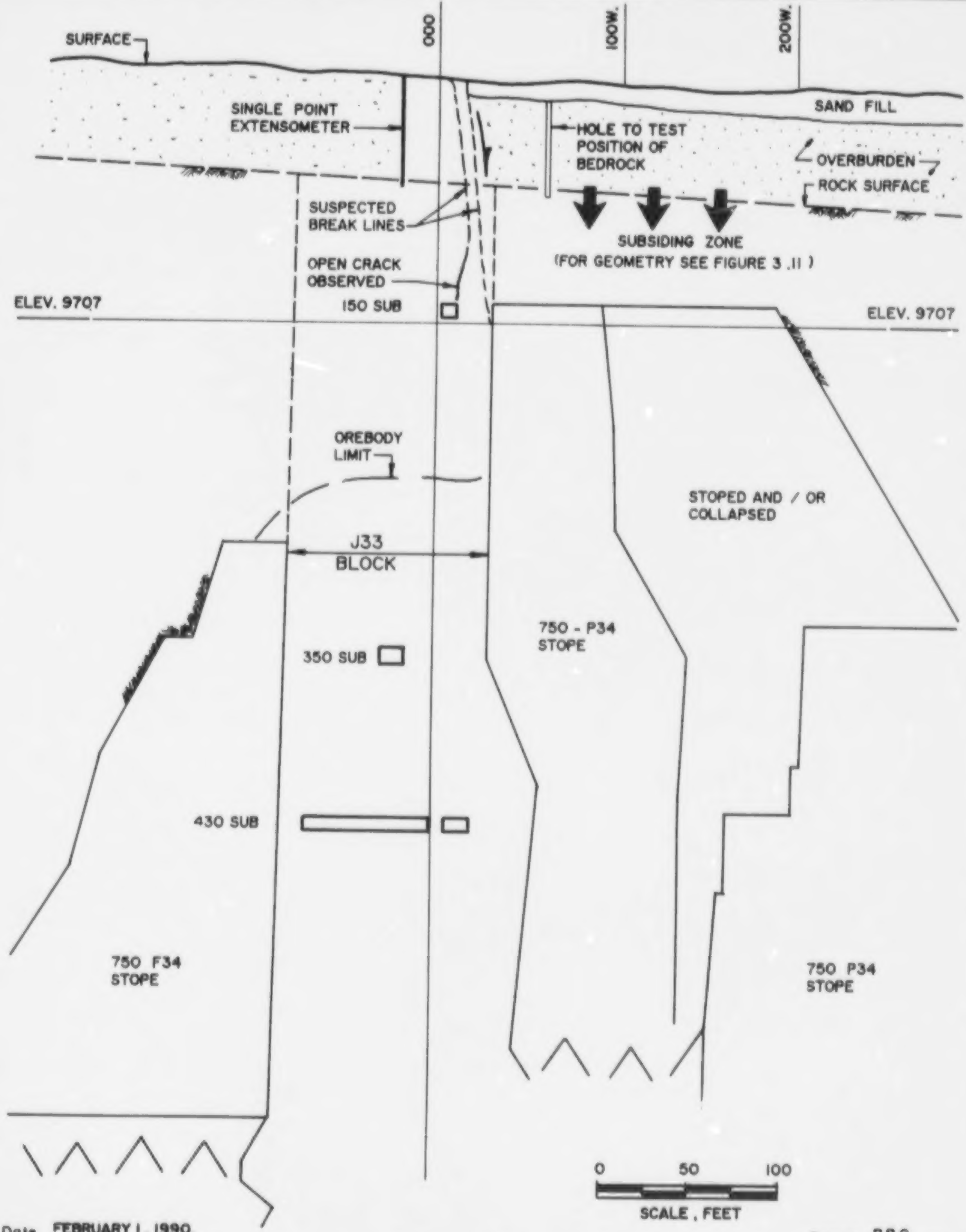

Date FEBRUARY 1, 1990.
Project 881-1739-3

Golder Associates

Drawn R.B.C.
Chkd. TGr

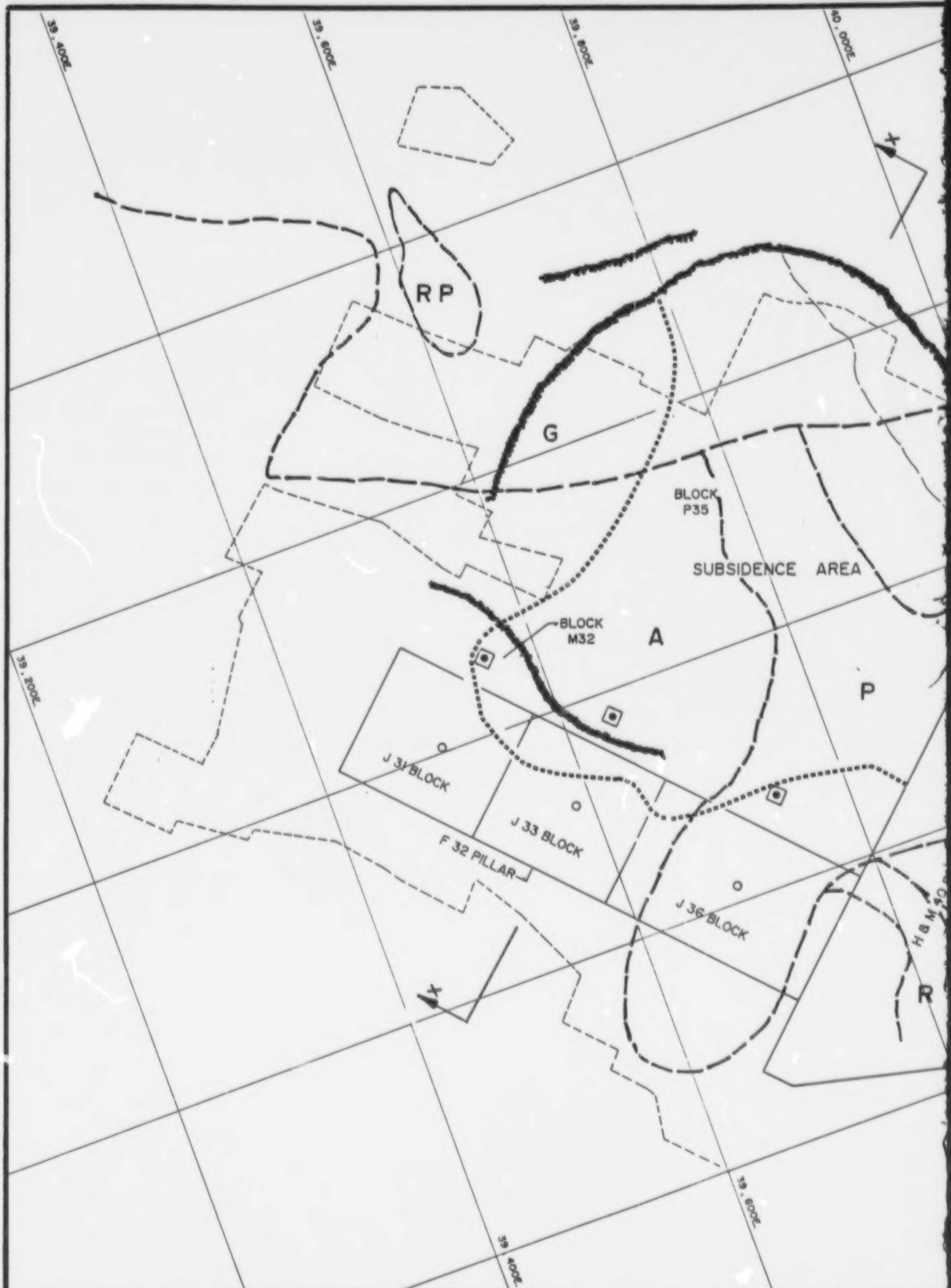
39,400E
39,600E
39,800E
40,000E
X
RP
G
BLOCK
P35
SUBSIDENCE AREA
39,200E
BLOCK
M32
A
P
J 31 BLOCK
J 33 BLOCK
F 32 PILLAR
J 36 BLOCK
H&M
R
X
39,600E
39,400E

SURFACE AND COMPOSITE PLAN OF CROWN PILLAR FAILURE AREA (MINE #12)

FIGURE 3.11

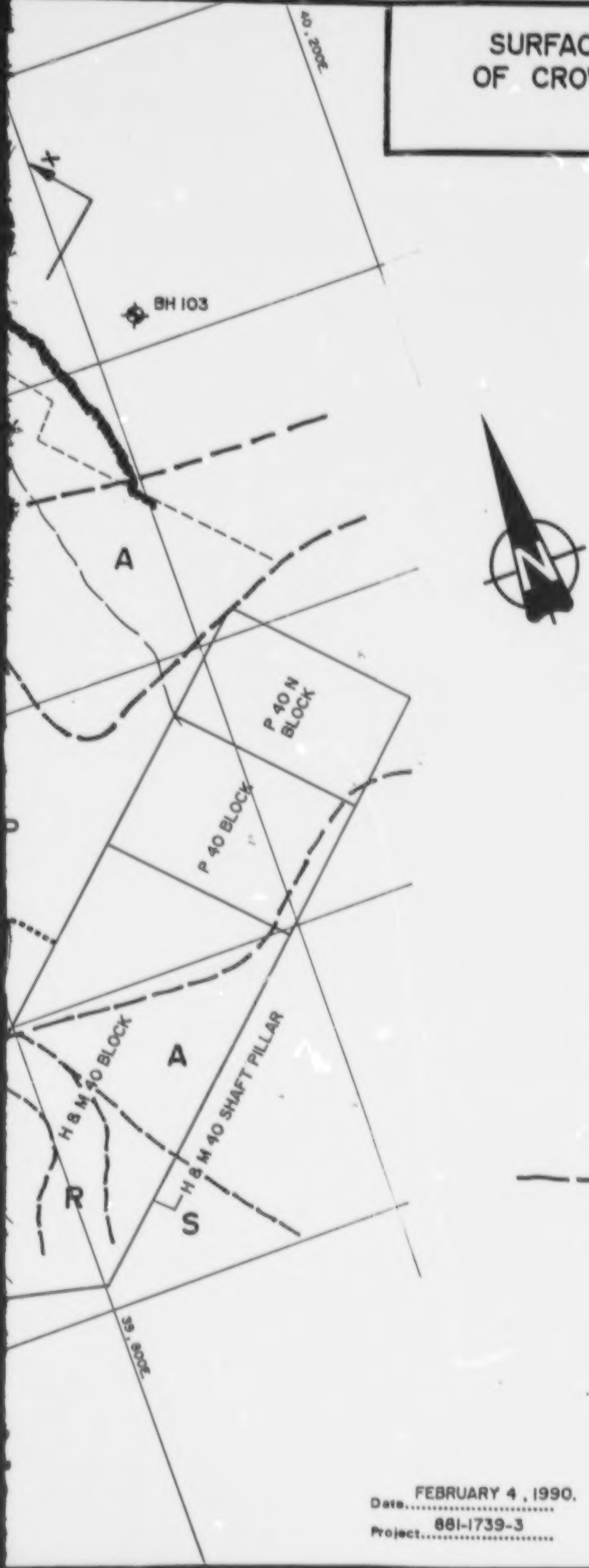

LEGEND

- ········ VISIBLE BOUNDARY OF SUBSIDENCE AREA
- ▬▬ CRACKS
- ▣ POSITION OF BEDROCK PROBE HOLES
- ○ POSITION OF SINGLE POINT EXTENSOMETERS
- ------ APPROXIMATE OUTLINE OF COMPLETED STOPES
- ⊕ BH 103 BOREHOLE

S	MASSIVE SULPHIDES
R	RHYOLITE
A	ANDESITE
G	GABBRO
RP	RHYOLITE PORPHRY
P	PERIDOTITE

— — — GEOLOGICAL BOUNDARIES

FOR SECTION X - X, SEE FIGURE 3.10

SCALE 1" = 100'

Date FEBRUARY 4, 1990.
Project 881-1739-3

Golder Associates

Drawn R.B.C.
Chkd TW

GENERALIZED GEOLOGICAL CROSS-SECTION AND DETAILED SECTIONS OF TYPICAL CAVE-IN ZONES (MINE #29)

FIGURE 3.12

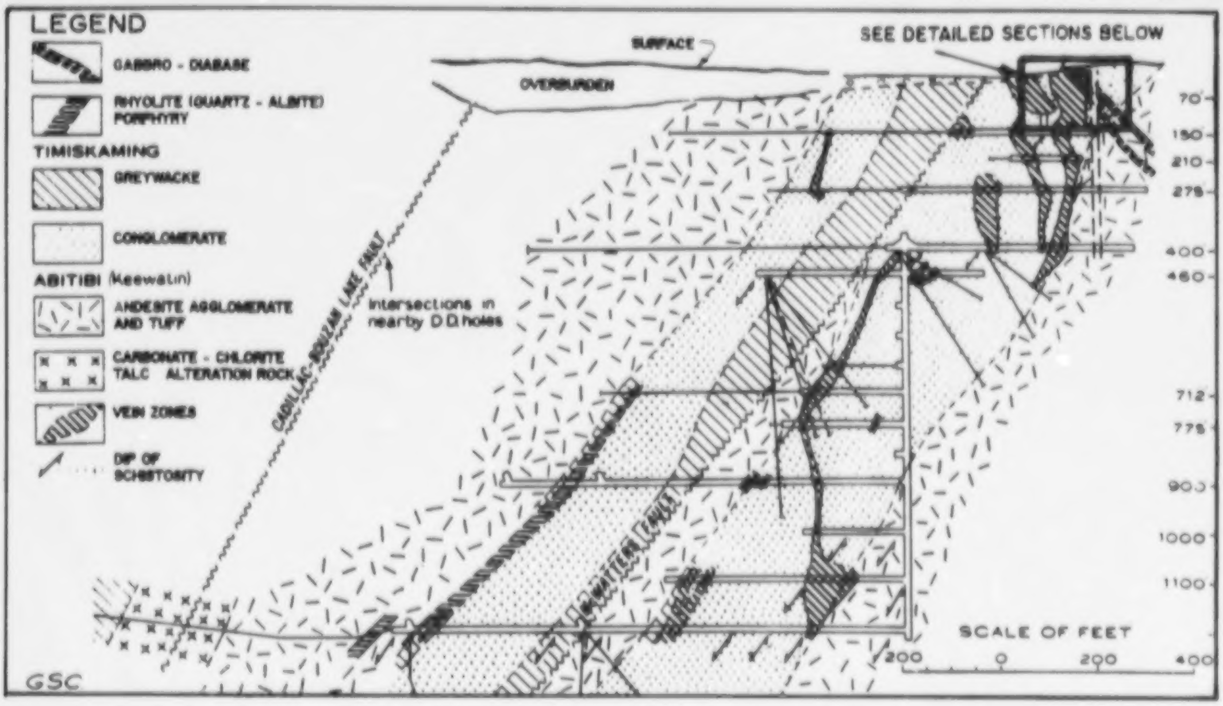
LEGEND
GABBRO - DIABASE
RHYOLITE (QUARTZ - ALBITE) PORPHYRY
TIMISKAMING
GREYWACKE
CONGLOMERATE
ABITIBI (Keewatin)
ANDESITE AGGLOMERATE AND TUFF
CARBONATE - CHLORITE TALC ALTERATION ROCK
VEIN ZONES
DIP OF SCHISTOSITY
SURFACE
OVERBURDEN
SEE DETAILED SECTIONS BELOW
CADILLAC - BOUZAN LAKE FAULT
Intersections in nearby D.D. holes
70
150
210
275
400
460
712
775
900
1000
1100
SCALE OF FEET
200
0
200
400
GSC

LONGITUDINAL SECTION

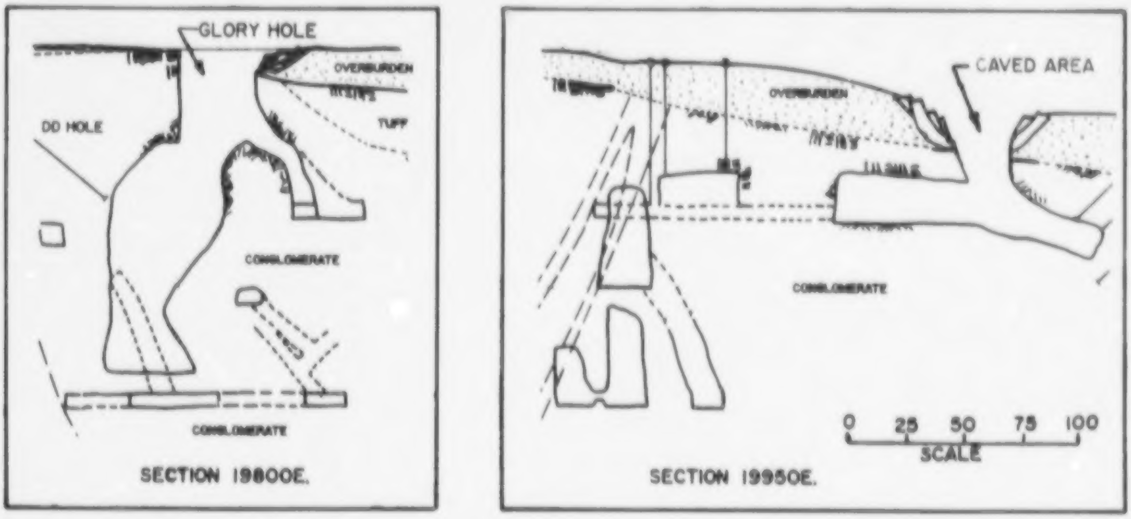

SECTION 19800E.

SECTION 19950E.

TYPICAL CAVE ZONE CONFIGURATIONS

Date JANUARY 31, 1990.
Project 881-1739

Golder Associates

Drawn R.B.C.
Chkd. TGr

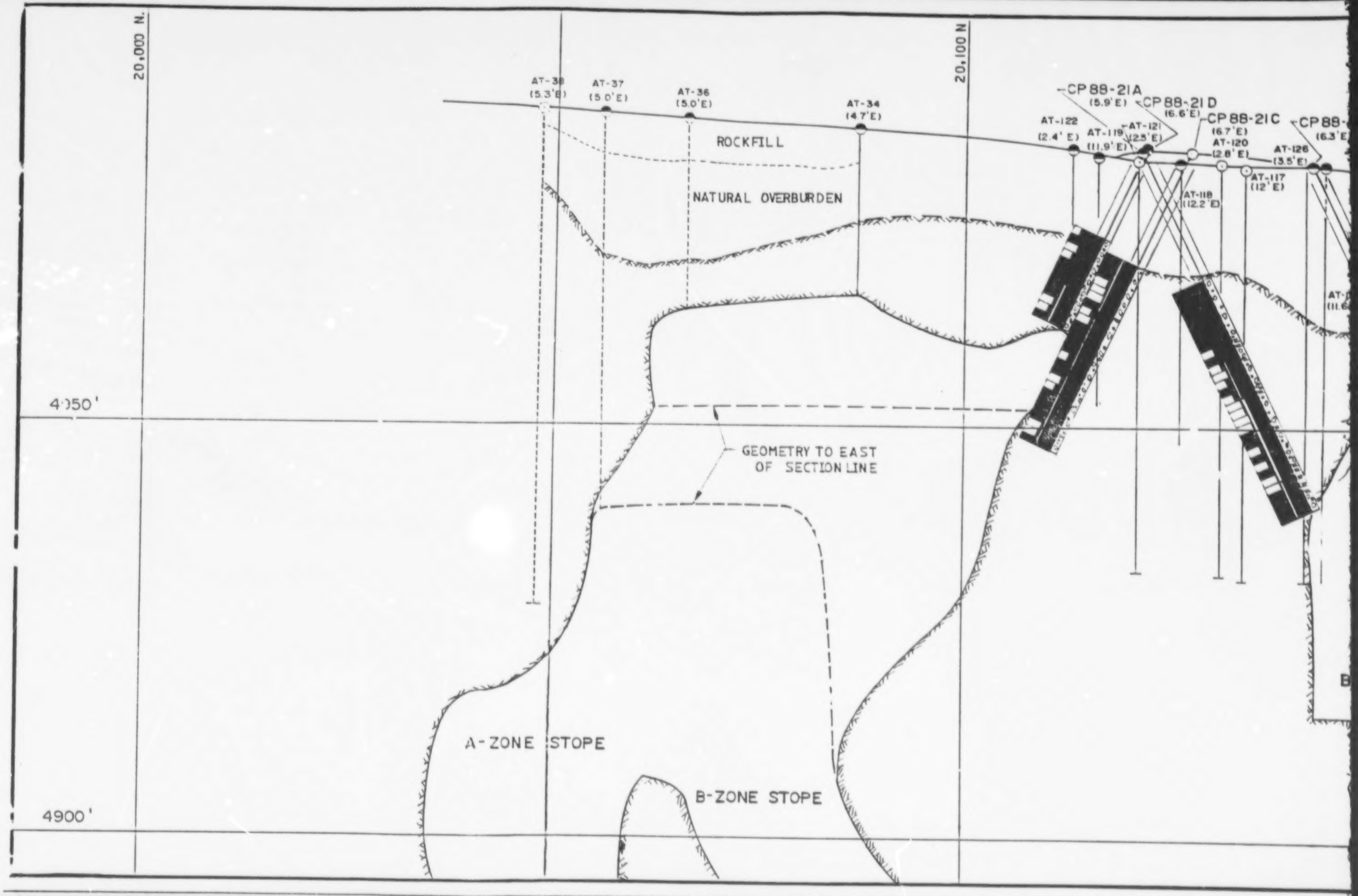
20,000 N.
20,100 N
AT-38
(5.3'E)
AT-37
(5.0'E)
AT-36
(5.0'E)
AT-34
(4.7'E)
CP 88-21A
(5.9'E)
CP 88-21D
(6.6'E)
CP 88-21C
(6.7'E)
CP 88-
(6.3'E)
AT-122
(2.4' E)
AT-119
(11.9'E)
AT-121
(2.5'E)
AT-120
(2.8'E)
AT-126
(3.5'E)
AT-117
(12'E)
AT-118
(12.2'E)
ROCKFILL
NATURAL OVERBURDEN
4950'
GEOMETRY TO EAST OF SECTION LINE
A-ZONE STOPE
B-ZONE STOPE
4900'

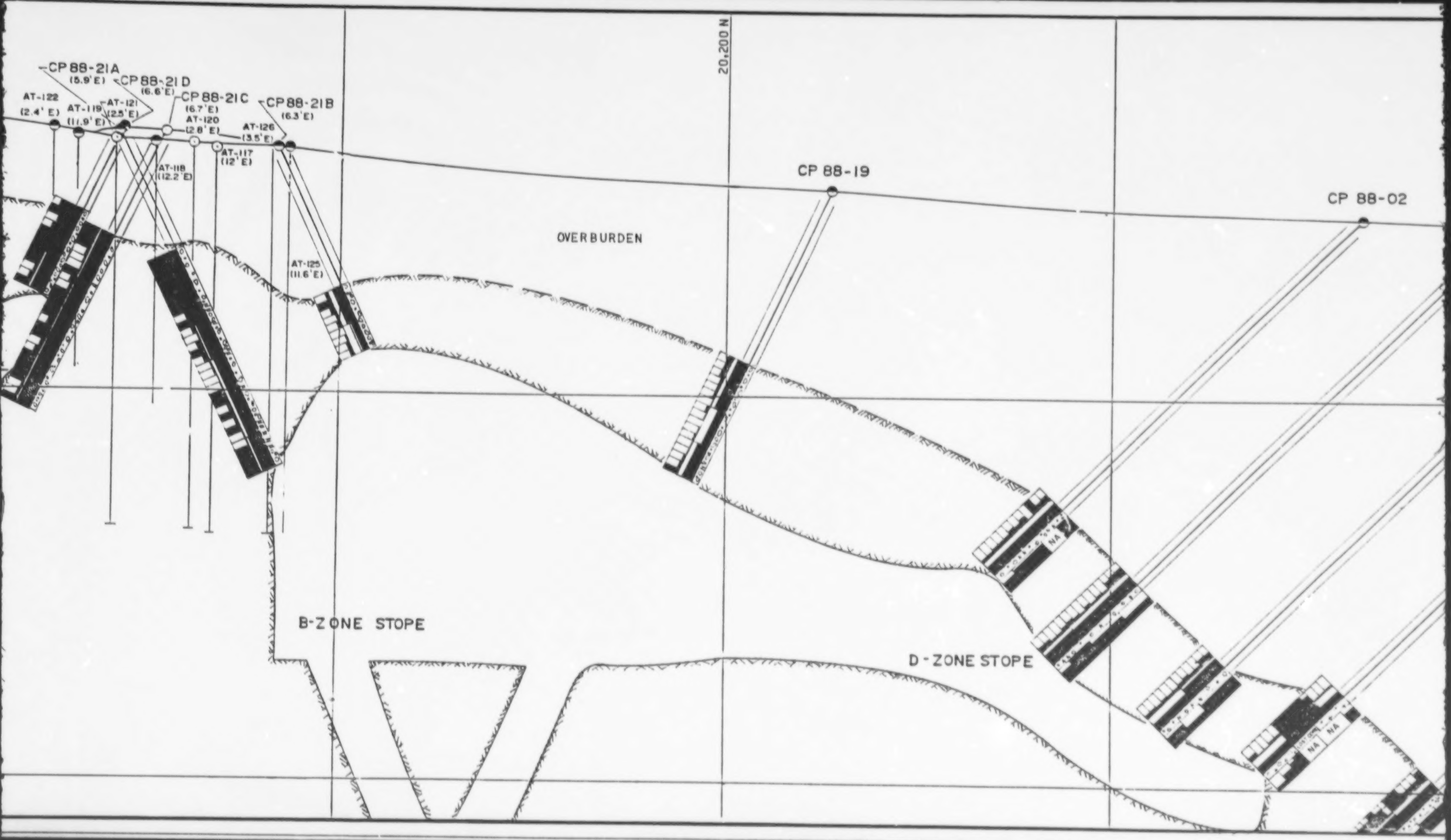
CP 88-21A
(5.9'E)
CP 88-21D
(6.6'E)
CP 88-21C
(6.7'E)
CP 88-21B
(6.3'E)
AT-122
(2.4' E)
AT-119
(11.9'E)
AT-121
(2.5'E)
AT-120
(2.8'E)
AT-126
(3.5'E)
AT-117
(12'E)
AT-118
(12.2'E)
AT-125
(11.6'E)
20,200 N
CP 88-19
CP 88-02
OVERBURDEN
B-ZONE STOPE
D-ZONE STOPE
NA
NA
NA

DETAILED GEOTECHNI
AT 20 025
SHOWING CROWN PILLAR GE

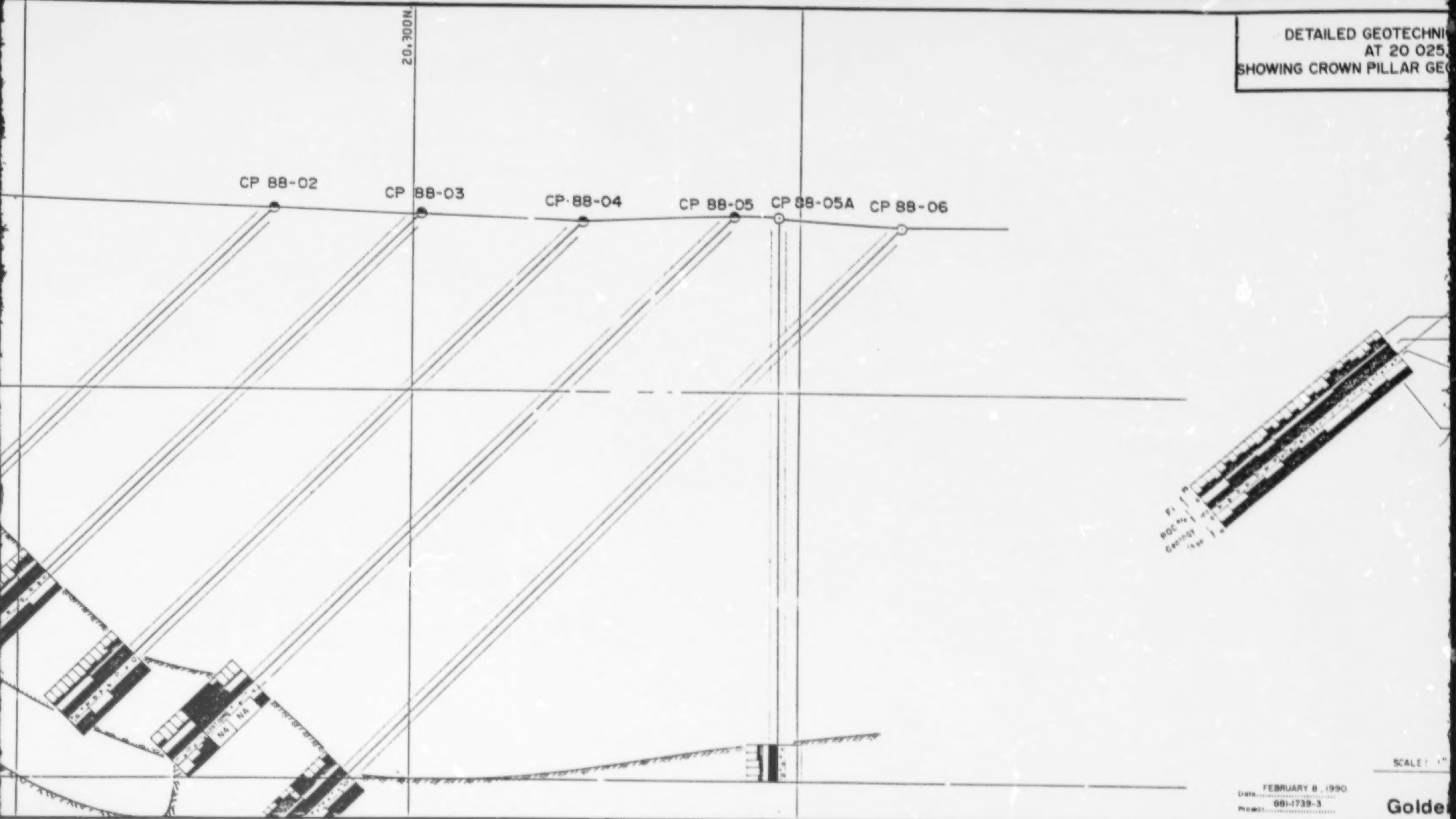

Date FEBRUARY 8, 1990

Project 881-1739-3

Golde

DETAILED GEOTECHNICAL SECTION AT 20 025 E. SHOWING CROWN PILLAR GEOMETRY (MINE #29)

FIGURE 3.13

LEGEND

TYPICAL DOWNHOLE
COMPOSITE LOG

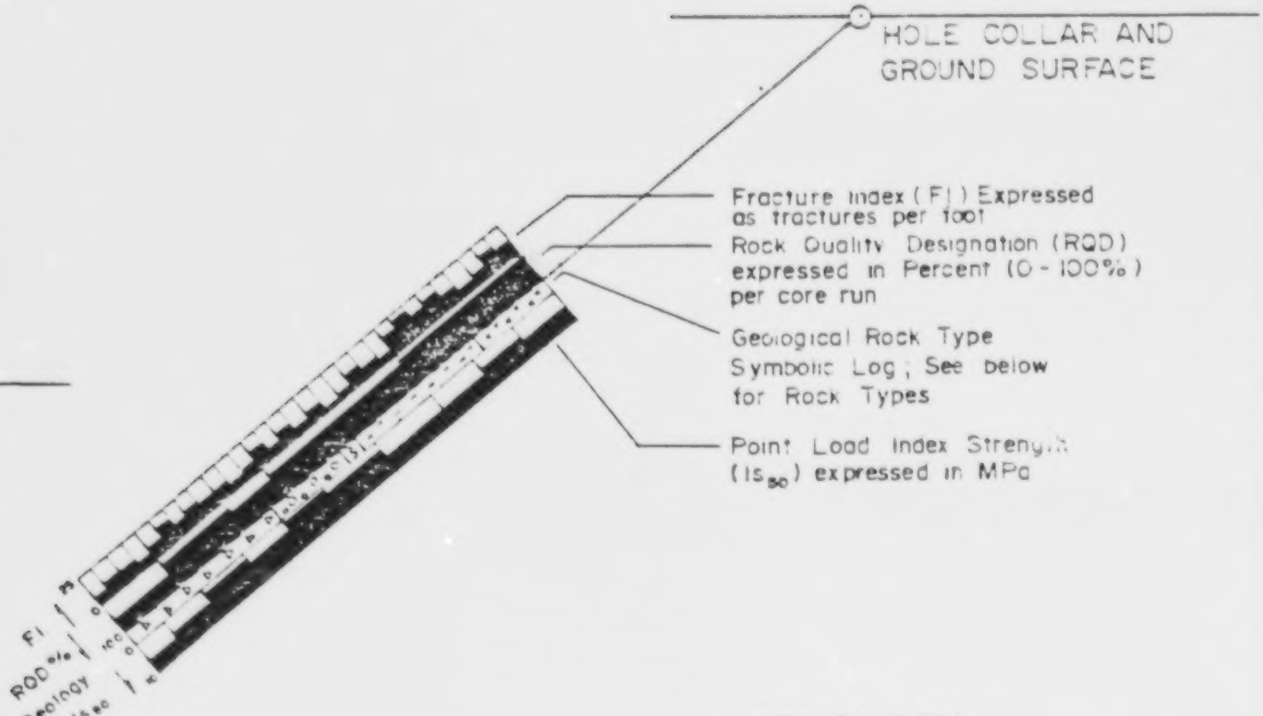
HOLE COLLAR AND GROUND SURFACE
Fracture index (FI) Expressed as fractures per foot
Rock Quality Designation (RQD) expressed in Percent (0 - 100%) per core run
Geological Rock Type Symbolic Log ; See below for Rock Types
Point Load Index Strength (Is_{50}) expressed in MPa
FI
RQD%
Geology
Is_{50}
0
100
0
10

LITHOLOGY

- ANDESITE
- DIABASE
- CONGLOMERATE
- AGGLOMERATE
- FAULT ZONE
- VEIN

SCALE: 1" TO 10'

Date FEBRUARY 8, 1990.
Project 881-1739-3

Golder Associates

Drawn D M / R.B.C.
Chkd TGK

GEOMETRY OF INTACT AND COLLAPSED CROWN PILLARS (MINE #59)

FIGURE 3.14

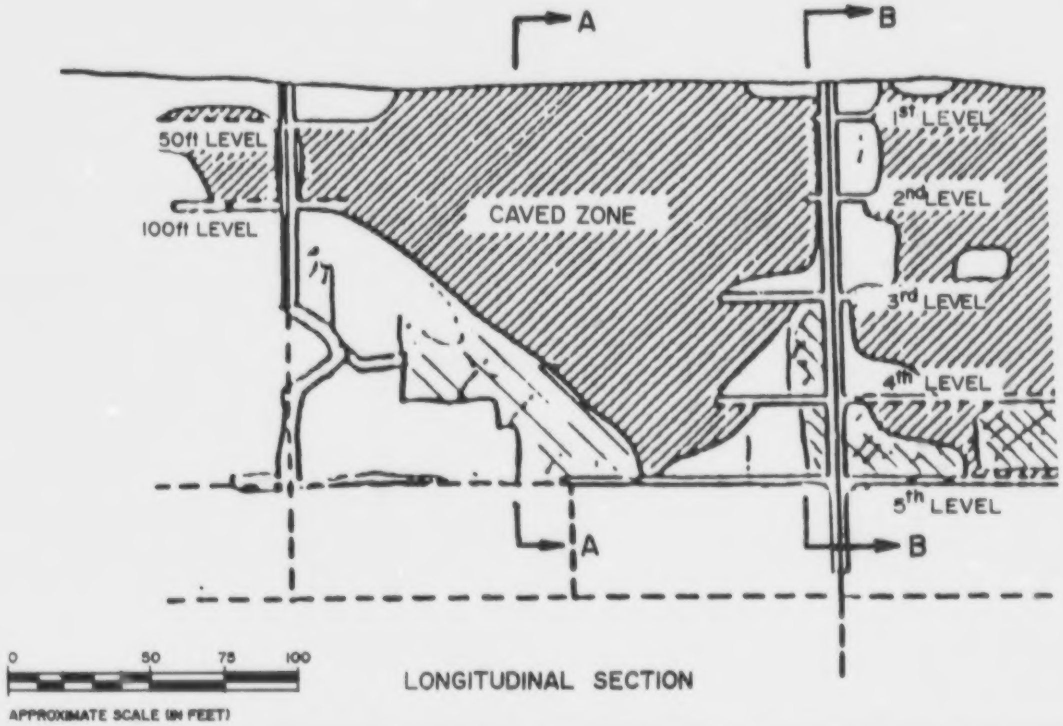

LONGITUDINAL SECTION

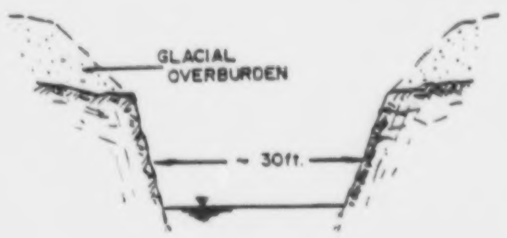

COLLAPSED CROWN LOCATION 30 ft. TO WEST OF AREA OF DIAGRAM B - B LOCATION.

SECTION A - A

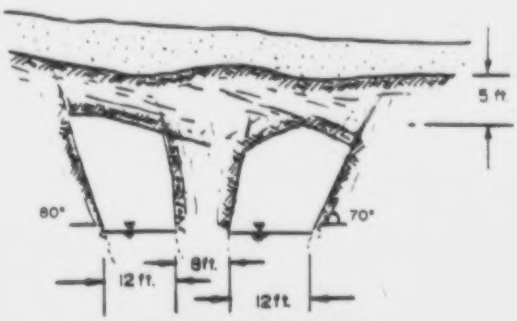

INTACT CROWN OVER TWIN STOPES SEPARATED BY STRIKE PILLAR

SECTION B - B

REFERENCE : KNIGHT C.W.,1915 ,"THE NORTH SHORE OF LAKE HURON", O.B.M. ANNUAL REPORT , VOL. 24 , PP 216 - 241

Date FEBRUARY 4 , 1990.
Project 881-1739-3

Golder Associates

Drawn R.B.C.
Chkd.

DETAILED ORE - ZONE CROSS - SECTION
(MINE #14)

FIGURE 3.15

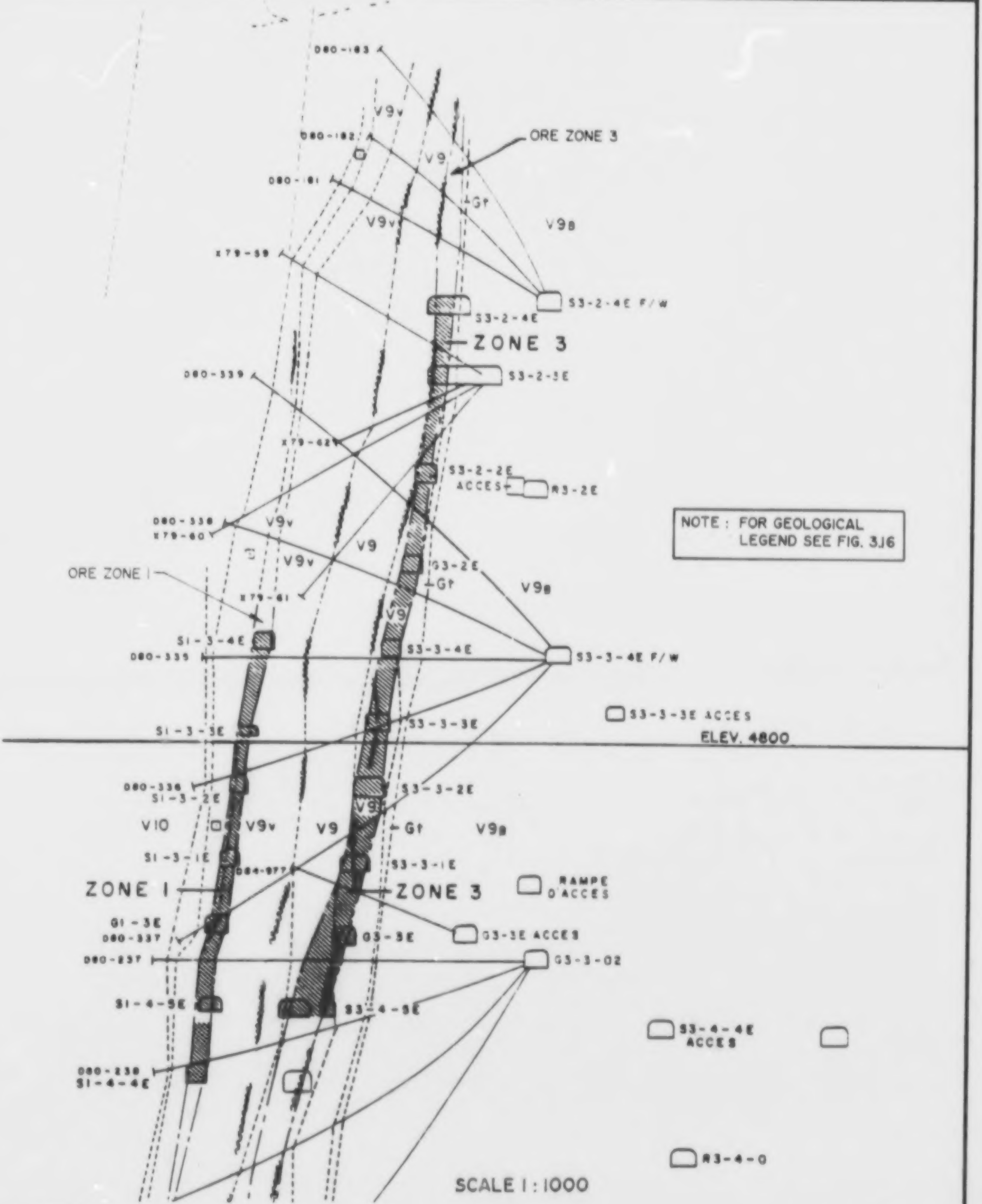

NOTE : FOR GEOLOGICAL LEGEND SEE FIG. 3.16

SCALE 1 : 1000

Date FEBRUARY 4 , 1990.
Project 881-1739-3

Golder Associates

Drawn R.B.C.
Chkd. TGC

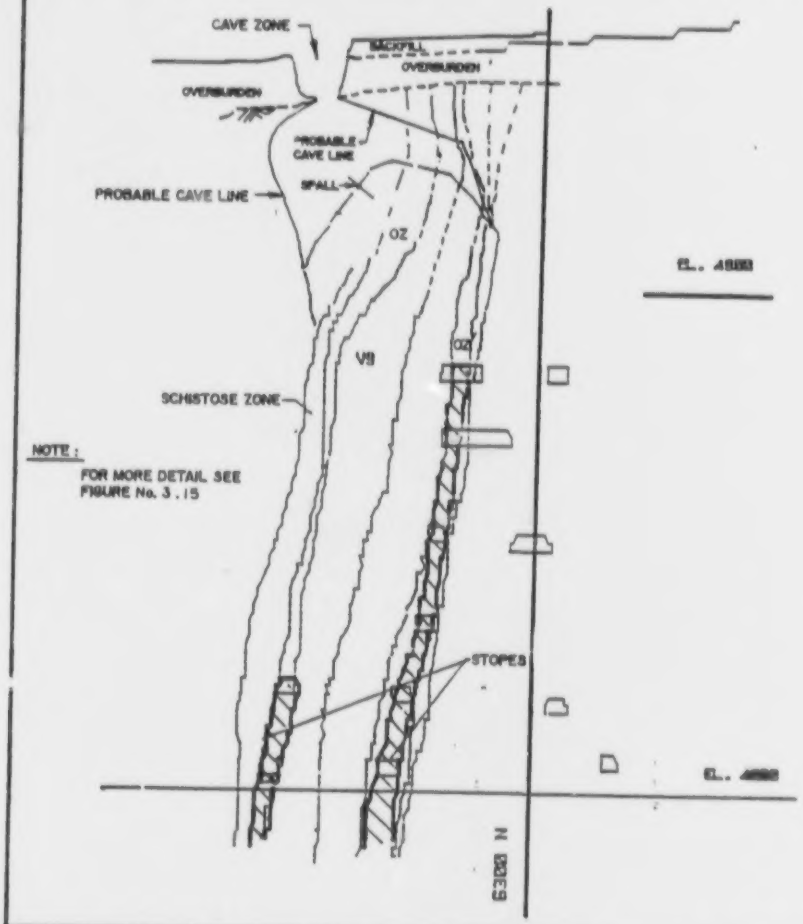

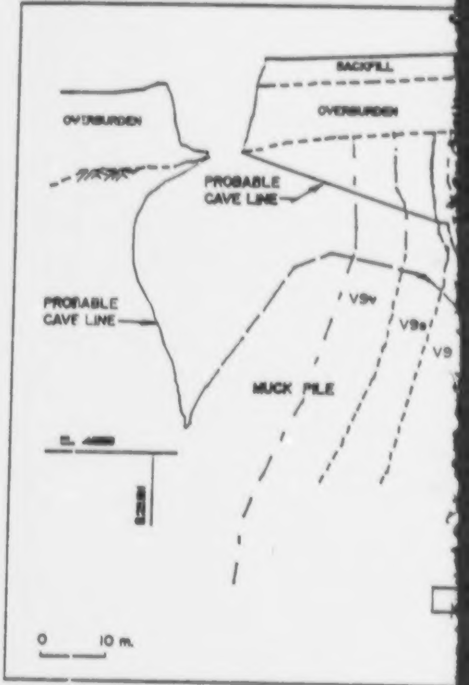

DETAIL OF SURFAC

SECTION 732

LOOKING WEST

LONGITUDINAL SECTION

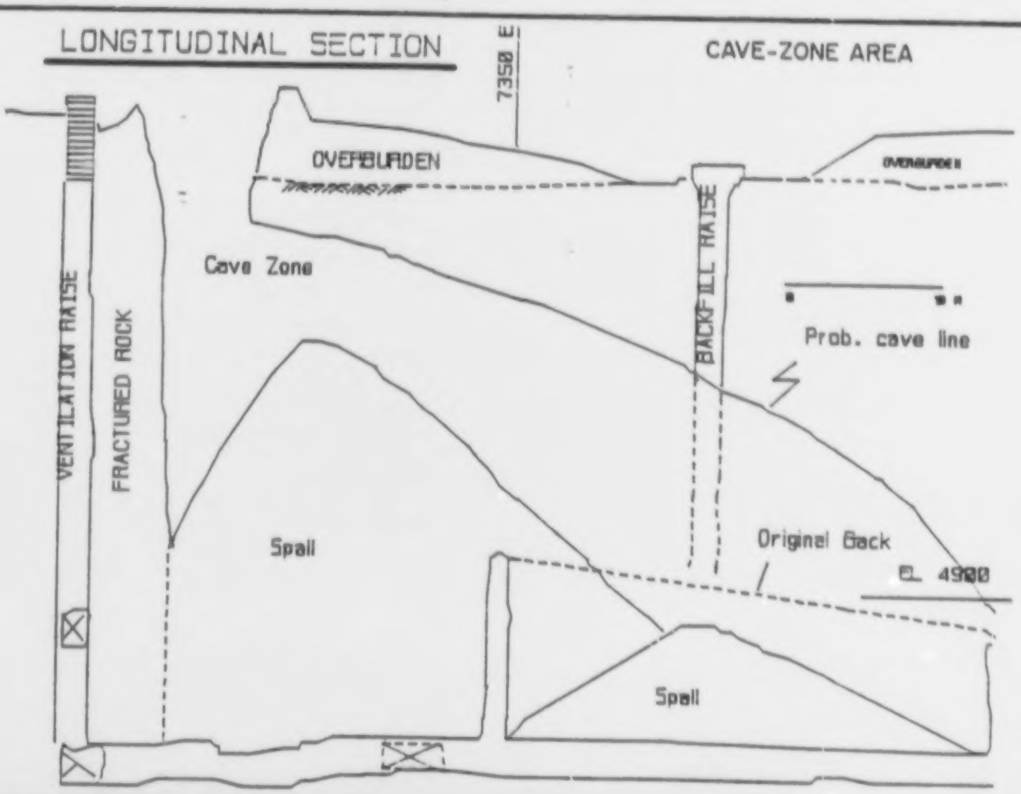

MINE #14 SUMMARY GEOTECHNICAL INFORMATION

FIGURE 3.16

PARAMETERS	DESCRIPTION (OR RANGE OF VALUES)	RATING N.G.I. Q	 C.S.I.R. R.M.R.
Drill Core Quality (R.Q.D.%)	ore zone 25-40, HW 40%, FW 60%	50	5
Number of Joint Sets (Jn)	schistocity, & 3 other sets	15	▩
Spacing of Joints (mm.) Fracture Index (/m.)	50 mm - 100 mm typical minimum 25 fractures/metre	▩	10
Condition of Joints : * Roughness (Jr)	planar, smooth, some slick	0.5	12
* Alteration/Contact Strength (Jc)	sericitic and chloritic coatings	4	
Intact Sample Strength (σc)	170 250 MPa, some weaker zones	▩	15
Groundwater Conditions	essentially dry	1	10
	TOTAL INDEX : RATING VALUE	0.42	52

LITHOLOGICAL LEGEND

V9	HANGING WALL PORPHYRY TUFFS	OZ	ORE ZONE FELSIC VOLCANICS
MV9	FOOTWALL MAFIC VOLCANICS		

MODULUS, E_{Rock} = 60 GPa, E_{Shear} = 25 GPa

$\sigma_h = 2\sigma_v$

$\nu = 0.25$

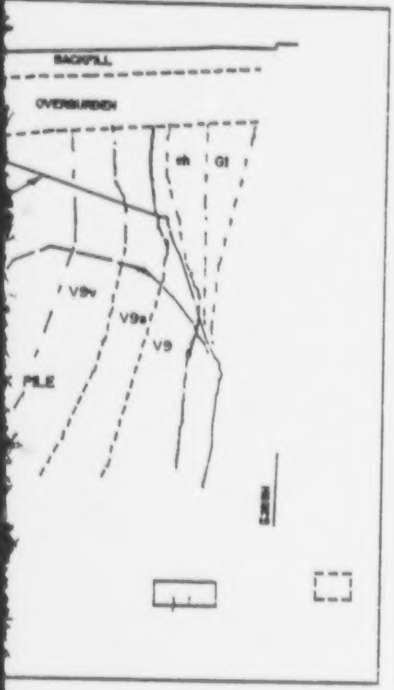

F SURFACE ZONE

ON 7320 E

OOKING WEST

PLAN

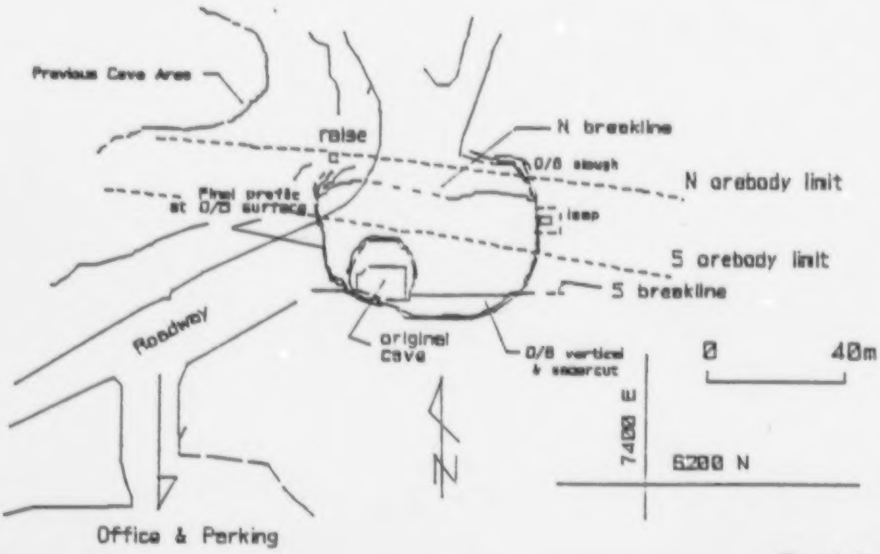

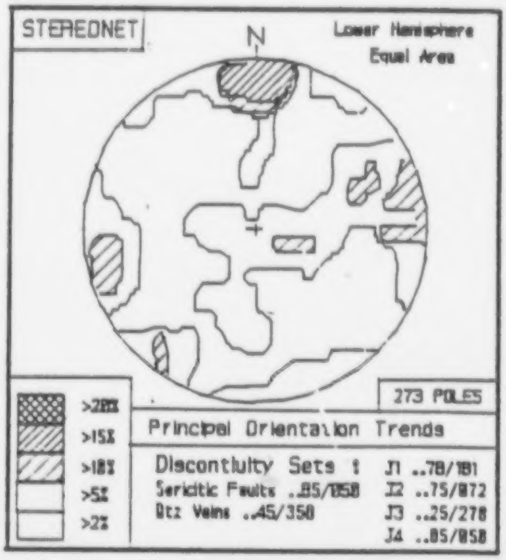

Golder Associates

MINE #22 CAVE ZONE GEOMETRY, AFTER CROWN PILLAR COLLAPSE

FIGURE 3.17

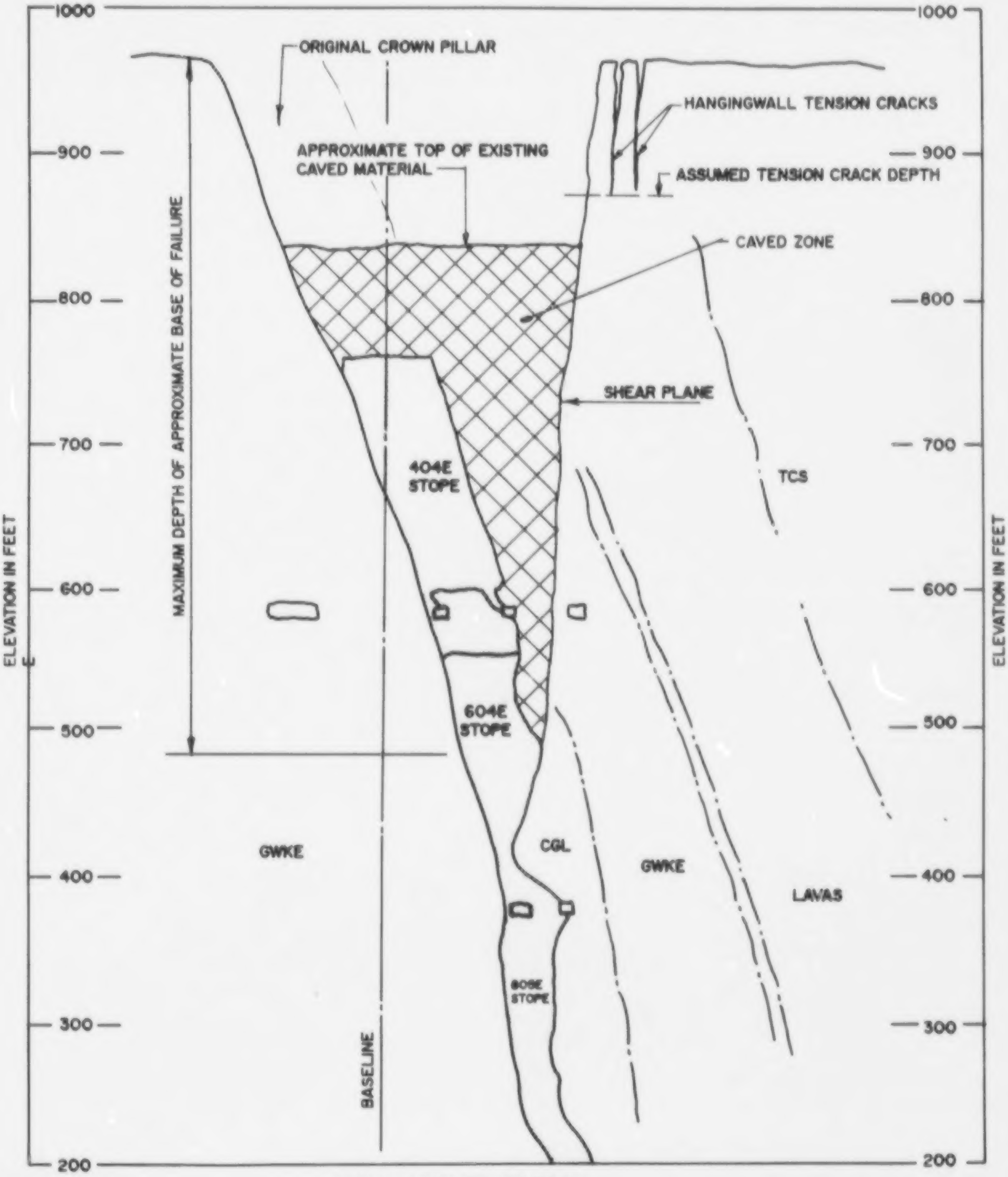

SCALE: 1 INCH TO 100 FEET

Date FEBRUARY 9, 1990.

Project 881-1739-3

Golder Associates

Drawn R.B.C.

Chkd TGC

DIMENSIONS AND LOCATION DETAILS FOR STOPE CAVE-INS AT MINE #25

FIGURE 3.18

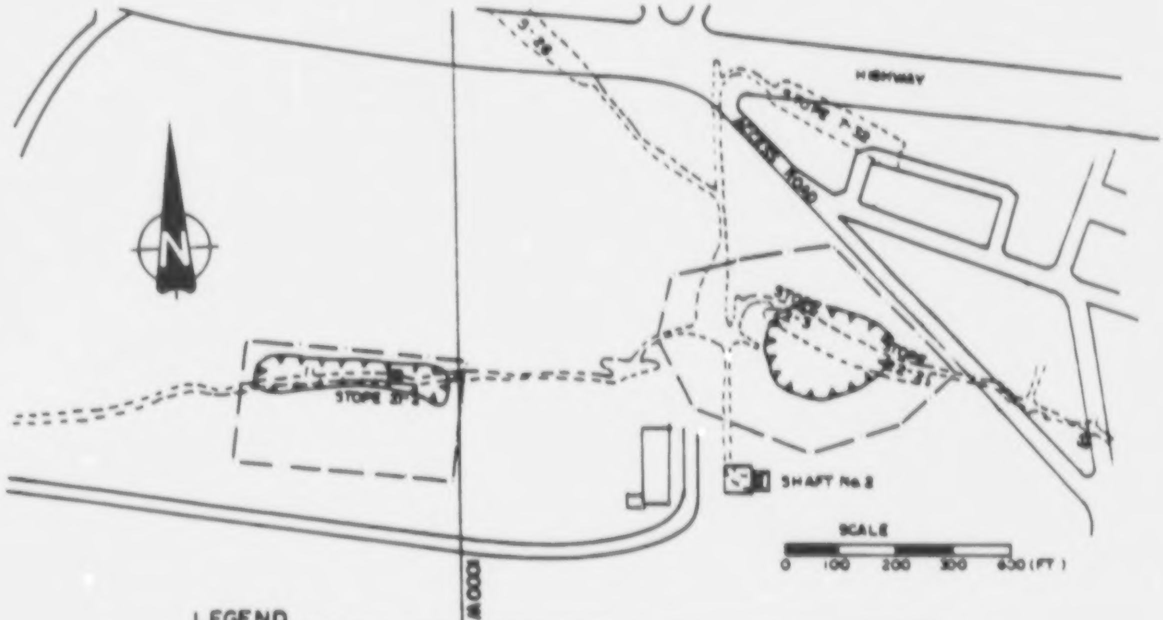

LEGEND

APPROX. SURFACE PROJECTION OF UNDERGROUND WORKINGS

ERECTED FENCE ON SURFACE

PLAN LOCATION OF RAISES

LOCATION OF SURFACE CAVED AREAS IN PLAN

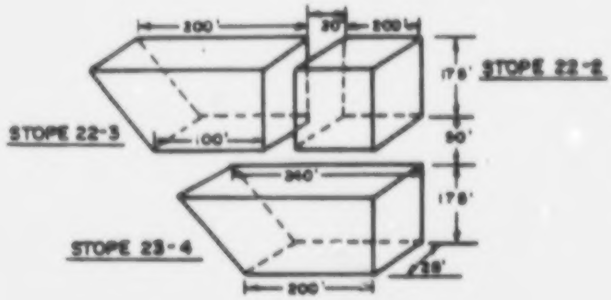

STOPE 22 - 3
ESTIMATED COVER ABOVE ROOF OF STOPE : 150 ft.
ESTIMATED VOLUME EXTRACTED : 656 x 10^3 cu. ft.

STOPE 22 - 2
ESTIMATED COVER ABOVE ROOF OF STOPE : 150 ft.
ESTIMATED VOLUME EXTRACTED : 875 x 10^3 cu. ft.

STOPE 23 - 4
ESTIMATED VOLUME EXTRACTED : 963 x 10^3 cu. ft.

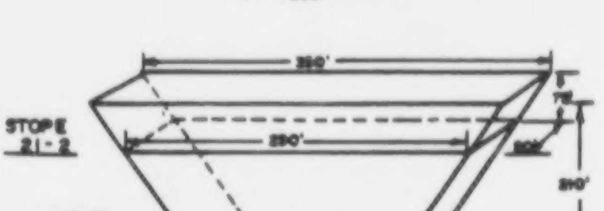

STOPE 21 - 2
ESTIMATED COVER ABOVE ROOF OF STOPE : 75 ft.
ESTIMATED VOLUME EXTRACTED : 460 x 10^3 cu. ft.

STOPE 22 - 4
ESTIMATED VOLUME EXTRACTED : 584 x 10^3 cu. ft.

NOTE:
ALL DIMENSIONS ARE APPROXIMATE

Date FEB. 9, 1990
Project 881-1739-3

Golder Associates

Drawn D.J.R
Chkd. TGr

OVERALL CONFIGURATION OF CROWN PILLAR FAILURE GEOMETRY (MINE #35)

FIGURE 3.19

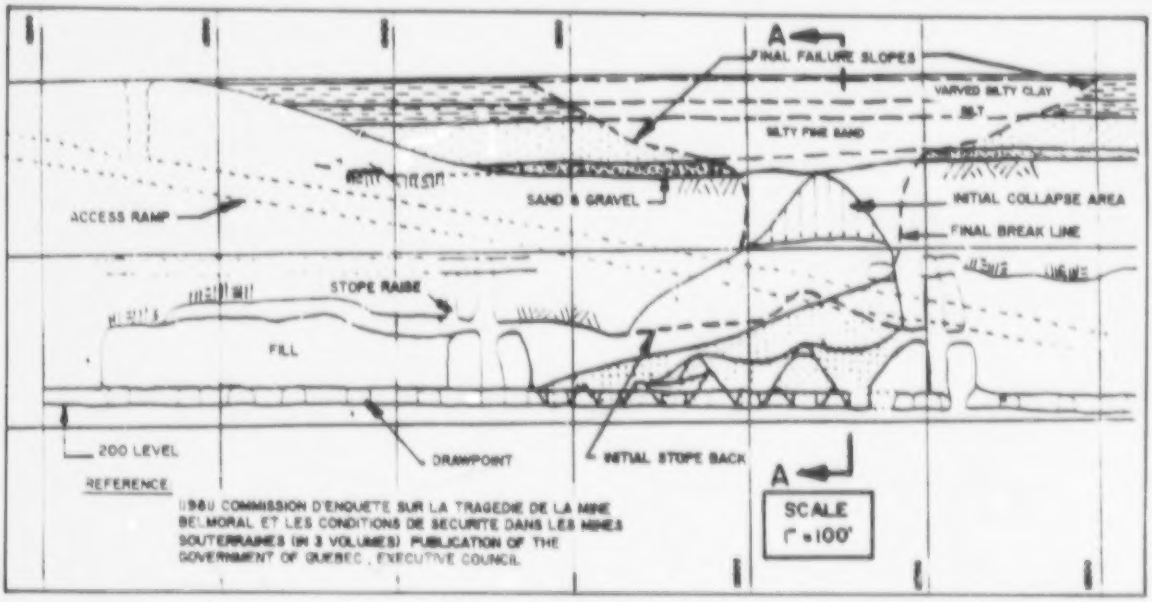

REFERENCE

(1981) COMMISSION D'ENQUETE SUR LA TRAGEDIE DE LA MINE BELMORAL ET LES CONDITIONS DE SECURITE DANS LES MINES SOUTERRAINES (IN 3 VOLUMES) PUBLICATION OF THE GOVERNMENT OF QUEBEC, EXECUTIVE COUNCIL

LONGITUDINAL SECTION

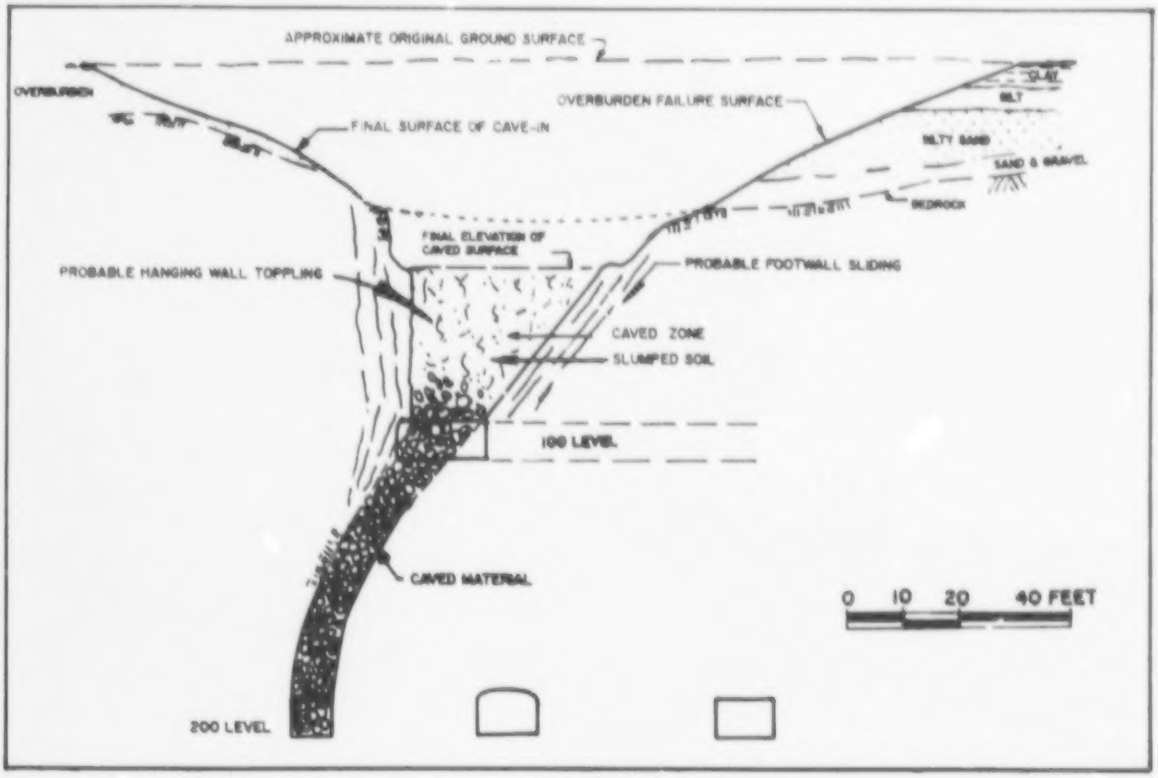
APPROXIMATE ORIGINAL GROUND SURFACE
OVERBURDEN
FINAL SURFACE OF CAVE-IN
OVERBURDEN FAILURE SURFACE
CLAY
SILT
SILTY SAND
SAND & GRAVEL
BEDROCK
FINAL ELEVATION OF CAVED SURFACE
PROBABLE HANGING WALL TOPPLING
PROBABLE FOOTWALL SLIDING
CAVED ZONE
SLUMPED SOIL
100 LEVEL
CAVED MATERIAL
0 10 20 40 FEET
200 LEVEL

CROSS-SECTION A-A AT 12620E.

Date FEBRUARY 2, 1990.

Project 881-1739-3

Golder Associates

Drawn R.B.C.

Chkd TG

LONGITUDINAL SECTION OF CROWN PILLAR FAILURE AT MINE #50

FIGURE 3.20

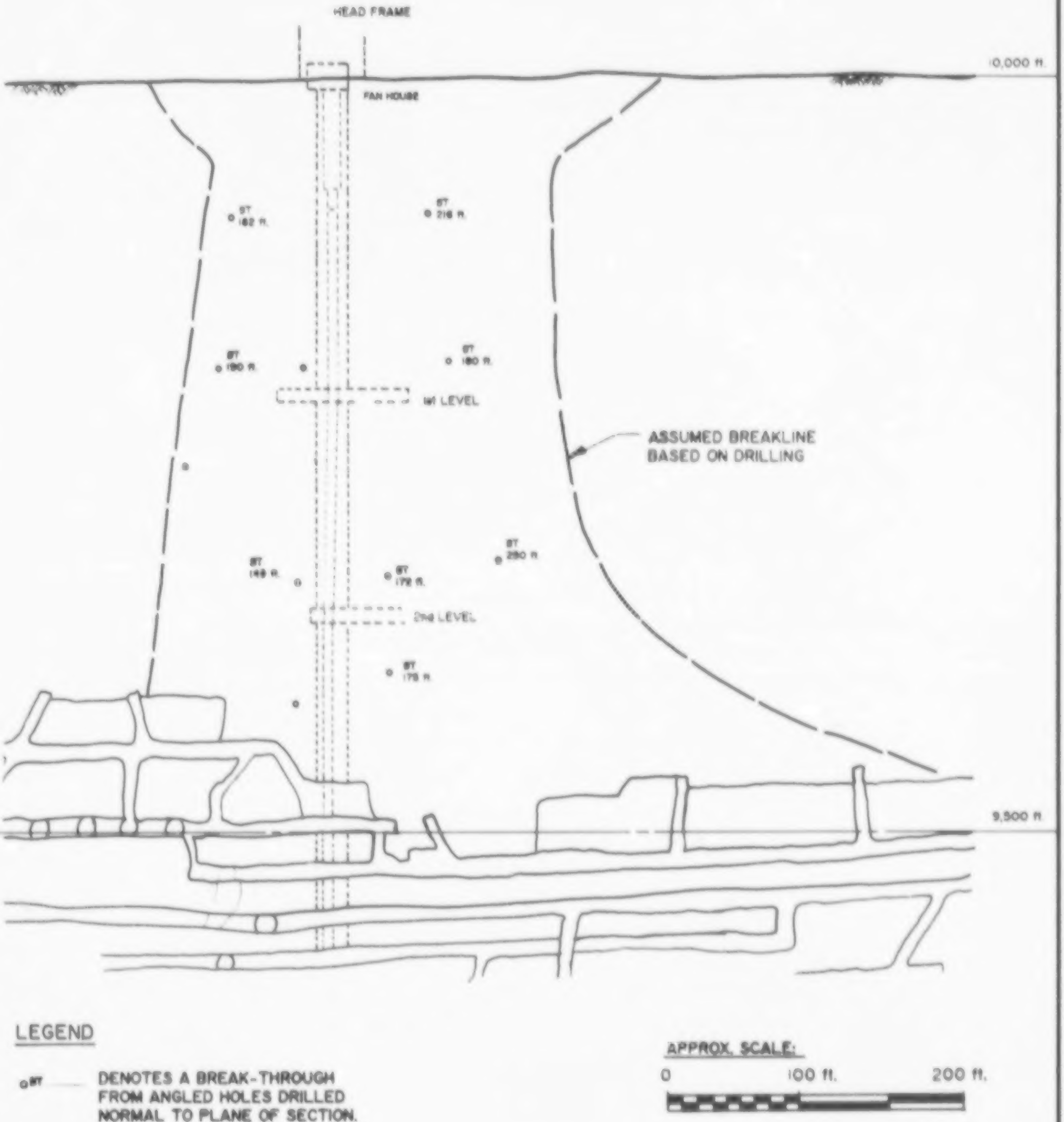

Date FEBRUARY 9, 1990.
Project 881-1739-3

Golder Associates

Drawn R.B.C.
Chkd TGu

CROWN PILLAR GEOMETRY AND CAVE - ZONE CONFIGURATION (MINE #41)

FIGURE 3.21

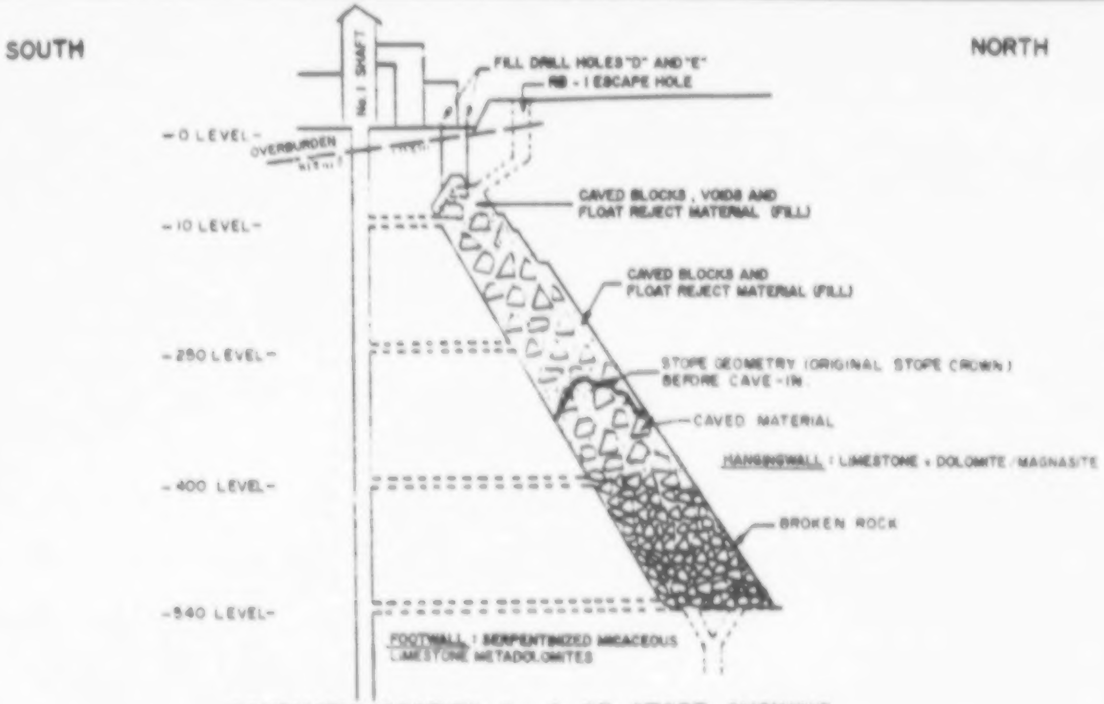
SOUTH
NORTH
No. 1 SHAFT
FILL DRILL HOLES "D" AND "E"
RB - 1 ESCAPE HOLE
– 0 LEVEL –
OVERBURDEN
– 10 LEVEL –
CAVED BLOCKS, VOIDS AND FLOAT REJECT MATERIAL (FILL)
CAVED BLOCKS AND FLOAT REJECT MATERIAL (FILL)
– 250 LEVEL –
STOPE GEOMETRY (ORIGINAL STOPE CROWN) BEFORE CAVE - IN
CAVED MATERIAL
HANGINGWALL : LIMESTONE + DOLOMITE / MAGNASITE
– 400 LEVEL –
BROKEN ROCK
– 540 LEVEL –
FOOTWALL : SERPENTINIZED MICACEOUS LIMESTONE METADOLOMITES

SCHEMATIC SECTION A - A OF STOPE SHOWING ORIGINAL CROWN AND EXTENT OF CAVED MATERIAL

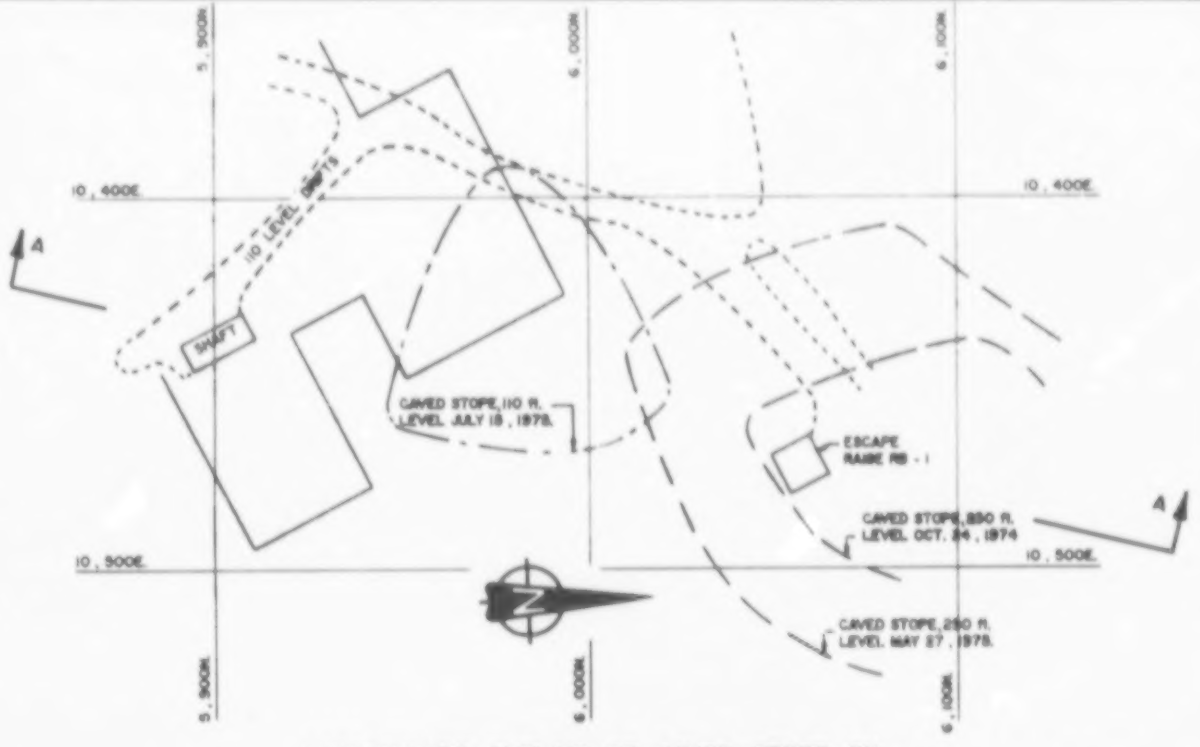

APPROXIMATE OUTLINE OF CAVED STOPE ON THE 110 AND 250 ft. LEVELS

Date FEBRUARY 4, 1990.
Project 881-1739-3

Golder Associates

Drawn R.B.C.
Chkd. TG

DETAILS OF PILLAR COLLAPSE AREAS
(MINE #67)

FIGURE 3.22

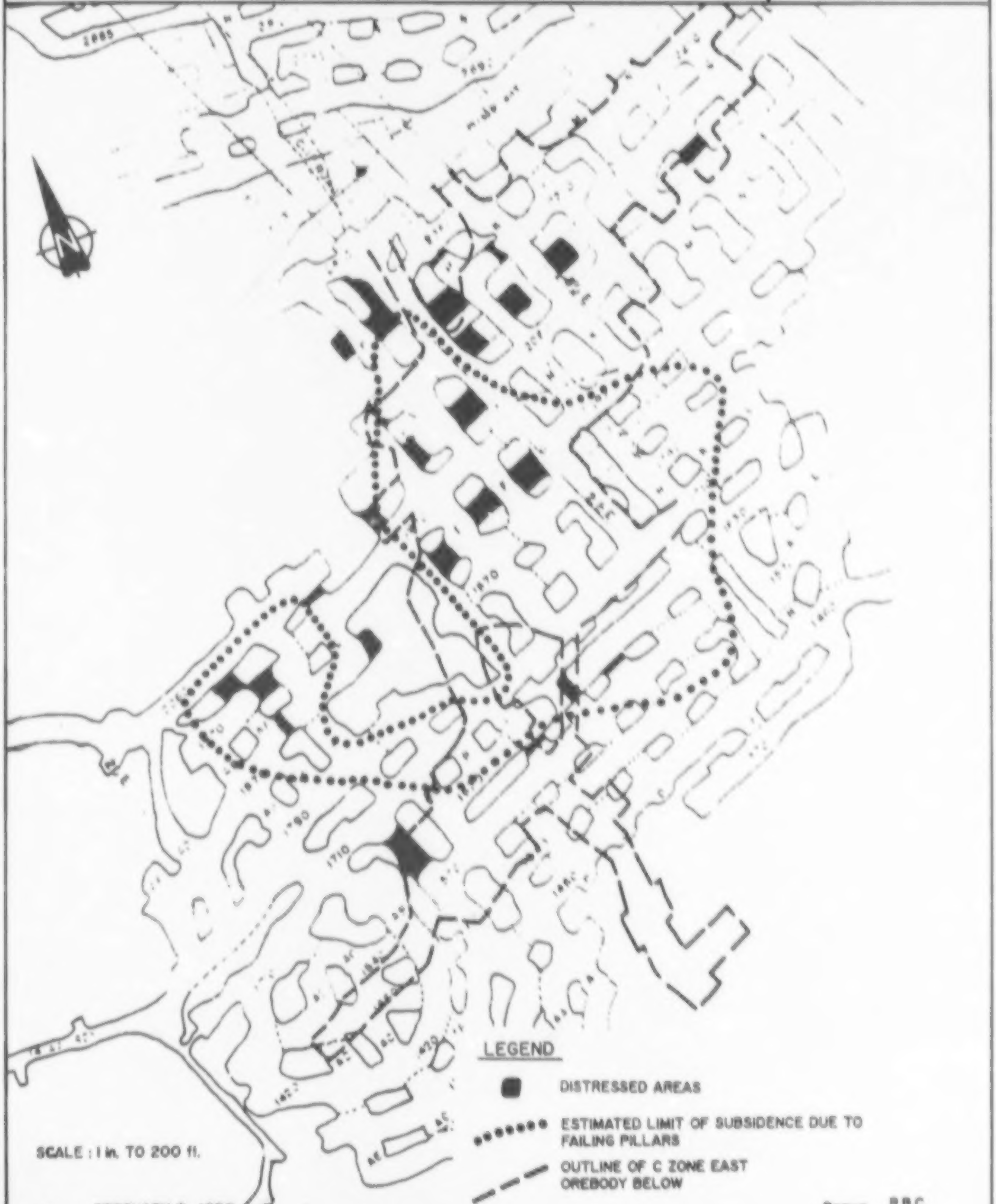
N
1870
1790
1710
LEGEND
■ DISTRESSED AREAS
●●●●●●● ESTIMATED LIMIT OF SUBSIDENCE DUE TO FAILING PILLARS
— — OUTLINE OF C ZONE EAST OREBODY BELOW

SCALE : 1 in. TO 200 ft.

Date FEBRUARY 9, 1990.

Project 881-1739-3

Golder Associates

Drawn R.B.C.

Chkd TGc

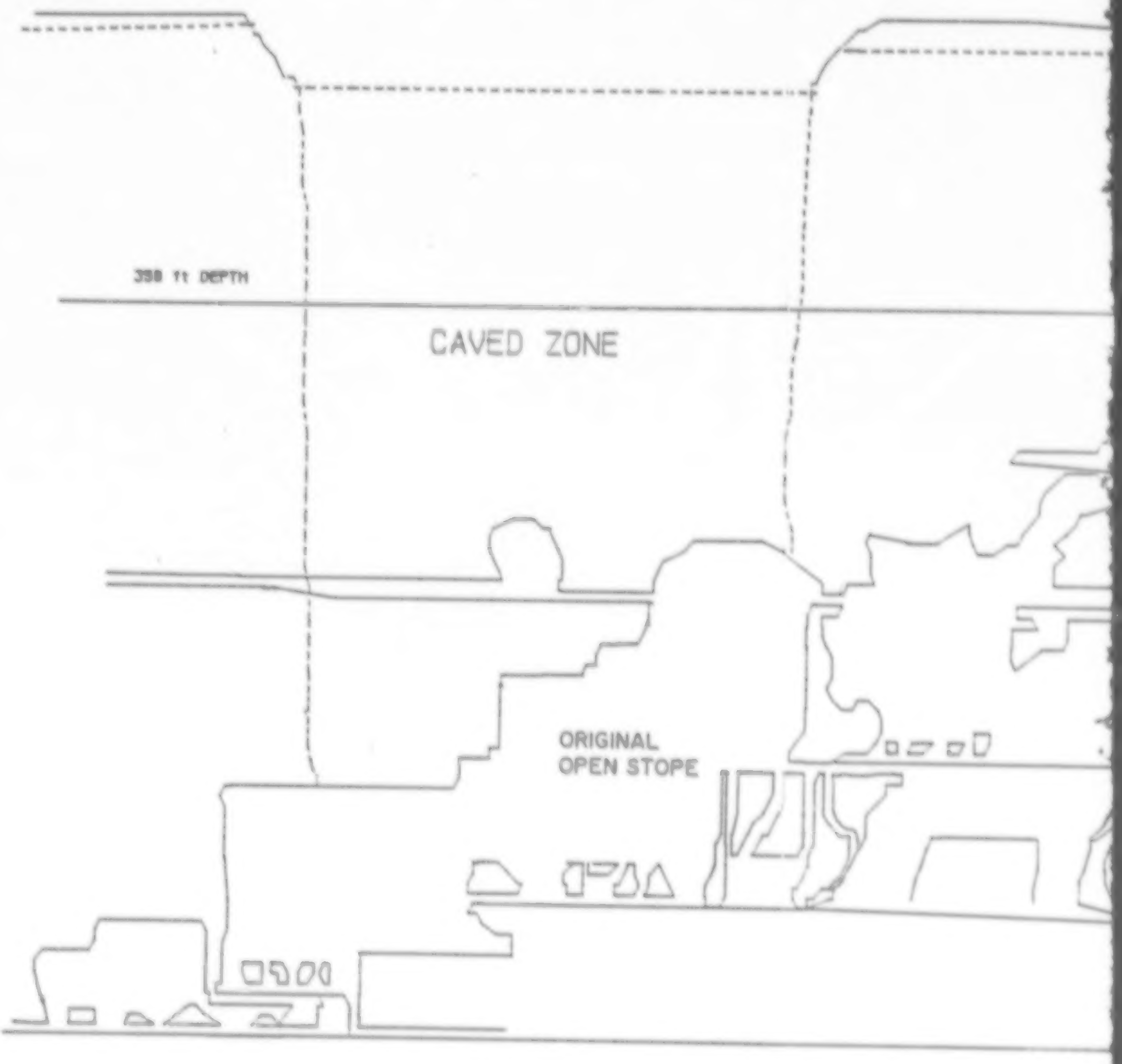

LONGITUDINAL SECTION

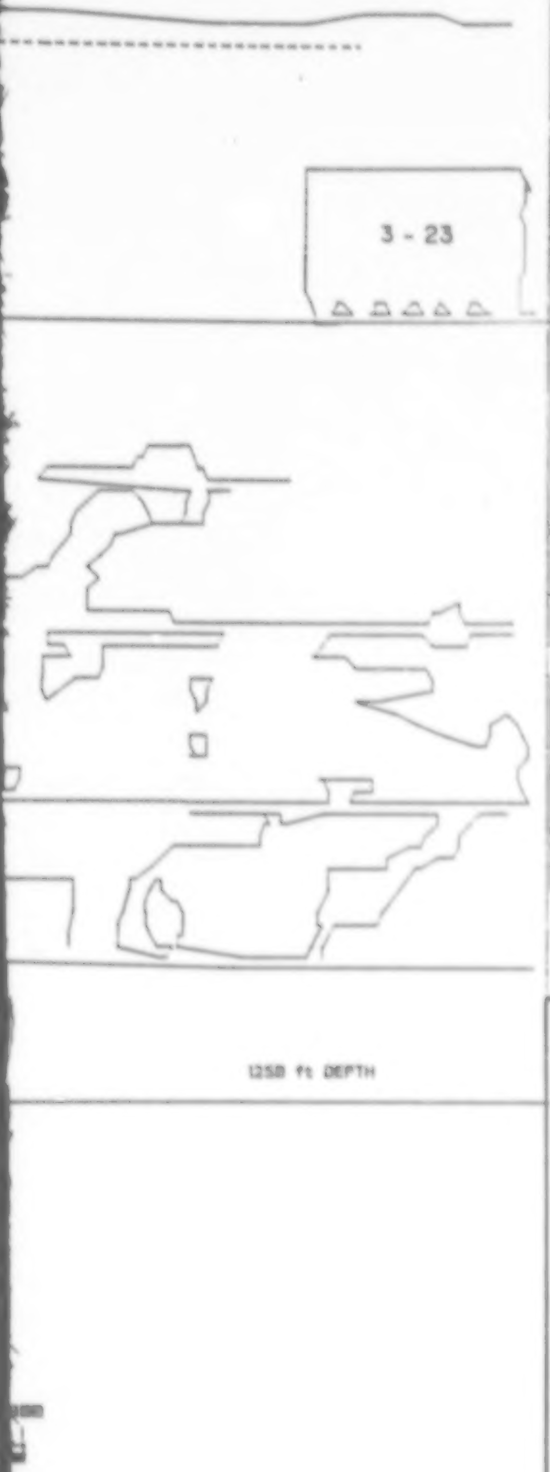

MINE #27 SUMMARY GEOTECHNICAL INFORMATION

FIGURE 3.23

PARAMETERS	DESCRIPTION (OR RANGE OF VALUES)	RATING	
		N.G.I. Q	C.S.I.R. R.M.R.
Drill Core Quality (R.Q.D.%)	Schistose, 20-30%	25	5
Number of Joint Sets (Jn)	Foliation plus 3 sets	4	▨
Spacing of Joints (mm.) Fracture Index (/m.)	Schistosity, less than 5 mm. 30-50 fractures/metre	▨	5
Condition of Joints : * Roughness (Jr)	Smooth, in pieces slickensided	0.5	6
* Alteration/Contact Strength (Jc)	Sericite/chlorite coated,some clay	4	
Intact Sample Strength (Qc)	Footwall schist zones c. 30 MPa	▨	4
Groundwater Conditions	Essentially dry except on fault	0.8	7
	TOTAL INDEX : RATING VALUE	0.625	27

LITHOLOGICAL LEGEND

SP	SYENITE PORPHYRY	FZ	CADILLAC BREAK - FAULT ZONE
P	PERIDOTITE		

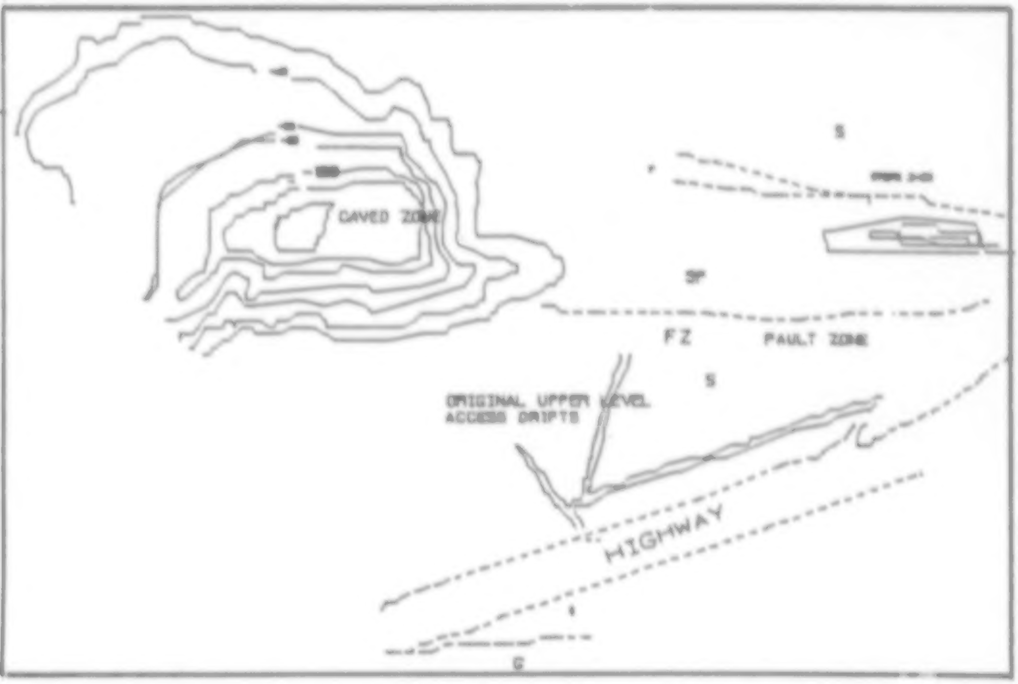

Golder Associates

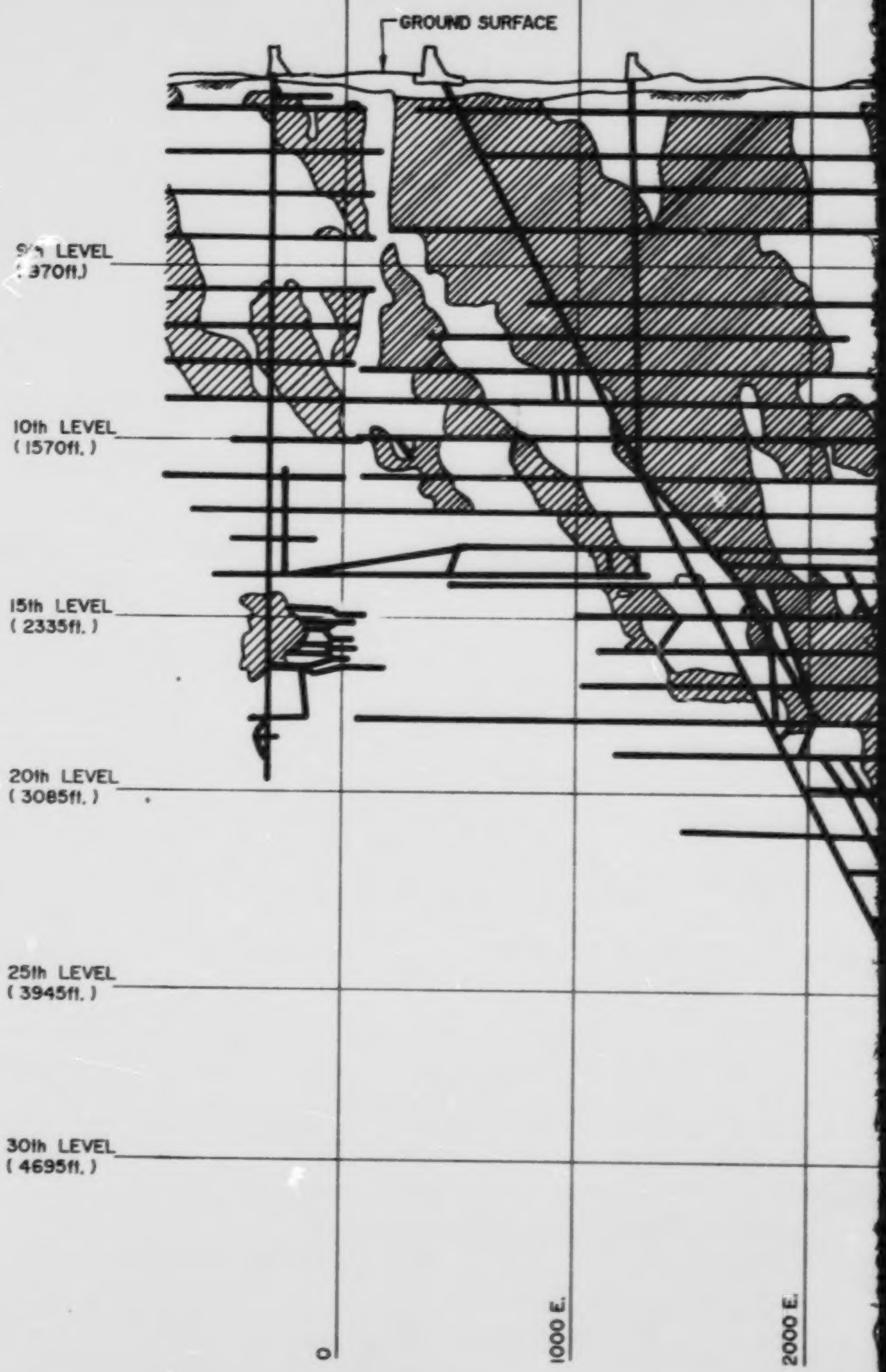
GROUND SURFACE
5th LEVEL
(870ft.)
10th LEVEL
(1570ft.)
15th LEVEL
(2335ft.)
20th LEVEL
(3085ft.)
25th LEVEL
(3945ft.)
30th LEVEL
(4695ft.)
0
1000 E.
2000 E.

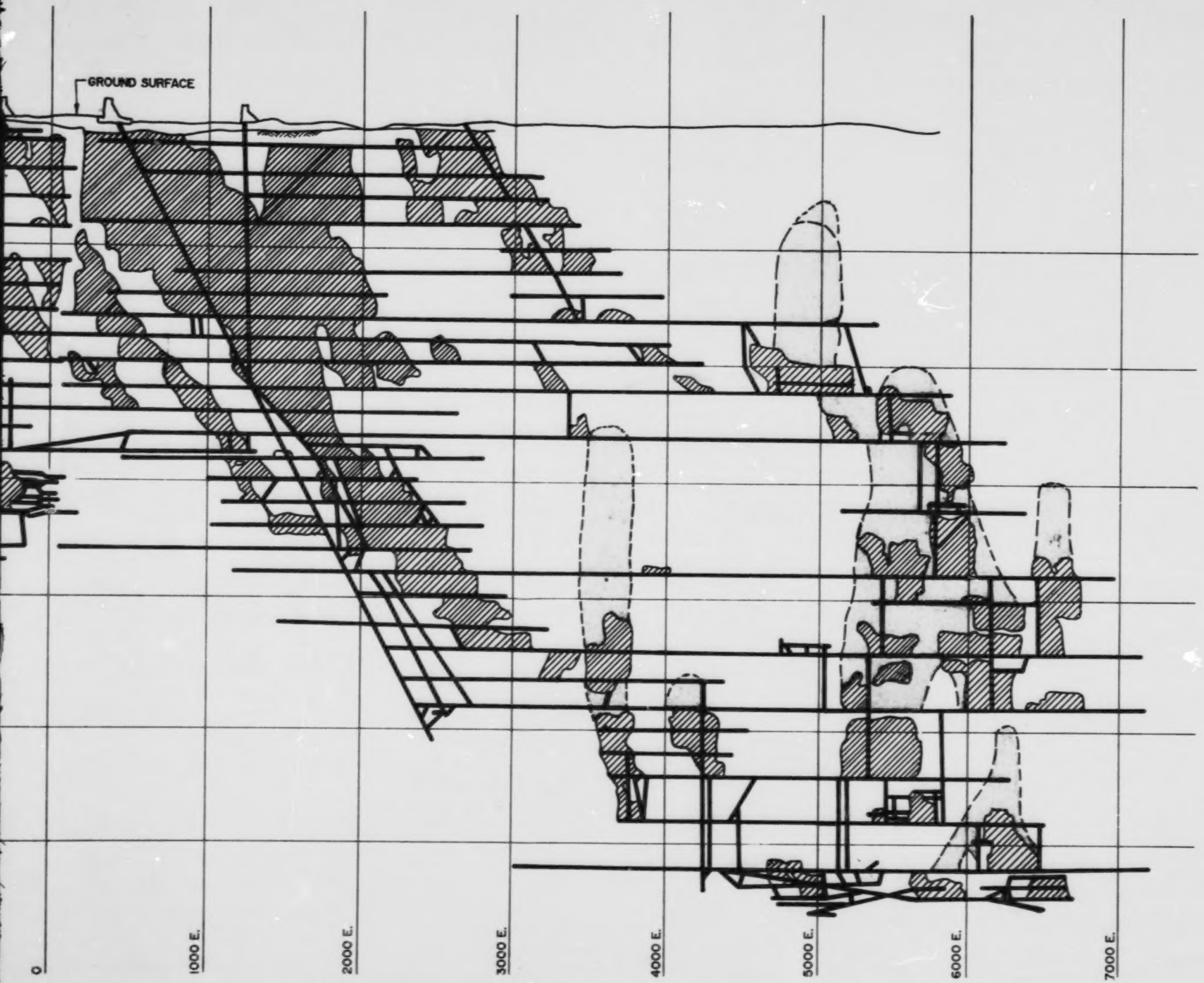

EAST - WEST SECTION THROUGH MINE #28 SHOWING CAVING STOPES

FIGURE 3.24

LEGEND

▨ AREAS OF MINE WORKINGS

☐ AREAS OF PROJECTED CAVING SUBSEQUENT TO MINING OPERATIONS

APPROXIMATE SCALE 1 INCH TO 700 FEET.

Date MAY 17, 1990.
Project 881 - 1739 -3

Golder Associates

Drawn R.B.C.
Chkd

GEOMETRICAL ARRANGEMENT OF CROWN FAILURE OF STOPE 2 - 15, MINE #62

FIGURE 3.25

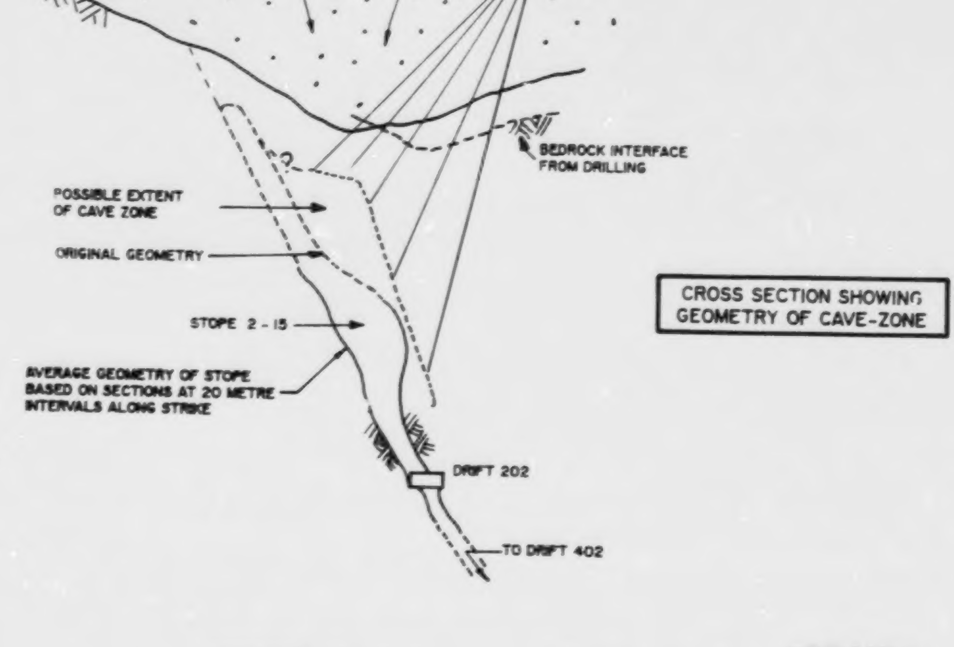
ELEV. 5 000 m
SUBSIDENCE ZONE
BEDROCK INTERFACE FROM DRILLING
POSSIBLE EXTENT OF CAVE ZONE
ORIGINAL GEOMETRY
STOPE 2 - 15
AVERAGE GEOMETRY OF STOPE BASED ON SECTIONS AT 20 METRE INTERVALS ALONG STRIKE
DRIFT 202
TO DRIFT 402

CROSS SECTION SHOWING GEOMETRY OF CAVE-ZONE

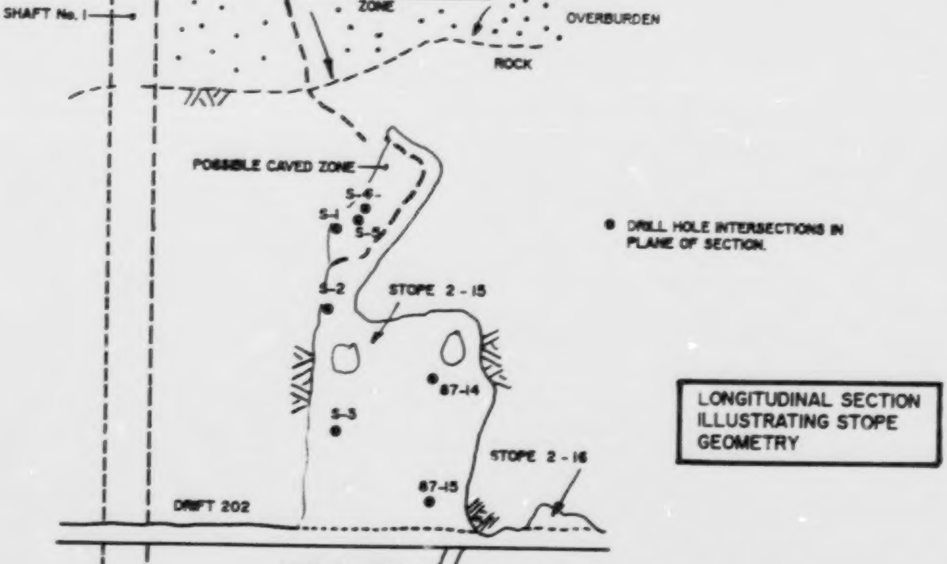

LONGITUDINAL SECTION ILLUSTRATING STOPE GEOMETRY

NOT TO SCALE

Date FEBRUARY 7, 1990.

Project 881-1739-3

Golder Associates

Drawn R.B.C.

Chkd.

CROSS SECTION SHOWING INSTRUMENTATION ARRAYS AND GEOLOGY OF AREA OF SLOUGHING HANGINGWALL (MINE #45)

FIGURE 3.26

NOTE : DRAIN AND VENT HOLES CASED THROUGH OVERBURDEN

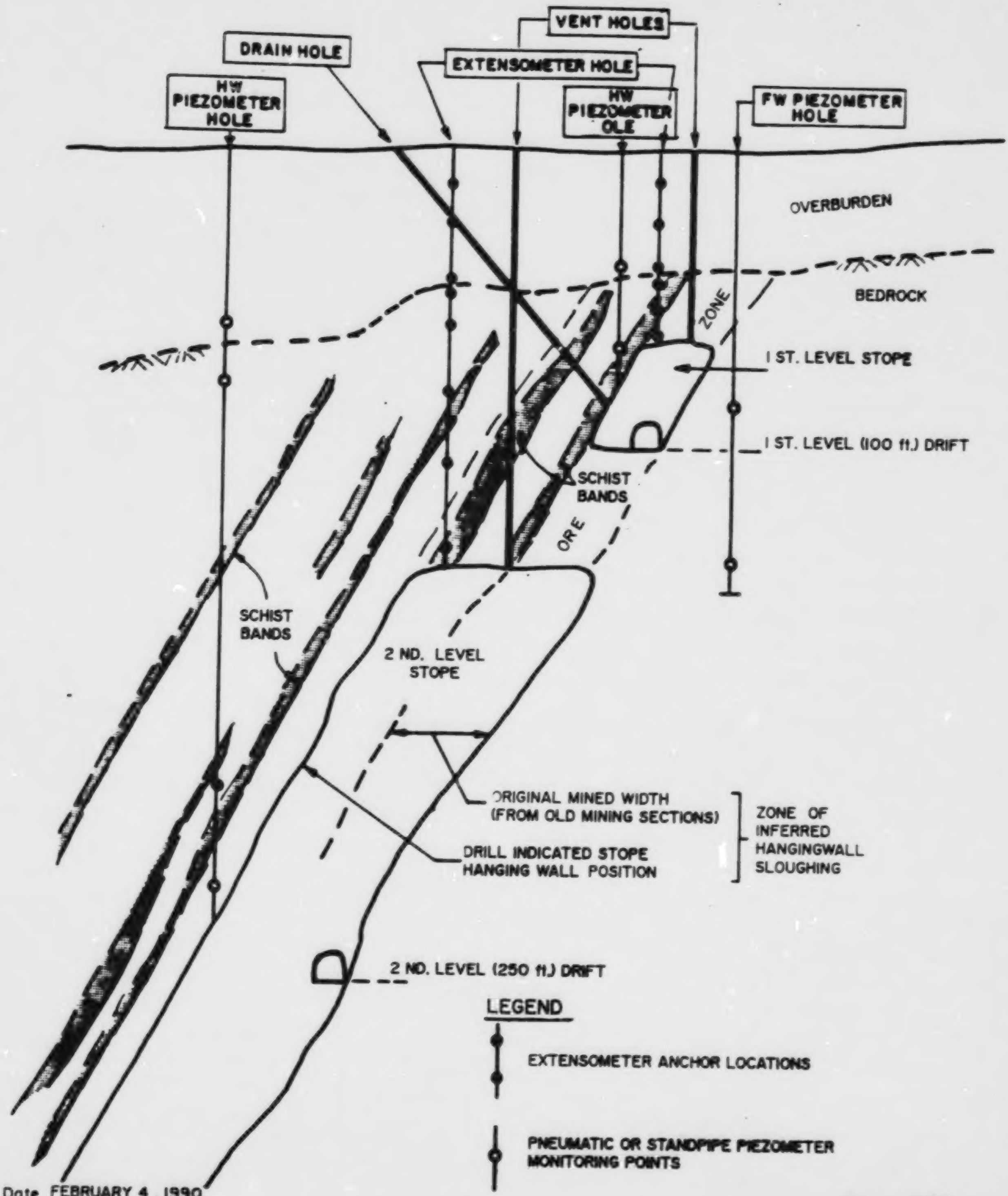
VENT HOLES
DRAIN HOLE
EXTENSOMETER HOLE
HW PIEZOMETER HOLE
HW PIEZOMETER OLE
FW PIEZOMETER HOLE
OVERBURDEN
BEDROCK
ZONE
I ST. LEVEL STOPE
I ST. LEVEL (100 ft.) DRIFT
SCHIST BANDS
ORE
SCHIST BANDS
2 ND. LEVEL STOPE
ORIGINAL MINED WIDTH (FROM OLD MINING SECTIONS)
DRILL INDICATED STOPE HANGING WALL POSITION
ZONE OF INFERRED HANGINGWALL SLOUGHING
2 ND. LEVEL (250 ft.) DRIFT
LEGEND
EXTENSOMETER ANCHOR LOCATIONS
PNEUMATIC OR STANDPIPE PIEZOMETER MONITORING POINTS

Date FEBRUARY 4, 1990.
Project 881-1739-3

Golder Associates

Drawn R.B.C.
Chkd. TGN

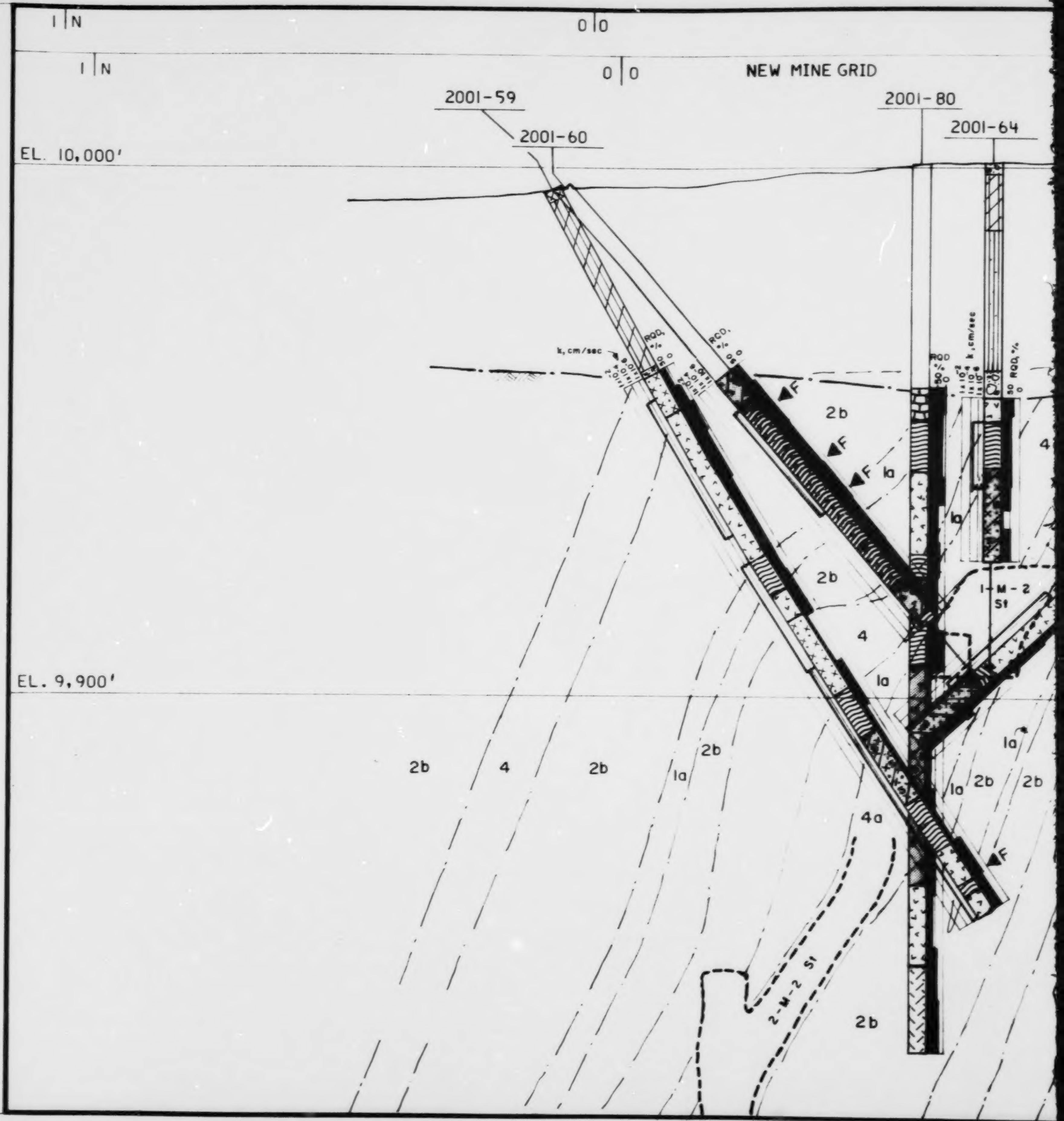
1 N
0 0
1 N
0 0
NEW MINE GRID
2001-59
2001-60
2001-80
2001-64
EL. 10,000'
EL. 9,900'
k, cm/sec
RQD, %
50 0
RQD, %
50 0
RQD %
50 0
k, cm/sec
1x10⁻²
1x10⁻⁴
1x10⁻⁶
RQD, %
50 0
F
F
F
F
2b
1a
4
1a
2b
1-M-2 St
4
1a
2b
4
2b
1a
2b
1a
1a
2b
2b
4a
2-M-2 St
2b

MINE #45 DETAILED CROWN PILLAR DRILL ARRAY FOR INSTRUMENTATION INSTALLATIONS

FIGURE 3.27

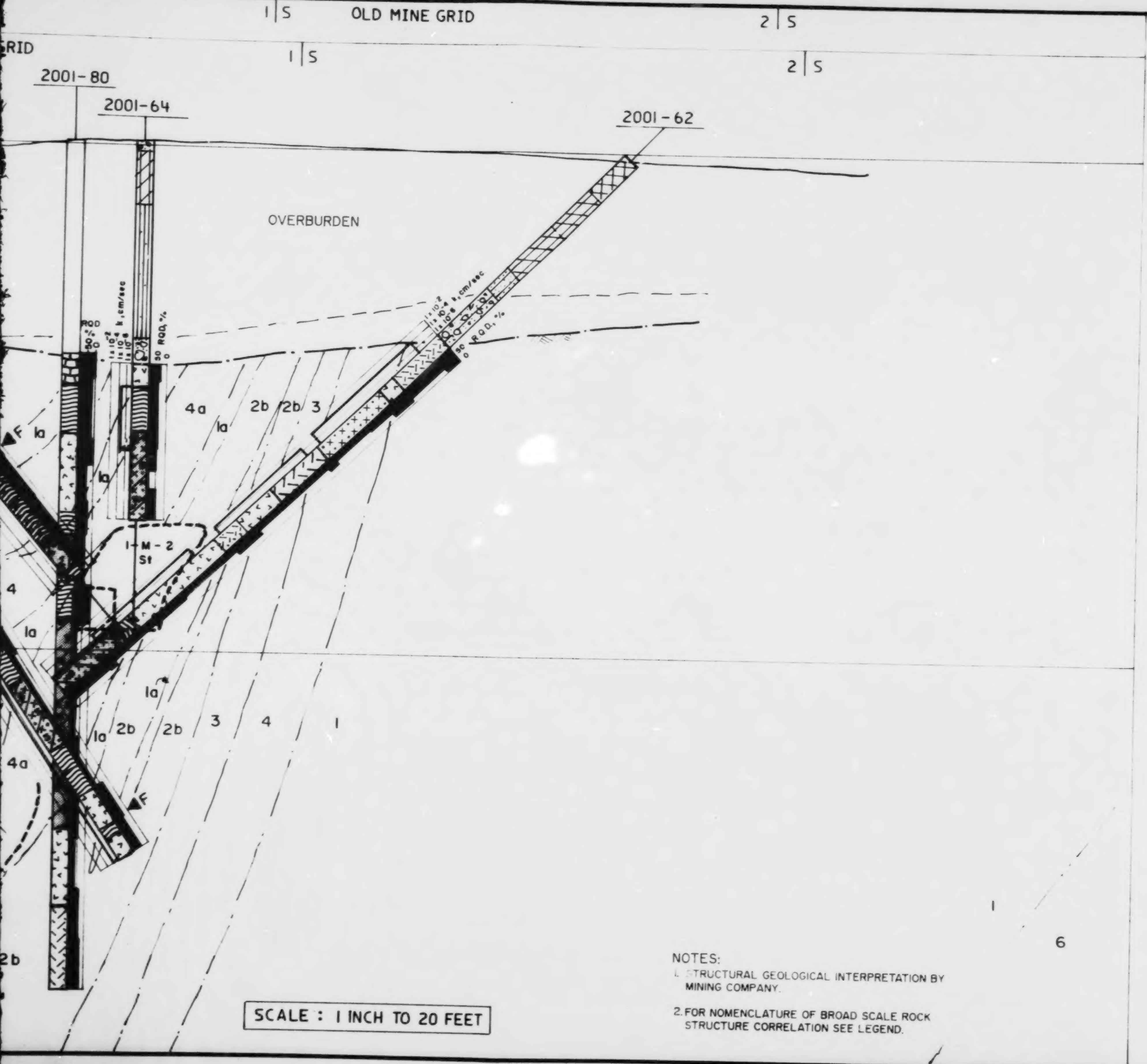

SCALE : 1 INCH TO 20 FEET

NOTES:

1. STRUCTURAL GEOLOGICAL INTERPRETATION BY MINING COMPANY.
2. FOR NOMENCLATURE OF BROAD SCALE ROCK STRUCTURE CORRELATION SEE LEGEND.

LEGEND

General

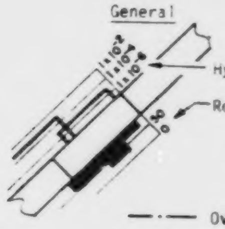

Hydraulic Conductivity (cm/sec)

Rock Quality Designation (RQD %)

(see Borehole Logs - Appendix I for details)

Overburden/bedrock contact

Stope back, from recent drilling

Underground openings (details from old mining records)

OVERBURDEN

▨	Mine Waste/rockfill
▨	Peat
▨	Weathered and Dessicated Crust (where defined)
▨	Rhythmically bedded clayey silts/silty clays
▨	Silty sands
▨	Tills

BEDROCK

6b	▨	Aplite	FELSIC INTRUSIVES
6a	▨	Granodiorite/Monzonite	
5	▨	Feldspar Porphyry	
4	▨	Porphyritic Diorite (Basic Syenite)	INTERMEDIATE INTRUSIVES
3	▨	Gabbro	
2b	▨	Dark green basaltic flows (non magnetic)	MAFIC VOLCANICS
1	▨	Blue grey komatiite flows (strongly magnetic)	ULTRAMAFIC VOLCANICS
1a	▨	Talc-chlorite schist	

▨	Zones of stockworked quartz silicification
▨	Carbonate Rich Zones
◀F	Fault Locations
▨	Shear Zones
▨	Mineralized Zones

Date.. FEBRUARY 9, 1990.

Project 881-1739-3

Golder Associates

Drawn PL / R.B.C.

Chkd

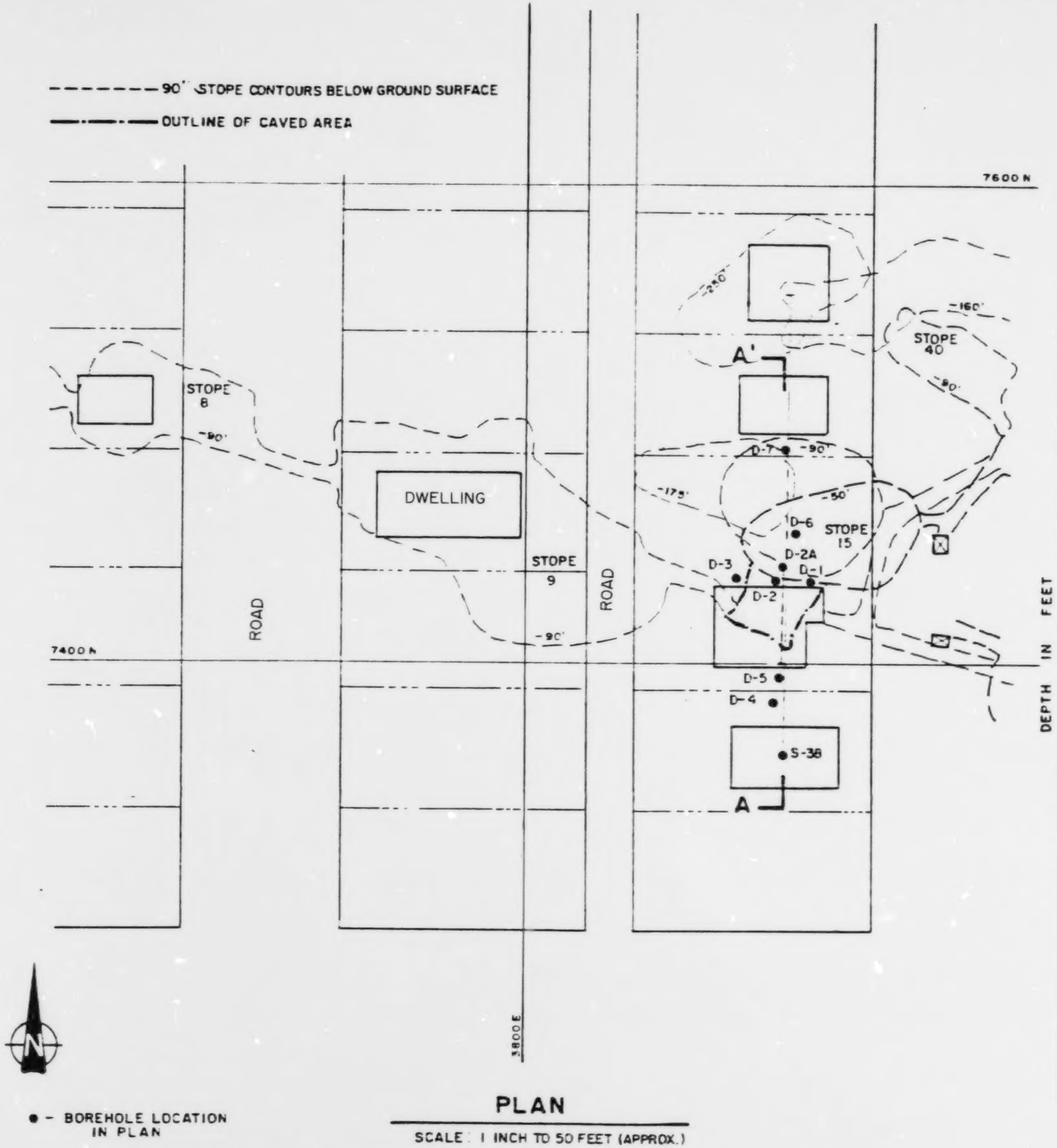

PLAN

SCALE: 1 INCH TO 50 FEET (APPROX.)

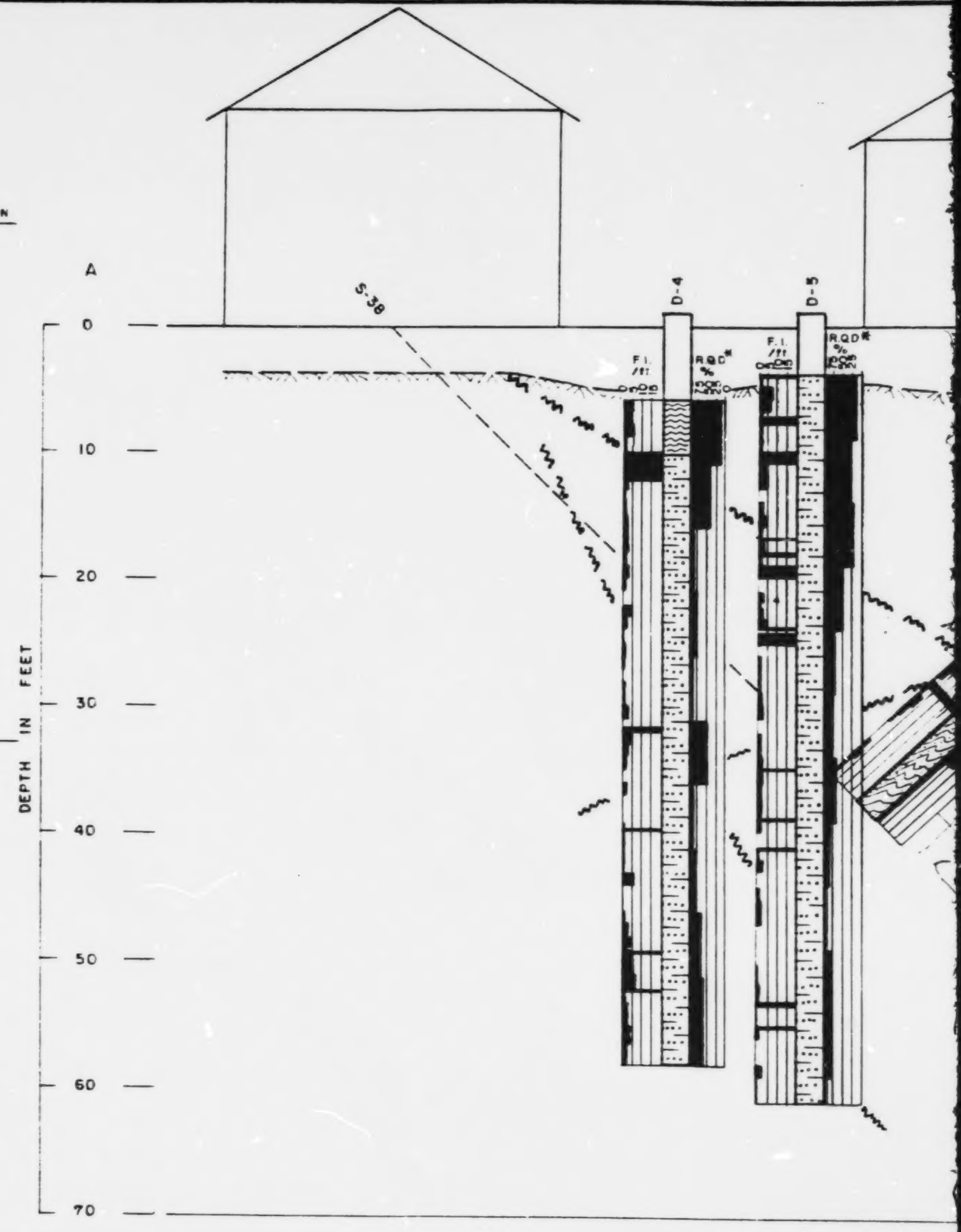

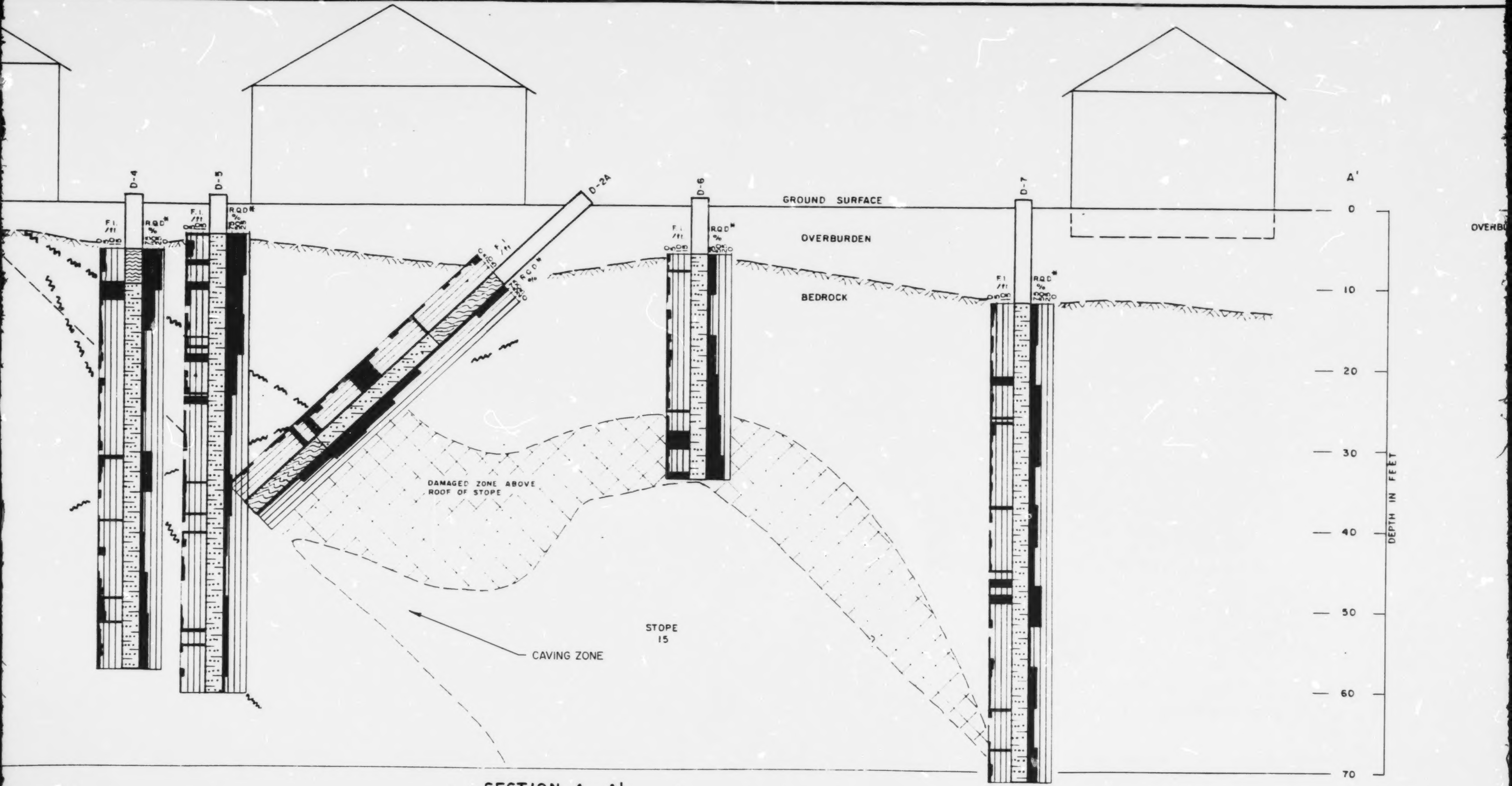

SECTION A - A'

SCALE : 1 INCH TO 10 FEET

MINE #26 DETAILED GEOTECHNICAL X - SECTION OF STOPING IN VICINITY OF PRIVATE DWELLINGS

FIGURE 3.28

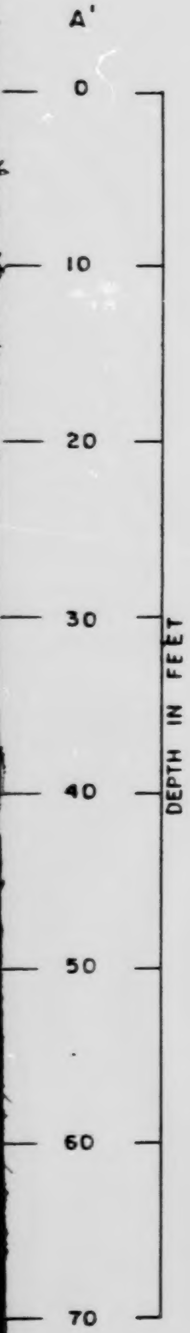

LEGEND

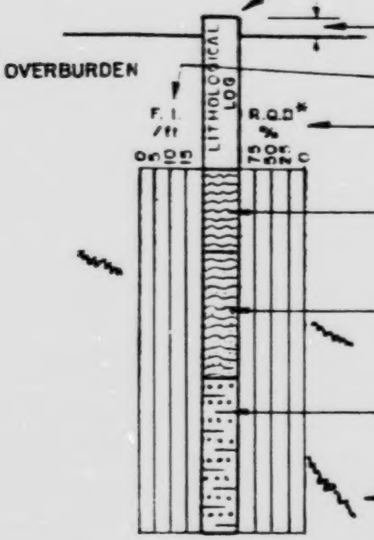

BOREHOLE COLLAR LOCATION IN SECTION

CASING STICK-UP (1 ft. above G.S.)

FRACTURE INDEX (fractures per foot)

MODIFIED ROCK QUALITY DESIGNATION,% (SEE NOTE 1 BELOW)

SCHIST (GREENSTONE); FAINTLY TO SLIGHTLY WEATHERED, WELL FOLIATED, DARK GREENISH-BLACK TO BLACK, MEDIUM GRAINED, BIOTITE - CHLORITE SCHIST

QUARTZITE; FRESH TO FAINTLY WEATHERED, THICKLY BEDDED, LIGHT GREYISH-WHITE TO GREYISH-BROWN, MEDIUM GRAINED, QUARTZITE

GREYWACKE/SILICEOUS GREYWACKE; FRESH TO FAINTLY WEATHERED, THICKLY BEDDED, WELL INDURATED, DARK GREYISH-BLACK TO BLACK, FINE GRAINED, GREYWACKE

INTERPRETED LOCATION OF SHEAR ZONE

NOTES

1. DRILL RUNS NOT SEPARATED DURING CORING OPERATIONS. MODIFIED ROCK QUALITY DESIGNATION PRIMARILY BASED ON A 5 FOOT LENGTH OF RETRIEVED ROCK CORE.

Date FEB. 8, 1990

Project 881-1739-3

Golder Associates

Drawn MHW

Chkd. JMS

Part 2
Analysis of Pillar Stability

Golder Associates

Section 4
Review of Design Methods

Golder Associates

4.0 REVIEW OF DESIGN METHODS

In this section of the report, currently available methods for evaluating surface crown pillar stability are each independently discussed. These comprise:

(i) empirical methods - either *rule of thumb* approaches, or more quantitative evaluations based on descriptive rock mass classifications,

(ii) analytical approximations using formulations for beams, plates and the like and,

(iii) numerical simulations using computer based modelling methods.

As with most rock mechanics problems, successful surface crown pillar design requires consideration of both the mechanical behaviour of the various materials present and an understanding of their geological structure. Evaluation of the stability of surface crown pillars is not as straightforward as many aspects of underground mine design because surface problems as well as rock mass weaknesses have to be assessed. This in turn reinforces the requirement that adequate data be obtained on crown conditions and that appropriate analysis procedures be utilized to assess stability.

4.1 Empirical Methods

Historically, *rule of thumb* design approaches, based on precedent practice, have been used as a guideline for optimising safe crown pillar dimensions. More recently, rock mass classification procedures have gained prominence as a rational method for categorizing the stability of surface pillars based on considerations of rock mass properties, including geological discontinuity conditions, groundwater and stress effects.

4.1.1 Rules of Thumb

In its most basic form, crown pillar design merely involves the selection of an appropriate pillar thickness, based on a thickness to span ratio, since the spans themselves, and the lengths of the stopes are largely governed by other mining considerations. Historical precedent is a major factor in this evaluation and provides a basis for the *rule of thumb* guidelines still in current usage.

This strong dependence on historical precedent is, in part, because acceptable analytical methods have not been available. In part, however, it is because the complexities of geometry and geology have not made it easy for the casual practitioner to select critical parameters appropriate to quantifying governing weaknesses. Recent publications (e.g.Bétournay, 1987) providing plotted compilations of thickness to span ratios used by the industry illustrate this problem. Figure 4.1 shows quite clearly:

- that other factors, i.e. details of geology, need to be taken into account and,
- that current *rule of thumb* guidelines are not being consistently applied, or that they do not provide consistent results.

4.1.2 Rock Mass Classifications

One possible approach to resolve the first uncertainty of current *rule of thumb* methods would be to make use of formal rock mass classification procedures. These recognize some of the missing geological data from the thickness-to-span ratio approach and thus could create a framework for better application of precedent practice.

A number of graphs have been produced by various authors including the originators of the NGI-Q and CSIR-RMR systems for evaluating stable spans (Figure 4.2). The database from which both classifications were developed, however, comes almost entirely from civil engineering openings located relatively deep within the rock mass. As such, the experience is not directly transferable to a crown pillar situation, unless detailed calibration to other stable and/or failed pillars in the same rock mass at shallow depth have been previously undertaken.

This necessity to restrict the use of classification systems to cases which fall within the confines of the data from which the classification was derived is a universal caveat which is all too often ignored. It is undoubtedly a contributing factor to the variability in predicted stable spans which can be derived from Figure 4.2 and from other references in the literature (e.g. Bieniawski, 1984, Hoek and Brown, 1980).

Barton had recognized this problem in 1976 and therefore undertook a careful examination of the Q-system to determine the specific requirements necessary to ensure that safe spans predicted by such graphs could be achieved in practice.

The requirements suggested for use of the Q-system for permanently unsupported openings are:

$J_n < 9$, $J_r > 1.0$, $J_a < 1.0$, $J_w = 1.0$, SRF < 2.5
with the following conditional requirements:

1. If RQD <40%, should have $J_n < 2$
2. If $J_n = 9$, should have $J_r > 1.5$ and RQD >90%
3. If $J_r = 1$, should have $J_n < 4$
4. If SRF >1, should have $J_r > 1.5$
5. If SPAN >10 m, should have $J_n < 9$
6. If SPAN >20 m, should have $J_n < 4$ and SRF <1

Obviously, considerable care is necessary if graphs such as shown on Figure 4.2 are to be used alone as a method for sizing a surface crown pillar, particularly since the database was derived from excavations at depth, and may therefore not be valid in some near-surface situations.

In spite of these limitations, the use of formal classification methods to reduce the complexity of geological conditions to manageable proportions is an attractive concept that has warranted additional work. As a first step in developing some more generic guidelines, specifically for crown pillars, an attempt was made to combine all available span to rock quality curves onto a single chart. The results for published civil engineering correlations are shown on chart (a) of Figure 4.3. A similar plot showing correlations based on the 1981 Golder Associates deep stope design approach and the modified method by Potvin (1988) for open stopes is included in chart (b) on the same figure. The similarities are encouraging.

Combining a *rules of thumb* approach to crown pillar design, based on precedent experience, with systematic application of appropriate methods of rock mass classification of crown rock conditions is considered to be one of the most important areas for improvement to the empirical treatment of surface crown pillar design.

In Section 6 of this report, this type of combination approach is followed as a means to evaluate the 237 individual case records included in the database presented in Appendix A.

As discussed later, these new correlations allow much better definition of the zone of marginal stability than the existing published data compiled on Figure 4.3. Several points however are evident even from Figure 4.3 and from attempts to cross-correlate *rule of thumb* precedents with span predictions based on more quantitative rock mass classification approaches, namely:

- at least two independent classifications of any rock unit should be completed as each of the classification methods emphasises or derates different features of the rock mass;
- both the NGI-Q and the CSIR-RMR classifications should be used for assessment of rock quality. Each should be used independently, then results compared to develop a breadth of appreciation for the rock mass being examined;
- for consistency of comparison, a stress reduction factor (SRF) of 1 should be used for the NGI system (medium stress, structurally controlled), and the CSIR system should not be derated for orientation effects;

- the resulting RMR and Q values should be checked against one another by plotting both sets of results as independent lines on charts such as shown on Figure 4.3. The two lines will provide bounds to an envelope or statistical error band defining the condition of the rock mass; and,

- the rocks comprising the wall and crown of the stope should be assessed independently and special consideration should be given to the contact areas between wall rocks and crown rocks. In the event that the Q index or RMR value for the crown is better than that for the wall rock, or better than that for the contact zone, then serious consideration should be given to use of the lower Q or RMR values for design purposes.

4.2 Analytical Approximations

Analytical approximations that may be used to assess crown pillar stability are based on the assumption that a crown pillar would behave as a continuous member (such as a beam or plate) or would act as an assemblage of discrete structural elements (Voussoir blocks).

Various formulae are available from civil and structural engineering texts that allow analysis of these types of structural models. They have, in general, been developed for analysis of masonry or concrete structures or other homogeneous isotropic man-made materials. In consequence, this imposes a severe restriction on their use for most rock mechanics applications. Invariably gross over-simplification of both the geometry and the mechanical characteristics of the rock mass are a necessary requirement for their application. In addition, the effect on crown stability of the stope beneath the crown pillar is generally ignored in such analyses.

4.2.1 Bending of Beams

Simple formulae to determine the flexural and shear resistance of beams provide a quick method to roughly ascertain a safe span for a given crown pillar in competent rock.

In applying beam theory to evaluate safe spans in rock, the following simplifications and assumptions, however, need to be made:

- the strike length of the rock beam must be greater than twice its span over the mine opening,

- the rock composition of the beam must be sufficiently consistent that it can be assumed homogeneous, isotropic and perfectly elastic,

- loads can only be applied normally to the longitudinal (strike) and transverse (dip) axes of the beam considered to represent the crown pillar (i.e. plane strain conditions prevail),

- the geometry of the rock beam and underlying opening must be essentially two dimensional and, of uniform, or only slowly varying cross-section, along the beam, and

- the rock mass forming the *beam* has to be assumed integral with the hangingwall and footwalls of the stope such that the beam can be considered as *rigidly attached* to the abutment rock areas.

With these conditions met, evaluation of safe spans can be made by considering two potential failure modes: tensile (flexural) failure and shear failure.

o Tensile Failure

For beams with large spans and limited thickness, the dominant mode of failure is the development of tensile cracking at the point of maximum tensile bending stress. These theoretical maximum tensile stresses occur in the immediate area of each abutment; and can be deduced as follows:

$$\underset{\text{(abutment)}}{\sigma_t\ (\text{max})} = \frac{\gamma \ell^2}{2t} + \frac{P\ell^2}{2t^2} \qquad (4.1)$$

where: t = thickness of beam
P = overburden load
ℓ = beam span
γ = unit weight of rock

Using equation 4.1, the maximum tensile fibre stress near the abutment zone within the rock beam can be calculated, and as shown on Figure 4.4, a series of 'design' curves can be developed for various overburden loadings for a range of beam thickness to span ratios. In order to evaluate stability the values of induced tensile stress plotted on the y-axis can then be compared with the available inferred tensile strength of the rock mass.

More complex beam configurations can be modelled with structural analysis computer packages such as P-Frame. Models can be developed incorporating non-uniform cross sections, varying material properties, etc. Much more representative geometry and loading conditions can thus be modelled and the effects of confining stresses can also be estimated.

The effect of horizontal confining stress has a major impact on tensile failure in simple beams.

Any *clamping* of the crown *beam* reduces tensile stress development significantly, as shown by the revised equation presented below.

$$\sigma_t \text{ (max)} = \frac{\gamma \ell^2}{2t} + \frac{P\ell^2}{2t^2} + \sigma_o \qquad (4.1a)$$

where: σ_o = in situ or induced compressive horizontal stress acting onto the sides of the crown beam.

- Shear Failure

For beams of relatively square cross section, i.e. with thickness to span ratios greater than about 0.2, shear failure, rather than tensile flexure dominates behaviour. For this condition, the available shear strength at any section along the beam can be determined using the following expression:

$$\text{Shear strength} = (\sigma_n \times d/2) \times B \times \tan \phi' + c' \qquad (4.2)$$

where:
σ_n = normal compressive stress on the beam section
B = width of the beam
d = beam thickness
ϕ' = friction angle on a potential shear plane/joint in the direction of the shear force
c' = cohesion on the same shear plane, acting over the area of the actual compression zone

For validity, this expression assumes that plane sections in an unloaded beam remain in plane strain after bending and that the neutral axis of the beam remains at mid-depth within the beam. This implies that the normal stresses at the top and bottom of the beam due to pure bending are equal in magnitude but opposite in sign, i.e. only compressive normal stresses are considered to contribute to the resistance to vertical shear.

This simple approach can also be extended to evaluate the effects on stability of pre-existing in situ horizontal stresses, or of additional compressive stresses induced by stress concentration in the abutments. Such stresses can be incorporated into the σ_n term in equation 4.2.

4.2.2 Arch Analysis

As a result either of the original excavation process or as a consequence of subsequent rock failure, the back of an underground stope may assume an arched shape. From the structural point of view, arching can allow larger stable spans for the same structural member thickness, provided that the abutments are sufficiently stable to sustain the lateral thrust and bending moment created by such arch action.

For arches of circular geometry and uniform cross section, established formulae for arch analysis are readily applicable. Thus calculation of shear stresses, bending moments and stresses and arch thrust can be carried out to allow some assessment of crown stability (Figure 4.5). However, in most crown pillar situations, the underside of the pillar may be of arched shape while the surface of the pillar could be approximately horizontal. Under these conditions, computer analyses, using programs such as P-frame are appropriate. In general terms, though, such analyses confirm the intuitive observation that a crown pillar with an arched shape is more stable than a crown pillar of similar thickness/span ratio with a stope crown that is essentially flat.

4.2.3 Plate Analysis

Stopes in most narrow vein situations (e.g. gold mines), are usually very long compared with their spans. The crown pillar can therefore be treated as a one way slab spanning the short dimension of the stope. In general, as indicated in Figure 2.2, slabs are considered to span in one direction when the ratio of long span: short span exceeds 4:1.

In many base metal mines, where ore bodies are more massive, the ratio of strike length to span of the stopes often ranges from 2:1 to 0.5:1. In these cases, it is appropriate to consider the crown pillar as a slab spanning in two directions. Where such two-way spanning occurs, it is also more appropriate to analyse the crown pillar as a plate supported on four edges rather than as a beam. The basic assumptions, however, are very similar to those described earlier for beams. Equation 4.3 provides the maximum fibre stress of a plate (at the centre of the long edge) due to two-way bending.

$$\sigma_x \text{ (max)} = \frac{6\,\beta\,q\,a^2}{t^2} \tag{4.3}$$

where: β = coefficient which varies with the span ratio
a = short span of the plate
t = thickness of the plate
q = loading on the plate per unit area

In order to examine the behaviour of a crown pillar as a two-way plate, a series of analyses were carried out to compute the maximum tensile stresses that could be developed in a crown pillar. The following range of dimensions and loadings were assessed:

short span = 20 m
long span = 20 to 60 m
thickness = 1 to 8 m
overburden depth = 0 to 20 m

Figure 4.6 shows the results which generally indicate that:

- beyond a long span to short span ratio of about 2, the maximum tensile stress stays approximately constant, however
- tensile stresses increase as the thickness of the crown pillar decreases and/or the overburden loading is increased.

In reality, the mode of failure of plates, (like the simplistic analyses with 2-D beams) will be largely governed by the homogeneity of the rock mass on the scale and extent of the stope crown pillar being considered. The geological structure at most mines, on a stope scale is very two-dimensional, particularly if the rock mass is schistose. Hence, plate theory would only become potentially usable in blocky rock masses with thin crown pillars. Even in these situations the method is of limited application as the kinematics of individual wedges and blocks within the overall stope crown is generally much more important than overall flexure of the crown itself.

4.2.4 Voussoir Beams

Rather than treating the crown pillar as homogeneous and isotropic, there is some merit in considering it to be composed of discrete blocks like bricks in a masonry arch. The theory of voussoir arching has been recognized and utilized for many years in bridge designs and masonry works as arching can greatly increase the load carrying capacity of a beam. At equilibrium, once arch action has developed, the lateral thrust is transmitted within the beam via an approximately parabolic curve to the abutments as illustrated in Figure 4.7.

The basic assumptions for Voussoir beam analysis are that:

- the rock mass is fractured (essentially along strike) by smooth subparallel breaks such that the crown pillar can be considered as a series of parallel blocks or plates,
- the crown pillar is essentially de-stressed in a direction normal to the fabric weaknesses, i.e. no clamping action exists between the individual plates,
- each individual plate is delaminated from its neighbour such that the overall beam can be considered a *no-tension* material, and
- the distribution of compressive stress at the centre and the abutments of the crown beam varies linearly with the depth of the voussoir beam section.

If the above conditions are satisfied and the beam remains stable, it can be considered to behave elastically and analytical simulation of failure behaviour can be appropriately analysed. Beer and Meek (1982) have identified three possible failure modes for rock beams considered as voussoir arches:

(i) shear at the abutment when the vertical reaction at the abutment (fixed end) is greater than the shearing resistance mobilized by the induced lateral load;

(ii) crushing at the hinges formed between voussoirs at the top central section of the beam and in the lower abutment contact areas, and

(iii) buckling of the beam with increasing eccentricity of the lateral thrust line, thus giving rise to a *snap-through* failure mechanism.

Based on examination of a variety of the case records, this type of model seems to be appropriate for a large number of situations where the ore body is essentially linear and broken up by numerous sub-parallel strike-oriented, steep angle joints or shears that separate discrete blocks or slabs of essentially unfractured rock.

Figure 4.8 illustrates clearly the change in voussoir beam behaviour with decreasing thickness to span ratio for three different rock mass qualities. It shows that if a roof beam has a high thickness to span ratio and weak discontinuity surfaces are present at the abutments, it is likely to fail in shear at the abutments. If the thickness to span ratio is low, then span stability is limited by compressive failure inducing crushing at the voussoirs and/or buckling of the beam. For beams composed of rock of low material strength, the tendency will be towards crushing or spalling at centre span or abutment areas. For thicker beams, where shear overstress may develop, any clamping action due to in situ confining stresses can aid significantly in improving the stability of the voussoir beam due to the increased normal stress acting on the joints.

4.2.5 Gravity and Structurally Controlled Failures

One of the more common mechanisms of crown failure is sliding or dislocation of individual blocks on unfavourably oriented pre-existing geological weaknesses. Identification of this type of failure mechanism (sometimes called a gravity or kinematic failure) requires a detailed knowledge of the geology and also consideration of the manner in which the geometry of the excavation interacts with the geology. Stress levels around the excavation are also a factor which can assist in identifying specific areas within which such failures are more likely than others; but the principal factors are geometry and geology.

Diagram A on Figure 4.9 shows an idealized two-dimensional section of a cross-cut in the sort of geology which could give rise to major kinematic failures in a blocky rock mass. In this situation a set of pervasive planar discontinuities dips obliquely to the geometry of the excavation and strikes approximately parallel to the crown axis. This type of weakness might be caused by bedding planes in a blocky sedimentary rock mass, or by major foliation discontinuities in a hard rock environment. A number of small joint features which are less continuous down-dip are shown cross-cutting this set. These cross joints effectively divide the rock mass up into a series or plates or blocks.

With differences in orientation of the geological structure, particularly dip with respect to the excavation shape, the stability of the crown may become affected to different degrees by the influence of such joints. For the sketch shown on Diagram A, the left-hand sidewall and the crown of the stope are both at risk. There is less likelihood of failure from the right-hand sidewall since the surface of sliding failure would largely involve the cross joints rather than the continuous features, and as these are secondary, they may be rougher and hence provide more shear resistance than the primary joints.

The scale of the individual blocks defined by the geology is also important especially where this *block size* is of the same order as the proposed excavation dimension. Quite clearly, as the spacing of the individual joints or discontinuities becomes small with respect to the dimension of the excavation, the opportunity for such failures increase but the size of individual block failures decreases. As this spacing becomes very small the type of failure progressively changes from block dropout to a form of ravelling where it may become more and more difficult to identify the structural control imposed by the geology. By contrast, as potential block dropouts become larger and the surface area on which sliding must take place increases, the roughness of the discontinuity surfaces plays a much more significant part in stabilization. Local variations in discontinuity orientation effectively become a part of the overall roughness of the individual surfaces and the tendency of the blocks to interlock becomes more significant.

In addition to stress effects arising from the shape of the excavation itself with respect to the crown geometry, stress changes due to the effects of proximity to surface or due to effects of adjacent mining could lead to loosening of individual blocks under some circumstances. These effects are particularly noticeable in the event of a steeply dipping tabular ore body where sliding failure of slabs can develop from the crown or sidewalls. These can be particularly large in areas where cross joints are throughgoing. Combinations of joint planes which are stable under the stress regime that exists at the time of initial drifting and development mining can become unstable as mining of the stope continues or as mining of an adjacent ore body occurs.

Recognizing the potential for kinematic failures requires an understanding of the structural geology of the area into which the stope has been excavated. Kinematic failures are most easily recognized in circumstances where regular patterns of geological discontinuities are evident. Such failures also occur, however, in more random geological settings where joint set orientations may vary over relatively short distances. In these situations, individual features which cross-cut regular fracture patterns often create locally difficulties.

Where the geology is regular, the possibility of kinematic failures can be evaluated relatively simply by means of a stereonet. A discussion of such methods can be found in a number of places in the literature, (ref. in particular, Chapter 4 of Hoek and Brown - "Underground Excavations in Rock" and texts such as "Methods of Geological Engineering in Discontinuous Rocks" by R.E. Goodman).

A typical stereonet plot for use in evaluation of a crown pillar from the viewpoint of structural stability is shown on Figure 4.9. The factors that need to be examined for assessing the stability of the crown to this mode of failure are:

- the shape and character of the rock blocks (possibly derived using the quotient RQD/J_n as an indicator of block size in centimetries - ref. Figure 2.3);
- the roughness, planarity and surface condition of the joints (ref. Figure 2.8); and
- the character of the joints and rock mass in the near surface zone, including effects due to weathering and other factors (e.g. blasting close to the stope crown).

Although such analyses can be carried out by hand using the methods discussed in Chapter 7 of Hoek and Brown, 1980, several computer codes are also available for solution of these problems. In order of increasing sophistication, these range from the simple underground wedge analyses presented in Hoek and Brown, 1980, through to the limit equilibrium key block solutions by Goodman and Shi and others.

4.2.6 Chimney Failure Analyses

The case of block sliding of the entire crown pillar on major planar bounding discontinuities is just a special form of gravitational sliding and can equally easily be treated by limit equilibrium methods.

Several of the larger and more dramatic crown pillar failures have, in fact, occurred by block collapse of a chimney of rock from the level of the stoped area through to surface. Such chimney failures seem to have developed either in very schistose rock masses where low shear strength foliation planes bound the limits of the chimney collapse on the one side and predominant slickensided cross joints form the other surfaces of failure. Some chimney caves are also reported within the core of fault blocks where the surfaces are again bounded by discrete low strength discontinuities. In some cases, water pressure effects (due to contrasting permeability characteristics of the shear planes with respect to the adjacent rock mass) may have influenced the development of the failure. In most situations, however, water has not been reported to be of major significance.

o Shear Controlled Chimney Failures

Absolute, shear controlled chimney failures are, by their very nature, less common than ravelling failures or minor instability initiated collapses, in that they assume no break-up and bulking of the rock mass during failure and full discontinuity-controlled shear behaviour of the entire four sides bounding the failure block. This type of chimney caving (known as plug subsidence) also requires an equally dimensioned void in plan beneath the crown into which the crown rock mass can slide. It thus tends to occur only in continuous schistose/foliated rock masses or in fault-bounded blocky rock mass situations.

Although these types of failures are infrequent, as the mechanism provides some reasonable measure of the behaviour of the entire crown zone, some limit equilibrium solutions have been developed to examine the problem (Brady and Brown, 1985, pp. 410 - 414 and Hoek, 1989). Figure 4.10 presents both the typical geometry assumed for such failures and the governing limit equilibrium solutions to determine the factor of safety against shear on the bounding surfaces of the failure block.

For the limit equilibrium analysis approach outlined on the diagram, it is assumed that sliding occurs when the total shear strength of the surfaces which define the boundaries of the pillar, are overcome by the weight of the pillar. For this situation, the total shear strength is considered to be dependent not only on the properties of the rock mass but also on the horizontal in situ stresses acting upon the pillar, compounded by any effects due to groundwater pressures within the pillar.

o Progressive Ravelling Type Failures

Two basic types of progressive, ravelling failures have been identified to affect crown stability conditions. These are:

- ravelling failure of the crown zone by break-down and disaggregation of schistose, or weak rock material, and
- unravelling and flexural hangingwall slabbing in moderately steeply-dipping ore bodies adjacent to a foliated, but competent footwall rock mass.

These types of failure are similar in nature to the condition created in block caving mining situations where it is the intention of the mining approach to disaggregate and progressively cave the rock mass.

4.2.7 Block Caving Analogies

Addressing the complexities of ravelling types of crown pillar failures can be regarded as the inverse of a block caving design. In the former, the objective is to maximise the stable span and minimise the stable thickness. In the latter, the objective is to ensure the development of an unstable span whatever the thickness. In this regard, the lower limits of caveability for a block caving concept might usefully define an upper limit for a stable crown pillar span.

Deiring & Laubscher, (1987), suggested a procedure for designing block caving stope layouts. This is based on a relationship between an adjusted Rock Mass Rating value and the hydraulic radius of the undercut required to initiate caving. The graph which they developed, shown on Figure 4.11, allows some appreciation of the likely onset of caving conditions for differing rock quality characteristics. The adjustments that Diering and Laubscher suggested simply reflect modifications to the standard CSIR-RMR rating for variations in dip of the ore body and geological structure, along much the same lines as the tunnel orientation adjustment originally suggested by Bieniawski (Figure 2.5).

For crown pillar design, it is instructive to consider some of the problems which have been known to occur in block caving operations as they help to define many of the reasons why crown pillars remain stable when, based on described geological conditions, they would be expected to have failed. Several block caving situations are shown on Figure 4.12. The desired caving form is shown on the cross section and on the upper longitudinal section on the right hand side of the page. The two lower longitudinals show problem situations when caving operations have stopped; for example, when natural arching of the roof span occurs (middle right drawing) or when funnelling develops (lower drawing).

Natural arching in caving situations can sometimes be prevented by excavating vertical boundary slots at the sides of the block cave. The presence of naturally weak features in these locations are therefore conducive to crown pillar collapse. In other circumstances, the presence of a central core of tougher rock which does not fracture as easily as the surrounding material, can stop a block cave. Such features clearly improve the stability of a crown pillar.

In most cases where the rock mass is relatively competent, the size and character of the cave zone and possible surface chimney collapse area depends only on the size of the undercut relative to the block size of the rock material. However, particularly in weak ore zone material, rather than an entire block caving, funnelling may develop through to surface (as shown on the lower right longitudinal on Figure 4.12). This type of caving, which may be as rapid as a plug or chimney collapse, is a common problem in schistose rock where stope spans are frequently too wide for even temporary stability. The onset of caving, even in these situations, can be evaluated either from the chart presented on Figure 4.11 or from considerations of the dimensions of the maximum credible rubble arch that can be developed for the block size of the rock fragments, (Coates, 1981).

It is noteworthy that self-caving stope operations that have naturally occurred (and often uncontrollably) tend to be associated either with very blocky ground conditions or with schistose rock masses (i.e. within the "readily cavable zone" of the Diering and Laubscher spectrum, Figure 4.11).

Assessing the geometry of the failure zone induced by progressive caving-type failures in real rock mass environments is difficult, but some guidelines can be inferred from studies of bulk flow of materials in silos and other containers. Model studies of sands and small fragments in cylindrical and rectangular containers has been found to have direct application to design of block caving and sub-level caving mining layouts (Janelid and Kvapil, 1975, Free, 1970).

Available modelling results make it apparent that no simple mathematical function can adequately describe the geometry of the actual failure zone, due to the many variables affecting its shape (such as material block size, broken and intact material properties, dip of the ore-body, scale of the undercut and cave opening and in situ confining stress conditions). Relationships of material flow patterns derived from these physical models, however, make it possible to predict the extent of propagation of a caving stope. On the basis of these studies and using data from actual mine behaviour, an approximation of the geometry of failure of the rock mass can be derived. This can then be extended to examine the onset of caving as a crown pillar design approach.

The basic premise is that the flow of material in actual caving operations tends to follow the same ellipsoidal draw patterns as seen in model studies. In some respects, the drawpoint analogy models crown collapse by progressive upward ravelling failure. To evaluate the point where the natural stability of a given crown pillar breaks down and the stope becomes self-caving to surface, it is convenient to examine the relationships of the draw ellipsoid (or ellipsoid of motion, as defined in Figure 4.13) to the shape of the limit ellipsoid shown also on the same diagram. The draw ellipsoid is defined as the envelope bounding the source of all material, pre-bulking, that falls from the crown zone into the stope. The limit ellipsoid defines the zone of broken material that has expanded and moved down under gravity to fill the void left by drawing of the fallen rock from within the draw cone, the height and width of which is defined by the volumetric relationship between the limit ellipsoid and the ellipsoid of motion (Figure 4.13).

If more material is removed from the stope drawpoints (i.e. during ongoing mining), the ellipsoids of motion and limit expand, as illustrated on Figure 4.13 by the sequence of events from Stage 1 to Stage 2. If the limit ellipsoid extends to ground surface, extensive surface subsidence begins to occur, depending on the competence of the hangingwall and footwall. Such conditions can be disastrous where flow sensitive overburden exists over the ore zone at the bedrock surface.

The principal relationships which have been developed to describe the extent of the limit ellipse bounding the broken zone of caving rock are expressed in terms of the eccentricity (ϵ) relative to the limit and motion ellipsoids, (Janelid and Kvapil, 1966, Free, 1970, Just and Free 1971); i.e.

$$\epsilon = \frac{1}{a}\sqrt{a^2 + b^2} = \sqrt{\frac{3W^2}{4h^2} - \frac{6V_e}{h^3} + 1} \qquad (4.4)$$

where:
a = semi-major axis of the draw ellipsoid
b = semi-minor axis of the draw ellipsoid
W = width of outlet (stope span)
h = height of draw, $= 2a$
V_e = volume of ellipsoid of motion $= 4/3\ \pi a b^2$

When applied to crown pillar collapse, determination of the eccentricity of the two ellipsoids demands that information be obtained on a number of factors including width of the stope crown opening, characteristic rock block particle size, and an approximate volume for the available open excavation space below the caving crown. Some inferences must also be made regarding typical ellipsoid eccentricities, specifically by reference to known empirical observations.

From model studies for design of sub-level mining operations, it has been found that actual eccentricities range between 0.92 and 0.98 for models that match field draw heights in excess of 15 m. Further, based on model and silo studies of granular materials, the volume of the ellipsoid of limit has been consistently found to be about 15 times greater than the volume of the draw ellipsoid. Therefore, using these empirical factors in the geometrical relationships for eccentricity given in equations 4.4, a simple relationship can be postulated between the approximate height of the limit ellipsoid and that of the draw ellipsoid. Based on these values, the height of the limit ellipsoid works out to be roughly 2.5 times the height of the draw ellipsoid. An approximation for the height of potential caving for any given rock mass above a mined-out stope, can therefore be made if the volume of the draw ellipsoid is determined. This required some knowledge of rock mass quality, and hence of block size and potential bulking characteristics for the rock mass of concern.

Using this approach it becomes feasible to rationalize limit zones if it is assumed that the ellipsoid of motion and hence that of limit are generated simply by the falling out of caved material from the crown area into a previously excavated open stope, and that 40 per cent bulking occurs as the broken rock falls into the stope. Thus, depending on the volume of available underground space and the span of the caving crown, it is possible to compute the theoretical height of the limit ellipsoid, thus defining the extent of the height of caving ground. This has been graphed on Figure 4.14 with respect to rock quality Q for a variety of stope heights, based on the relationship, Span = $4.4\ Q^{0.32}$ given on Figure 4.3.

It should be appreciated that the relationships plotted on Figure 4.14 provide only a generic estimate of the height of potential cave development, as such caving is rock mass dependant. Caving in a given rock mass may not even develop, due simply to rock block size. In this regard, it should be appreciated that these concepts of a flow ellipsoid are based on flow of relatively uniform material, thus structural variations in the rock mass may constrict cave development. In fact, caving will not occur where there is a lack of individual structural weaknesses. The graph on Figure 4.14 is therefore limited in application to those conditions where caving is suggested by the curve on Figure 4.11. Further, the model test results for predicting caving are generally based on observations of fairly homogeneous material. The interlocking effects of blocks of various assortments of sizes in a caving stope might invalidate the flow ellipsoid concept. Nevertheless, this approach holds promise for at least a preliminary determination of caveability and for allowing estimates to be made of maximum crown thickness and span dimensions for a particular rock mass. Further, the method in fact, checks very closely with estimates of actual caving at Mine #28 (see Figure 3.24).

4.2.8 Analytical Methods Summary

Many of the presented analytical approximations are potentially suitable for crown pillar stability evaluation and some have distinct application under particular circumstances. Although the assumptions pertaining to each procedure are in some cases restictive, in many situations application of these approaches provides considerable insight for rationalizing crown pillar designs.

The conditions under which each individual procedure may be applicable, and the important uses of each procedure are summarized below:

- Analytical approximations, in general, focus on the crown pillar as a single structural element. The interacting effects between the crown pillar, the stope and the surrounding rock are ignored. They should therefore be used with caution and discretion. However, they do provide a means for conducting a quick first assessment of crown pillar stability and a ready means for rapidly conducting a wide range of parametric estimations. The limitations of their applicability, however, should be duly recognized.

- The analytical procedures for beams, plates and arches offer simple and quick assessment of crown pillar stability with respect to tensile and shear failures. In situ stress effects can also be readily included in the analysis. It should be noted, however, that the intrinsic assumption of homogeneity in the beam material, in most cases, over-simplifies actual geological situations.

- Beam, arch and plate analyses are potentially useful in situations where the rock mass is intact (free of throughgoing adversely oriented joints) or has a sufficient number of interlocking discontinuities such that it behaves as a *jointed* rock mass. A rock mass with a set of predominant discontinuities will be controlled by the kinematics of individual wedges and blocks rather than the flexural behaviour due to beam bending effects.

- The voussoir beam formulation features a concept of interaction between discrete blocks. It takes into account a set of prominent joints parallel to the strike of the ore zone which separates the crown pillar into discrete blocks. It therefore has potential application to evaluating crown pillars in slabby or schistose rock. In situ stresses (if known) can also be included in the stability evaluation of the crown pillar. As each voussoir (block) forming the crown beam is considered to be homogeneous, secondary cross jointing through the crown may constrain the application of this procedure to other than strike-oriented discontinuity situations.

- The procedure of rock mass characterization, using established rock classification systems such as the CSIR RMR and the NGI-Q index, is applicable to derivation of rock mass parameters for use in almost all of these analytical formulations where the crown pillar rock mass is considered as a "jointed" element.

- Two forms of caving analysis are applicable for evaluation of crown pillars within rock units which are susceptible to this type of failure mechanism. Chimney caving or plug failures which are analyzable using limit equilibrium methods can provide considerable insight into controls on failure geometry. The concept of the limit and draw ellipsoid can also aid in assessing progressive failure situations.

4.3 Numerical Procedures

With the ever increasing range of computer programs available for use in analysis of stress conditions adjacent to and around mined openings, it is remarkable how few of the codes are directly applicable to evaluation of problems involving the complex geometrical characteristics of many surface crown pillars.

Straightforward elastic stress analysis, even for complex geometries, is relatively easily accomplished with most of the available codes (such as those based on boundary element and/or finite element or finite difference formulations). However, when attempting to model the post-failure behaviour of surface crown pillars or crown pillars of extreme geometrical shape, the capability of available codes is limited and in many cases the results are very sensitive to choice of input parameters and accuracy of model geometry.

Further, very large strains and even significant block displacements occur in a large number of crown pillar collapse situations, prior to actual failure. It is therefore essential that appropriate computer codes be used, otherwise severely biased results may be obtained. Currently, two commercially available 2-D computer codes are available for modelling large displacements. The two codes: FLAC (Fast Lagrangian Analysis of Continuum) and MUDEC (Micro Distinct Element Code), both can provide elastic solutions, and can model post-failure processes and compute the associated strains and displacements. In the case of MUDEC, large interblock movements can also be modelled.

In addition, based on field assessment, it has been recognized that in some crown pillar situations, crown stability is significantly influenced by complex three-dimensional geometrical effects. In such situations, it is unrealistic to simply analyse the problem in two dimensions. However, at the current state of the art, many three dimensional stress analysis packages are cumbersome to utilize for undertaking more than simple examination of the 3-D stress conditions around a complex crown geometry. Even for relatively simple geological and geometrical situations, meshing of a finite element grid for 3-D modelling can be rather expensive and time-consuming. Thus, until 3-D codes can be made more versatile, only limited application is currently seen for such sophistication. For the present, reliance will have to be largely placed on use of superposition and multiple 2-D analyses to facilitate evaluation of complex 3-D situations.

Nevertheless, despite these limitations numerical procedures hold great promise for ultimately improving our insight into crown stability controls.

4.3.1 Boundary Element Method

Use of the boundary element method for stress analysis of the rock mass around underground openings has been well established as a viable approach over the last five to ten years. Most commercially available boundary element codes assume that the rock mass surrounding the opening is an isotropic homogeneous medium. As the solution is very fast, this approach offers a means for rapidly evaluating two dimensional stress conditions around both near-surface and/or deep underground openings.

The latest free-surface version of the boundary element program EXAMINE, developed at the University of Toronto, was extensively used on this project to examined the stress environment around most of the documented crown pillars. The program allows three options of in situ stress input:

Case 1 - gravitational vertical stress with a given ratio of horizontal to vertical stress, (K_o)

Case 2 - elevated horizontal stress in the very near surface zone plus gravitational stress conditions with a given K_o at depth, and

Case 3 - uniform horizontal and vertical stresses with a constant K_o ratio

Cases 1 and 2 generally represent the in situ stress condition for most crown pillar situations, while case 3 tends more to represent in situ stress conditions at depth.

To illustrate the application of the boundary element method, two mines in particular were analysed: Mine #26 and Mine #22. In situ stress conditions pertaining to case 1 and case 2 with 8 MPa elevated horizontal stress (Herget, 1980) were examined. A K_o value of 1 was assumed, representing a probably conservative in situ stress state for the surface crown pillar situation.

- Mine #26

For Mine #26, the thickness to span ratio of the crown pillar is about 0.5. Figure 4.15 shows computed contours of the major and minor principal stresses (σ_1 and σ_3 respectively) around the stope and in the surface crown pillar zone for case 1 a gravitational stress field. (Note: the input parameters are shown on the margin of the Figure). The results indicate that stress concentrations occur within the surface crown pillar and near the bottom of the stope. In general, the major principal stress within the crown pillar is sub-horizontal and compressive. However, there is a zone where the minor principal stress is tensile over a large area beyond the hangingwall and into a limited area beyond the footwall.

Figure 4.16 shows the corresponding stress contours for the case 2 input stress condition (elevated horizontal stress in the near-surface zone). The general trend of the stress distribution for cases 1 and 2 is similar but the stress concentration effects are more pronounced for case 2. Further, the area of tensile minor principal stress increases in the footwall zone for the case 2 in situ stress condition.

o Mine #22

For modelling the two level stope geometry of Mine #22, prior to crown failure the entire near surface zone including the surface crown pillar and the sill pillar between the two stopes was evaluated as shown in Figure 4.17. The thickness to span ratio of the surface crown pillar above the smaller, upper stope is about 1:1, and as shown on Figures 4.17 and 4.18, the stress distributions for the case 1 and case 2 input stress states respectively are similar to those for Mine #26. Stress concentrations again occur in the surface crown pillar zone with the effects, for the case 2 input stress condition being more pronounced. As with the Mine #26 analyses large zones of tensile minor principal stress are also predicted to exist, notably for the case 2 input stress condition (Figure 4.18).

Several salient points can be noted from the above results:

- For the assumed in situ stress states, clamping stresses are predicted to exist in the crown pillar due simply to stress concentration effects (provided that the rock mass is sufficiently competent to transmit such stresses).
- The predictions suggest that the hangingwall, and, to a lesser extent, the footwall are de-stressed in the minor principal stress direction but sufficient confinement still exists in the major principal stress component. While such conditions may not necessarily signify failure, there is potential for the initiation of tensile delamination on joints or schistocity in the plane of the stope strike, ie., normal to the direction of the minor principal stress.
- With an assumed elevated horizontal stress in the near-surface zone, a significant increase in stress concentration occurs within the crown pillar compared with a straight gravitational stress field condition. In addition, a larger zone of tensile minor principal stress develops alongside the stope.

It is important to note that these boundary element results suggest that the presence of any significant stress concentration in the near surface zone of a surface crown pillar would, likely enhance the stability of the crown pillar by providing significant clamping (confinement) to the crown rock mass. It is also noteworthy that elevated stresses could theoretically exist in the crown pillar due to stress redistribution alone. This may account for the stability of some very thin crown pillars. Unfortunately, it is impossible to verify this inference as currently there is no stress measurement data in the crown areas any of the mines studied. The inclusion of stress measurement programs in crown pillars in any future study would certainly enhance the evaluation procedure for determining crown pillar stability.

In general, because the boundary element method provides a quick and reilable tool for analysing two dimensional stress distributions around underground openings, it has wide applicability. However, certain precuations must be taken to ensure that the code is capable of realistically accounting for free surface conditions for use in assessing crown pillars. Further, when utilized for modelling surface crown pillars and stopes it must be appreciated that the actual rock mass can only be approximately represented by a homogeneous medium, thus care again needs to be taken with parameter selection. Currently, codes allow incorporation of either the Mohr-Coulomb or Hoek-Brown failure criterion to provide an assessment of rock mass strength properties. The codes are however, limited in the capability of readily modelling different material parameters and in handling post-failure stress transfer effects such as realistically can occur in a complex crown pillar situation.

4.3.2 Finite Element and Finite Difference Methods

Both finite element and finite difference methods are capable of handling inhomogeneity in the rock mass much better than is possible with the boundary element method. The finite element method, however, assumes small strain in its formulation, whereas with finite difference codes such as FLAC (Fast Lagrangian Analysis of Continua) modelling is possible for cases where large strains or significant displacements develop. As most of the case records for failed crown pillars exhibited substantial displacement prior to failure, stress analyses using FLAC were undertaken to attempt to back-analyse failure development.

Within the finite difference code for FLAC, five different constitutive models can be utilized:

1. Elastic	the rock material is assumed linearly elastic, homogeneous and isotropic,
2. Anisotropic	the rock is assumed elastic but transversely isotropic,
3. Mohr-Coulomb	the rock material is assumed perfectly elastic below peak strength and perfectly plastic after yield, and the material follows a Mohr-Coulomb failure criterion up to its yield,
4. Ubiquitous	the material is assumed essentially as a Mohr-Coulomb solid with embedded planes of weakness. Failure can occur within the solid or along the weakness planes, and
5. Strain-softening	the material is assumed to follow a Mohr-Coulomb failure criterion, however, once the material reaches peak strength, critical post-peak behaviour of the material can be defined.

With the explicit finite difference calculation scheme employed in the formulation of FLAC, the code is well suited for modelling progressive destabilization. For crown pillar work the ability within the FLAC code to continually update the co-ordinates (configuration) of the finite difference grid as stress changes occur is of considerable advantage to assessing failure behaviour. As the code allows ready visual presentation of the distorted shape of any stope geometry as failure develops, it is particularly useful in providing insight into initiation of failure and into propagation mechanisms.

o **Mine #42**

Mine #42 was analysed using the FLAC model to assess the code's applicability to crown pillar assessment. The in situ stress condition was assumed to be gravitational and the input parameters for the rock mass were set as follows:

Bulk modulus (K) = 24 GPa
Shear modulus (G) = 40 GPa
Cohesion (c′) = 0
Friction angle (ϕ') = 40°
Stress ratio K_o = 1
Density(γ) = 2700 kg/m^3

The geometry of the stope and the crown pillar is shown in Figure 4.19 which illustrates the results of the initial elastic stress analysis. The stress trajectories and the zone where tension occurs in the minor principal stress field are also shown. The results for Mine #42 are consistent with those computed using the boundary element method for Mine #26 which has a similar geometry (Figure 4.15). The general pattern of stresses are similar for both analyses and the extent of the zone of tension in the minor principal stress field is also similar. As the two numerical methods give comparable results this gives confidence for inter-changeability in the use of these two methods for evaluation purely of elastic stress conditions.

FLAC, however, offers post-failure stress analysis by transferring excess stresses from failed elements to the adjacent elements and redistributing the unbalanced stresses in an iterative manner until equilibrium conditions are again reached. As this facility could be of considerable value for assessing stress transfer effects during failure, an attempt was made to analyze the post-failure conditions for the Mine #42 crown pillar. A Mohr-Coulomb model with the following three sets of parameters was analyzed:

(a) ϕ' =40°, c′ =o, σ_t=0 (no tension cut-off)
(b) ϕ' =63°, c′ =1.25MPa, σ_t=0 (no tension cut-off)
(c) ϕ' =63°, c′ =1.25MPa, σ_t=1MPa (no tension cut-off)

These parameters were chosen specifically to assess the sensitivity of the computed results to the selected model behaviour even though it is recognized that set (a) might be totally unrealistic for the rock mass at Mine #42.

a) Post-Failure Analysis ($\phi' = 40°$, $c' = 0$, $\sigma_t=0$)

Figure 4.20 shows the displacement predicted from the model after stress transfer in the post failure analysis. Large displacements of up to 2.5 m. are computed for the footwall side of the stope associated with development of a curvilinear failure surface. An extensive near-surface zone of tension is also predicted as shown in the lower diagram on the Figure.

It is considered that some of the effects shown on Figure 4.20 basically stem from idiosyncrasies within the numerical computation which relate to the behaviour of the rock mass model during post-failure analysis for the specified set of model parameters. By virtue of the specified characteristics of the modelled rock mass with a "no tension" cut-off, $c' = 0$ and an elastic, perfectly plastic, post-peak behaviour, the material is considered by the model to have failed once one of the principal stresses goes tensile. The excess stresses are then redistributed to adjacent elements in a progressive manner. In view of the large tension zones, adjacent to the footwall of the stope (see Figure 4.19), the numerical stress transfer process for this model has been extensive and plastic displacements have continued to take place in those elements undergoing stress transfer. As more elements have become overstressed due to the stress transfer process, the resulting plastic deformations have created excessive displacements of the footwall as shown on Figure 4.20.

Examination of the model results also show some inconsistencies in the displacement vectors. There may, in fact, indicate numerical instability in the displacement computations. On the other hand, as there is relatively little displacement of the rock mass on the hangingwall side, these displacements may again result from stress transfer effects due to the fact that any excess stresses that persisted in the vicinity of the hangingwall have become redistributed in order to reach equilibrium conditions.

The fact that no evidence of this type of failure mechanism is apparent at Mine #42 suggests that this type of post-failure model, is inappropriate for representing the behaviour of relatively competent rock masses.

b) Post-Failure Analysis ($\phi' = 63°$, $c' = 1.25$ MPa, $\sigma_t = 0$)

As Mine #42 is classified with an RMR in the 70 to 80 range and the hangingwall and footwall rock masses surrounding the tabular, narrow vein ore zone are competent, (see Appendix A), a c′- ϕ' Mohr-Coulomb FLAC model was utilized to check the program's applicability to evaluate conditions for a no-tension situation, but with higher strengths.

Post-failure analyses identical to those run under case (a) were repeated using a revised set of parameters, and the calculated displacements and stress distributions are shown on Figure 4.21. Large displacements are predicted at the hangingwall and the trend of the displacement vectors are generally consistent with expected behaviour. The tensile zone shown on Figure 4.20 has been eliminated as shown in the lower diagram in Figure 4.21, due primarily to the "no-tension" behaviour specified for the model. However, large displacements are still predicted which indicate potential instability in the hangingwall. Again, as there is absence of any significant hangingwall instability at the mine site, it suggests that these input parameters may still be too conservative for modelling the actual rock mass conditions at the site.

c) Post-Failure Analysis ($\phi' = 63°$, $c' = 1.25$MPa, $\sigma_t = 1$MPa)

The computed displacements and stress distributions for this analysis are shown on Figure 4.22. The displacements are small, but the tensile zone in the footwall is still present, albeit of a slightly reduced extent, as the specified tensile strength in the model has allowed tensile stresses to be sustained with the rock mass. Hence stress redistribution in this model run, has only occurred in elements where the tensile stress has exceeded the specified tensile strength. It is apparent from the results that with these input parameters, only a modest stress transfer takes place within the rock mass. Hence the tension zone remains relatively unchanged and the resulting displacements are small, and consistent with field based expectations.

The problems inherent in reaching correct parameter matching in these modelling runs is clear from the output plots and the summary given on Table 4.1. These results reinforce previous analytical concerns that correct parameter selection is critical to achieving rational results that match reality. Examination of Figures 4.19 through 4.21 suggest that the parameters used in the initial runs were overly conservative. Matching of actual results to observed conditions suggests that both cohesion and a tension cut-off condition are required. For this case, values of $c' = 1.25$ MPa, $\phi' = 63°$ and $\sigma_t = 1$ MPa appear to provide consistent results with the observed behaviour of the rock mass.

This series of comprehensive parametric analyses, however, demonstrates that it is possible through careful back-analyses to ascertain appropriate rock mass strength parameters for most actual rock environments. It is recognized, however, that other factors, such as the magnitude of any in situ stress within the crown zone could also affect the outcome of the results. The need to verify in situ stress conditions for such situations is again key to the interpretation of the analysis results.

While this type of homogenous Mohr-Coulomb failure model allows quite useful appreciation to be gained of rock mass behaviour, it is limited by the intrinsic continuum approach and thus not flexible enough to allow examination of the influence of prominent discontinuity sets within the rock mass. As block movement is commonplace at failure in crown pillar zones, evaluation of these areas for marginally stable or failing cases can best be undertaken with a discrete block code model such as MUDEC, the MICRO Distinct Element Code developed by ITASCA in the United States.

4.3.3 Distinct Element Method

The distinct element method has been formulated based on a discontinuum approach to simulate jointed rock masses as assemblages of blocks. Block interaction is analysed through the stresses and displacements at the common cover and edge contact points, while the discontinuities themselves are modelled by boundary behaviour at block intersections.

The MUDEC code used in this study allows the modelling of 3 different joint behaviours:

1. point contact; with elasto/plastic material and a Mohr-Coulomb failure criterion,
2. joint area contact; with elasto/plastic material with Mohr-Coulomb failure criterion, and
3. same as #2, except that cohesion and tension are ignored after peak strength has been reached.

Within each of the discrete blocks defined within the model, the MUDEC program subdivides them into triangular finite difference zones using much the same internal algorithm as FLAC. Two constitutive models can be used within the blocks:

1. linearly-elastic and isotropic, and/or
2. Mohr-Coulomb elastic/plastic failure

Initial modelling, using MUDEC, suggested that by use of this code for a number of cases, reasonably accurate correlations could be made between model results and reality. In consequence, as a means to develop a greater understanding of failure mechanisms and modelling capabilities, a series of parametric studies were undertaken of a conceptual range of typical crown pillar geometries. The cases analysed and the parameters used are summarized in Table 4.2 while the schematic layout of the stope and the crown pillar configuration that was modelled is presented on Figure 4.23. Two rock mass conditions within the five-point CSIR scale of descriptions; namely, poor and good, with CSIR-RMR values of 23 and 65 respectively were selected as base cases for the evaluation.

The input parameters for these comparative analyses were developed using the methods discussed in Section 2 of this study and the in situ stresses were based on gravitational vertical stress and a K_o value of 1.

For each of the cases analysed, stresses and displacements were accumulated until sufficient computation steps had been taken to achieve equilibrium. This was verified by tracking the displacement of a particular element at a critical boundary (e.g. an element at the centre of the crown pillar). Continued displacement after a large number of computational steps signified that the geometry was unstable, while equilibrium was defined as the point when no further displacement of the element occured.
Each of the 24 geometry situations examined was run until sufficiently stable output results were obtained or until failure trends were apparent. A matrix table of the various runs undertaken is included as Table 4.2 and the results of the analysis are summarized on Tables 4.3 and 4.4 for the poor and good rock mass conditions, respectively. The behaviour of the crown and wall rock zones, for each case evaluated are summarized on these tables.

Three classic behaviour patterns were evident from the modelling, as shown on Figure 4.24.

This drawing also illustrates several important points which affect crown pillar stability:

(a) Crown pillars with a thickness to span ratio (T/S) of 0.15 are generally de-stressed and are unstable for the case of shallow stope geometries even for good rock conditions. Although they fail for poor rock conditions for steeply inclined stopes, they are marginally stable with better rock conditions (see for example Figure 4.25).

(b) Stopes with 45° inclination are potentially unstable regardless of T/S ratios and rock condition (see Figures 4.24 and 4.25).

(c) Most of the crown pillars are stable when a compression arch can be developed through the pillar (see Figure 4.24). For pillars with stopes at shallower dips (45° to 60°), or where crowns are thin, the compression arch may not be fully developed (see Figure 4.25). Under these circumstances, large progressive movements are predicted to occur in the hangingwall and in the crown pillar, and, in consequence, this leads to instability of the crown, and ultimately to failure.

(d) With dipping stopes, most of the initial movements occur in the hangingwall, then blocks release within the crown pillar. Very little movement seems to occur of the footwall blocks. For stable crown pillar situations, movements stabilize after some initial block adjustments such that no further displacements occurs. If the crown becomes unstable, rock block movements continue, ultimately leading to instability of the entire crown pillar zone. This progressive sequence and mode of failure predicted by the model seems generally consistent with observed instability behaviour for most of the failed crown pillars.

As rock mass parameters are common throughout each of the two sets of rock mass conditions analysed and as the various cases only reflect changes in geometry, the results highlight the relationship between crown geometry and overall stability. These parametric analyses also provide considerable help towards understanding the mechanisms of failure. In addition, they illustrate the potential of using this program or the more sophisticated version of this program (UDEC) to model the complex rock mass conditions existing in many surface crown pillars.

4.3.4 Three-Dimensional Stress Analysis

Because of the complex geometry of a number of the crown pillars, there is often a need to examine stress conditions in three dimensions. However, due to limited financial resources for this research project, only a limited programme of three-dimensional modelling was carried out. A solid block model of only one mine (which exhibited particularly complex geometry) was developed to examine stress conditions throughout the crown pillar zone. This modelling was undertaken by the Rock Engineering Group at the University of Toronto. The I-DEAS Solid Modelling/Finite Element Analysis package, produced by the Structural Dynamics Research Corporation (SDRC), was used for building and numerically analysing the crown geometry of Mine #29.

The geometry of the model is illustrated in Figure 4.26 in which the stopes are represented by the pink and green openings with the blue block representing the rock mass. The finite element mesh for the model is shown in the lower photograph on Figure 4.26.

To reduce the number of elements to be used in the model to a reasonable number, the stopes were assumed to be symmetrical about the vertical, y axis; i.e. only the left half of the stopes were included in the block model shown on Figure 4.26. The rock mass was assumed to be isotropic, elastic and homogeneous with an in situ vertical stress based on a gravitational stress increase with a K_o value of 1.

The results from the modelling (presented as various colour shades corresponding to increasing stress levels around the stopes) are shown on the upper and lower diagrams of Figure 4.27 for the major and minor principal stresses respectively. Figure 4.28 shows a cut-away section of the model illustrating the stress distribution along the underside of the crown pillar. The following points can be noted from examination of the stress distributions:

(a) Zones of marked tensile stress occur along the top supported edge of the crown pillar (see Figure 4.27). (Positive stress values indicate tension in Figures 4.27 and 4.28). Similarly, the underside of the crown slab is also in tension at the centre (Figure 4.28). The magnitude of the predicted maximum tensile stress is about 3.6 MPa at the centre of the crown with the rest of the crown either in slight compression or somewhat de-stressed.

(b) At some distance from the open stopes, the rock mass is in compression as anticipated.

The presence of tensile stresses in the crown slab is consistent with the typical stress pattern for a plate supported on four edges. The location of the higher tensile stresses within the crown predicted by the model is also consistent with the position of a crown breakthrough that occurred at the mine site.

Although the analysed problem has been over-simplified to minimize computational time, it shows that there is potential for the use of three-dimensional analysis to study complex stope and crown pillar geometries. However, for 3-D modelling considerable sophistication is required in order to successfully characterize the geometry and geology of a real situation.

In some cases, though, this may provide the only method of realistically determining the stress distribution in a crown area. Currently, however, one of the most significant limitations on the use of 3-D methods is the requirement to input a considerable amount of geometric data in order to accurately define crown geometry. Further, it may be prohibitively expensive for mines or small institutions to conduct such sophisticated methods of crown pillar analysis on any sort of regular basis. In this light, it is currently considered that the development of design guidelines, based on the results of two-dimensional stress analysis and other numerical procedures, would be more useful for practitioners involved in crown pillar design than widespread use of 3-D methods. In fact, as the results of these three-dimensional analyses can be matched, in general, by results from carefully calibrated 2-D models it is considered more appropriate that future modelling be addressed towards evaluating the behaviour of discontinuity controlled failures. In this light, Figure 4.29 shows the comparitive configurations of the geometry of Mine #29 modelled in the three-dimensional case compared to the mesh arrangement used for examining part of the crown of the A-zone stope using FLAC. The configuration for a boundary element arrangement and for a P-Frame structural assessment are shown on Figure 4.30.

To examine the stability of various crown geometries all of these models can be applied, within certain limitations. Comparison of the results obtained by running each of these models for the Mine #29 crown pillar situation, has provided a quite useful indication of modelling applicability, and suitability, (see Table 4.5). This comparison table suggests that, with care, simple solutions can in most circumstances be utilized to gain rapid appreciation, even of complex situations. Resort to 3-D analyses may therefore only be warranted for particularly severe geometrical configurations that are not amendable to 2-D simplifications.

4.3.5. Block Theory Applications

Some considerable advances have been made towards development of computer codes which will extend current limitations of handling jointed rock block problems. The limitations of such procedures, as proposed by Goodman and Shi (1981) and by Warburton (1983), when applied to realistic problems such as determining rock block interactions within a complex jointed rock zone within a crown pillar, are still appreciable. Failure analysis for the interaction of even a few blocks is a formidable computational problem. Thus, resort has to be made to simplifications. This again focuses attention towards use of generic modelling as a means for extending current understanding of failure behaviour. It also suggests that probabilistic techniques, not only should be applied to geological data collection (e.g. using stereonet plotting and other approaches) but also should be incorporated into stability evaluations. Development of rational methods of probability evaluation is seen as of prime importance to reducing current limitations to analytically assessing actual crown pillar situations.

4.4 Failure Probability Appraisal

Throughout the foregoing discussion and for almost all of the analyses presented in this report, considerable reliance has been placed on defining accurately the parameters used in the modelling. This in not a trivial task, as, in reality, such wide variations in rock types and properties can occur within a crown zone that selecting representative controlling parameters may be difficult. In consequence, some study needs to be undertaken of probabilistic approaches. The value of this approach can be illustrated by the results for some limit equilibrium calculations for chimney failure for two rock types, as shown on Figure 4.31.

Hoek, 1989, as part of this study, addressed the possible use of some initial probability assessments as a means for improving deterministic evaluation of factors of safety for crown pillar conditions. Refering to Figure 4.10 it will be assumed that the pillar dimensions, defined by x,y and z, and the unit weights of rock (τ_R) and water (τ_W), are known with a high enough degree of precision that they can be assigned unique values. The other six parameters that control failure behaviour for chimney collapse are the water pressure conditions in the pillar (Z_W), the rock mass rating (RMR), the uniaxial compressive strength of the intact rock material (σ_C), the value of the Hoek-Brown constant m for the intact rock material (m_i), the horizontal to vertical stress ratio (K_x) in the x direction and the horizontal to vertical stress ratio (K_y) in the y direction. These six parameters can be examined probabilistically if each is defined by a mean value and a standard deviation and it is assumed that the values are normally distributed around the mean.

For probabilistically determining the risk of failure, it is necessary to develop a distribution for each of the variables of concern. For each of the parameters of interest, the mean, $\bar{V}$ of a set of observations of each variable, V can be expressed by:

$$\bar{V} = \frac{\sum V_i}{n} \tag{4.5}$$

where V_i is the i th observation and
n is the number of observations

The sample variance S^2 is the square of the standard deviation S and is given by:

$$S^2 = \frac{\sum (\bar{V} - V_i)^2}{n - 1} \tag{4.6}$$

With these known, the coodinates (Y, V_i) of the curve defining the normal distribution of the variable V can be calculated from:

$$Y = \frac{1}{S\sqrt{2\pi}} e^{-\frac{1}{2}\left(\frac{V_i - \bar{V}}{s}\right)^2} \tag{4.7}$$

One of the most rigorous methods that could then be used to investigate the distribution of factors of safety for a given problem, such as this crown pillar analysis would involve use of the Monte Carlo technique. In applying this method to this type of problem, a random number generator would be used to determine a value V_i for each of the six normally distributed variables and these values would then be used to compute a factor of safety. If this process is repeated say 1000 times, a histogram of the factor of safety distribution can be plotted.

The Monte Carlo technique, however, is computationally intensive, and often, for the level of accuracy required in most engineering situations, it can be replaced by use of Rosenbleuth's point estimate method (Rosenbleuth, 1972). This approach is based upon the fact that a quantity, calculated from an equation containing a number of normally distributed variables, will itself be normally distributed. Hence, for each variable, two point estimates are made at fixed values of one standard deviation on either side of the mean ($\bar{V} \pm s$) and the equation is solved for every possible combination of point estimates. This produces 2^m solutions, where m is the number of normally distributed variables involved.

In the case of this limit equilibrium assessment of crown pillar chimney failure, the factor of safety equation contains six normally distributed variables and hence 64 values of the factor of safety are obtained from this process. The mean and standard deviation for the factor of safety are calculated by means of the equations given previously and thus the normal distribution can also be plotted. Figure 4.31 illustrates the normal distribution of the factor of safety calculated using Rosenbleuth's method for two rock quality conditions. The distribution is plotted for a range of ± 3 standard deviations on either side of the mean factor of safety and the probability of failure is given by the ratio of the area under the normal distribution curve for factor of safety values from $-\infty$ to 1 (shown shaded on the diagram on Figure 4.31).

It should, however, be appreciated that in order to facilitate more widespread application of probabilistic techniques to evaluation of crown pillar situations, certain assumptions must be made, namely that:

- the failure mechanism for a given crown pillar situation is known, and
- an analytical model is available which adequately replicates actual failure behaviour.

It is clear from the foregoing discussion that neither of these situations apply at the current state-of-the-art. Further research is therefore essential not only on probabilistic approaches to geological data collection and evaluation but also on refining and improving available analysis methods such that crown stability conditions can be reliably analyzed.

TABLE 4.1 - Summary of Post Failure Analysis Results (Wright-Hargreaves - Mine 42)

Strength Parameters			Summary of Results
c' [MPa]	ϕ' [°]	σ_t [MPa]	
0	40	0	• Excessive displacement of FW - up to 2.5 m indicating FW collapse. • Excessive displacement in CP. • Excessive tension zone near ground surface.
1.25	63	0	• Excessive displacement of upper HW and CP. Displacements > 0.5 m. • Very little displacements in FW. • HW and CP unstable.
1.25	63	1.0	• Compression arch formed in CP. • Extensive tension zone in HW and upper part of FW.

CP = Crown Pillar
HW = Hangingwall
FW = Footwall

TABLE 4.2 - Generic Analysis of Stopes Using MUDEC

T/S	θ=90°	θ=75°	θ=60°	θ=45°
	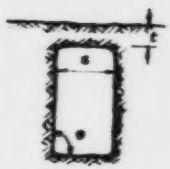	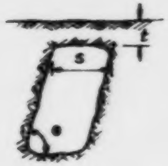	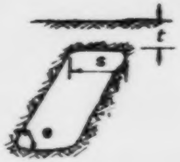	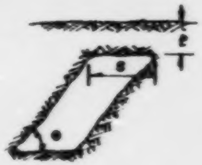
0.15 STOPE GEOMETRY SPAN = 7.5 m HEIGHT = 25.225 m	CASE 1 = poor rock properties CASE 13= good rock properties	CASE 4 = poor rock properties CASE 16= good rock properties	CASE 7 = poor rock properties CASE 19= good rock properties	CASE 10= poor rock properties CASE 22= good rock properties
0.5 STOPE GEOMETRY SPAN = 7.5 m HEIGHT = 22.5 m	CASE 2 = poor rock properties CASE 14= good rock propeties	CASE 5 = poor rock properties CASE 17= good rock properties	CASE 8 = poor rock properties CASE 20= good rock properties	CASE 11= poor rock properties CASE 23= good rock properties
1.5 STOPE GEOMETRY SPAN = 7.5 m HEIGHT = 15 m	CASE 3 = poor rock properties CASE 15= good rock properties	CASE 6 = poor rock properties CASE 18= good rock properties	CASE 9 = poor rock properties CASE 21= good rock properties	CASE 12= poor rock properties CASE 24= good rock properties

T/S = crown pillar thickness/span ratio
θ = inclination of stope with respect to horizontal
CP = crown pillar
HW, FW = hangingwall, footwall
• see Figure 4.23 for rock properties

TABLE 4.3 - Summary of MUDEC Analysis for Schistose Rock Conditions (Poor Rock Quality, Q = 0.1, RMR = 23)

T/S	θ=90°	θ=75°	θ=60°	θ=45°
0.15	CASE 1 • CP generally de-stressed • Sidewall movements up to 0.1 m • CP movements up to 0.7 m • CP sagged and collapsed	CASE 4 • CP generally de-stressed • Large movements in HW and CP • CP unstable	CASE 7 • CP generally de-stressed • Very large movement in CP (> 0.9 m) • CP unstable	CASE 10 • CP generally de-stressed • Very large movement in CP (> 0.4 m) • CP unstable
0.5	CASE 2 • Compression arch formed in CP • Very little movement in sidewalls • CP movement stabilized	CASE 5 • CP generally de-stressed • Very large movement in HW and CP • CP unstable	CASE 8 • CP generally de-stressed • Very large movement in HW and CP • CP unstable	CASE 11 • CP generally de-stressed • Very large movement in CP (> 0.3 m) • CP unstable
1.5	CASE 3 • A compression arch is formed in CP • Very little movement in sidewalls • CP movement stabilized soon after initial block movements	CASE 6 • Compression arch formed in CP • Moderate movements in HW • CP movement stabilized	CASE 9 • Compression arch not fully formed • Large movements in HW and abutment of CP • CP unstable	CASE 12 • CP generally under slight compression • Very large movement in CP and HW • CP unstable

T/S = crown pillar thickness/span ratio
θ = inclination of stope with respect to horizontal
CP = crown pillar
HW,FW = hangingwall, footwall
• shaded regions denote unstable or potentially unstable crown pillars

TABLE 4.4 - Summary of MUDEC Analysis for Competent, Slabby and Blocky Rock Conditions (Good Rock Quality, Q = 10, RMR = 65)

T/S	θ=90°	θ=75°	θ=60°	θ=45°
0.15	CASE 13 • CP generally de-stressed • Very little movements in side walls • CP movements in the order of cm. • CP movements continueing, potentially unstable	CASE 16 • CP generally de-stressed • Very little movements in sidewalls • CP movements continueing, potentially unstable	CASE 19 • CP generally de-stressed • Movements in HW in the order of cm. • CP movements continueing, potentially unstable	CASE 22 • CP generally de-stressed • Movements in HW in the order of cm. • CP movements continueing, potentially unstable
0.5	CASE 14 • Compression arch formed in CP • Very little movement in sidewalls • CP movement stabilized	CASE 17 • Compression arch formed in CP • Very little movement in sidewalls • CP movement stabilized	CASE 20 • CP generally de-stressed • Large movement in HW (>4 cm) • CP unstable • CP movements continueing, potentially unstable	CASE 23 • Compression arch formed in CP • Movements in HW and CP in the order of cm. • CP movement continueing, potentially unstable
1.5	CASE 15 • Compression arch formed in CP • Very little movement in sidewalls • CP movement stabilized soon after initial block movements	CASE 18 • Compression arch formed in CP • Very little movements in sidewalls • CP movement stabilized soon after initial block movements	CASE 21 • Compression arch formed in CP • Very little movements in sidewalls • CP movement stabilized soon after initial block movements	CASE 24 • Compression arch not fully formed in CP • Movements in HW in the order of cm. • CP movements continueing, potentially unstable

T/S = crown pillar thickness/span ratio
θ = inclination of stope with respect to horizontal
CP = crown pillar
HW,FW = hangingwall, footwall
• shaded regions denote unstable or potentially unstable crown pillars

TABLE 4.5 - Comparison of Advantages and Disadvantages of Various Available Numerical Methods

Numerical Method	3-D Finite Element Analysis	2-D Finite Difference Analysis	2-D Boundary Element Analysis	Structural Analysis
Software	I-DEAS	FLAC	EXAMINE package	P-Frame
Advantages	• Allows three dimensional analysis of mine geometries. • Good graphical output.	• Non-linear analysis which allows large deformation. • Good graphical output. • Model can accommodate different material parameters. • Automatic mesh generator.	• Model complicated geometries easily and quickly. • Good tool for parametric studies. • Good graphical output.	• Relatively easy to set up. • Flexible geometry. • Can perform quick parametric studies. • Good graphical output.
Disadvantages	• Difficult to set up model and mesh. • Experienced operator required. • Homogeneous and elastic model only. • Structural engineering based software not designed for geotechnical problems. • Extensive computer time required.	• Extensive computer time required. • Applicable only to 2-D problems. • Experienced operator required.	• Applicable only to 2-D problems. • Homogeneous and elastic model only.	• Structural engineering based software.

TYPICAL THICKNESS TO SPAN CORRELATIONS FOR VARIOUS CROWN PILLARS (AFTER BÉTOURNAY, 1987)

FIGURE 4.1

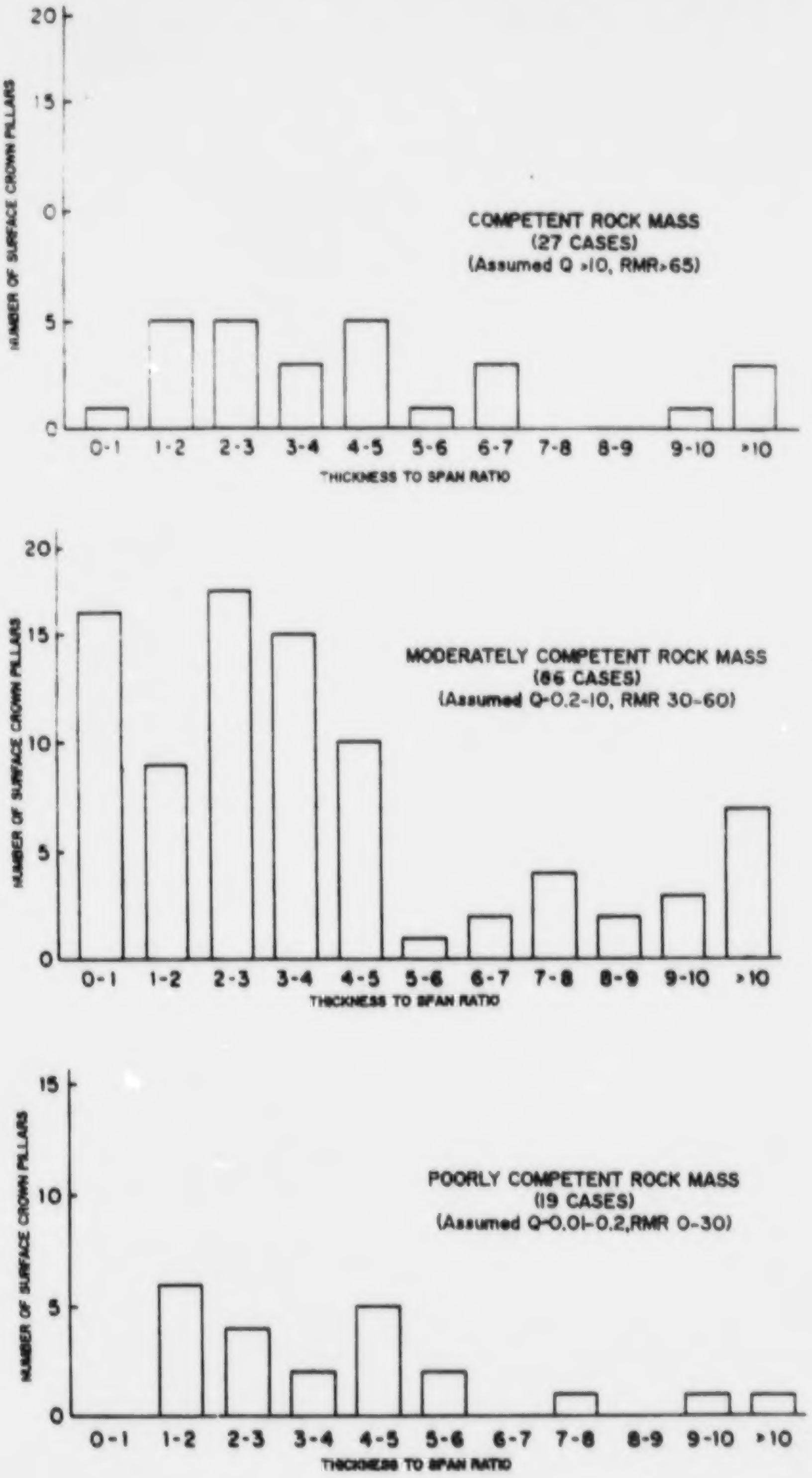
COMPETENT ROCK MASS
(27 CASES)
(Assumed Q >10, RMR>65)

MODERATELY COMPETENT ROCK MASS
(86 CASES)
(Assumed Q-0.2-10, RMR 30-60)

POORLY COMPETENT ROCK MASS
(19 CASES)
(Assumed Q-0.01-0.2,RMR 0-30)

Date FEBRUARY 7,1990
Project 881-1739-3

Golder Associates

Drawn R.B.C.
Chkd. TGL

CSIR GEOMECHANICS (RMR) AND NGI Q-SYSTEM CORRELATIONS TO UNSUPPORTED SPANS & STAND-UP TIME

FIGURE 4.2

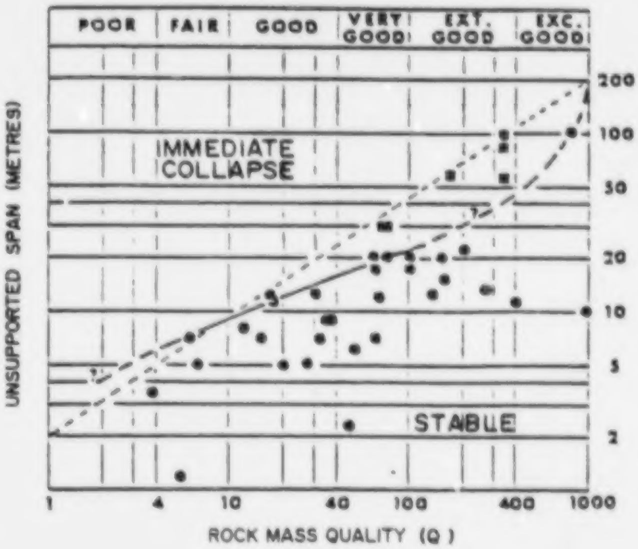

NGI Q-SYSTEM CORRELATION
AFTER BARTON (1974)

NOTE : CIRCLES REPRESENT THE MAN-MADE UNSUPPORTED EXCAVATIONS REPORTED IN THE LITERATURE. SQUARES REPRESENT SOME NATURAL OPENINGS FROM CARLSBAD, NEW MEXICO. THE CURVED ENVELOPE IS AN ESTIMATE OF THE MAXIMUM DESIGN SPAN FOR PERMANENTLY UNSUPPORTED MAN-MADE OPENINGS.

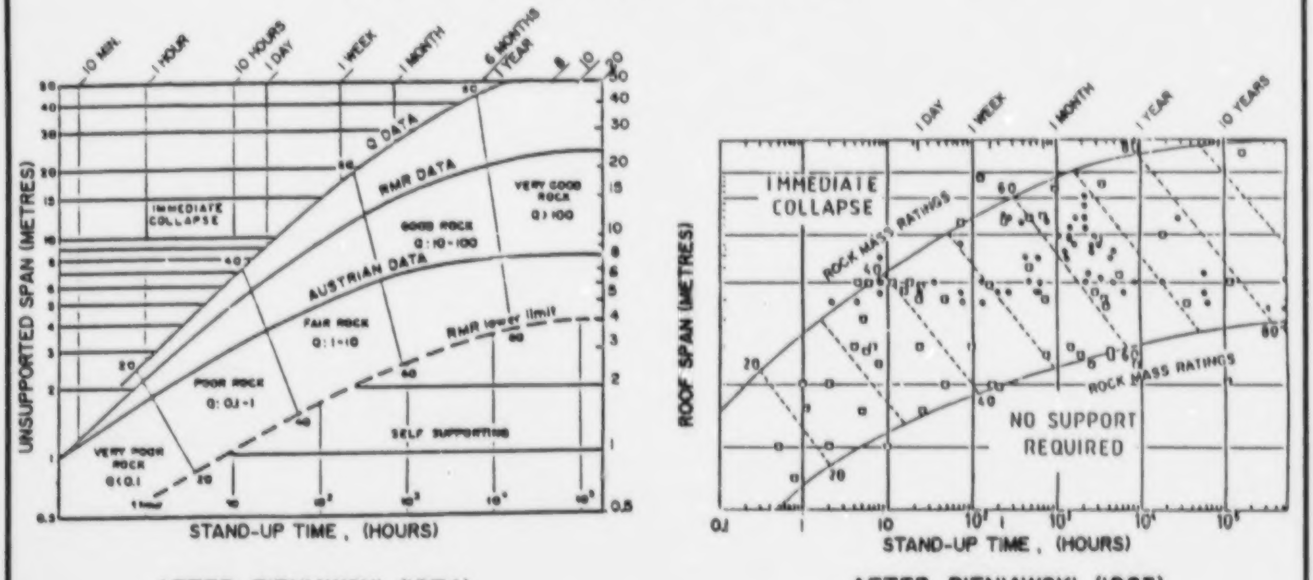

RMR & AUSTRIAN CORRELATIONS

Date FEBRUARY 12, 1990.
Project 881-1739-3

Golder Associates

Drawn R.B.C.
Chkd. TJL

COMPARISON CHARTS FOR EVALUATION OF STABLE SPANS USING PUBLISHED ROCK MASS CLASSIFICATION PROCEDURES

FIGURE 4.3

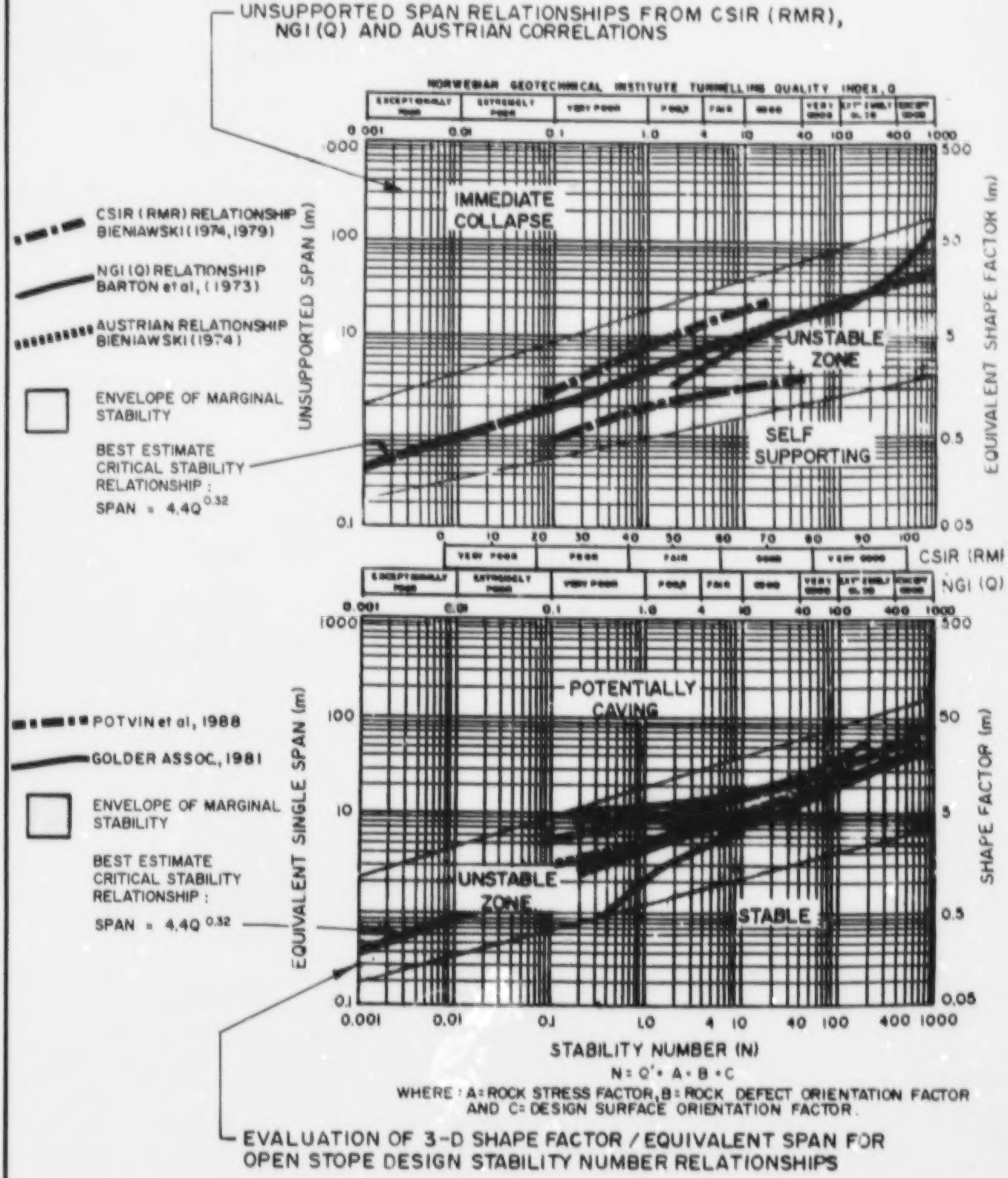

UNSUPPORTED SPAN RELATIONSHIPS FROM CSIR (RMR), NGI (Q) AND AUSTRIAN CORRELATIONS

$N = Q' \cdot A \cdot B \cdot C$

WHERE : A = ROCK STRESS FACTOR, B = ROCK DEFECT ORIENTATION FACTOR AND C = DESIGN SURFACE ORIENTATION FACTOR.

EVALUATION OF 3-D SHAPE FACTOR / EQUIVALENT SPAN FOR OPEN STOPE DESIGN STABILITY NUMBER RELATIONSHIPS

Date FEB. 12, 1990

Project 881-1739-3

Golder Associates

Drawn TDR

Chkd. TGr

GENERIC BEAM THEORY DESIGN CURVES ILLUSTRATING MAXIMUM TENSILE STRESS FOR VARIOUS OVERBURDEN DEPTHS

FIGURE 4.4

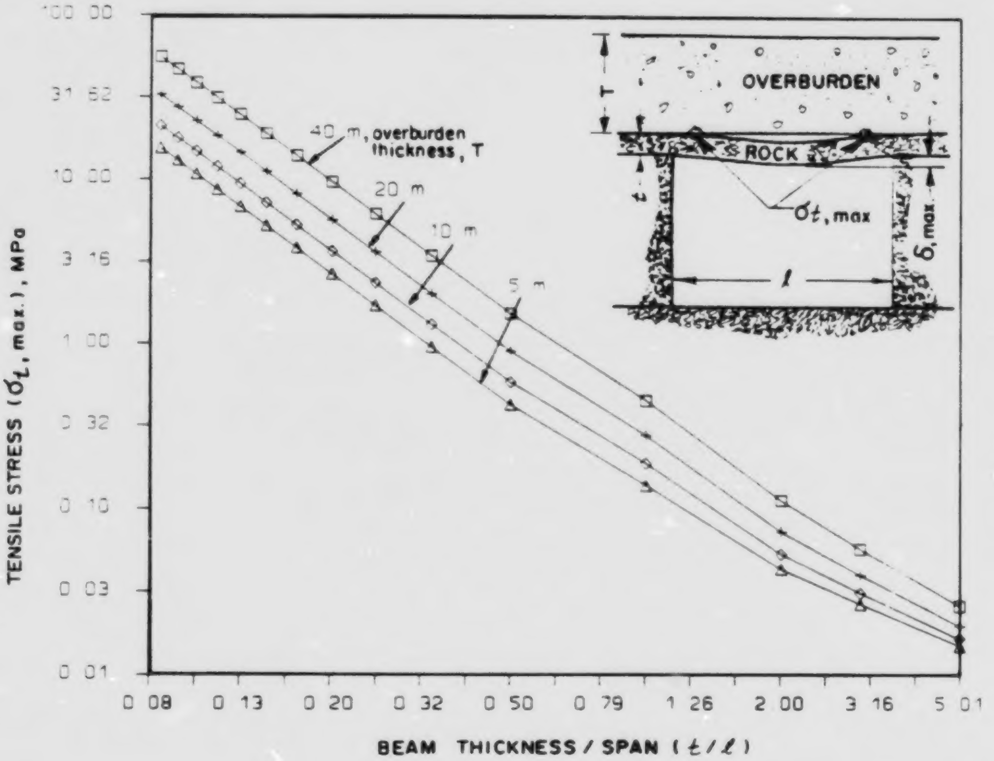

ROCK = 2700 kg/m^3

SOIL = 1600 kg/m^3

BEAM SPAN = 10.0 m

	V. POOR	POOR	FAIR	GOOD	V.GOOD
NGI - Q	0.01	0.1	1.0	10.0	100.0
RMR	3	23	44	65	85
INFERRED ROCK MASS TENSILE STRENGTH (MPa)	0.002	0.02	0.15	1.0	3.0

Date FEBRUARY 12, 1990.

Project 881-1739-3

Golder Associates

Drawn R.B.C.

Chkd.

COMPARATIVE SHEAR AND BENDING MOMENT DIAGRAMS FOR FLAT AND ARCHED CROWN ANALOGIES

FIGURE 4.5

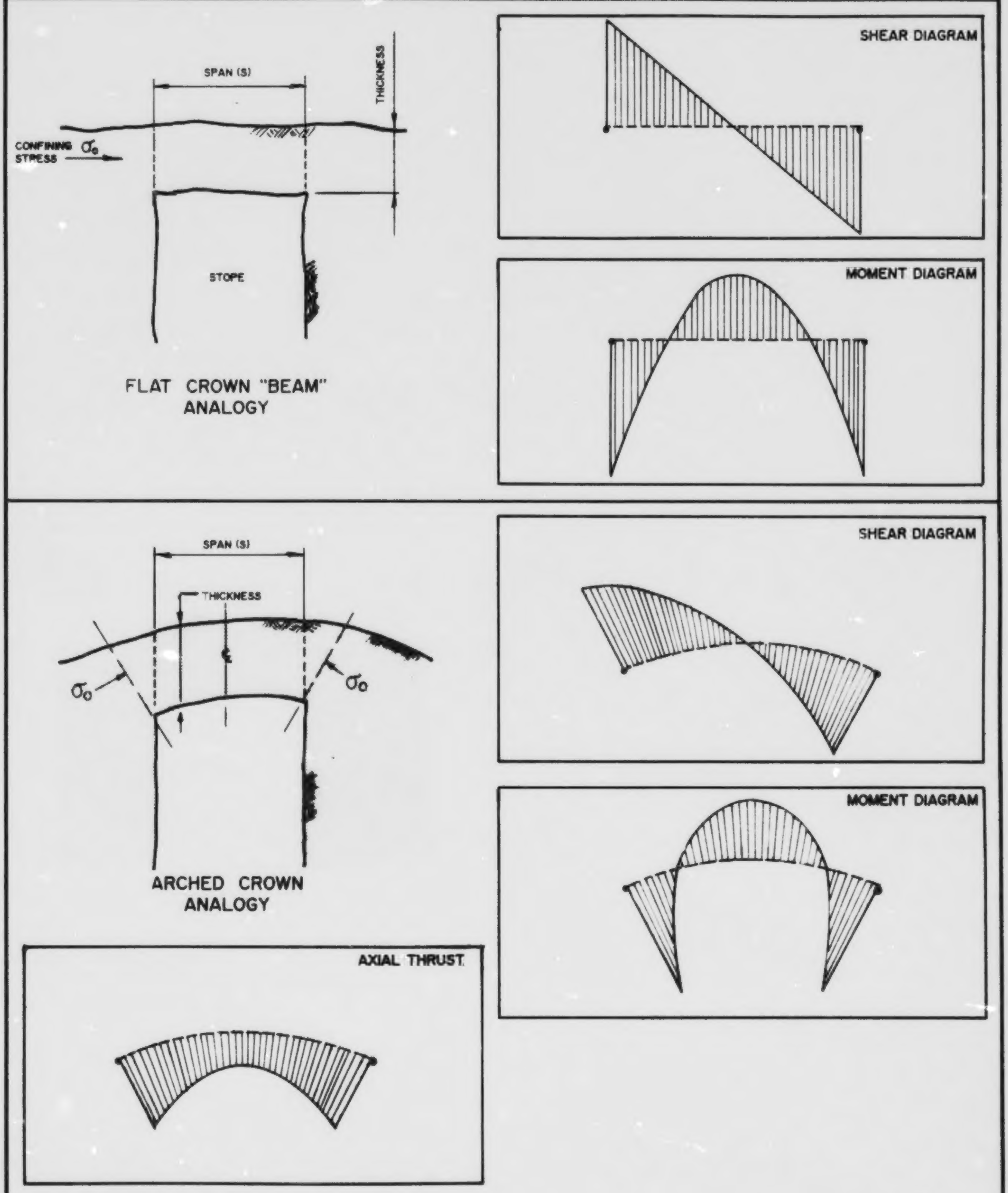

Date FEBRUARY 12, 1990.
Project 881-1739-3

Golder Associates

Drawn R.B.C.
Chkd. TGL

GENERIC RELATIONSHIPS FOR CROWN PILLARS ANALYSED AS TWO-WAY SPANNING PLATES

FIGURE 4.6

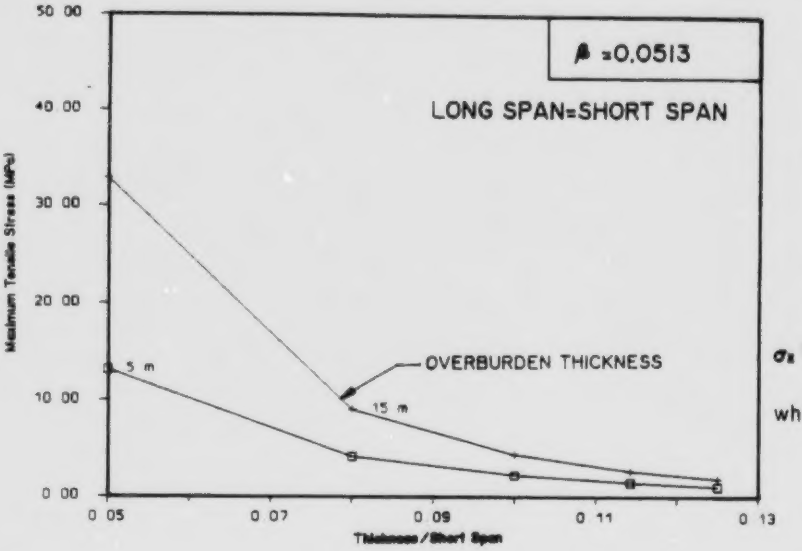

$$\sigma_x \max = \frac{b\beta q a^2}{t^2}$$

where q= applied overburden loading

LONG SPAN / SHORT SPAN	1.00	1.25	1.50	1.75	2.00	∞
β	0.0513	0.0665	0.0757	0.0806	0.0829	0.0833

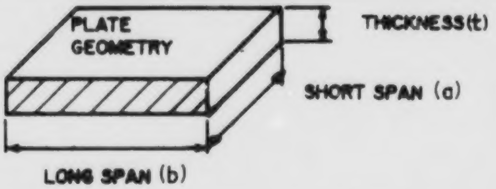

β IS A SIMPLIFYING NUMERICAL COEFFICIENT USED IN THE PLATE EQUATIONS , ROARKE (1965)

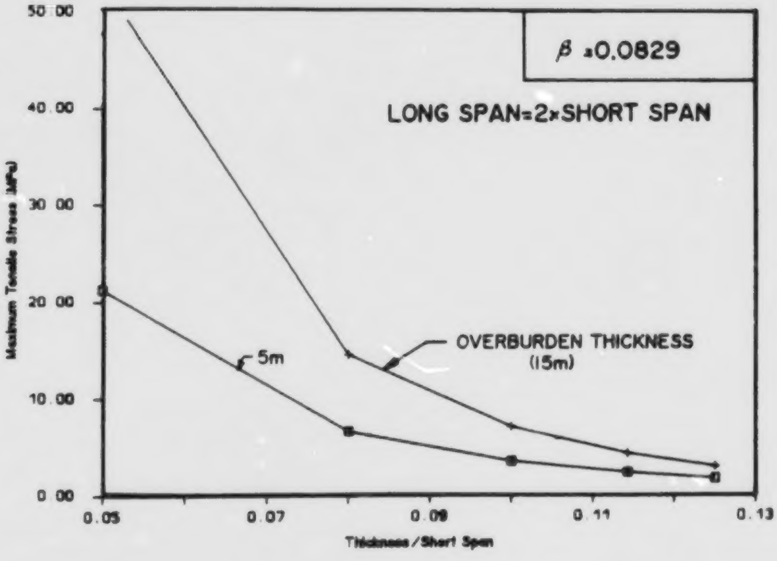

Date FEBRUARY 1990
Project 881-1739

Golder Associates

Drawn RBC
Chkd. TGL

CONCEPT OF ARCH ACTION OF VOUSSOIR BEAMS FOR CROWN PILLAR ANALYSIS

FIGURE 4 7

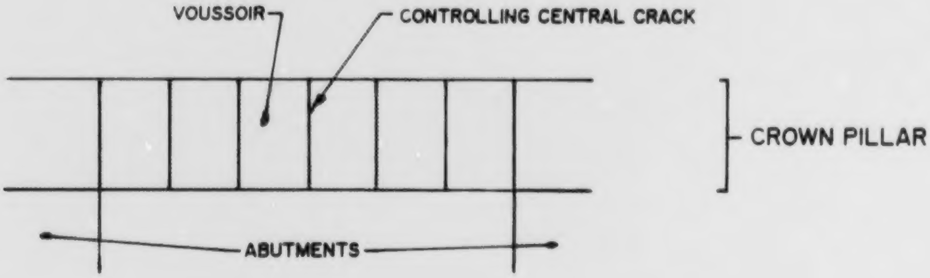

IDEALIZED GEOMETRY OF CROWN PILLAR WITH ASSUMED VERTICAL WEAKNESS PLANES

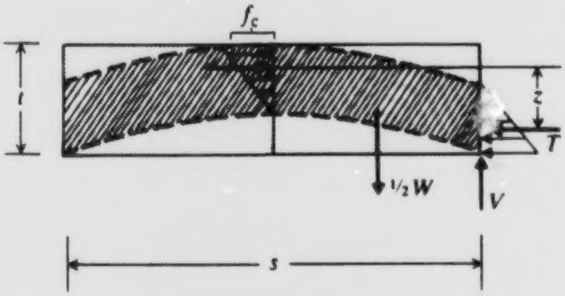

APPROXIMATE PARABOLIC ARCH ACTION

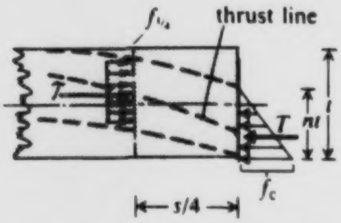

ASSUMED THRUST GEOMETRY AT ABUTMENTS

(AFTER BRADY & BROWN, 1985)

Date FEBRUARY 12, 1990.
Project 881-1739-3

Golder Associates

Drawn R.B.C.
Chkd.

RESULTS OF VOUSSOIR BEAM ANALYSES FOR VARIOUS ROCK QUALITY AND BEAM GEOMETRIES	FIGURE 4.8

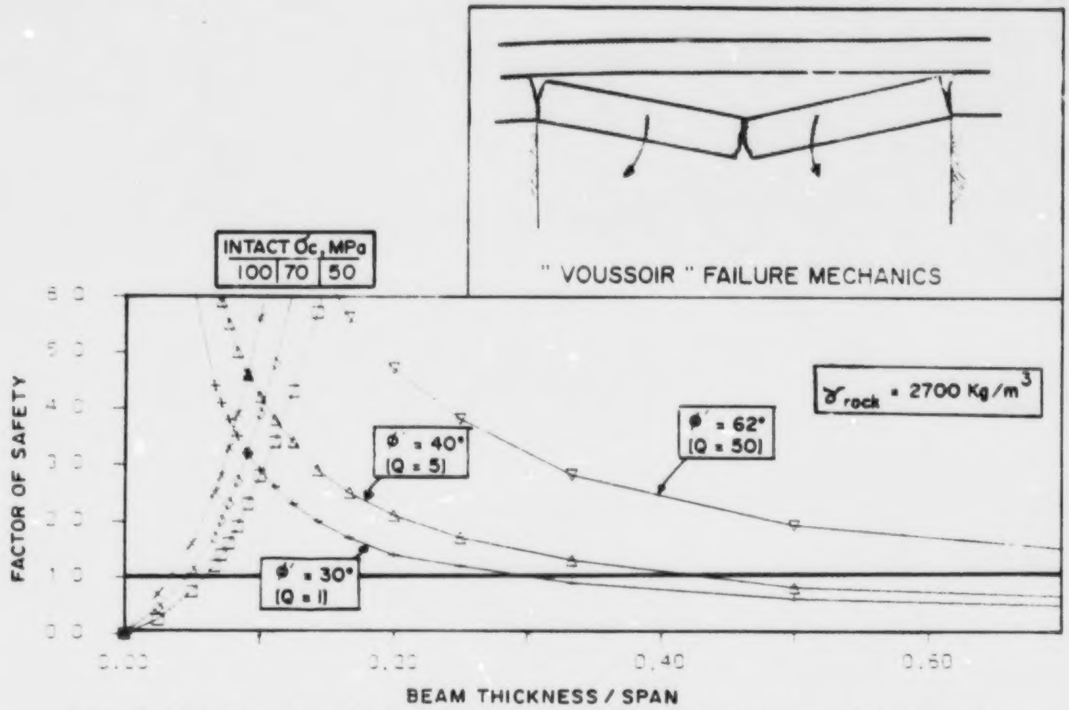

RELATIONSHIPS FOR SHEAR AND COMPRESSIVE FAILURE MECHANISMS FOR HORIZONTAL VOUSSOIR BEAMS

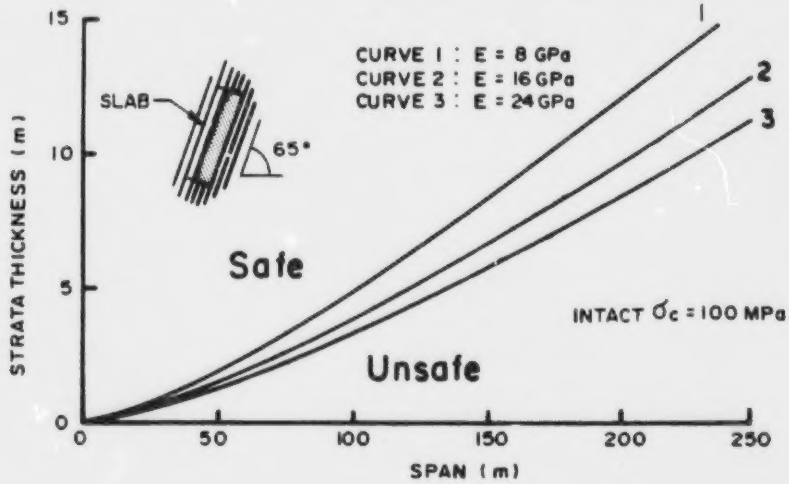

CURVES FOR 65° INCLINED SLABS SUBJECT TO "VOUSSOIR" ACTION (AFTER BEER AND MEEK, 1982.)

Date FEBRUARY 12, 1990.
Project 881-1739-3

Golder Associates

Drawn R.B.C.
Chkd. TGL

MECHANISMS OF KINEMATIC FAILURE OF CROWN PILLARS AND METHODS OF GEOLOGICAL DATA PRESENTATION FOR KINEMATIC STABILITY EVALUATION

FIGURE 4.9

STOPE / CROWN GEOMETRY
IN BLOCKY CONDITIONS

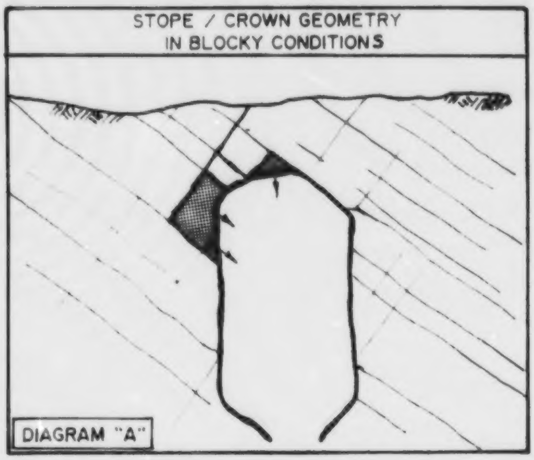

DIAGRAM "A"

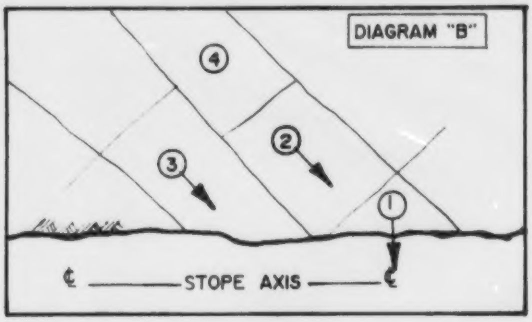

DIAGRAM "B"

STOPE / CROWN GEOMETRY
IN SLABBY CONDITIONS

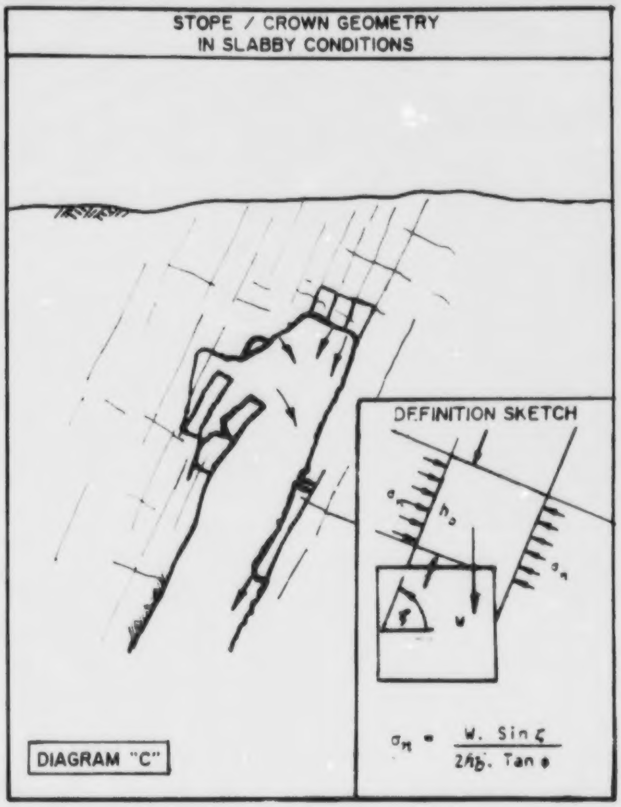

DIAGRAM "C"

$$\sigma_n = \frac{W.\ \sin\xi}{2h_o.\ \tan\phi}$$

TYPICAL PRESENTATION OF STRUCTURAL GEOLOGY DATA

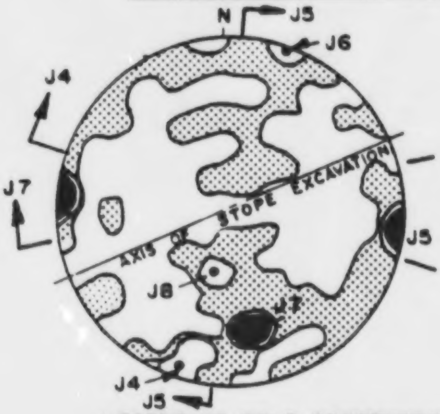

LEGEND OF POLE CONCENTRATION
AS PERCENTAGE OF TOTAL POLES

- ■ 4 - 10%
- ☐ 2 - 5%
- ▨ < 2 %
- J4• JOINT NUMBER AND CENTRE OF CONCENTRATION
- ↳ STRIKE DIRECTION OF CRITICAL JOINTS

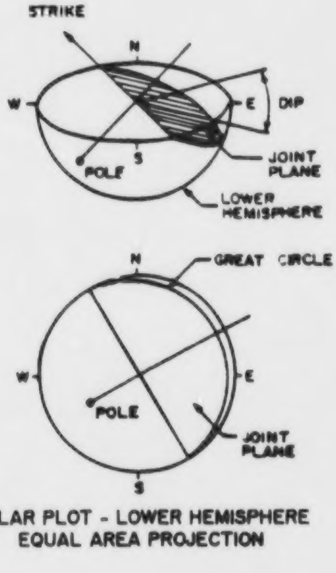

POLAR PLOT - LOWER HEMISPHERE
EQUAL AREA PROJECTION

Date FEBRUARY 12, 1990.
Project 881-1739-3

Golder Associates

Drawn R.B.C.
Chkd. TG

Form GA-D-4 (Imperial)

TYPICAL GEOMETRY FOR CROWN CHIMNEY CAVING ANALYSIS

FIGURE 4.10

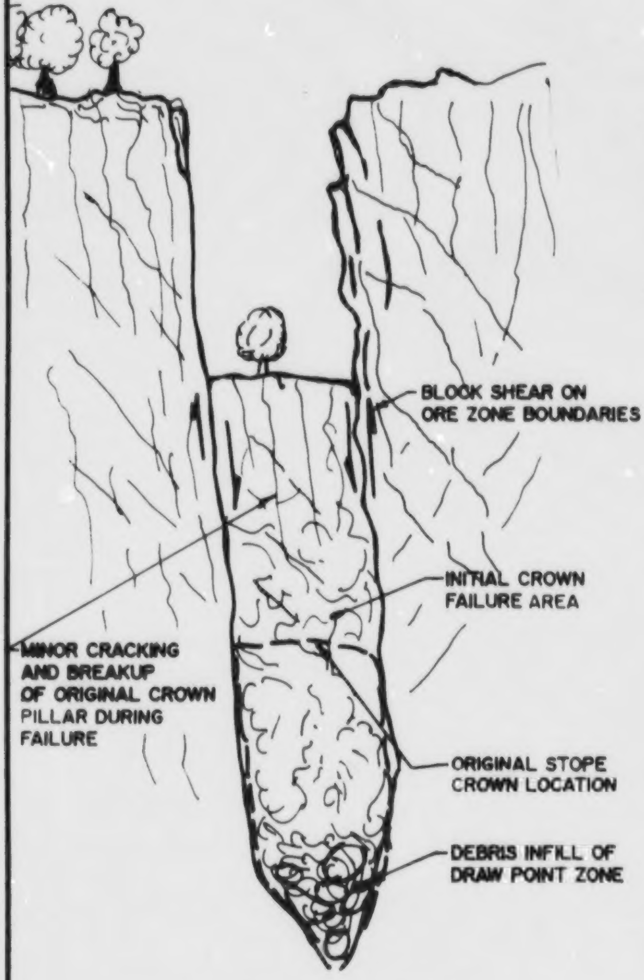
BLOCK SHEAR ON ORE ZONE BOUNDARIES
INITIAL CROWN FAILURE AREA
MINOR CRACKING AND BREAKUP OF ORIGINAL CROWN PILLAR DURING FAILURE
ORIGINAL STOPE CROWN LOCATION
DEBRIS INFILL OF DRAW POINT ZONE

GENERAL FAILURE GEOMETRY

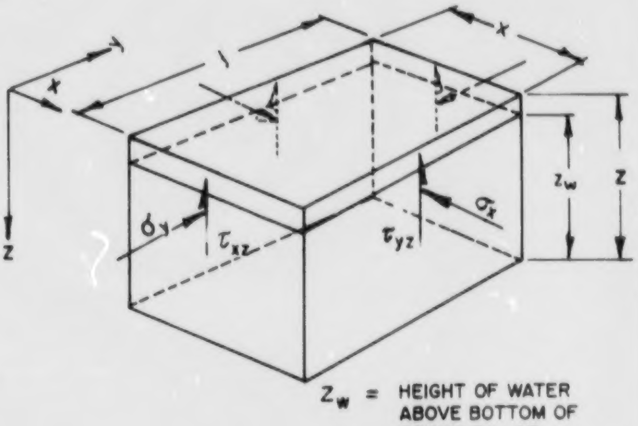

Z_w = HEIGHT OF WATER ABOVE BOTTOM OF CROWN PILLAR BLOCK

DEFINITION SKETCH

FACTOR OF SAFETY AGAINST VERTICAL DOWNWARD SLIDING :

$$F = \frac{2}{\gamma_r}\left(\frac{\tau_{xz}}{y} + \frac{\tau_{yz}}{x}\right)$$

WHERE γ_r IS THE UNIT WEIGHT OF ROCK AND τ AND τ ARE THE SHEAR STRENGTHS OF THE END WALL (x z) AND STOPE STRIKE SIDEWALL (y z) FACES RESPECTIVELY.

REFERENCES:

- BRADY and BROWN (1985), ROCK MECHANICS FOR UNDERGROUND MINING PAGES 410 TO 414.
- HOEK (1989), A LIMIT EQUILIBRIUM ANALYSIS OF SURFACE CROWN PILLAR STABILITY. PROCEEDINGS: INTERNATIONAL CONFERENCE ON SURFACE CROWN PILLARS, TIMMINS.

Date JANUARY 30, 1990.
Project 881-1739-3

Golder Associates

Drawn R.B.C.
Chkd. TGL

TRANSITION FROM CAVING TO STOPING CONDITIONS FOR VARIOUS ROCK MASS QUALITIES

FIGURE 4.11

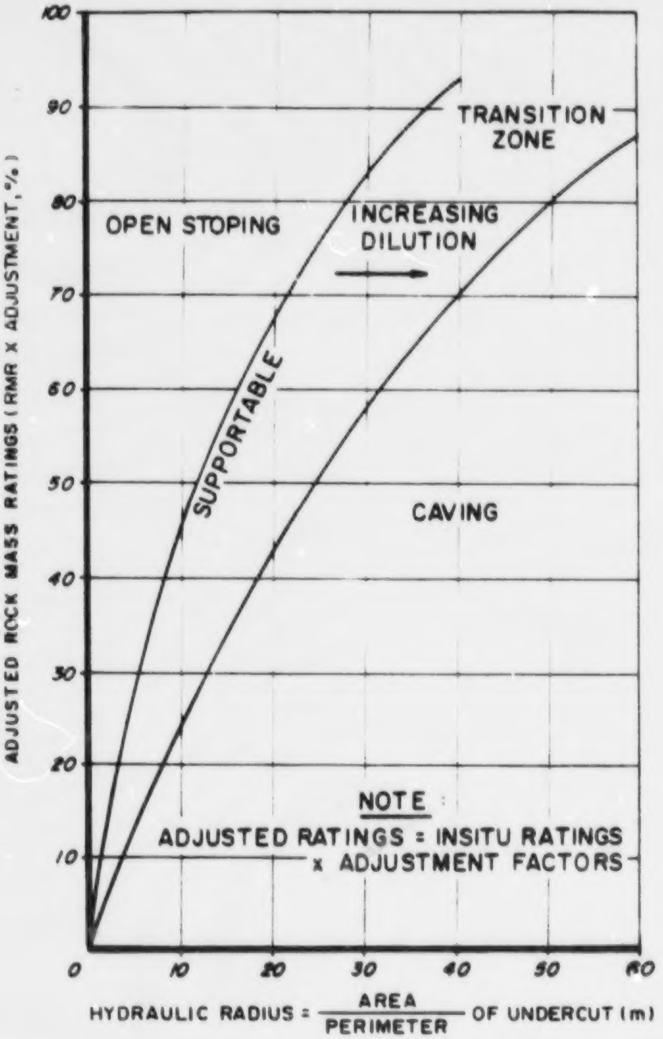

ORE BODY ATTITUDE ADJUSTMENTS:

Dip of surface	**Adjustment, %**
0–30°	80
30–50°	85
50–70°	90
70–80°	95
80–90°	100

REFERENCE: DIERING, J.A.C. AND LAUBSCHER, D.H., (1987) PRACTICAL APPROACH TO THE NUMERICAL STRESS ANALYSIS OF MASS MINING OPERATIONS. TRANS. I.M.M., VOL. 96 pp A179 - A188.

Date FEBRUARY 12, 1990
Project 881-1739-3

Golder Associates

Drawn P L
Chkd.

GEOMETRICAL CHARACTERISTICS FOR VARIOUS CAVING SITUATIONS

FIGURE 4.12

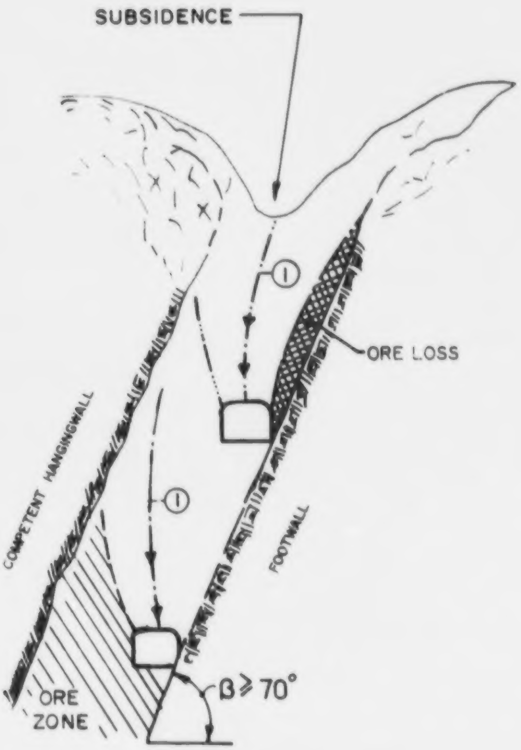

GENERALIZED CAVING GEOMETRY WITHIN DEFINED ORE LIMITS

① CENTRE LINE OF GRAVITY FLOW

(DIAGRAMS MODIFIED FROM MATHEWS , 1978.)

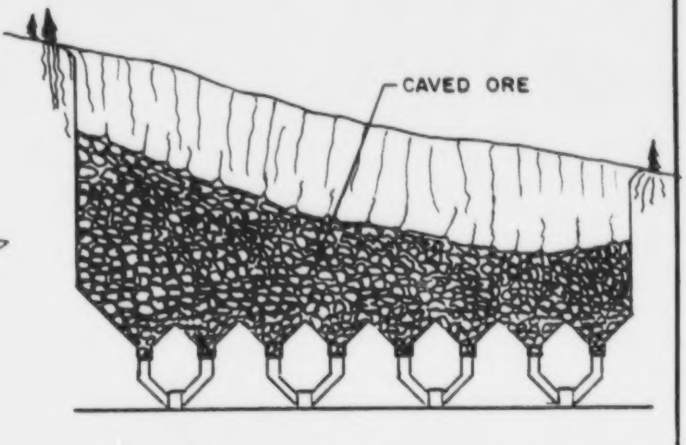

EFFECTIVE CAVING AND UNIFORM SUBSIDENCE

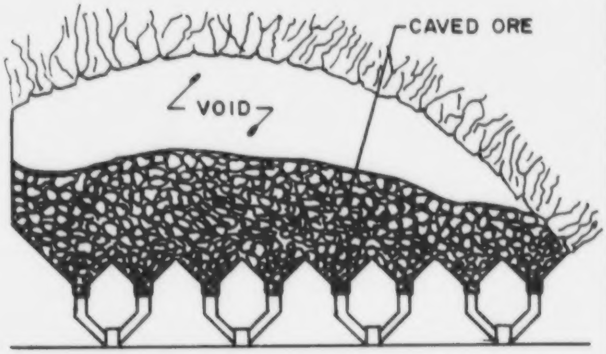

DEVELOPMENT OF UNDESIRABLE STABLE ARCHING

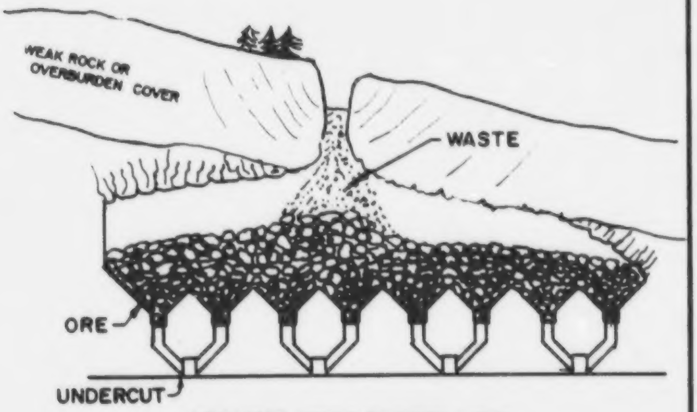

ARCHING WITH FUNNELLING

Date JANUARY 31, 1990

Project 881-1739-3

Golder Associates

Drawn R.B.C.

Chkd. TGL

DRAWING PATTERNS FOR CAVED ROCK

FIGURE 4.13

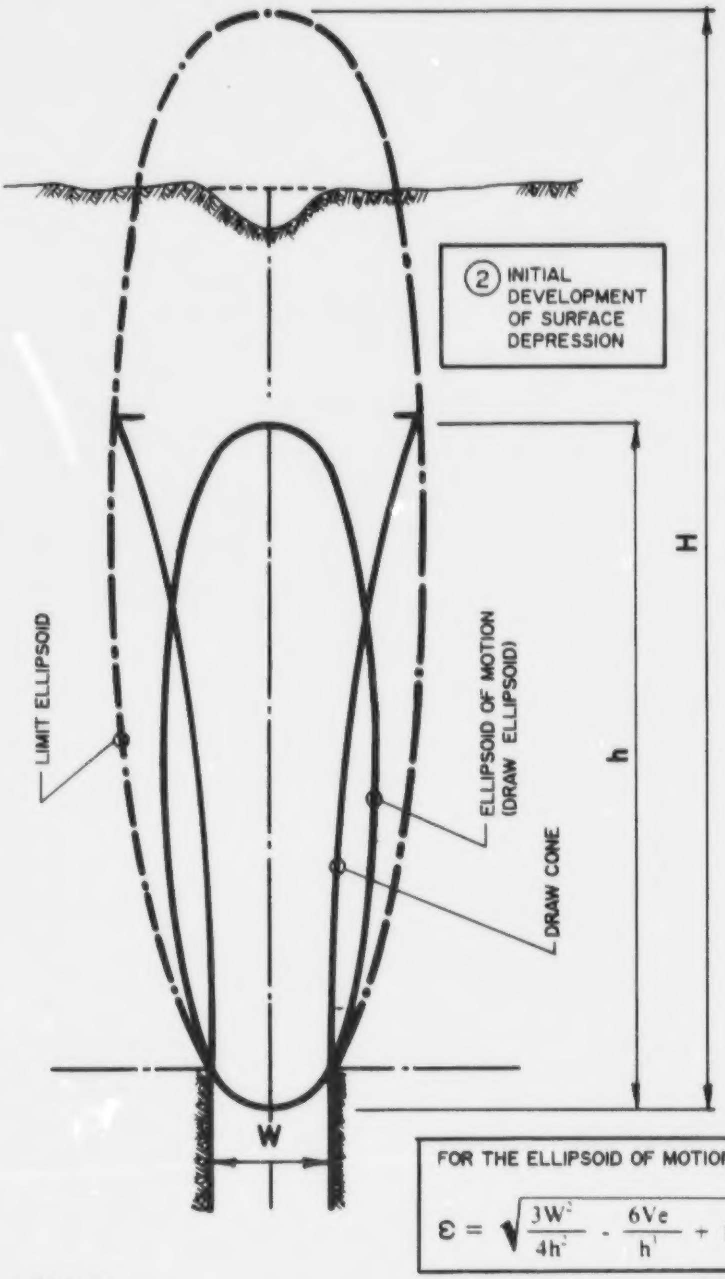
② INITIAL DEVELOPMENT OF SURFACE DEPRESSION
H
h
LIMIT ELLIPSOID
ELLIPSOID OF MOTION (DRAW ELLIPSOID)
DRAW CONE
W

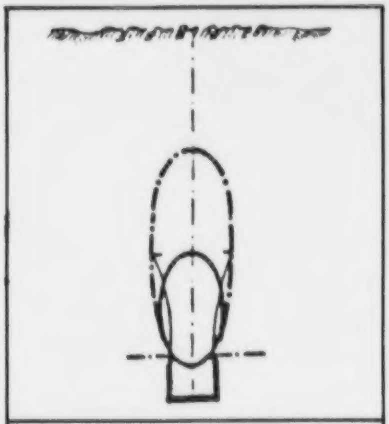

① INITIAL CAVE - DEVELOPMENT BEFORE ELLIPSE OF MOTION FULLY DEVELOPED.

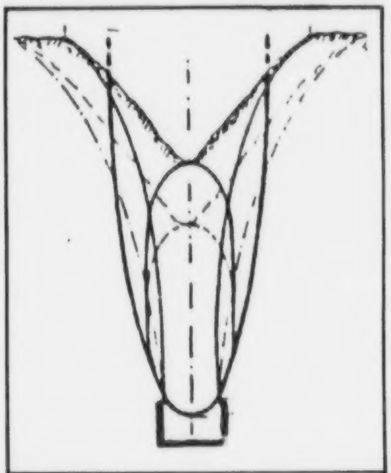

③ COMPLETE DRAW THROUGH TO SURFACE, WHEN h BECOMES SAME AS ORIGINAL CROWN THICKNESS.

FOR THE ELLIPSOID OF MOTION

$$\varepsilon = \sqrt{\frac{3W^2}{4h^2} - \frac{6Ve}{h^3} + 1}$$

LEGEND

ε = ECCENTRICITY
a = SEMI-MAJOR AXIS OF THE DRAW ELLIPSOID
b = SEMI-MINOR AXIS OF THE DRAW ELLIPSOID
W = WIDTH OF OUTLET (STOPE SPAN)
h, H = HEIGHT OF DRAW AND LIMIT ELLIPSOIDS
Ve = VOLUME OF DRAW ELLIPSOID

REFERENCES:

- JANELID and KVAPIL (1966)
- (FREE, 1970 ; JUST and FREE, 1971)

Date JANUARY 30, 1990.
Project 881-1739

Golder Associates

Drawn R.B.C.
Chkd. TGC

CRITICAL STOPE HEIGHTS FOR LIMITATION OF CAVING (ASSUMING COMPLETE STOPE FILLING BY CAVED ROCK)

FIGURE 4.14

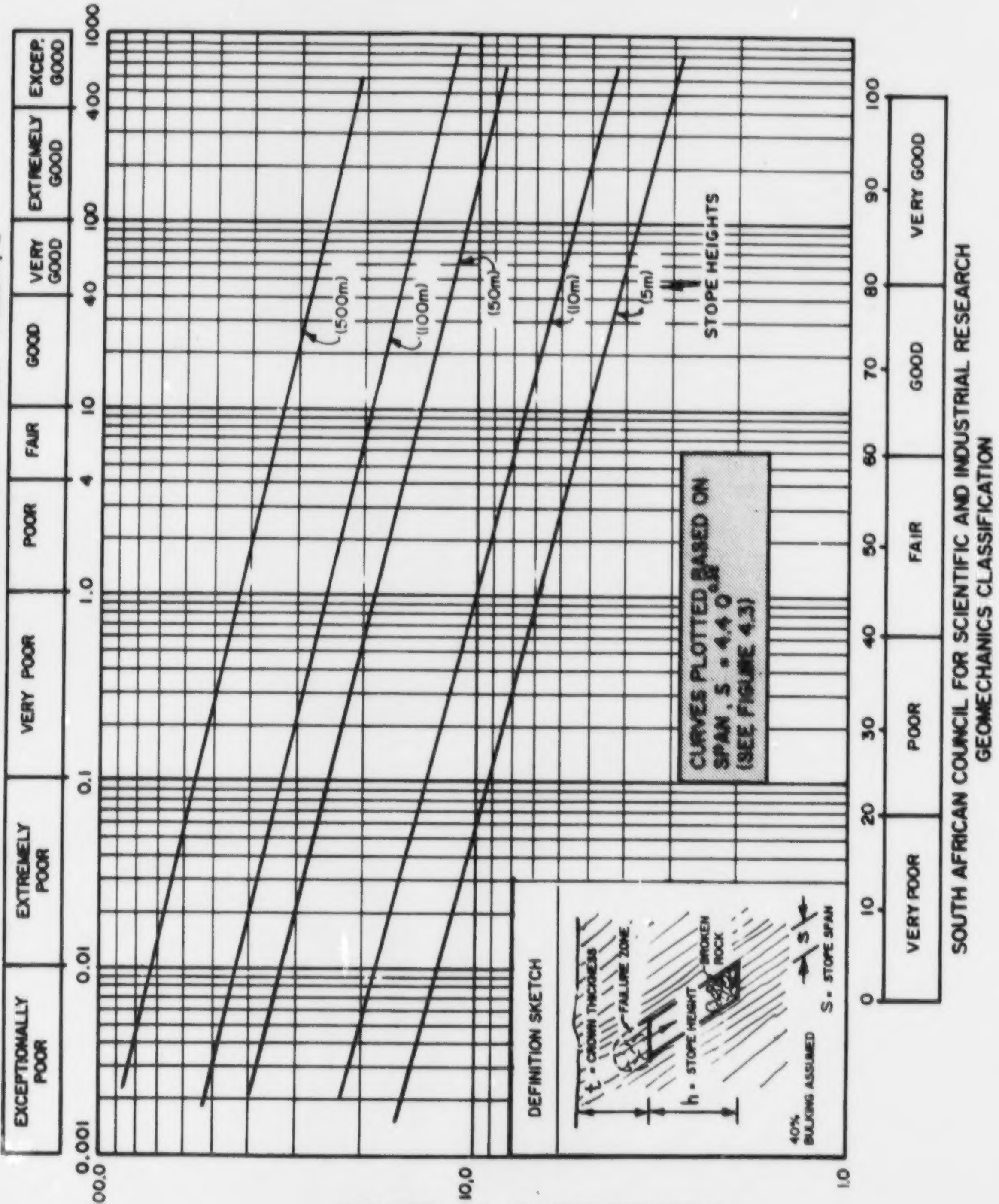

Date FEB. 14, 1990

Project 881-1739-3

Golder Associates

Drawn RBC

Chkd. Tgh

MINE #26 - CASE I STRESS INPUT
2 - D BOUNDARY ELEMENT ANALYSIS RESULTS

FIGURE 4.15

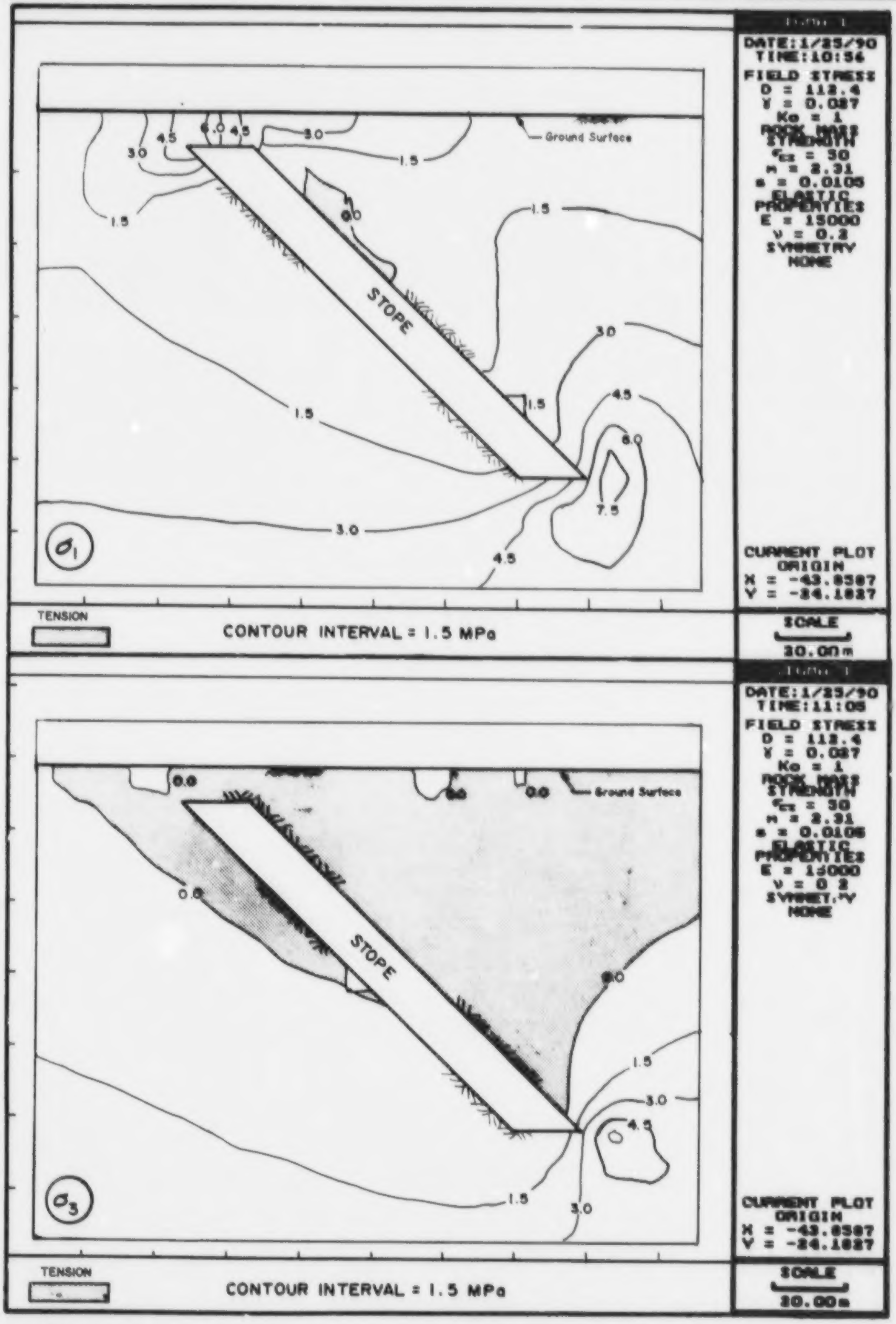

DATE:1/25/90
TIME:10:56
FIELD STRESS
D = 112.4
γ = 0.027
Ko = 1
ROCK MASS
STRENGTH
σ_{ci} = 30
m = 2.31
s = 0.0105
ELASTIC
PROPERTIES
E = 15000
ν = 0.2
SYMMETRY
NONE

CURRENT PLOT
ORIGIN
X = -43.8587
Y = -24.1827

CONTOUR INTERVAL = 1.5 MPa

SCALE
30.00m

DATE:1/25/90
TIME:11:05
FIELD STRESS
D = 112.4
γ = 0.027
Ko = 1
ROCK MASS
STRENGTH
σ_{ci} = 30
m = 2.31
s = 0.0106
ELASTIC
PROPERTIES
E = 15000
ν = 0.2
SYMMETRY
NONE

CURRENT PLOT
ORIGIN
X = -43.8587
Y = -24.1827

CONTOUR INTERVAL = 1.5 MPa

SCALE
30.00m

Date FEBRUARY 11, 1990.
Project 881-1739-3

Golder Associates

Drawn R.B.C.
Chkd. TGC

MINE #26 - CASE 2 STRESS INPUT
2 - D BOUNDARY ELEMENT ANALYSIS RESULTS

FIGURE 4.16

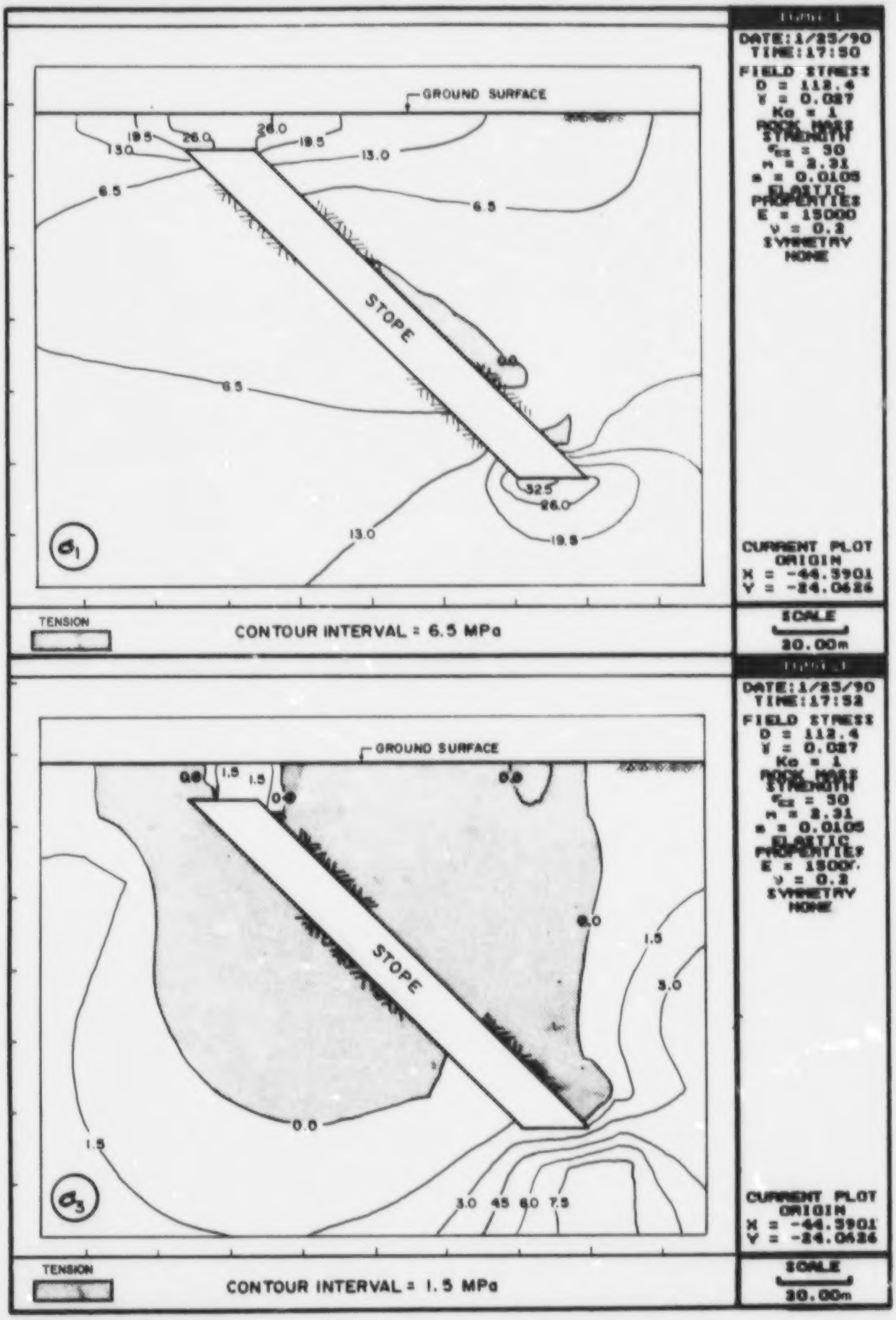

Date FEBRUARY 11, 1990.

Project 881-1739-3

Golder Associates

Drawn R.B.C.

Chkd. TGL

MINE #22 - CASE I STRESS INPUT
2 - D BOUNDARY ELEMENT ANALYSIS RESULTS

FIGURE 4.17

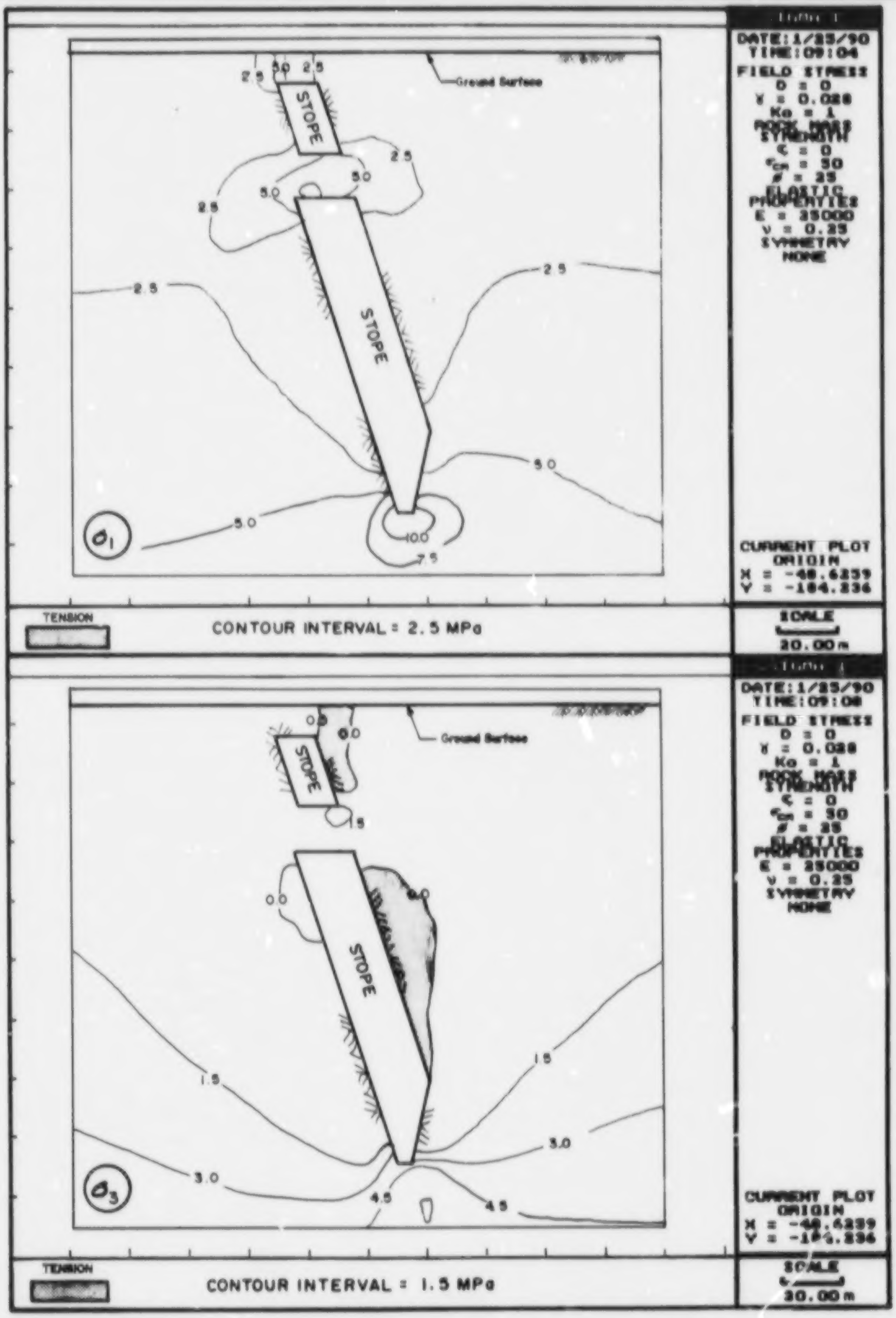

Date FEBRUARY 9, 1990.

Project 881-1739-3

Golder Associates

Drawn R.B.C.

Chkd Tgr

MINE #22 - CASE 2 STRESS INPUT
2 - D BOUNDARY ELEMENT ANALYSIS RESULTS

FIGURE 4.18

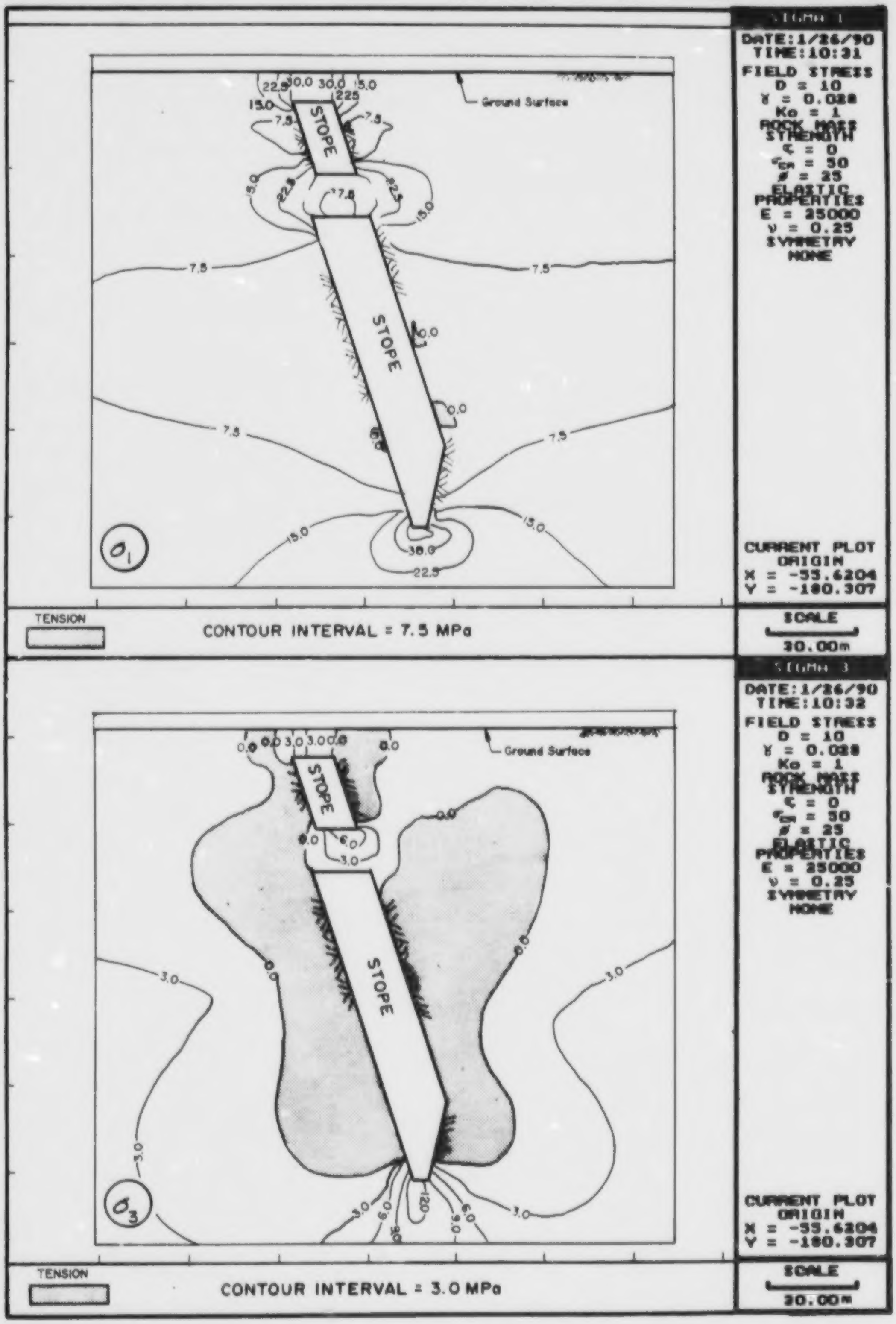

Date FEBRUARY 11, 1990.

Project 881-1739-3

Golder Associates

Drawn R.B.C.

Chkd. TGr

RESULTS OF FLAC ANALYSIS
PLOT OF PRINCIPAL STRESS TRAJECTORIES AND TENSION ZONE FOR MINE # 42 (ELASTIC MODEL)

FIGURE 4.19

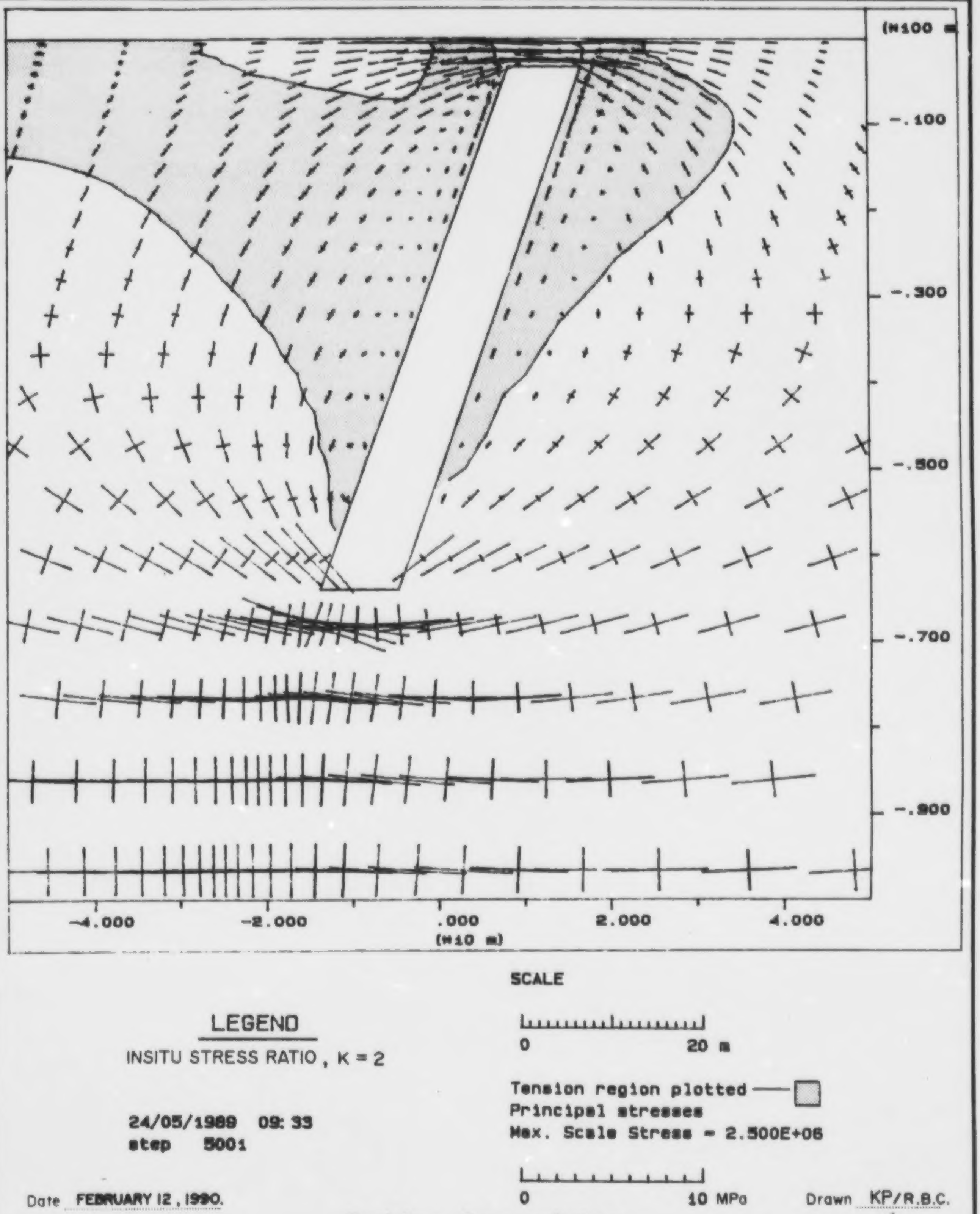

Date FEBRUARY 12, 1990.

Project 881-1739-3

Golder Associates

Drawn KP/R.B.C.

Chkd.

RESULTS OF FLAC MODELLING FOR MINE #42
USING MOHR - COULOMB MODEL
(NO TENSION : NO COHESION)

FIGURE 4.20

DISPLACEMENT VECTORS

0 5m

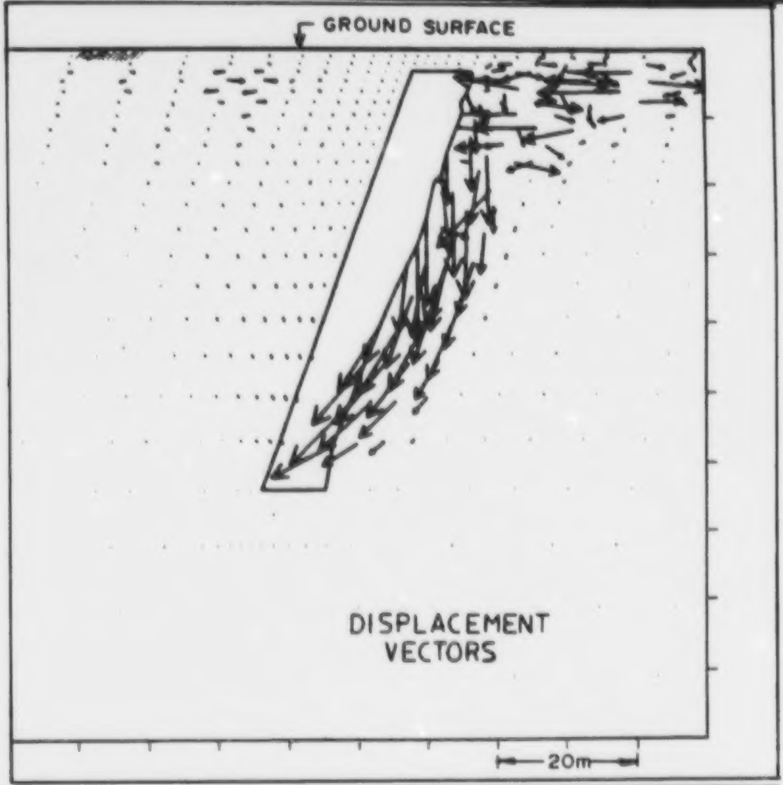

PRINCIPAL STRESS VECTORS

0 10 MPa

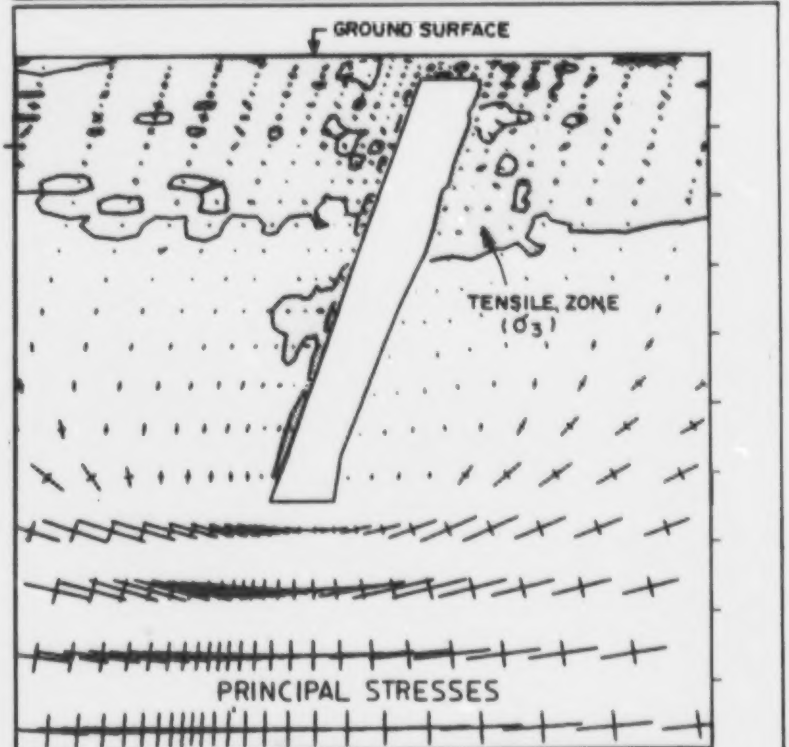

Date FEB. 14, 1990
Project 881-1739-3

Golder Associates

Drawn RBC, MHW
Chkd. TGC

RESULTS OF FLAC MODELLING FOR MINE #42 USING MOHR-COULOMB MODEL WITH $C' = 1.25$ MPa , $\phi' = 63°$, $\sigma_t = 0$

FIGURE 4.21

DISPLACEMENT VECTORS

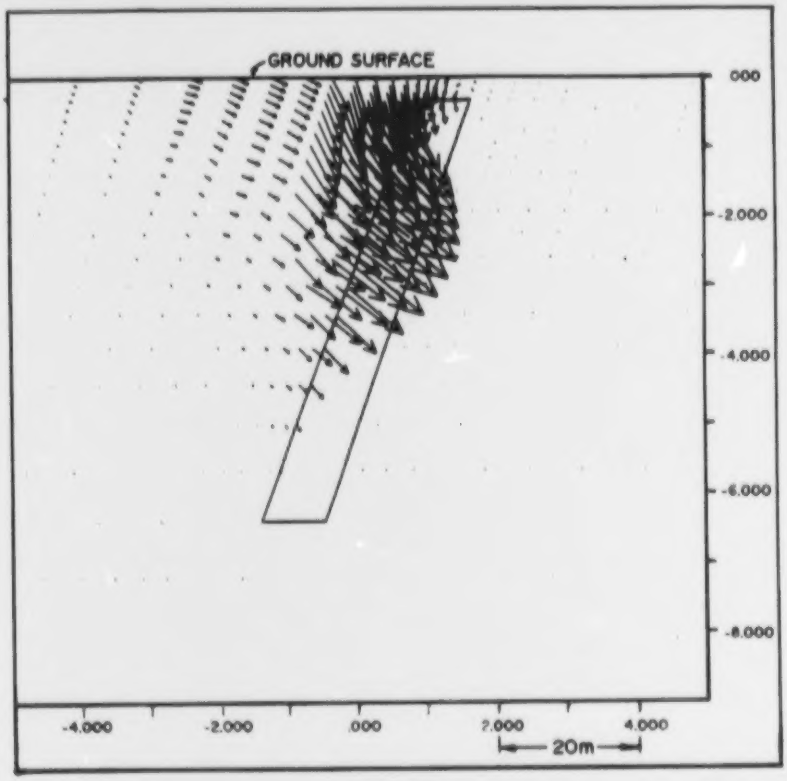

PRINCIPAL STRESS VECTORS

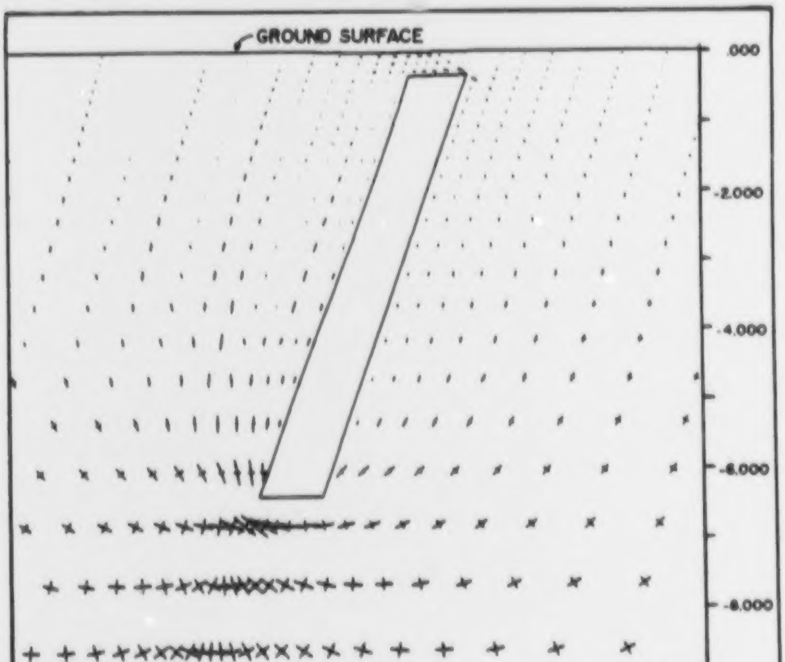

Date FEBRUARY 14, 1990.
Project 881-1739-3

Golder Associates

Drawn R.B.C./P.L.
Chkd. Tgc

RESULTS OF FLAC MODELLING FOR MINE #42 USING MOHR - COULOMB MODEL WITH $c' = 1.25$ MPa, $\phi' = 63°$, $\sigma_t = 1.0$ MPa

FIGURE 4.22

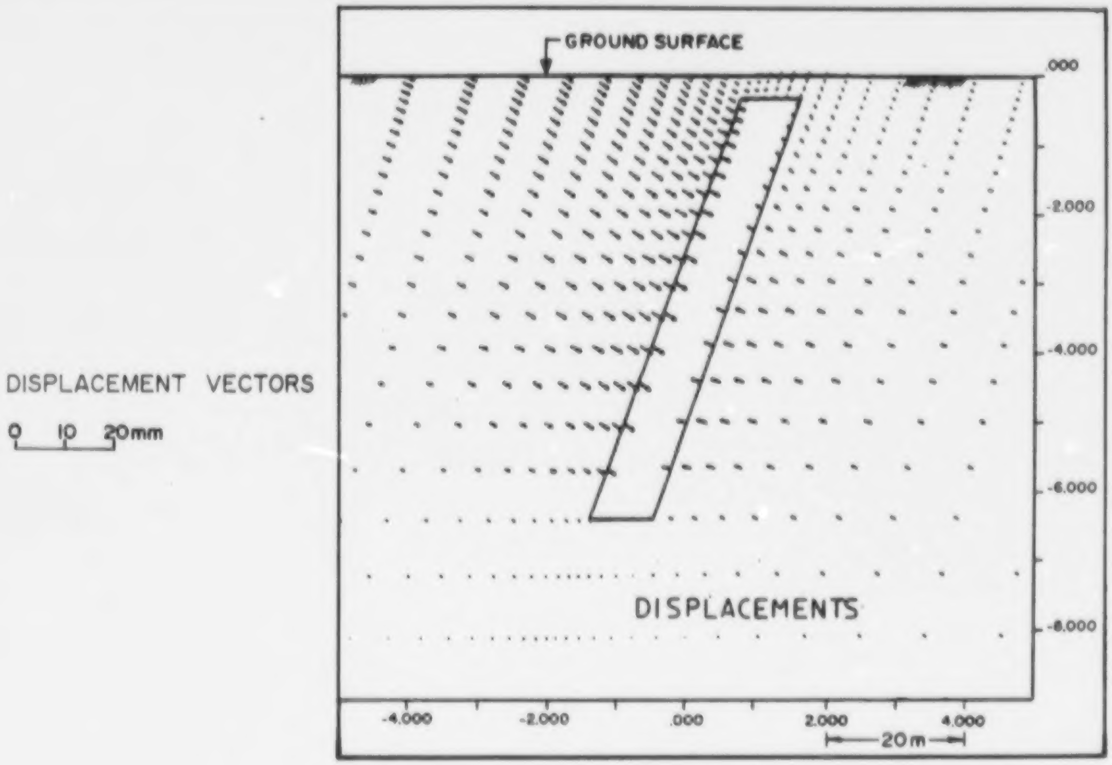

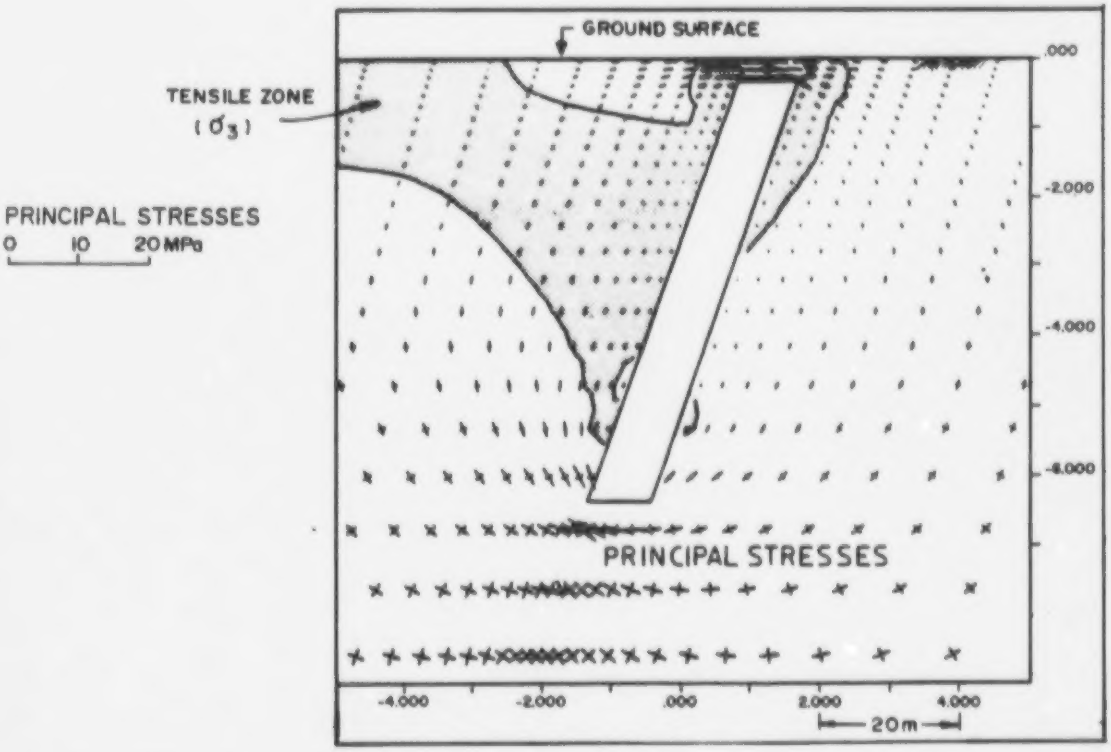

Date FEBRUARY 14, 1990.
Project 881-1739-3

Golder Associates

Drawn R.B.C. / M.H.W.
Chkd.

GEOMETRICAL LAYOUT FOR PARAMETRIC SERIES OF MUDEC ANALYSES

FIGURE 4.23

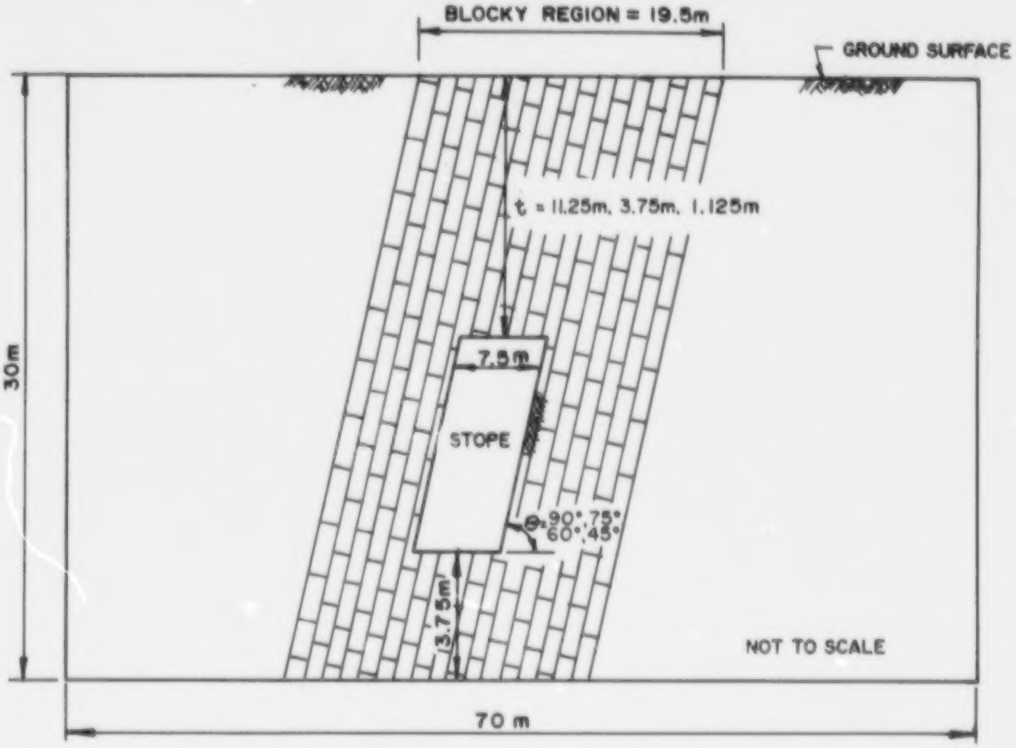

MATERIAL PARAMETERS USED IN PARAMETRIC STUDY

Joint							Rock		
ρ [kg/m^3]	G [GPa]	K [GPa]	c' [MPa]	ϕ' [°]	Jkn [GPa/m]	Jks [GPa/m]	ρ [kg/m^3]	G [GPa]	K [GPa]
Poor Rock Quality									
2000	2.4	5.1	0.02	61	42	21	2700	2.4	5.1
Good Rock Quality									
2000	11.3	20.2	1.3	64	391	196	2700	11.3	20.2

- Jkn = Joint normal stiffness
- Jks = Joint shear stiffness

Date 881-1739-3

Project 881-1739-3

Golder Associates

Drawn TDR / R.B.C.

Chkd.

REPRESENTATIVE RESULTS FROM MUDEC ANALYSES FOR OVERALL RANGE OF CROWN PILLARS EXAMINED

FIGURE 4.24

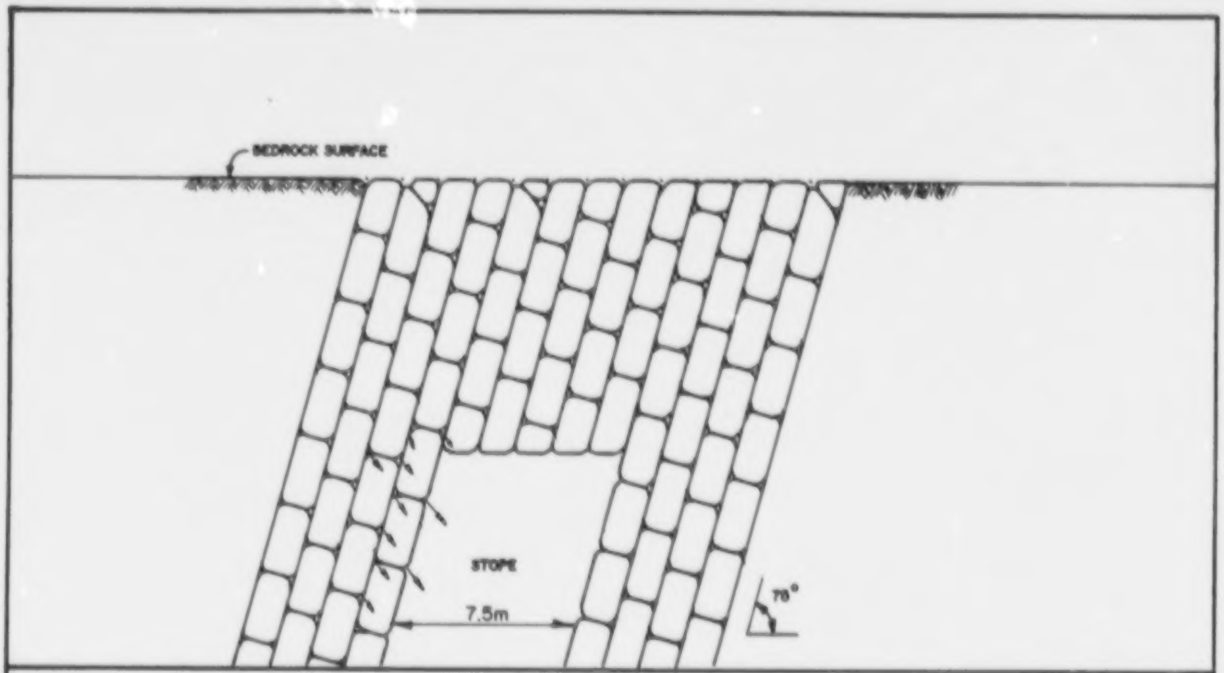

TYPICAL ONSET OF CROWN PILLAR FAILURE
INDUCED BY HANGINGWALL DESTABILIZATION

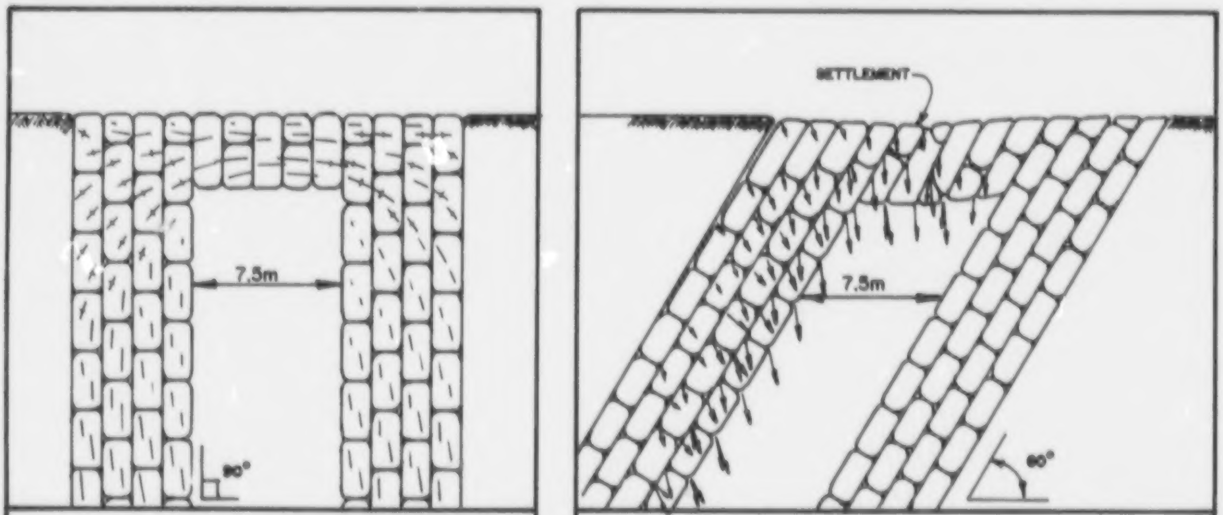

STRESS ARCH DEVELOPED IN
CROWN PILLAR
FOR GOOD ROCK CONDITIONS

SIGNIFICANT HANGINGWALL SLABBING AND
CROWN PILLAR DISTRESS

(NOTE DELAMINATION OF HANGINGWALL BLOCKS AND
SETTLEMENT OF SURFACE)

Date FEBRUARY 8, 1990.
Project 881-1739-3

Golder Associates

Drawn R.B.C.
Chkd. TG

MODEL RESULTS FOR STOPE GEOMETRY SHOWING CROWN STRESS CONDITIONS

FIGURE 4.25

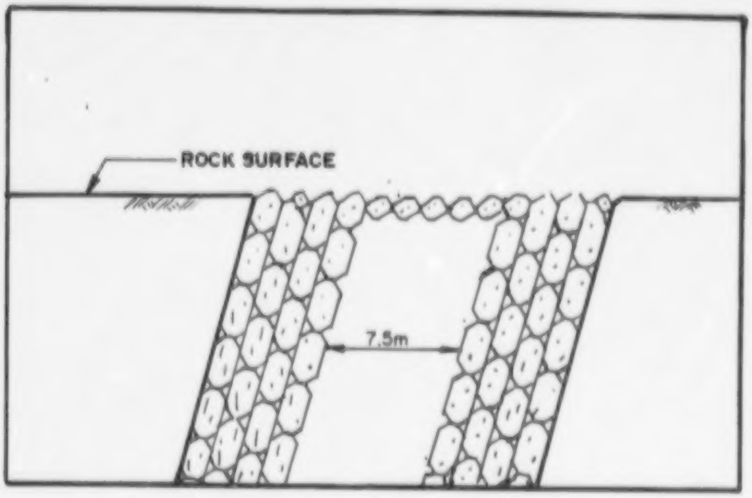

DE-STRESSED CROWN ZONE

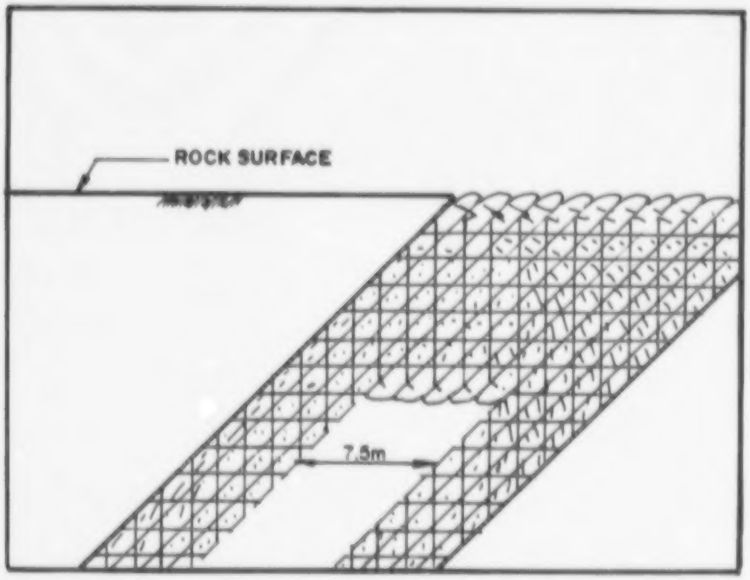

PARTIAL DEVELOPMENT OF COMPRESSION ARCH THROUGH CROWN

Date FEB. 14, 1990
Project 891-1539-3

Golder Associates

Drawn TDR
Chkd Tgc

GEOMETRICAL CONFIGURATIONS FOR SOLID MODEL AND FINITE ELEMENT MESH FOR MINE #29 CROWN PILLAR AND STOPE LAYOUT

FIGURE 4.26

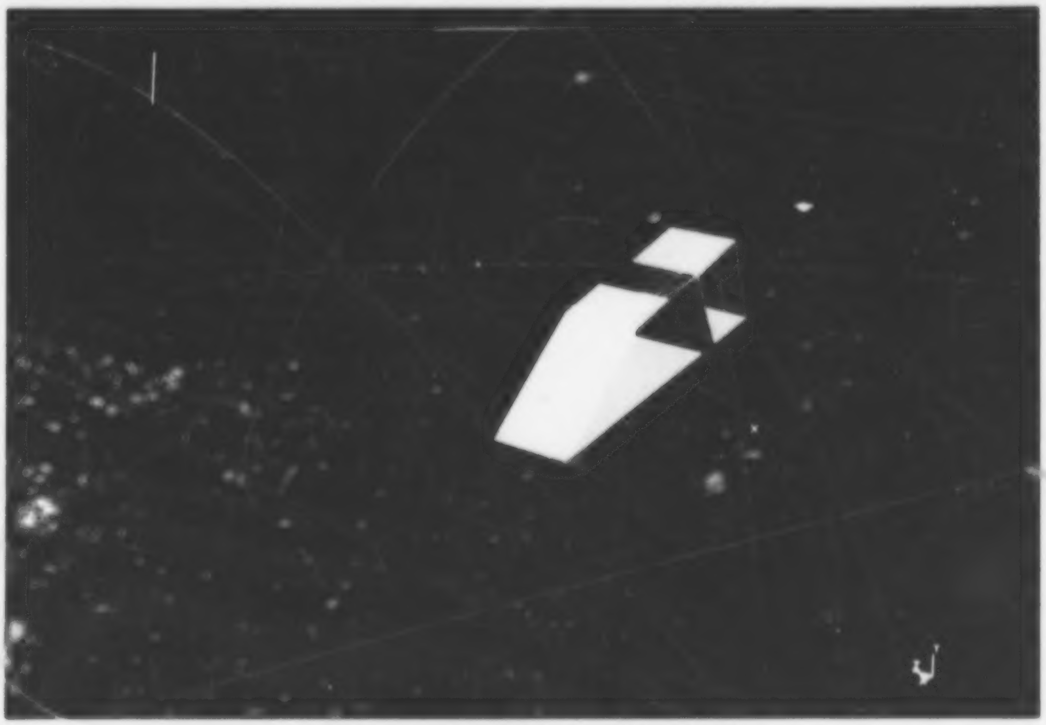

SOLID MODEL OF STOPE CONFIGURATION

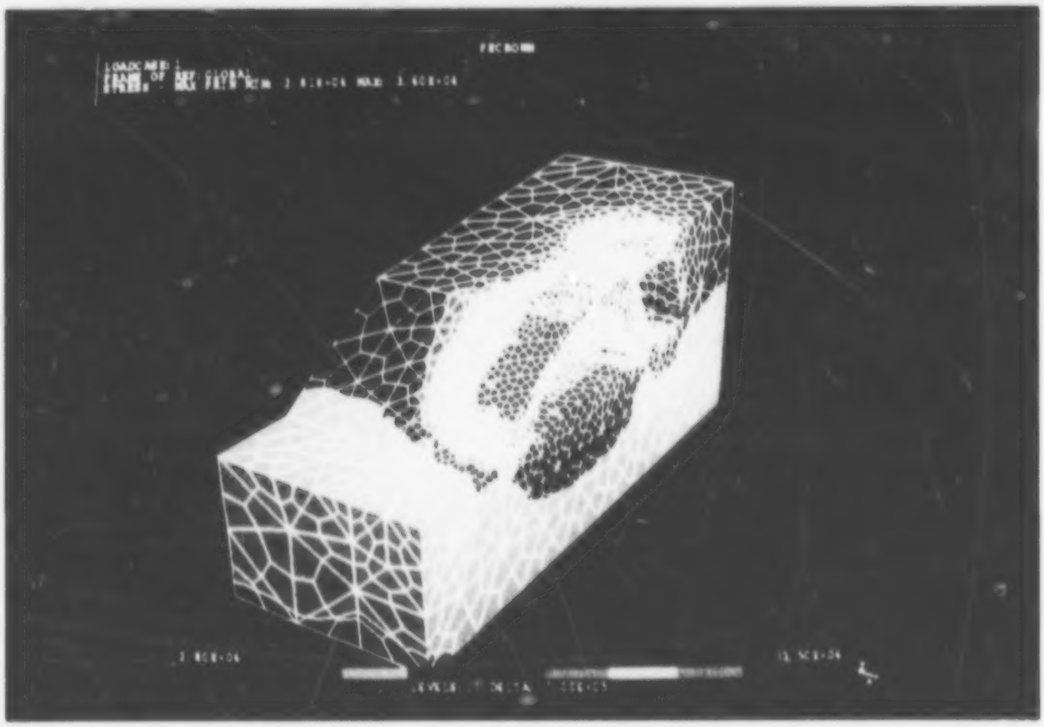

FINITE ELEMENT MESH LAYOUT

Golder Associates

STRESS CONFIGURATIONS ON UPPER SURFACE AND WITHIN ROCK MASS 3-D MODEL - MINE #29

FIGURE 4.27

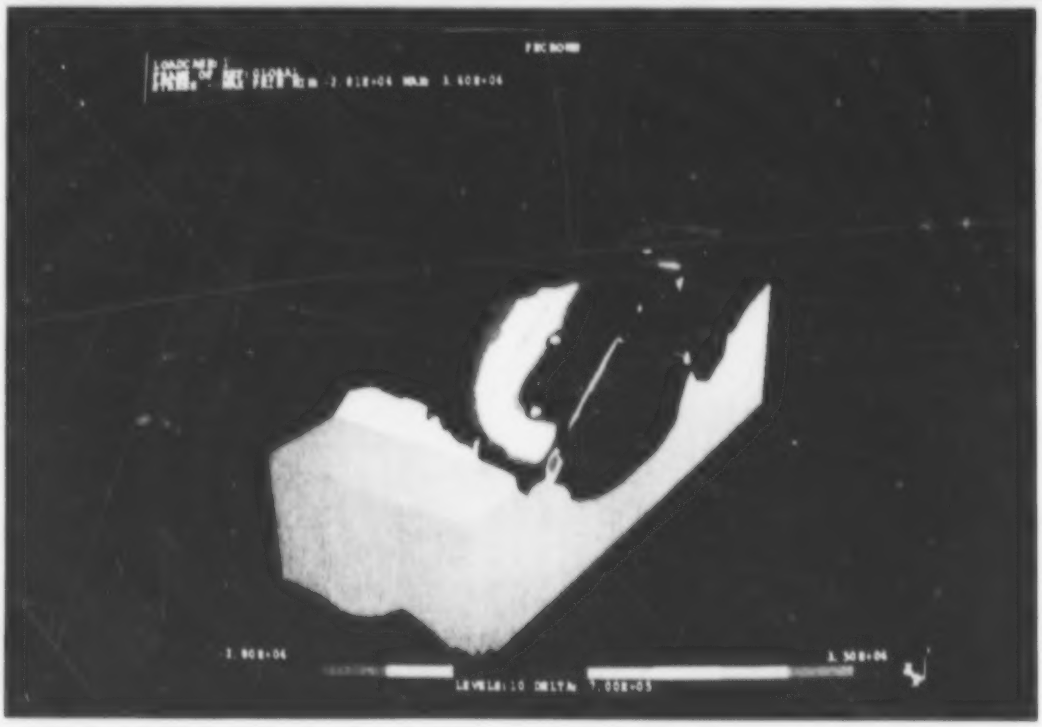

σ_1 - MAJOR PRINCIPAL STRESS DISTRIBUTION

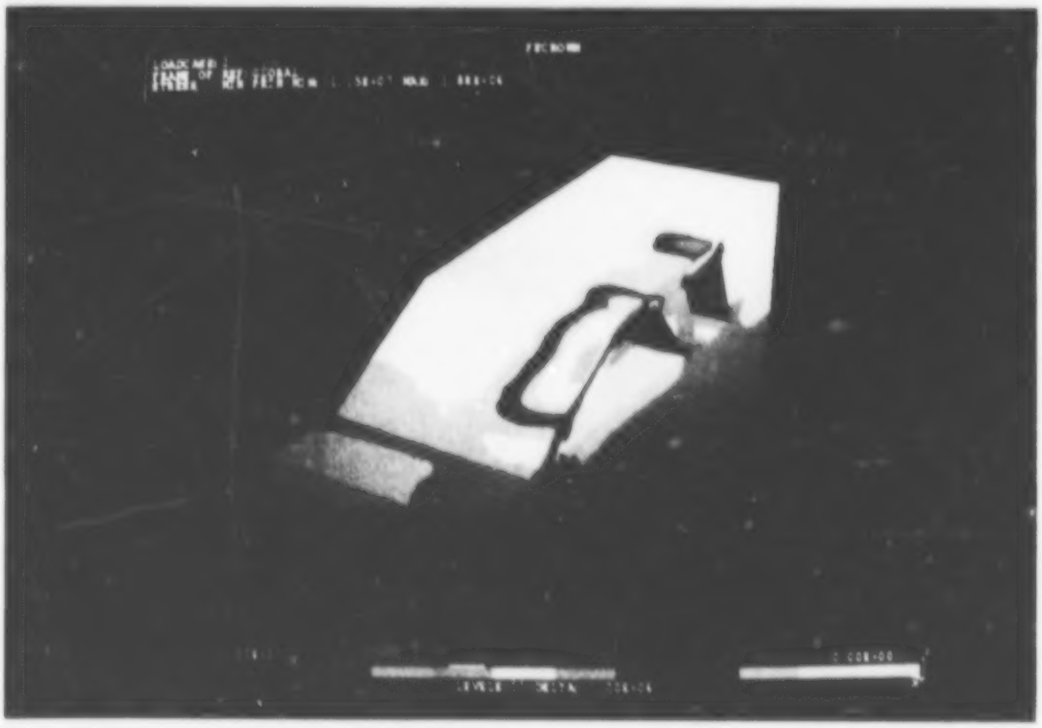

σ_3 - MINOR PRINCIPAL STRESS DISTRIBUTION

Golder Associates

STRESS CONFIGURATIONS - UNDERSIDES OF STOPE CROWN PILLARS AND WITHIN STRIKE PILLAR REGION - MINE #29

FIGURE 4.28

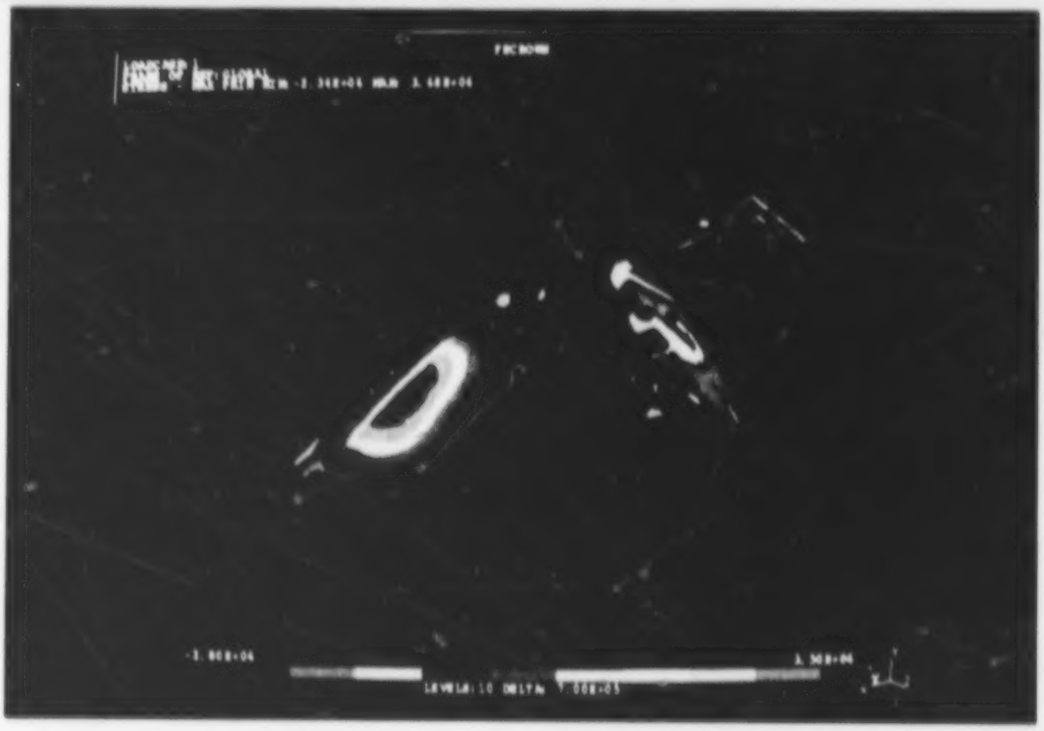

σ_1 - MAJOR PRINCIPAL STRESS DISTRIBUTION

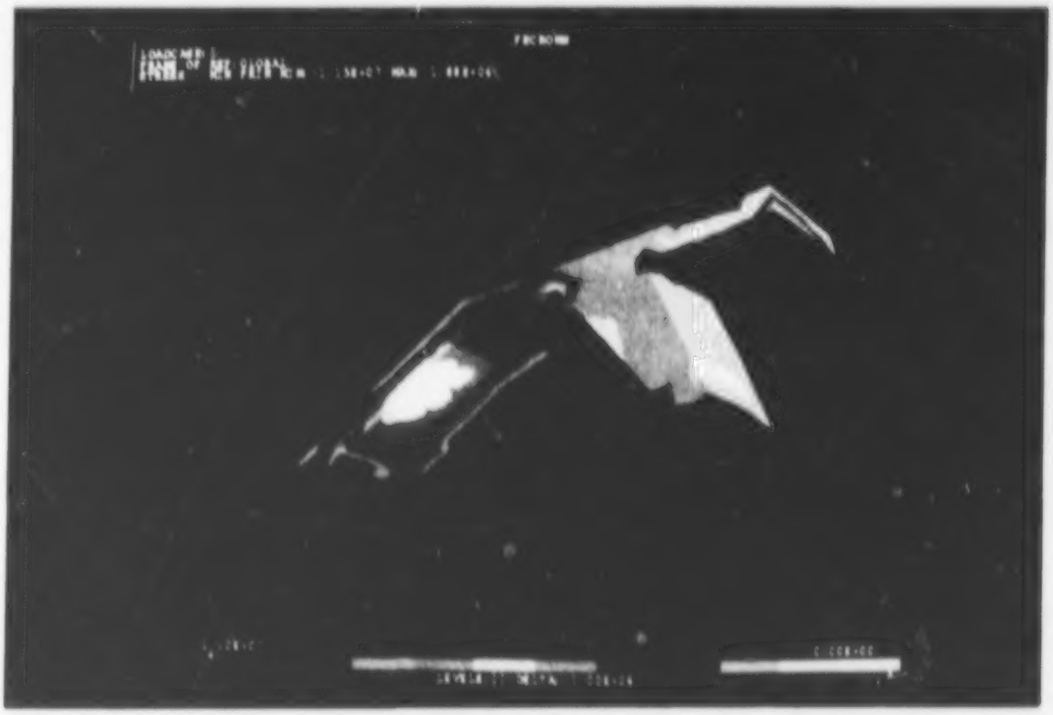

σ_3 - MINOR PRINCIPAL STRESS DISTRIBUTION

Golder Associates

COMPARISON BETWEEN MESH ARRANGEMENTS FOR 2-D FLAC MODEL AND 3-D I-DEAS GEOMETRY
(MINE #29)

FIGURE 4.29

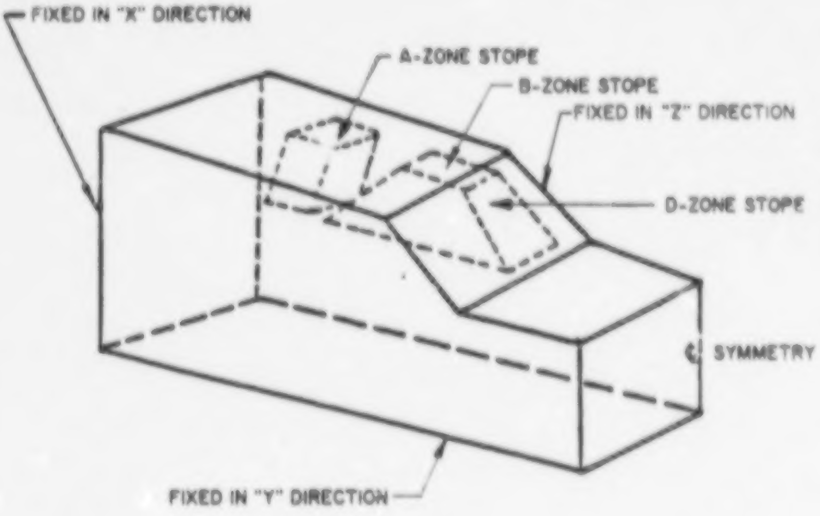

3-D FINITE ELEMENT MODEL (I-DEAS)

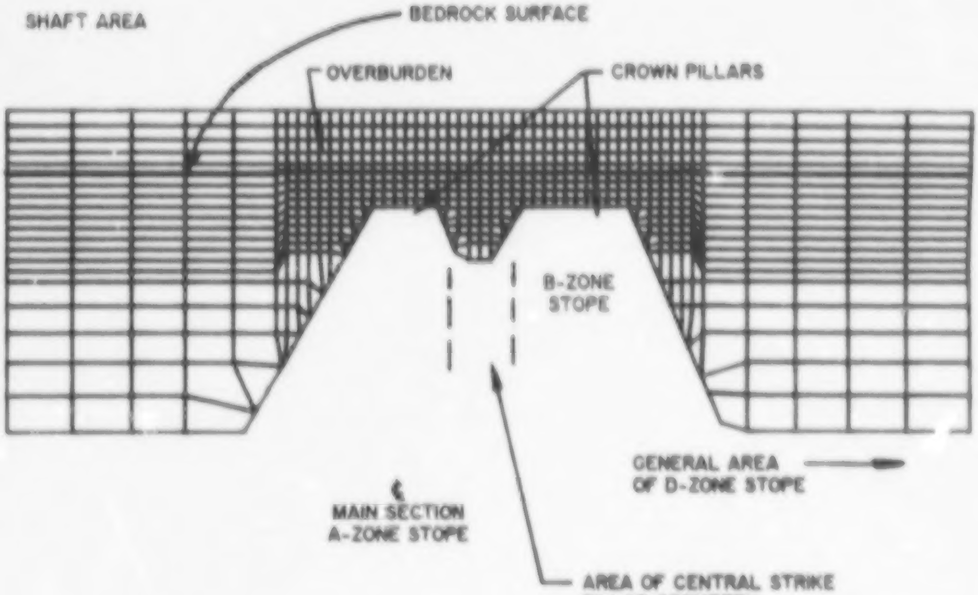
SHAFT AREA
BEDROCK SURFACE
OVERBURDEN
CROWN PILLARS
B-ZONE STOPE
GENERAL AREA OF D-ZONE STOPE
℄ MAIN SECTION A-ZONE STOPE
AREA OF CENTRAL STRIKE PILLAR GEOMETRY

2-D FINITE DIFFERENCE MODEL (FLAC)

Date FEBRUARY 12, 1990.
Project 881-1739-3

Golder Associates

Drawn D.J.R
Chkd

MODELLING CONFIGURATIONS FOR 2-D BOUNDARY ELEMENT AND P-FRAME STRUCTURAL SOLUTION APPROACHES (MINE #29)

FIGURE 4.30

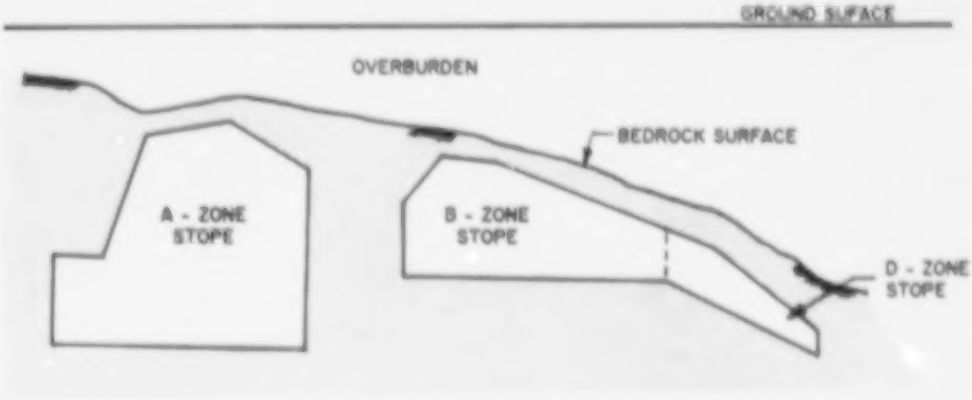

2 - D BOUNDARY ELEMENT MODEL (EXAMINE)

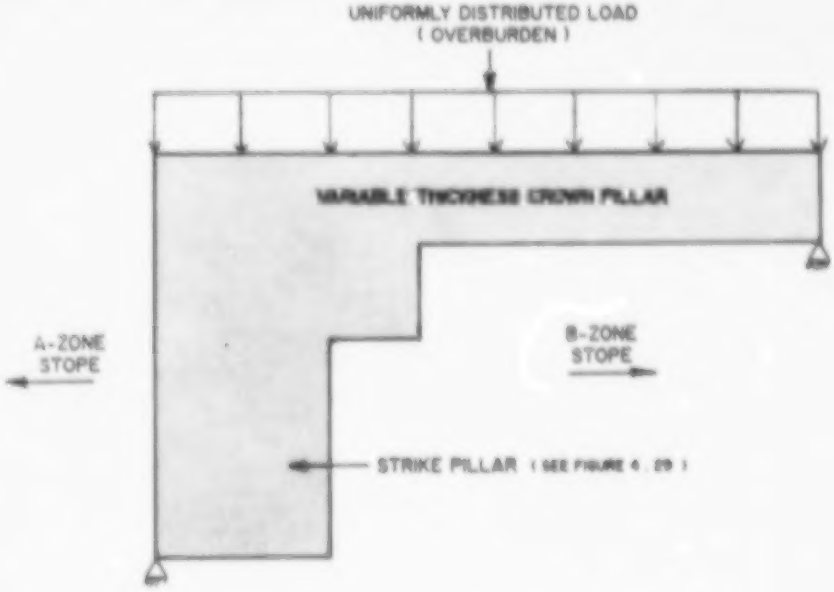
UNIFORMLY DISTRIBUTED LOAD (OVERBURDEN)
VARIABLE THICKNESS CROWN PILLAR
A-ZONE STOPE
B-ZONE STOPE
STRIKE PILLAR (SEE FIGURE 4 . 29)

STRUCTURAL MODEL (P - FRAME)

Date FEBRUARY 12 , 1990.
Project 881-1739-3

Golder Associates

Drawn DJR / R.B.C
Chkd Tgc

RESULTS OF CHIMNEY FAILURE ANALYSES FOR TWO DIFFERENT ROCK QUALITIES

FIGURE 4.31

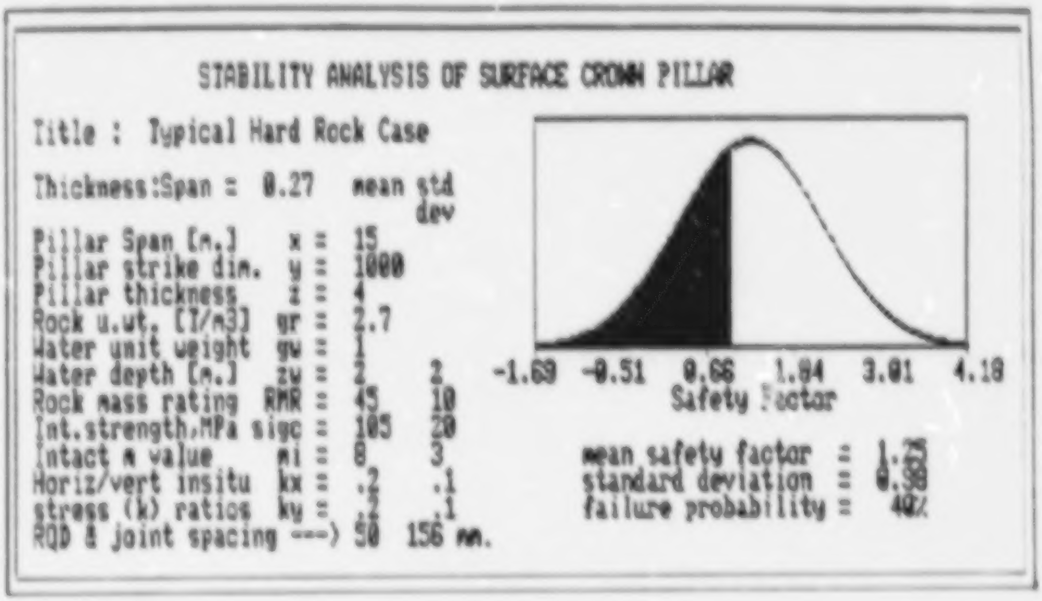

```
              STABILITY ANALYSIS OF SURFACE CROWN PILLAR

Title :  Typical Hard Rock Case

Thickness:Span =  0.27   mean std
                              dev
Pillar Span [m.]     x =  15
Pillar strike dim.   y =  1000
Pillar thickness     z =  4
Rock u.wt. [T/m3]   gr =  2.7
Water unit weight   gw =  1
Water depth [m.]    zw =  2     2
Rock mass rating   RMR =  45    10
Int.strength,MPa sigc =  105    20
Intact m value      mi =  8     3
Horiz/vert insitu   kx =  .2    .1
stress (k) ratios   ky =  .2    .1
RQD & joint spacing ---) 50  156 mm.

                          mean safety factor  =  1.25
                          standard deviation  =  0.98
                          failure probability =   40%
```

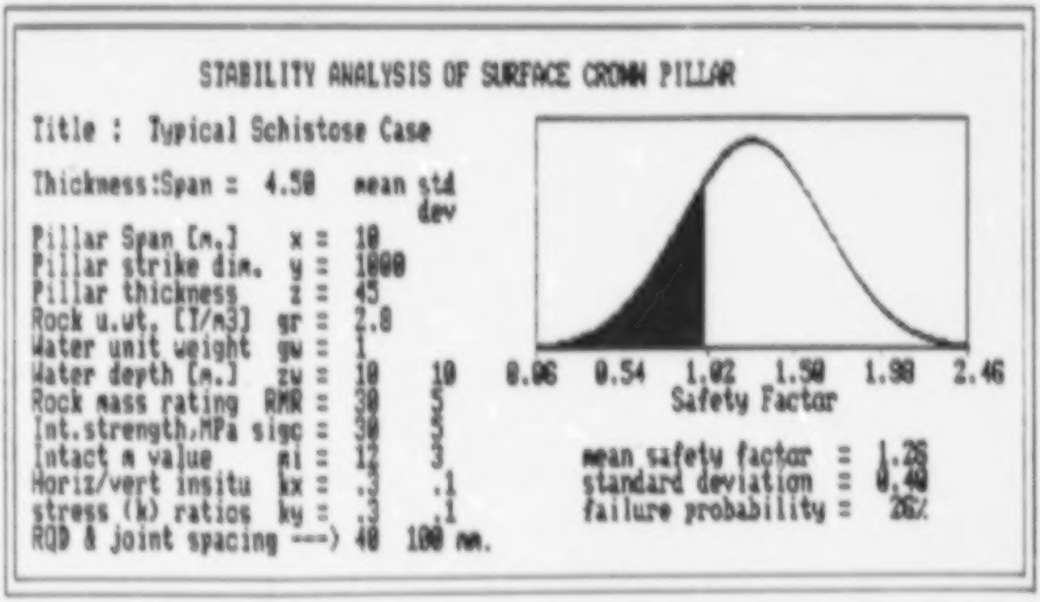

```
              STABILITY ANALYSIS OF SURFACE CROWN PILLAR

Title :  Typical Schistose Case

Thickness:Span =  4.50   mean std
                              dev
Pillar Span [m.]     x =  10
Pillar strike dim.   y =  1000
Pillar thickness     z =  45
Rock u.wt. [T/m3]   gr =  2.8
Water unit weight   gw =  1
Water depth [m.]    zw =  10    10
Rock mass rating   RMR =  30    5
Int.strength,MPa sigc =  30     5
Intact m value      mi =  12    3
Horiz/vert insitu   kx =  .3    .1
stress (k) ratios   ky =  .3    .1
RQD & joint spacing ---) 40  100 mm.

                          mean safety factor  =  1.26
                          standard deviation  =  0.40
                          failure probability =   26%
```

Date FEBRUARY 14, 1990.
Project 881-1739-3

Golder Associates

Drawn R.B.C./P.L.
Chkd TG

Section 5
Application of Evaluation Procedures

Golder Associates

5.0 APPLICATION OF EVALUATION PROCEDURES

In this section of the report, a number of the case records discussed in Section 3 have been analysed to assess the validity of various available approaches to crown pillar stability evaluation. These approaches are summarized on Table 5.1

5.1 Category A Crown Pillars

Several mines in the list presented on Table 2.2 are grouped under Type A - tabular ore zones. The crown pillars for most situations of this type are rectangular and of relatively simple geometry. Beam formulae, plate formulae and Voussoir beam analysis can therefore be considered suitable and were used. Numerical analyses using FLAC were also carried out in some cases to determine ambient stress conditions and to assess overall stability conditions on a mine-wide scale. Five representative mines with both past history of failure or stable conditions were chosen. These are Mine #44, Mine #42, Mine #38, Mine #26 and Mine #33. Analytical and numerical procedures were applied as appropriate to model the known behaviour of the crown pillars.

- Mine #44

The essentially two-dimensional, relatively narrow vein-type geological environment at Mine #44 (see Figure 5.1 and the definition sketch at the bottom of Figure 5.2), is well suited for analysis using structural analysis procedures. The P-Frame program was therefore used for evaluating factor of safety values with respect to shear and tensile modes of failure for a range of crown pillar geometry and geomechanical parameter variations.

The modelled geometrical characteristics of the crown pillar and the rock properties used for the analysis are as follows;

Geometry of modelled crown pillar

span = 12 m
beam depth = 4.5 m
width = 1 m (unit width)

Rock Properties (intact rock)

E = 55 GPa
G = 22.9 GPa
σ_c = 50 MPa, σ_t = 5 MPa
ϕ' = 30° to 55°
c' = 0 to 825 kN

In situ or induced compressive stress = 1 MPa

Loading

Self weight @ 26 kN/m^3
Overburden load = 120 kN per metre length along the crown beam

Figure 5.2 shows typical output data from the program, assuming the crown pillar geometry and loading configuration shown in the sketch at the base of the drawing. Information is provided on deflections, on distribution of vertical shear force within the beam and on the bending moment distribution along the crown.

The factor of safety against shear failure along the beam for a representative friction angle, ϕ' of 30° (with $c'=0$) is presented on the top diagram in Figure 5.3. This is computed for the point where the bending stress is lowest and thus the influence of any normal confining stress necessary to develop shear resistance is at a minimum. At the mid-span of the beam, shear stress is zero, as expected, therefore, the factor of safety against shear failure is theoretically infinite. Under the loading condition described above, assuming only frictional characteristics for the rock, the shear factor of safety is below 1, over two thirds of the span.

The beam was then analysed with higher, (somewhat unrepresentative) friction angles but keeping $c'=0$. The results, which are shown on the lower diagram in Figure 5.3 indicate that there is only a marginal increase in the shear factor of safety with increase in friction angle. If cohesion is introduced, the second curve on the upper diagram in Figure 5.3 shows that a minimum value of c' of 825 kN is required to achieve a factor of safety of 1. For a rock beam which is fairly homogenous and free of adversely oriented schistosity, a significant measure of cohesion will exist in the rock mass. However, for a rock beam with adversely oriented structural discontinuities (e.g., sheared graphitic schists or mylonitic zones), cohesion values would likely be low or zero.

The effects of in situ or induced compressive stresses on crown pillar stability are significant as shown on the top diagram on Figure 5.4. By including a uniform compressive stress of 1 MPa normal to the direction of span, the factors of safety markedly increase. This compressive (clamping) action puts the crown pillar beam into compression, thereby increasing normal stresses acting on any existing shear planes and significantly increasing shear resistance. The lower graph in Figure 5.4 provides a plot of the factor of safety against flexural tensile failure with no induced compressive stress acting along the beam. The results shown indicate that even without clamping action there is little risk of tensile failure of the beam under the prescribed loading conditions.

The results of the analyses for Mine #44, have raised several interesting points:

- the stability of the crown pillar is markedly improved if the pillar is subjected to internal compression, analogous to a prestress loading,
- if cohesion cannot be mobilized along the rock joints, a thicker crown pillar may not necessarily be safer than a thin pillar with respect to potential shear failure, as the normal stresses along the beam are generally low for thick beams and the dead weight of the beam is correspondingly higher than for a thin pillar. This fact may be of considerable importance if the rock is schistose and the schistosity dips in the direction of the maximum shear forces, and
- any cohesion that can be mobilized along the weaker, adversely oriented rock joints is very important as it can strongly influence the stability of the crown pillar with respect to shear.

On the basis of the structural analysis, the current stability of the crown pillar at Mine #44 may be attributed to the presence of clamping stresses and or cohesion on the primary discontinuities in the rock mass.

o Mine #38

For Mine #38, the ore vein forms a relatively thin, low strength, very steeply dipping discontinuity within an otherwise competent conglomeratic host rock. Thus, rather than a fabric weakness being present throughout the crown pillar, stability is largely controlled by the strength of the ore veins and the somewhat wider zone of shearing and disturbance immediately adjacent to such veins.

Two simple geometries were postulated based on examination of the numerous open stopes and existing thin crown pillars at the mine (Figure 5.5). For Case 1, the main ore zone is assumed to occur at the stope centre, often below a natural depression in the bedrock, while for Case 2, the main vein is assumed to occur adjacent to one wall of the stope. These geometries are shown on Figure 5.5, for the crown pillar modelled as a fixed end beam. Three typical spans were examined - 1.5 m., 3 m. and 4.5 m.; and four loading conditions were checked - self weight, a triangular overburden load to approximate soil arching (3 m. deep at mid span), a uniformly distributed load (UDL) due to an overburden soil 3 m. deep and a UDL due to soil 6 m. deep.

Of these, the most critical loading case is the combination of self-weight and UDL due to soil 6 m. deep, analogous to the geometry in the area of an actual cave-in. As available data on in situ properties of the rock mass fabric were limited, rock mass characterization methods were used to form the basis on which shear and tensile strengths were assigned for evaluation of static factors of safety against shear or flexural (tensile) failure of the crown pillar.

The intact rock strength and deformation properties and the rock mass quality (derived from using characterization procedures) and based on field exposures and diamond drillhole data are as follows:

Rock Mass Quality	Intact Argillite or Conglomerate (Country Rock)	Ore Vein or Contact Zone
RQD	40 - 70%	0 - 15%
NGI(Q)	140 - 400	0.1 - 60
CSIR (RMR)	80 - 95	40 - 60
m_i	20 - 25	7
Intact Rock Properties		
σ_c(MPa)	80 - 150	0.3 - 4
σ_t(MPa)	1.2 - 15	0.3 - 4
E (GPa)	70	7
G (GPa)	28	2.8
Unit Weight		
Rock (T/m/^{3})	2.6	2.4
Overburden (T/m^3)	2.4 (Overburden)	

where

m_i = rock mass parameter related to the shear strength of intact rock based on the Hoek-Brown (1981) failure criterion,

σ_c = uniaxial compressive strength of the intact rock,

σ_t = tensile strength of the intact rock,

NGI(Q) = rock mass classification index based on the method of characterization suggested by the Norwegian Geotechnical Institute, and

CSIR (RMR) = rock mass rating based on the rock mass classification approach suggested by the South African Council for Scientific and Industrial Research.

Using the CSIR-RMR rating or Q-index described above and the Hoek-Brown non-linear shear failure criterion, the Mohr-Coulomb rock mass shear strength parameters (c' and ϕ') were derived for various normal stresses appropriate to the situations analyzed (i.e. by using the equations presented in Section 2).

The range of shear strength parameters for typical vein material are tabulated below:-

Rock Mass Shear Strength Parameters

Normal Stress σ_n (kPa)	Effective Cohesion c′ (kPa)	Effective angle of internal friction ϕ' (degrees)
0 - 345	345	45
345 - 690	415	40
690 - 1035	480	37.5
1035 - 1380	550	35
1380 - 1720	620	33

For calculating the factor of safety against tensile cracking within or adjacent to the ore vein, a conservative lower bound value of 0.3 MPa contact tensile strength was assumed for the contact between the ore vein and the host rock.

For a symmetrical V-shaped beam of 4.5 m. span (Case 1 Model), the calculated minimum Factor of Safety against tensile cracking due to bending is greater than 10 for a thickness/span ratio of 1. Shear along the vein is also improbable for this geometry since the theoretical shear stress is zero at the vein. Of all the cases analysed, the most critical conditions identified were for failure of an asymmetrically located ore vein within a thin but relatively wide crown pillar. Critical bending and shear conditions exist for the vein occurring at the sidewall of the stope (i.e. the Case 2 Model). The results for this geometry for the 4.5 m. span have therefore been plotted in the lower half of Figure 5.5.

As noted in the generic beam analysis, the mode of failure differs with different thickness to span geometries. Specifically, the calculated factors of safety against tensile cracking due to bending within or adjacent to the calcite vein are greater than 1 at thickness to span ratios in excess of about 0.35. The calculated factor of safety against tensile cracking increases significantly as the thickness/span ratio increases. It is about 3 at a thickness to span ratio of about 0.6. These results are consistent with arching theory which indicates that flexural failure is not critical when the thickness/span ratio exceeds a relatively modest value.

By contrast, the calculated factors of safety against shear failure on or within the ore vein in the Case 2 model range from about 1.3 at a span ratio of 1, to about 1.5 at a span ratio of 1.5 (Figure 5.5).

It is of interest to note from Figure 5.5 that the factors of safety against tensile and shear failure both exceed unity for a thickness to span ratio greater than about 0.35. This appears to be consistent with field observations of failed crown pillars at Mine #38.

- Mine #42

As the geometry of the crown pillar at Mine #42 is relatively elongated along strike, but also exhibits several transverse pillars separated by openings, it was analysed both as a beam and as a plate. The geometry and input parameters respectively are sketched on Figure 5.6 and presented in Table 5.2. Since no detailed rock property data was available for this mine, rock properties were assessed from Q and RMR correlations and checked against those of the rock masses at Mine #38 and the hangingwall side at Mine #22 for which better information was available.

Figure 5.6 shows the results of the beam analysis. The plot gives maximum tensile stresses developed in the existing surface crown pillar for two specific pillar thicknesses and for a range of spans, assuming that the pillar is analysed as a fixed end beam. These are shown together with an indication of the applicable tensile strength of the rock comprising the crown pillar. For the actual pillar thicknesses existing at the site, tensile stresses in the pillar are very modest (below 5 MPa) for the range of actual spans (8-15 m). However, the tensile stresses are between 10 to 20 MPa for a 1 m thick pillar of the same span range.

As shown on the longitudinal section included on Figure 5.6, in some parts of the crown, relatively thin pillar sections exist. In these situations, there is potential for bending-induced tensile cracking. Elsewhere along the crown pillar at this mine, where thicknesses of the pillar are greater (refer longitudinal section on Figure 5.6), shear is a more likely mode of failure. In general, both shear strengths and tensile strengths are sufficiently high that failure of the crown beam has not occurred. This is despite the fact that some slabbing type instability of the walls of the stopes has been commonplace at this mine and at others along the "main break" through this mining belt. This type of slabbing is in fact also suggested by the results of some of the numerical analyses.

As this mine was used as a control case for evaluating the effectiveness and representativeness of the FLAC program, several checks were also possible on parameter selection as discussed in Section 4. In order to maintain consistency, the same basic geometry as shown on Figure 5.6 and used for the beam analyses, was used for the FLAC analyses. While the structural analysis, discussed in the previous paragraphs, has focused on the behaviour of the crown pillar itself, the numerical analysis discussed in Section 4 provides a somewhat more global evaluation of stress conditions which might induce failure of the crown pillar through instability of the stope. The modelling carried out for this mine clearly illustrates that stability of the crown is controlled by wall rock conditions in the stope below. If low shear strengths are assumed for either the hangingwall or the footwall, extensive displacements are predicted.

- Mines #25 and #26

The geometry and geology of the mine openings at Mine #26 and at the adjacent Mine #25 are relatively consistent, with stopes developed in rocks either side of and within the contact zone between a slabby suite of greywackes and a fairly competent syenite porphyry unit (for reference see Figure 5.7 and Figures 3.18 and 3.28 of Section 3).

The crown pillars in many parts of these two adjacent mines are fairly thin and in competent ground. As in these areas of competent ground, the crowns are generally supported on all four sides over reasonably short strike length, some preliminary analyses were undertaken using plate approaches to examine the minimum surface crown thicknesses that were sustainable in such rocks.

In view of the typical geometry of the stopes in competent rock at both mines, the crown pillar was analysed as a plate with a short span of 20 m. and with long spans varying between 20 and 60 m. The geometry of the plate analysed for this case is shown in Figure 5.8 and the input parameters used in the analysis are presented on Table 5.2. Assuming that the plate approach is valid and that the tensile strength of the rock mass is about 5 MPa, then with characteristic strike length/span ratios, minimum sustainable crown pillar thicknesses are of the order of 1.5 m for resisting failure by tensile cracking.

- Mine #33

Most of the rock mass at Mine #33 is competent, and in consequence, the majority of the narrow vein mining at the property did not experience problems, however some places exhibited progressive caving effects of the ore zone and immediate wall rocks.

The geometry of the vein systems at Mine #33 are relatively complex (see Figure 5.9), with numerous parallel ore zone structures occurring throughout the mining depth. In most locations crowns have remained stable, but one area of suspected surface crown pillar collapse occurred where a zone of parallel veins had been extracted. The location is situated adjacent to part of the main stoping on the #5 Vein system (as shown on the section at the base of Figure 5.9).

In 1982, depressions were noted in the overburden deposits and angled diamond drilling of the crown pillar rock mass over the stope was undertaken to evaluate the cause of the depressions. The possibility that some type of hangingwall or crown caving had developed was suggested by the fact that some 300,000 tons of "slough-muck" were recorded to have originated from above the 1000 ft. level on the #5 Vein.

Exact details of the extent of such sloughing problems were not achieved by drilling, although one hole intersected overburden and timber at a location which, based on the mine records, should have been 10-12 m. within the hangingwall rock mass. Nevertheless, as the surface depressions in the relatively thin overburden cover are in about the correct location for the effects that might be induced by local crown pillar collapse, some preliminary numerical analyses have been undertaken to evaluate likely failure mechanisms.

A FLAC model was set up to analyse the #5 Vein as a simplified single stope. Figure 5.10 shows the predicted elastic stress trajectories and zone of tensile minor principal stress. This tension zone encompasses both the upper part of the footwall rock mass and a sizeable zone on the hangingwall side. The crown pillar, however, remains in compression. It is noteworthy that the results are similar to those obtained from the analyses conducted for Mine #42 (refer to Figures 4.19 to 4.20). However, rock strengths at Mine #33 are less than those at Mine #42 as minor instability, somewhat analagous to the movements shown on Figure 4.20 likely occurred, giving rise to the extra ore material drawn from the stopes.

5.2 Category B Crown Pillars

Various examples of crown pillars in blocky rock mass conditions are tabulated in Appendix A. The most comprehensive geotechnical data however is available for Mine #29 (see Figure 3.13).

- Mine #29

Various approaches were used to assess the stability conditions of the hard blocky rock mass at Mine #29. These included P-Frame, boundary element and three-dimensional finite element analysis. All of the results gave rise to representatative predictions of critical stability zones, which closely match actual cave-in areas (see Figures 4.26 to 4.30 and detailed discussions in Section 4).

5.3 Category C Crown Pillars

Crown pillar stability in foliated rock masses is dominated by pervasive schistosity. The use of the Voussoir approach may provide realistic matching of such conditions as it takes into account dominant discontinuities as a set of discrete breaks between voussoirs. However, numerical analysis is often more appropriate for examination of schistose, foliated rock conditions because then the overall interaction between the stope and the crown can be checked, as these are often inter-related. The FLAC formulation is well suited to modelling foliated rock mass environments by means of the "ubiquitous joint model". However, because of the intrinsic characteristics of the elasto-plastic behaviour of the post-peak model in FLAC, especially in the case where a "no-tension" material is assumed, excessive displacements can often result unless very careful parameter matching and calibration is undertaken (see Figures 4.19 to 4.21 for the variations apparent from initial analysis of the Mine #42 case records). The use of appropriate input parameters is therefore critical, in order to obtain rational results.

In most steeply dipping, foliated rock environments, where displacements are controlled by the schistosity, and release surfaces are provided by other secondary cross joint sets, sliding and toppling failure modes are common. In de-stressed areas, where tensile delamination and rock movements take place along major discontinuity surfaces, a continuum approach may not be entirely applicable for assessing the stability of the stope and crown pillar. The discontinuum approach, using such computer block codes as MUDEC, can offer better insight into such problems.

The application of both of these approaches however is illustrated by reference to the four mines examined in this section of the report, namely Mines #15, #14, #22 and #45. For Mines #14 and #15, FLAC was used with the ubiquitous joint model as this was considered the most representative. For Mine #22, where distinct block sliding of the footwall and toppling of the hangingwall has been observed, MUDEC was used to examine the trend of interblock movements, while for Mine #45 limit equilibrium methods were applied to examine hangingwall slabbing as a possible mode for destabilization of the crown pillar.

o Mine #15

The FLAC program was applied to this mine in order to match known condtions. The ubiquitous joint model was used in the immediate area of the stope with the inherent weakness oriented parallel to the sidewalls, thus representing the graphite schist units. For areas away from the stope, a Mohr-Coulomb model was used as this can more accurately represent the far field rock mass.

From the geology plans provided by the mine and test results obtained by CANMET, several different material zones were defined in order to match known rock conditions. Input parameters for these zones are presented in Table 5.3. The results of the modelling using these Mohr-Coulomb parameters for the post failure analysis are shown in Figure 5.11.

It can be seen that the displacements at the sidewalls are primarily along the ubiquitous joint sets. Individual displacements are predicted to be of the order of 10 cm. Minor displacement at the crown and some settlement of the overburden is predicted. The trend of the displacements, as indicated by examination of history plots for individual elements at the centre of the crown, shows that stability has not been achieved for the sets of input parameters used in the model.

However, these predicted conditions seem to be relatively accurate and consistent with observations of instability noted within several sill pillars at the property.

- Mine #14

A similar ubiquitous joint FLAC model as that used for the analyses for Mine #15 (again with Mohr-Coulomb conditions included for the far-field zone away from the stopes), was set up for evaluating the crown pillar at Mine #14. Again, as extensive rock testing has been carried out, both by the mine and by CANMET, it was possible to define each of the major geological zones by appropriate material parameters. A complete set of these input parameters is presented in Table 5.3. As shown on Figure 5.12, the modelled cross-section matches that shown on Figure 3.16 with the two large stopes separated by an approximately 20 m. thick strike pillar. Again, as for Mine #15, the overburden was assumed to be an elastic cohesive medium, in this case approximately 7 m. thick.

Post failure analysis was again undertaken using a Mohr-Coulomb model with the following range of input parameters:

$\phi' = 63°$
$c' = 1.25$ MPa
$\sigma_t = 0$ to 1 MPa

From examination of Figure 5.12, it will be noted that very large displacements occur in the hangingwall of the shorter stope and relatively smaller displacements occur of the hangingwall of the taller stope. The trend of these displacements is such that progressive movements would continue in the hangingwalls of both stopes, ultimately causing destabilization of the pillar between the two stopes. Downward slip within the rock mass is suggested to develop above the shorter stope. It is likely that such movement would propagate further into the rock mass in both the vertical and lateral extent. It is interesting to note that the actual failure that occurred of this part of the crown pillar, in fact, appears to have been consistent with this predicted failure mode.

o Mine #22

As significant hangingwall toppling had occurred as part of the failure at Mine #22 (see Figure 5.13), the pre-failure situation was modelled using the MUDEC code so that individual block behavioural trends could be emulated.

The thinnest crown pillar cross-section was selected for modelling as it represents the most severe geometry. Two major joint sets (70° foliation and a 30° northward dipping set) were incorporated into the model (Figure 5.14). Displacement vectors, stress trajectories and deformed block geometries were monitored for a fairly long period run with relatively low moduli and shear strengths assumed for the slaty greywacke of the footwall area. Table 5.3 lists the input parameters used for this modelling and Figure 5.14 shows the predicted stress distribution around the stope. It is interesting to note that both the surface crown pillar and the sill pillar are under compression, but progressive displacements and block movements are occuring in the stope sidewalls, see Figure 5.15.

The computed displacements shown on the left hand plot on Figure 5.15 suggest that initial movements develop in the hangingwall of the larger lower stope. At the first stage, the maximum elastic displacement is only approximately 3 cm. at mid-height of the stope, but dislocation of the walls is beginning to occur and closure of the bottom of the stope at the draw-point is already evident. The crown and footwall are also exhibiting some movement such that shearing is being induced within the slaty footwall rock mass. Footwall displacements are only approximately 1 cm. and the crown pillar, at this stage, remains intact and relatively stable. With further deformation, hangingwall slabbing and crown pillar shear develops.

It is interesting, in the light of the failure events, to examine the stress trajectory plot shown on Figure 5.14. This indicates that both the footwall and hangingwall have become de-stressed and that stress concentrations within the surface pillar are also small. The results also indicate that the interface stresses between the elements at the footwall and hangingwall of the stope have become tensile because of tensile delamination along the schistosity due to stress relief. A large horizontal stress concentration, however, can still be observed at the sill pillar between the upper and lower stopes. This seems to persist almost until the point of final crown block sliding and collapse (see stages 2 and 3 on Figure 5.15).

Failure at the hangingwall of the lower stope appears to be initiated by slab delamination which then leads to toppling. Since the hangingwall almost immediately becomes completely destressed, the thin plates formed by the intersection of the major cross joints with the foliation are free to delaminate. In fact, some distortion of the hangingwall at mid-height is clearly developed at stage 3, as shown on Figure 5.15. As illustrated, once such a failure is initiated, progressive caving and upward ravelling develops. Ultimately, at the crown of both stopes, the blocks, bounded by the 70° schistosity and the 30° master joints, become free and begin to slide into the stope as the shear strength on the foliation is exceeded.

At the footwall of the large lower level stope, sliding along the low angle joints propagates as outward movement of the toe blocks continues towards the stope, thereby promoting large scale rock movement on the entire stope sidewalls (see stages 2 and 3 plots). Closure of the basal hangingwall section of the drawpoint also seems to contribute to the overall development of the hangingwall instability.

These numerical evaluations suggest that failure of the crown pillar was controlled by slabbing and delamination of the stope hangingwalls and by shear failure within the crown pillar footwall abutment area. It is significant that this failure mode is consistent with observed failure mechanisms seen in other stopes in similar ground conditions.

o Mine #45

As shown by the analyses for Mine #22, hangingwall slabbing and footwall delamination in schistose rocks is a common problem that historically can give rise to significant crown pillar failures. It is compounded by dewatering of old workings because rapid depressurization of a schistose rock mass by uncontrolled lowering of water levels can lead to severe pressure-induced instabilities first of the hangingwall and thence of the crown of near surface stopes. (viz. the Mine #60 situation refer: Section 3 of this report). Considerable care therefore needs to be taken in such cases to maintain controlled pressure regimes in the bedrock throughout dewatering. With too rapid lowering of water levels, severe pressure gradients can be induced, which

- can precipitate slabbing failure along schistosity planes in the stopes and
- induce block caving of fractured zones in thin crown pillars.

Any collapse of the crown pillar or progressive upward migration by tensile delamination of the stope backs could lead to surface breakthrough. In consequence, detailed parametric analyses were undertaken as part of an overall assessment of the stability of the workings at Mine #45. This work was carried out to control the rate of dewatering through the old workings. For both crown stability and hangingwall slabbing cases, the rock was analysed as an integral beam of given thickness and properties:

- for the hangingwall, a continuous slab (of full stope height) was considered as a fixed-end beam supported only at the stope crown and invert, and

- for the crown pillar, analysis was carried out in two ways. The first assumed that the crown pillar behaved as a cantilevered beam supported on the footwall side and cantilevered across the stope crown. The second assumed that the crown pillar behaved as a rigid block prevented from sliding into the stope by shear resistance developed on weak schistose bounding discontinuity surfaces on the footwall.

The idealized geometry considered for these analyses is shown on Figure 5.16 and the input parameters for the analyses are summarized in Table 5.2. Based on the analyses, stability conditions are extremely sensitive to water pressure effects. Slabbing of the hangingwall was found to be the critical mode of failure once the water level in the stopes was below the level of the stope crown, but when the water pressure head in the footwall side of the rock mass was at or above the crown of the stope, failure of the crown pillar was found to be more critical (Figure 5.17).

5.4 Category D and E Crown Pillars

Several failures of crowns in slabby or faulted situations have occurred where the rock mass was of low strength or the geometry of the excavations was adverse for kinematic stability. In most situations, such failures exhibit many of the features addressed under the previous types of crown geometry. Usually though, the geometry of individual fault controlled potential failure modes requires site specific conceptualization of 3-D geometry for rational analysis. Use of parametric analyses conducted with MUDEC in combination with application of statistical approaches to realistically quantify rock mass parameters, may allow more generic understanding to be made for prediction of which types of slabby, blocky and faulted situations are of critical concern. Key block modelling aided by simple kinematic stability checks using a stereonet, are however, essential for understanding possible failure mechanisms in very complex geological environments.

TABLE 5.1 - Summary of Numerical Analyses Undertaken for Crown Pillar Evaluation Project

	PROGRAM CODES				
Mine #	MUDEC	FLAC	EXAMINE	P-Frame	I-DEAS
14		◆	◆		
15		◆	◆		
22	◆		◆		
26			◆	◆	
29		◆	◆	◆	◆
33		◆	◆	◆	
35		◆	◆		
36		◆	◆		
38				◆	
42		◆	◆	◆	
44			◆	◆	
45		◆	◆		
46		◆	◆	◆	

TABLE 5.2 - Input Parameters for Beam, Plate & Voussoir Beam Analyses

Mine#	w [m]	t [m]	o/b [m]	E [GPa]	σ_c [MPa]	σ_t [MPa]
15*	3	25	30	56-106	96-166	17-22
26	20	8	3	55	50	5
35*	4	16	10	69**	77	13
42	8	3	0	64	144	19
44	4	2	10	50	150	10
45	5 or 15	5	25	20	50	5
46	5	2	20	50	100	10

- w = width of beam
- t = thickness of beam
- o/b = thickness of overburden

* data from CANMET report MRL 89-22 (INT)

** from dilatometer E < 10 GPa

TABLE 5.3 - Input Data for FLAC and MUDEC Analyses

FLAC	ROCK						JOINT		MODEL
	ρ [kg/m^3]	G [GPa]	K [GPa]	c' [MPa]	ϕ' [°]	σ_t [MPa]	c' [MPa]	ϕ' [°]	
Mine #14									
HW	2700	24	40	1.27	33	0.38	-	-	Mohr
FW	2700	24	40	2.42	49	0.368	-	-	Mohr
Schist	2700	8	13.3	0.93	22	0.0079	0	15	Ubiquitous
V9	2700	24	40	1.23	32	0.032	0	26	Ubiquitous
Mine #15									
V6-7	2700	35.2	58.7	1.41	41	13.6	-	-	Mohr
V8-9	2700	28.4	52.2	0.039	42	9.98	1.248	64	Ubiquitous
qtz	2700	33.3	39.39	0.039	42	9.98	1.248	34	Ubiquitous
gc	2700	8.0	13.33	0.416	22	0.341	0.014	26	Ubiquitous
Mine #35									
	2700	23.6	39.3	-	-	-	-	-	Elastic
Mine #42									
	2700	11.3	20.2	1.25	63	1.0	-	-	Elastic and Mohr
Overburden (where applicable)									
	1600	0.03	0.1	-	-	-	-	-	Elastic

MUDEC	ROCK						JOINT		MODEL
	ρ [kg/m^3]	G [GPa]	K [GPa]	c' [MPa]	ϕ' [°]	σ_t [MPa]	c' [MPa]	ϕ' [°]	
Mine #22									
	2800	16.7	10	-	-	-	0	15	Elastic - Block Mohr - Joint

- for all cases, $k_o = 1$

GENERALIZED GEOLOGICAL CROSS - SECTIONS AND PLAN (MINE #44)

FIGURE 5.1

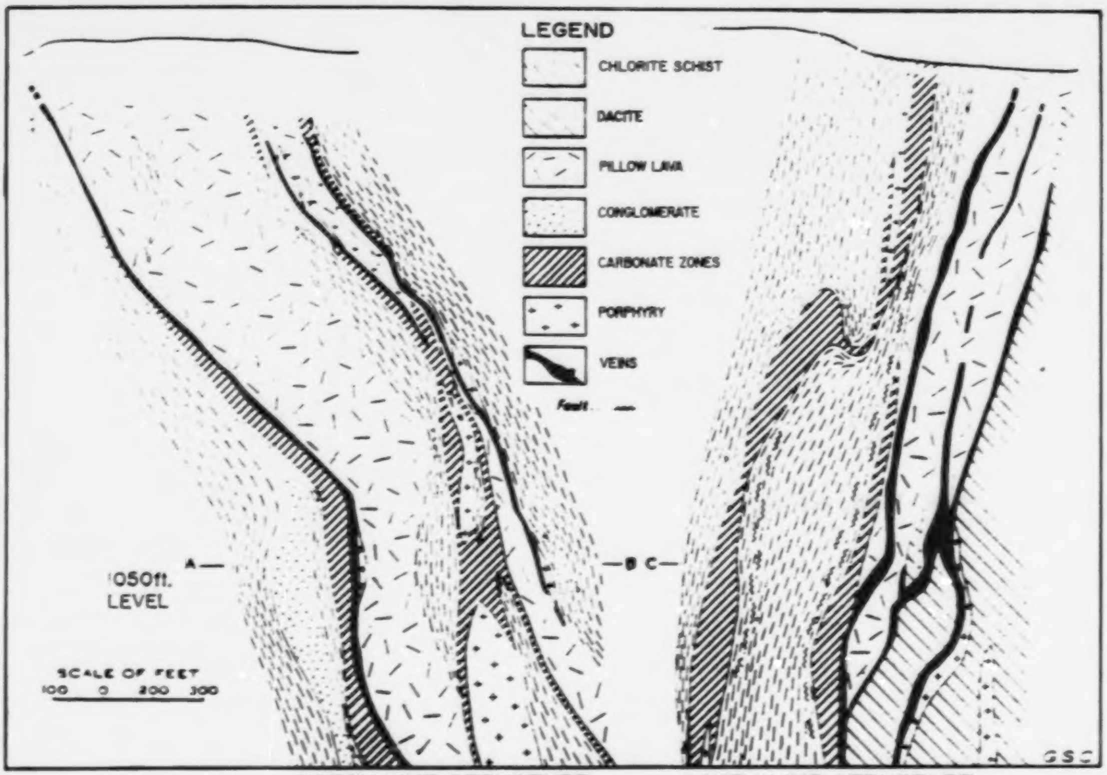

NORTH LIMB STRUCTURE SOUTH LIMB STRUCTURE

CROSS - SECTIONS

PLAN OF MINE AREA

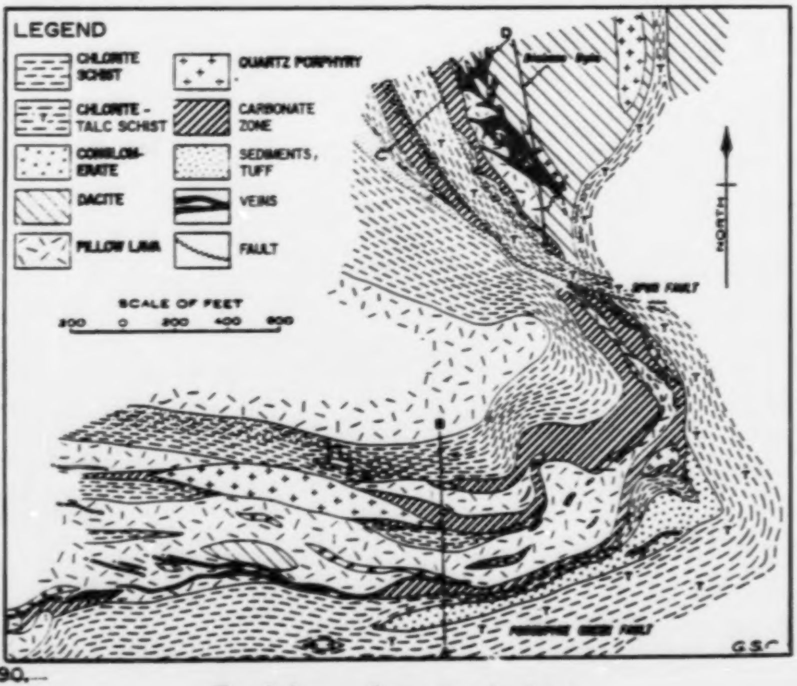

Date FEBRUARY 14, 1990.

Project 881-1739-3

Golder Associates

Drawn PL

Chkd.

TYPICAL P-FRAME OUTPUT FOR BEAM ANALYSIS DEFLECTION, SHEAR AND BENDING MOMENT PLOTS FOR CROWN PILLAR AT MINE #44

FIGURE 5.2

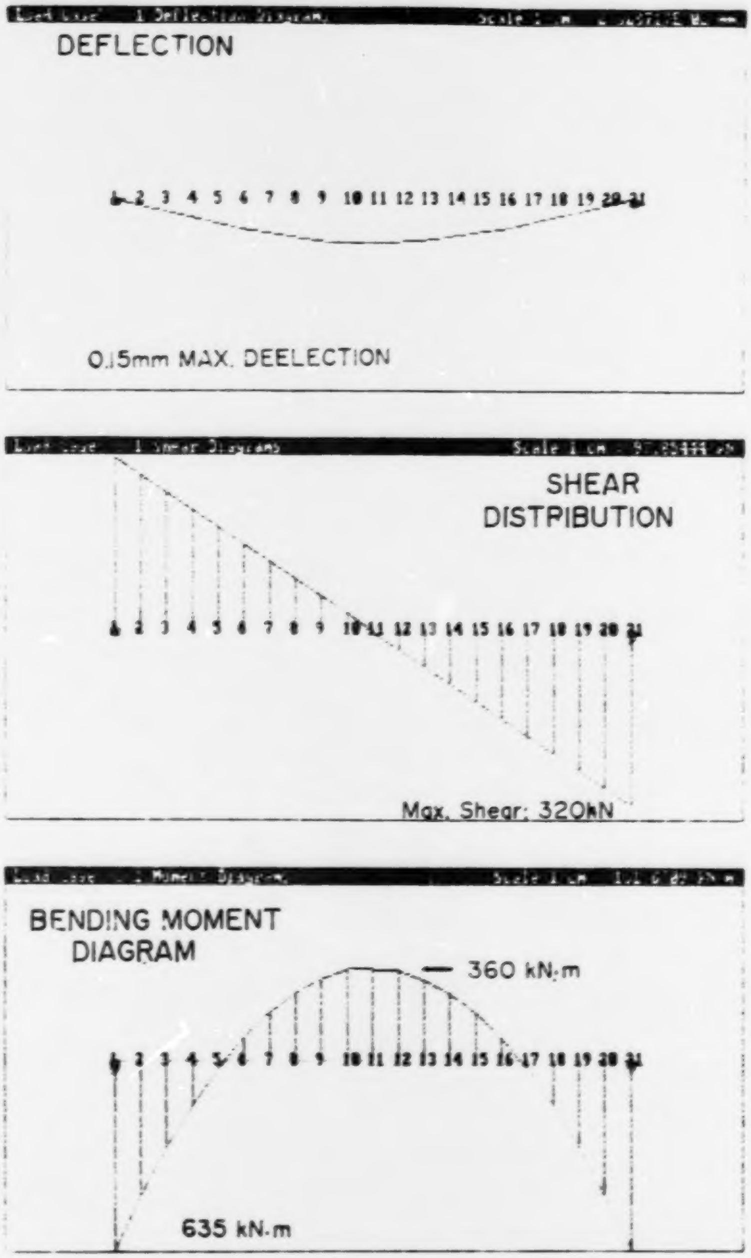

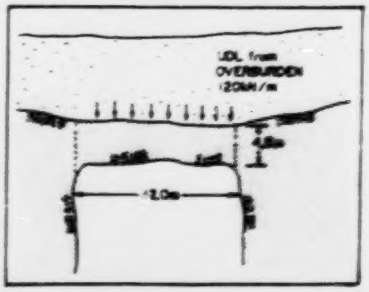

SKETCH OF ACTUAL GEOMETRIC CONFIGURATION

Date FEBRUARY 14, 1990.
Project 881-1739-3

Golder Associates

Drawn R.B.C./P.L.
Chkd TGC

APPRAISAL OF CROWN PILLAR STABILITY AT MINE #44 USING ELASTIC BEAM THEORY (P-FRAME)

FIGURE 5.3

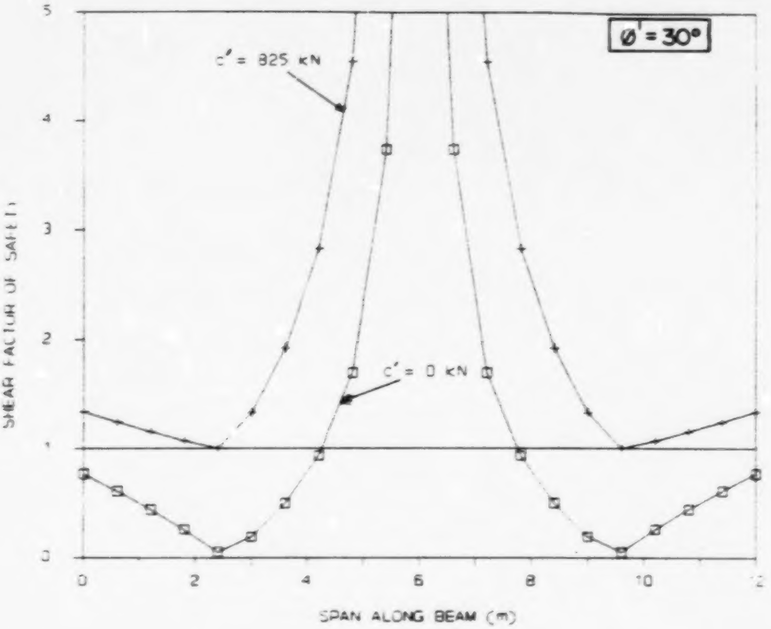

INFLUENCE OF COHESION ON
FACTOR OF SAFETY AGAINST SHEAR

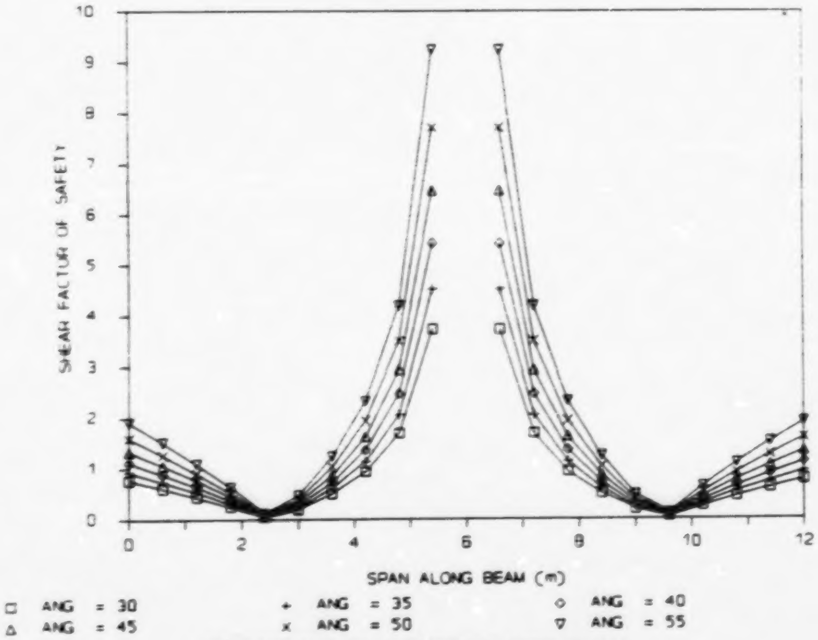

INFLUENCE OF FRICTION ANGLE ON
FACTOR OF SAFETY AGAINST SHEAR

Date FEBRUARY 14, 1990.
Project 881-1739-3

Golder Associates

Drawn R.B.C./P.L.
Chkd.

INFLUENCE OF LATERAL CONFINING STRESSES ON STABILITY OF CROWN PILLAR
(MINE #44)

FIGURE 5.4

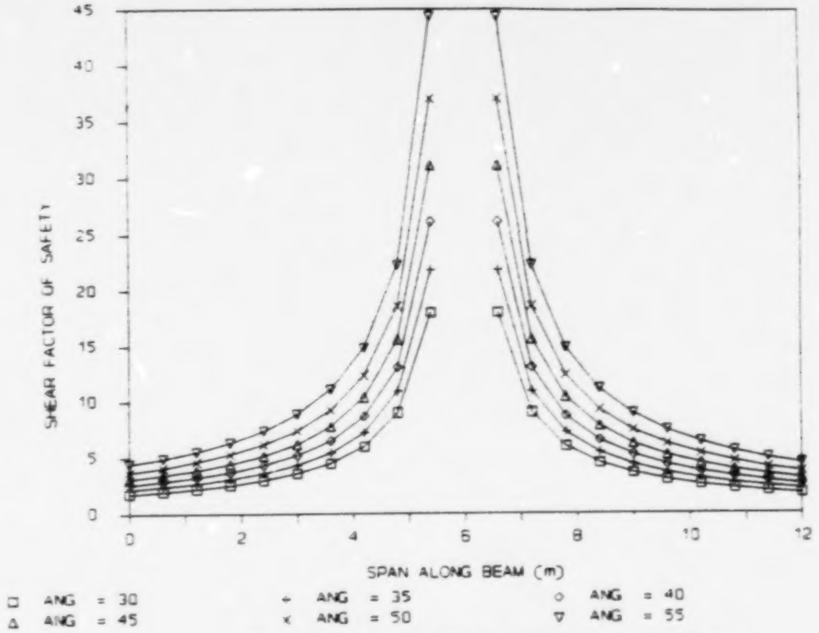

EFFECT OF 1 MPa HORIZONTAL "CLAMPING" COMPRESSION ON FACTOR OF SAFETY FOR FRICTION ONLY ANALYSES

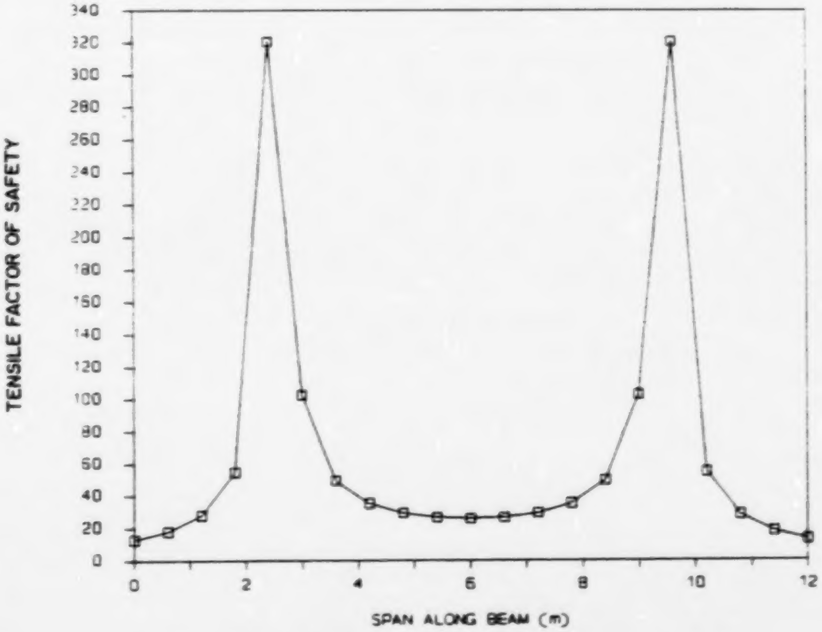

VARIATION OF TENSILE FACTOR OF SAFETY ALONG SPAN OF CROWN PILLAR BEAM

Date FEBRUARY 14, 1990

Project 881-1739-3

Golder Associates

Drawn R.B.C./P.L.

Chkd. ~~tk~~

CROWN PILLAR THICKNESS PARAMETRIC EVALUATION (MINE #29)

FIGURE 5.5

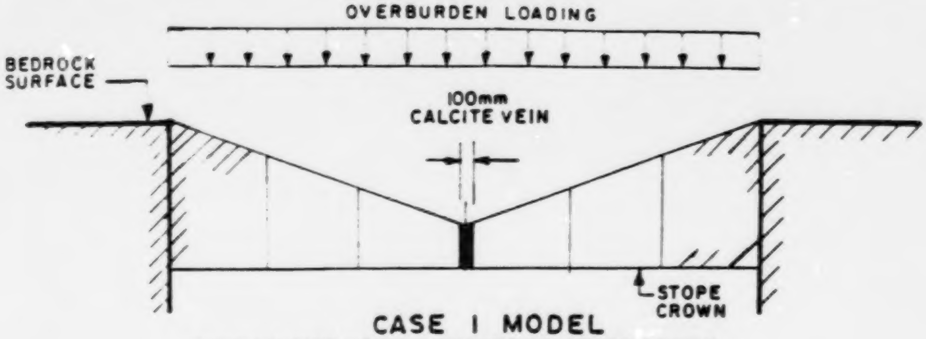

CASE 1 MODEL

MAIN CALCITE VEIN AT CENTRE OF STOPE CROWN

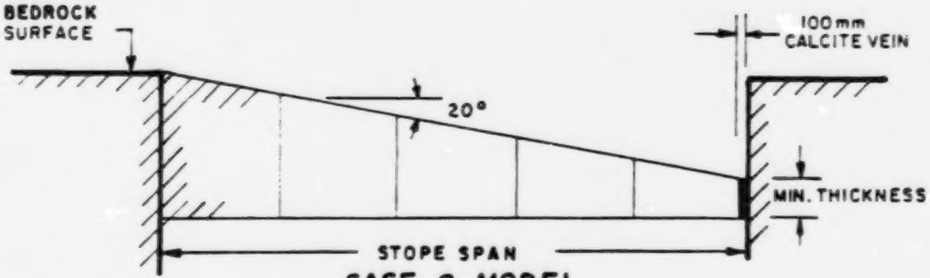

CASE 2 MODEL

MAIN CALCITE VEIN AT STOPE WALL

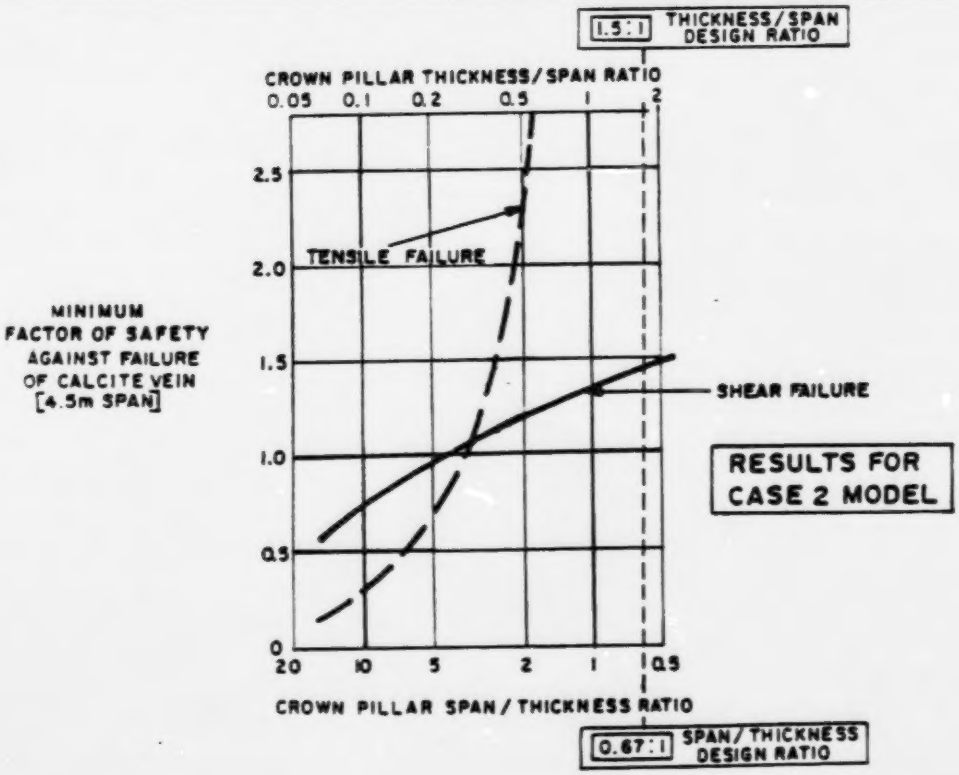

Date FEBRUARY 14, 1990.

Project 881-1739-3

Golder Associates

Drawn R.B.C./P.L.

Chkd TGC

EVALUATION OF CROWN PILLAR AT MINE #42 ANALYSED AS BEAM WITH FIXED ENDS

FIGURE 5.6

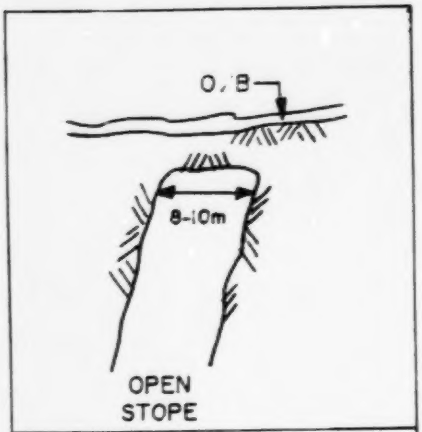

IDEALIZED CROSS SECTION

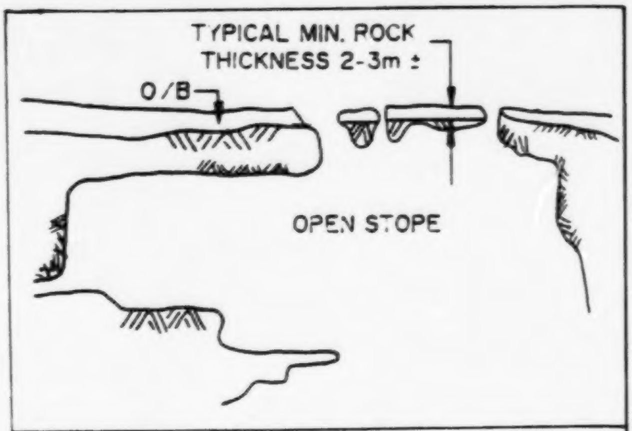

GENERALIZED LONGITUDINAL SECTION

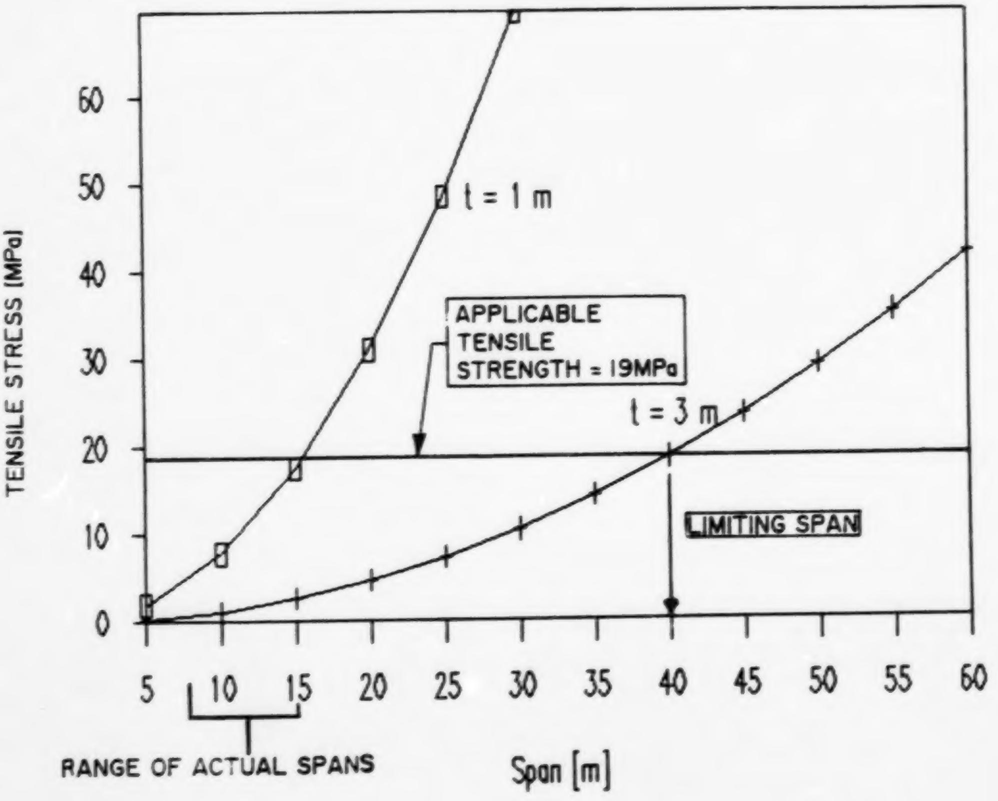

Date FEBRUARY 14, 1990.

Project 881-1739-3

Golder Associates

Drawn R.B.C./P.L.

Chkd.

ISOMETRIC DIAGRAM OF #1 AND SHAFT AREAS
(MINE #25)

FIGURE 5.7

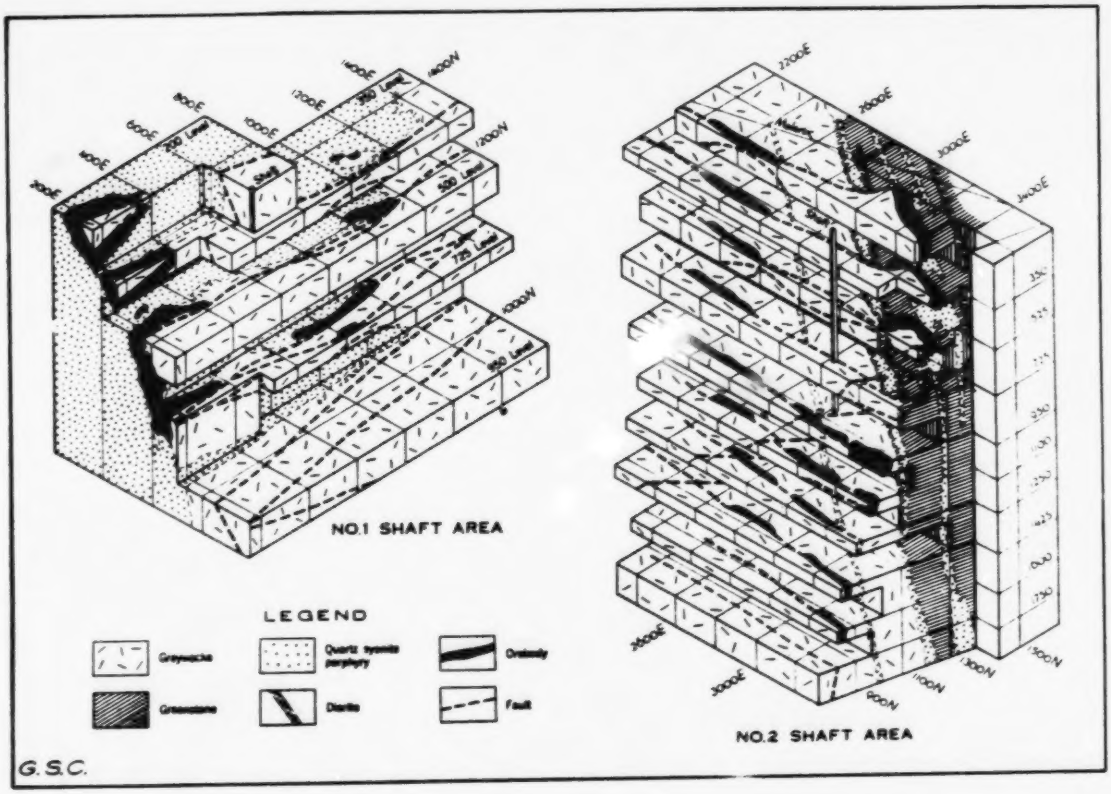

Date FEBRUARY 14, 1990.
Project 881-1739-3

Golder Associates

Drawn R.B.C./P.L.
Chkd. TGL

APPRAISAL OF CROWN PILLAR STABILITY FOR MINE #26 USING PLATE ANALYSIS METHODS (ASSUMING PLATES WITH FIXED ENDS)

FIGURE 5.8

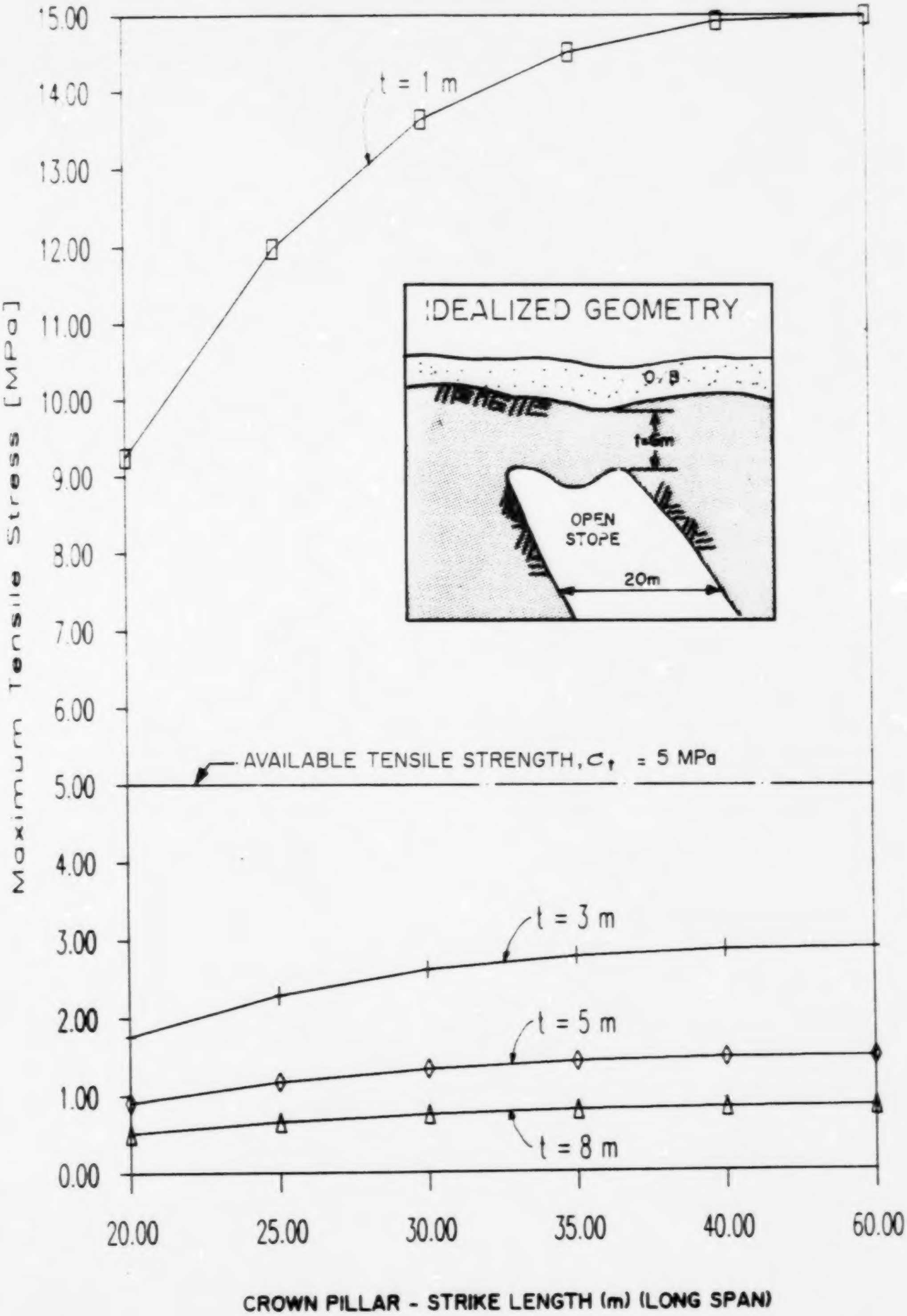

Date FEBRUARY 14, 1990.

Project 881-1739-3

Golder Associates

Drawn R.B.C./P.L.

Chkd 1G

OVERALL GEOLOGY AND GEOMETRY OF #3 , #5 AND #7 VEIN AREAS AT MINE #33

FIGURE 5.9

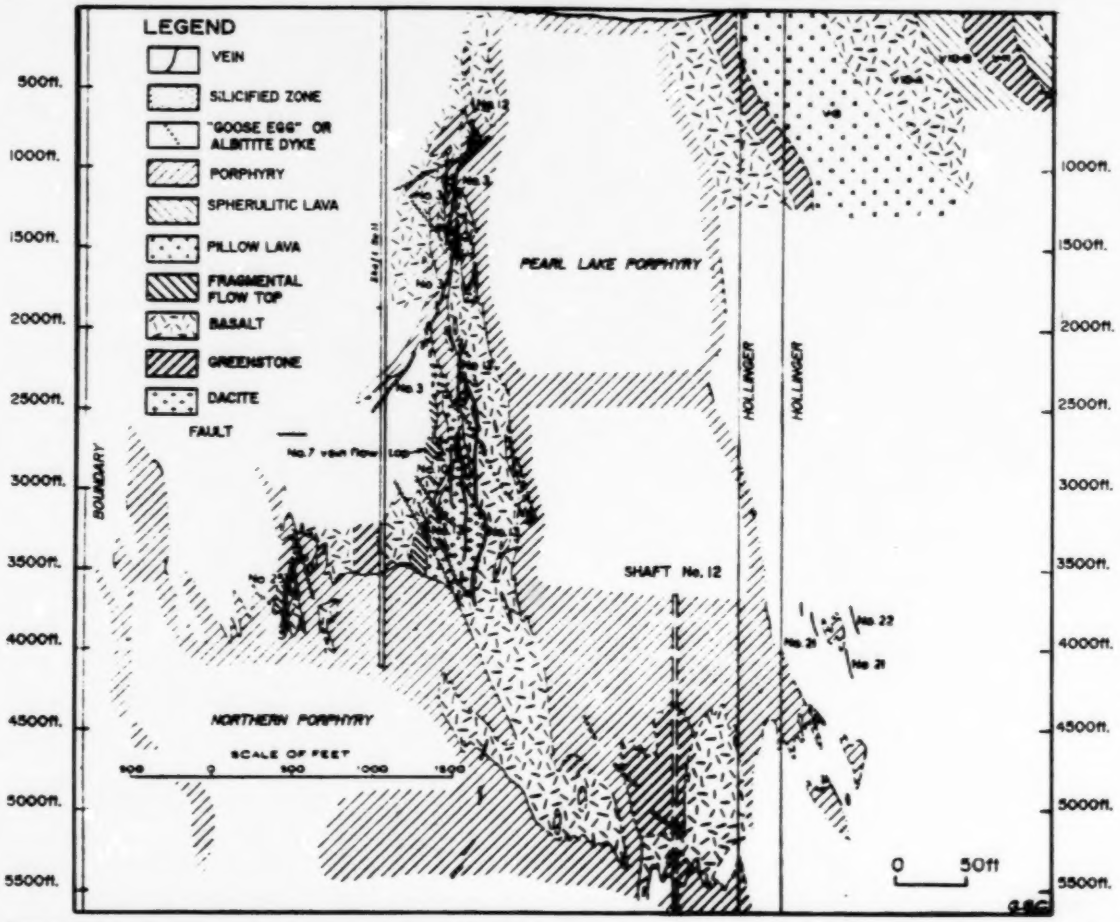

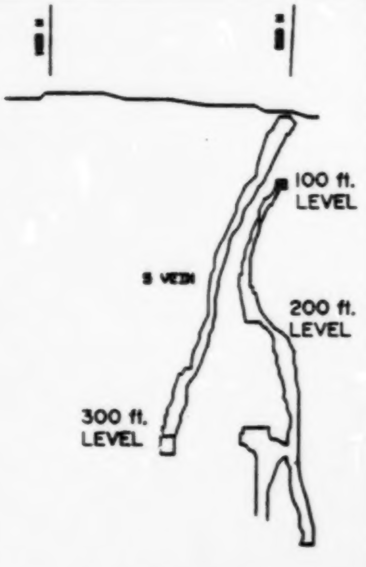

X - SECTION VEIN #5

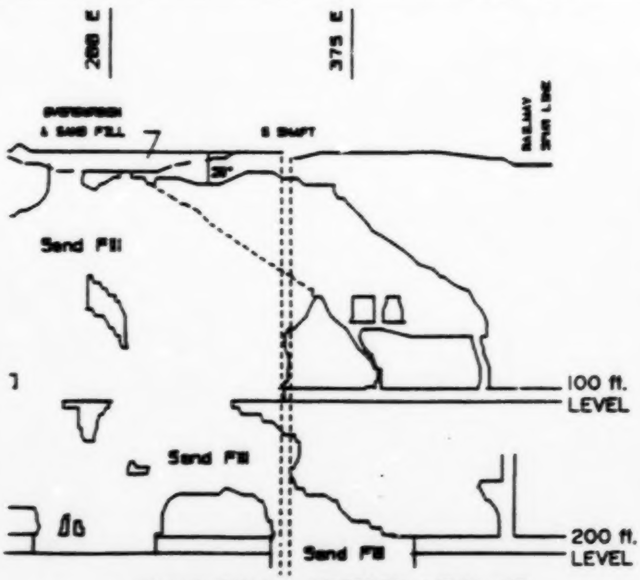

LONGITUDINAL SECTION VEIN #5

Date FEBRUARY 14, 1990

Project 881-1739-3

Golder Associates

Drawn P.L.

Chkd. TGL

RESULTS OF FLAC ANALYSIS SHOWING PLOT OF PRINCIPAL STRESS TRAJECTORIES AND TENSION ZONE FOR MINE #33 (ELASTIC MODEL)

FIGURE 5.10

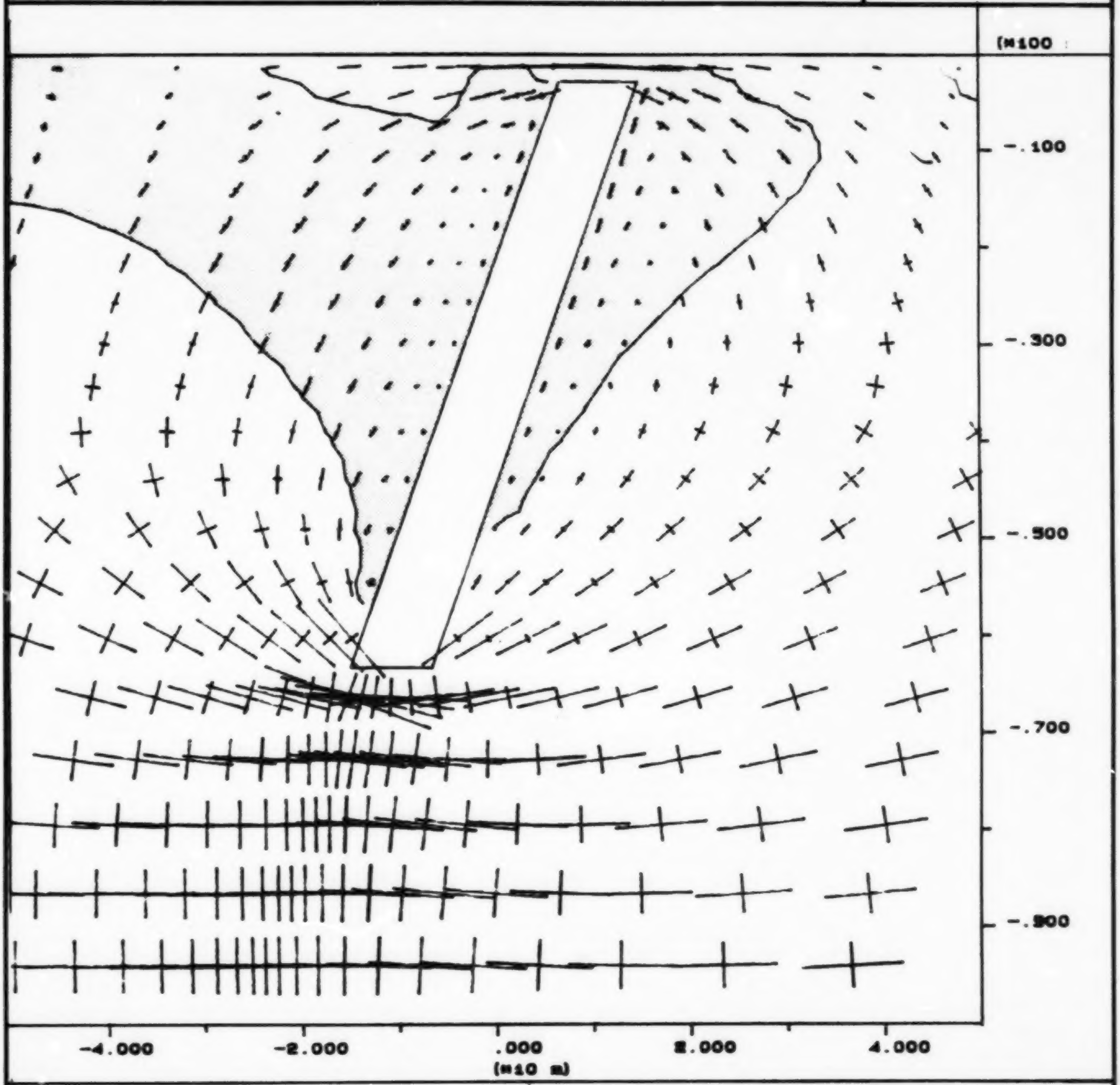

LEGEND

IN SITU STRESS RATIO , κ = 2

24 / 05/ 1989 08 : 44
STEP 1831

SCALE

0 20 m

TENSION REGION PLOTTED ▨
PRINCIPAL STRESSES
MAX. STRESS - 2.500E + 06

0 10 MPa

Date FEBRUARY 14, 1990.
Project 881-1739-3

Golder Associates

Drawn R.B.C./P.L.
Chkd. Tgl

RESULTS OF POST - FAILURE ANALYSIS USING FLAC DISPLACEMENT AND STRESS TRAJECTORY PLOTS (MINE #15)

FIGURE 5.11

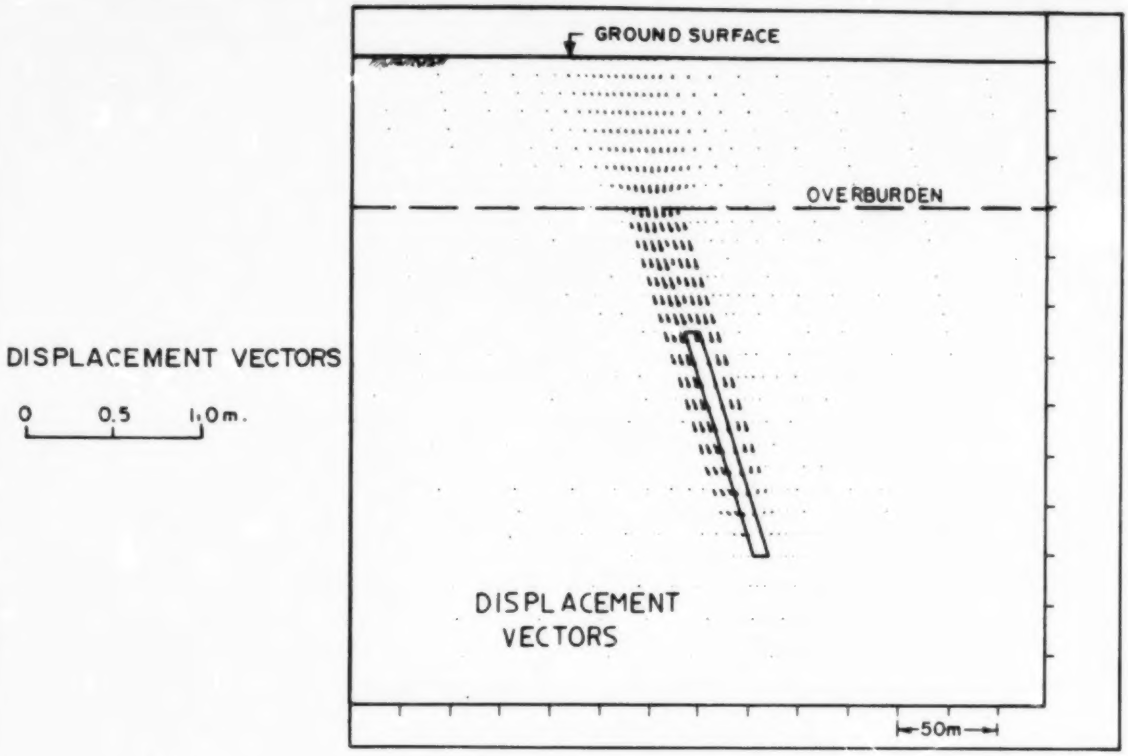

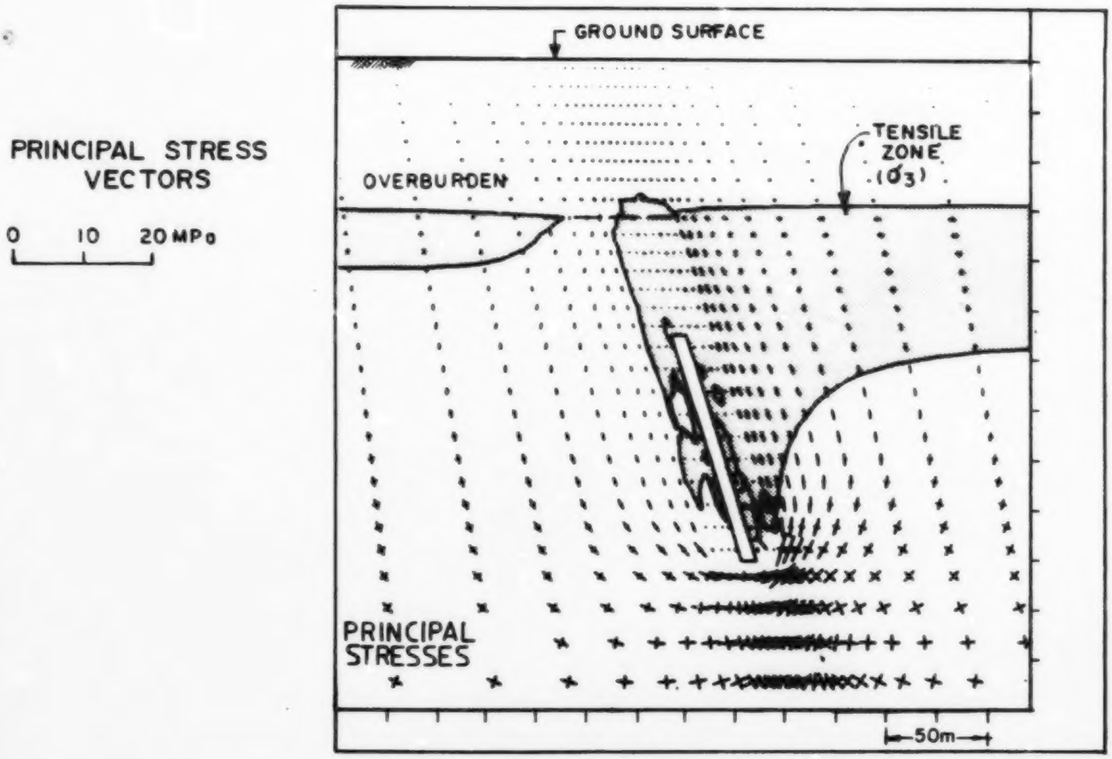

Date FEB. 14, 1990

Project 881–1739–3

Golder Associates

Drawn RBC, MHW

Chkd TGL

RESULTS OF POST - FAILURE ANALYSIS USING FLAC DISPLACEMENT AND STRESS TRAJECTORY PLOTS (MINE #14)

FIGURE 5.12

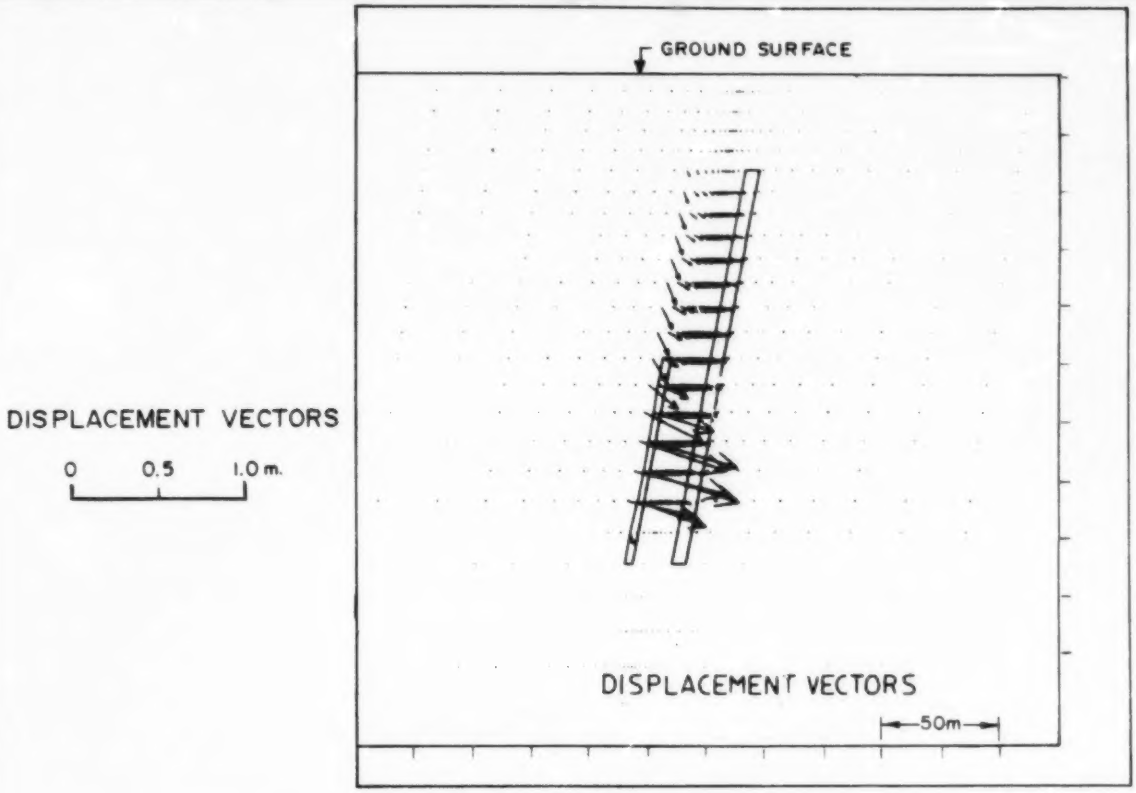

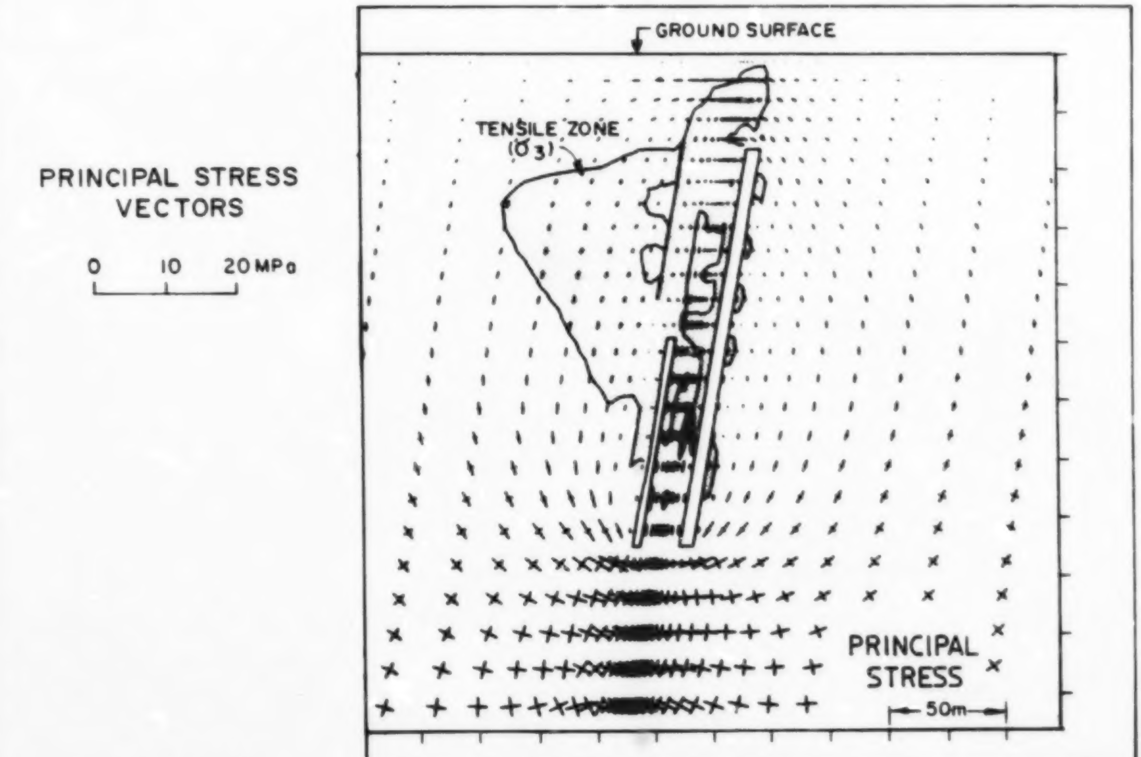

Date FEB. 14, 1990
Project 881—1739-3

Golder Associates

Drawn RBC, MHW
Chkd.

CONCEPTUAL SKETCH OF MINE #22 AFTER ORIGINAL CROWN PILLAR FAILURE

FIGURE 5.13

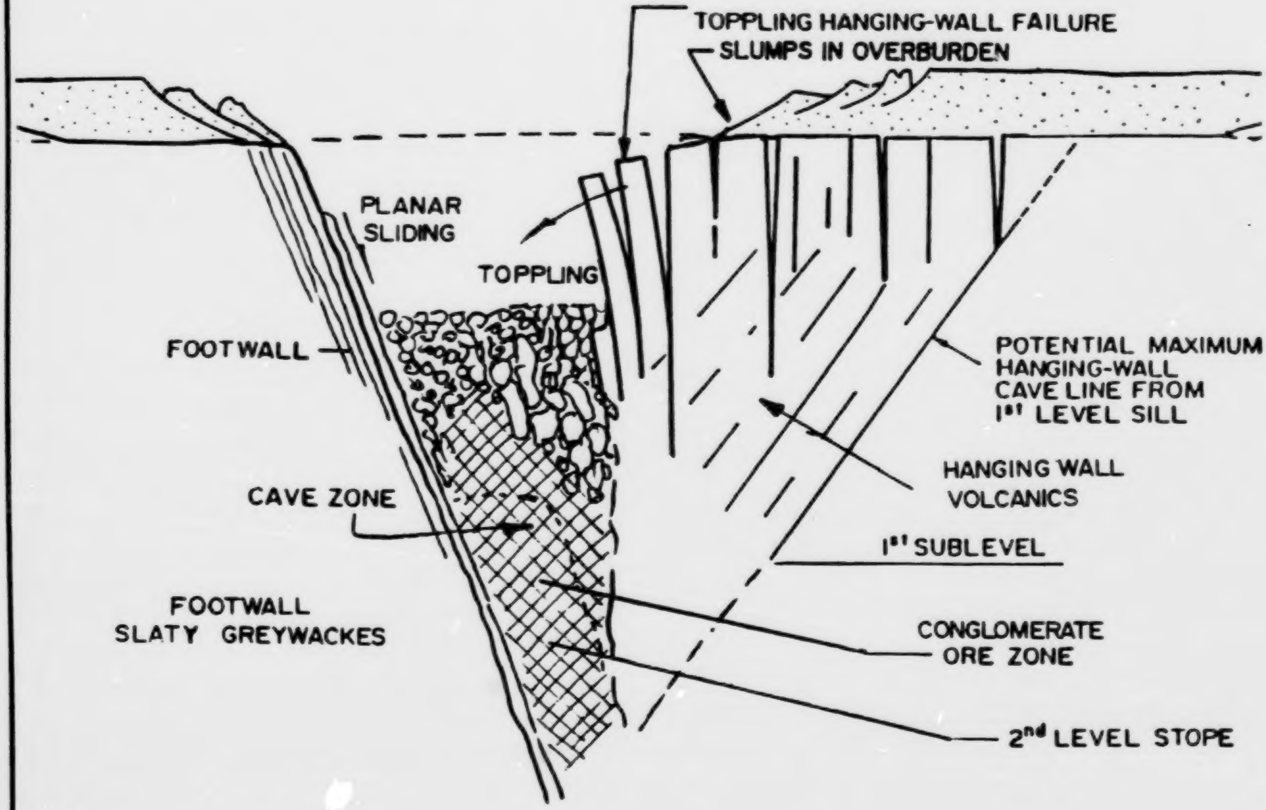

Date FEBRUARY 4, 1990.
Project 881-1739-3

Golder Associates

Drawn R.B.C
Chkd. 1GL

RESULTS OF MUDEC ANALYSIS PLOT OF PRINCIPAL STRESS TRAJECTORIES (MINE #22)

FIGURE 5.14

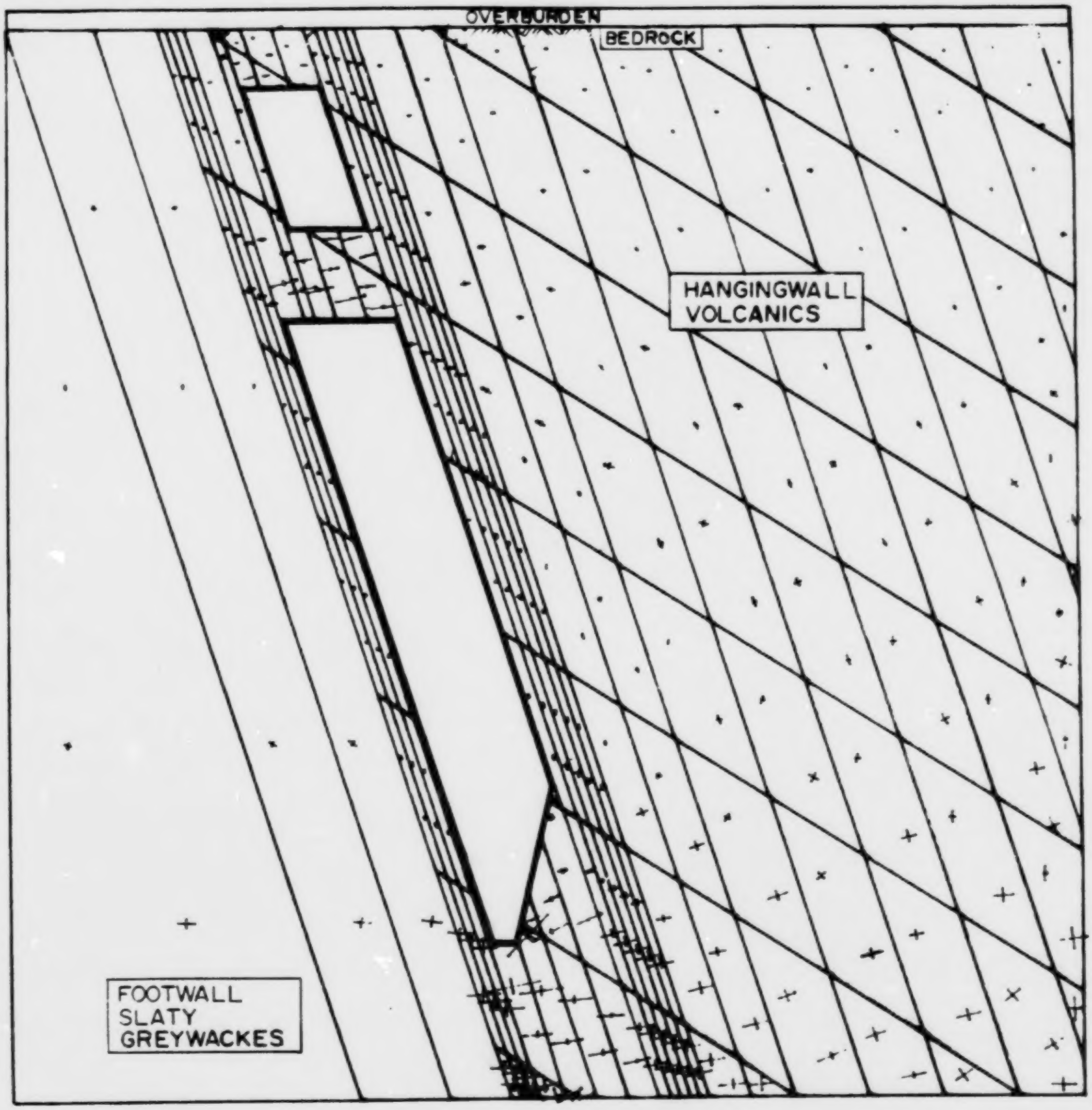

LEGEND

IN SITU STRESS RATIO, $K_o = 1$

29 / 05 / 1989 08 : 54
CYCLE 1844

SCALE

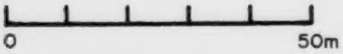

PRINCIPAL STRESSES
MAXIMUM = 2.442E 1 07

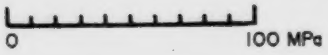

Date **FEBRUARY 14, 1990.**
Project 881-1739-3

Golder Associates

Drawn R.B.C./P.L.
Chkd TGL

OUTPUT PLOTS FROM MUDEC ANALYSIS FOR MINE #22 SHOWING CROWN PILLAR FAILURE SEQUENCE

FIGURE 5.15

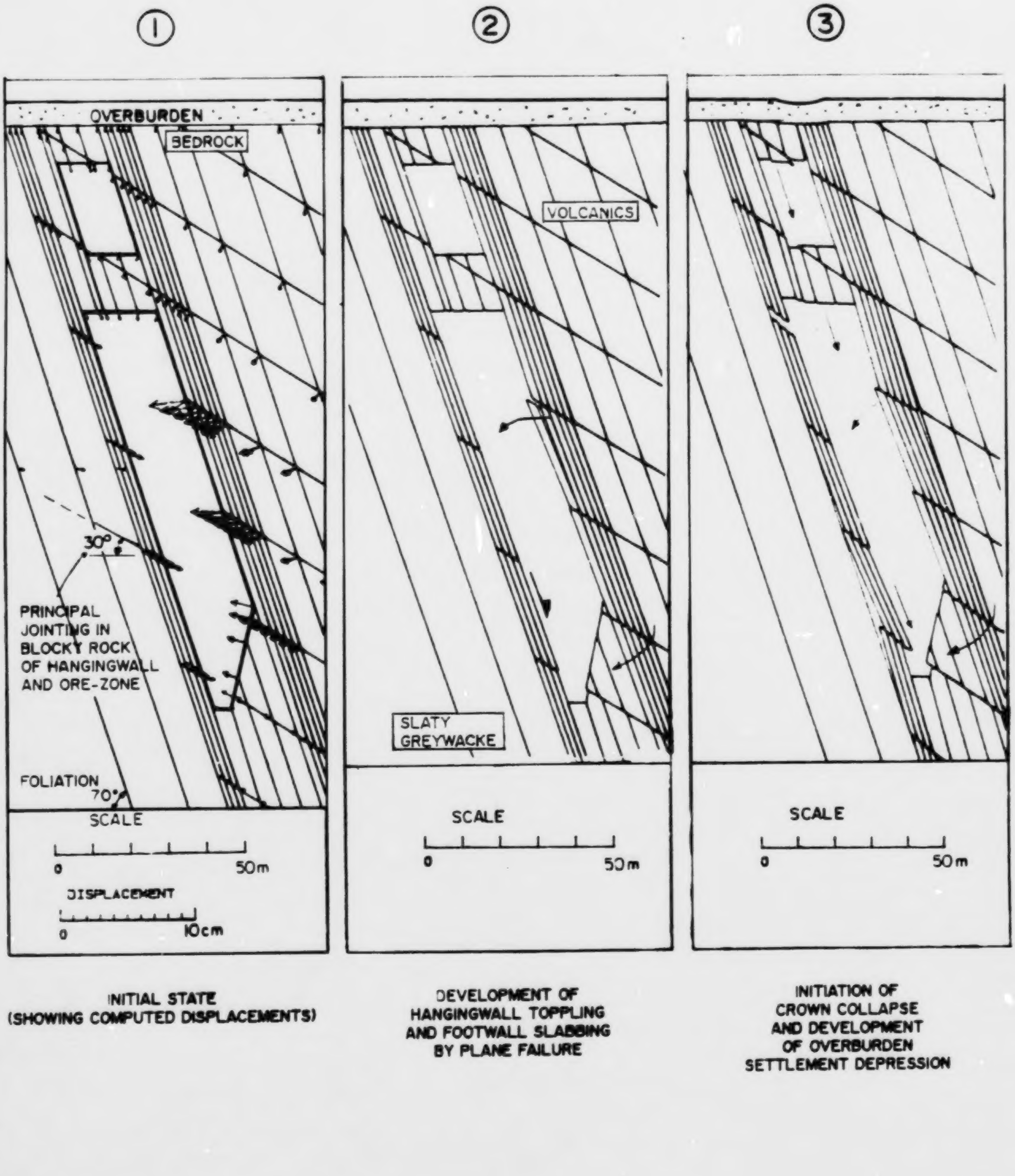

INITIAL STATE (SHOWING COMPUTED DISPLACEMENTS)

DEVELOPMENT OF HANGINGWALL TOPPLING AND FOOTWALL SLABBING BY PLANE FAILURE

INITIATION OF CROWN COLLAPSE AND DEVELOPMENT OF OVERBURDEN SETTLEMENT DEPRESSION

Date FEBRUARY 14, 1990
Project 881-1739-3

Golder Associates

Drawn R.B.C./P.L.
Chkd. TGC

IDEALIZED STOPE GEOMETRY FOR STABILITY ANALYSIS OF CROWN PILLAR AND HANGINGWALL ZONE FOR DEWATERING OF MINE #45

FIGURE 5.16

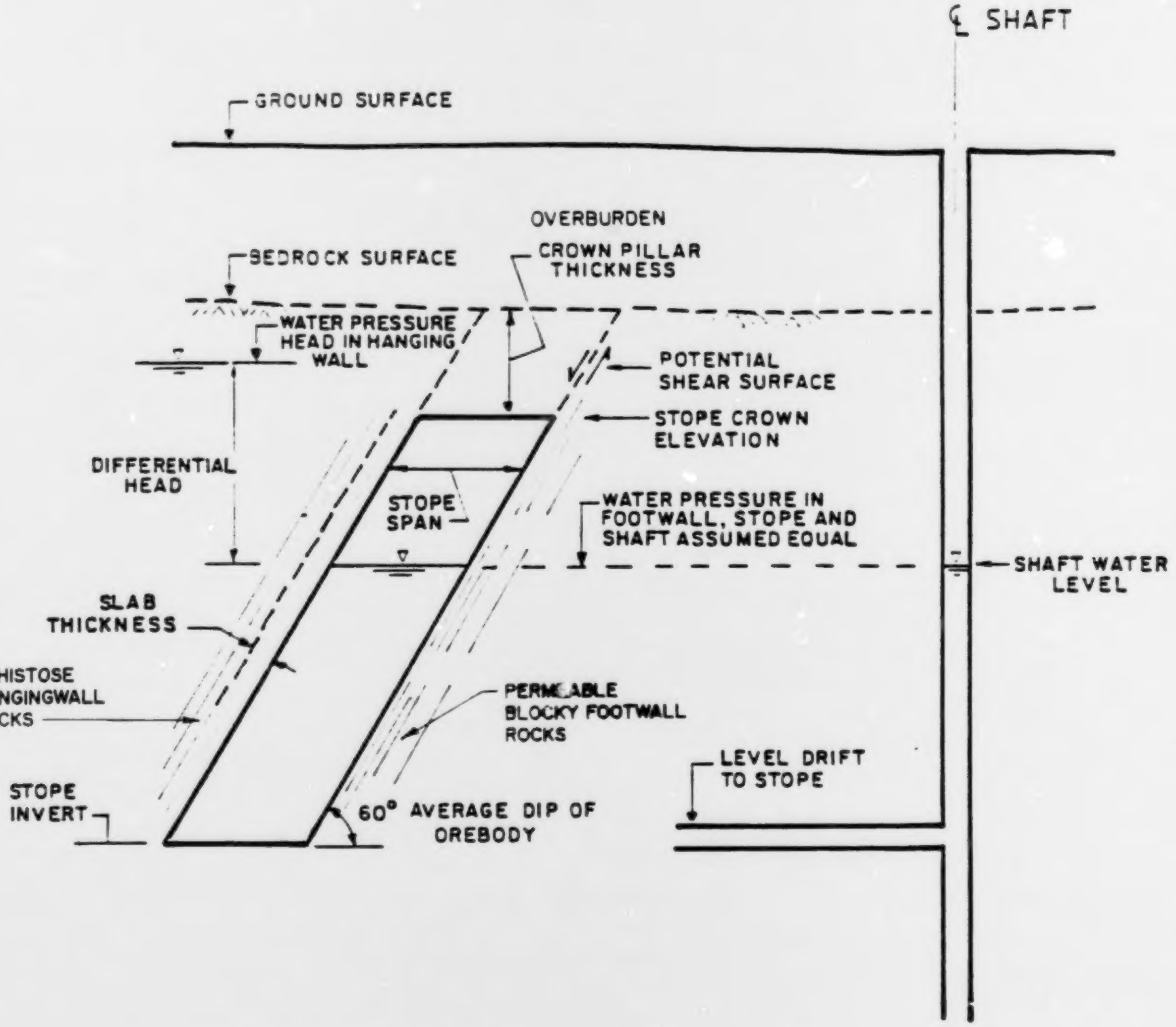

Date FEBRUARY 14, 1990.
Project 881-1739-3

Golder Associates

Drawn R.B.C./P.L.
Chkd. TGL

STABILITY ASSESSMENT - Ist LEVEL STOPE (MINE #45)

FIGURE 5.17

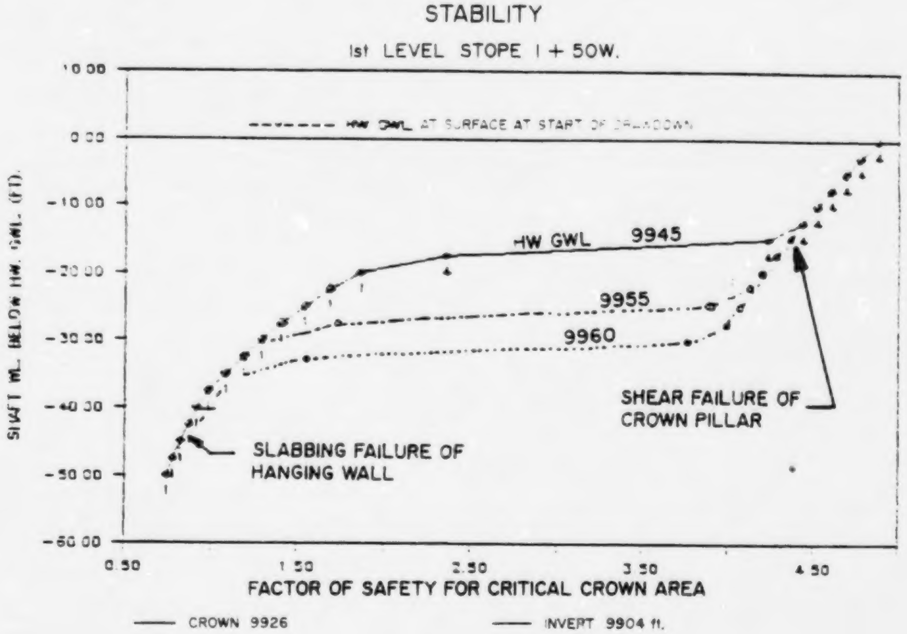

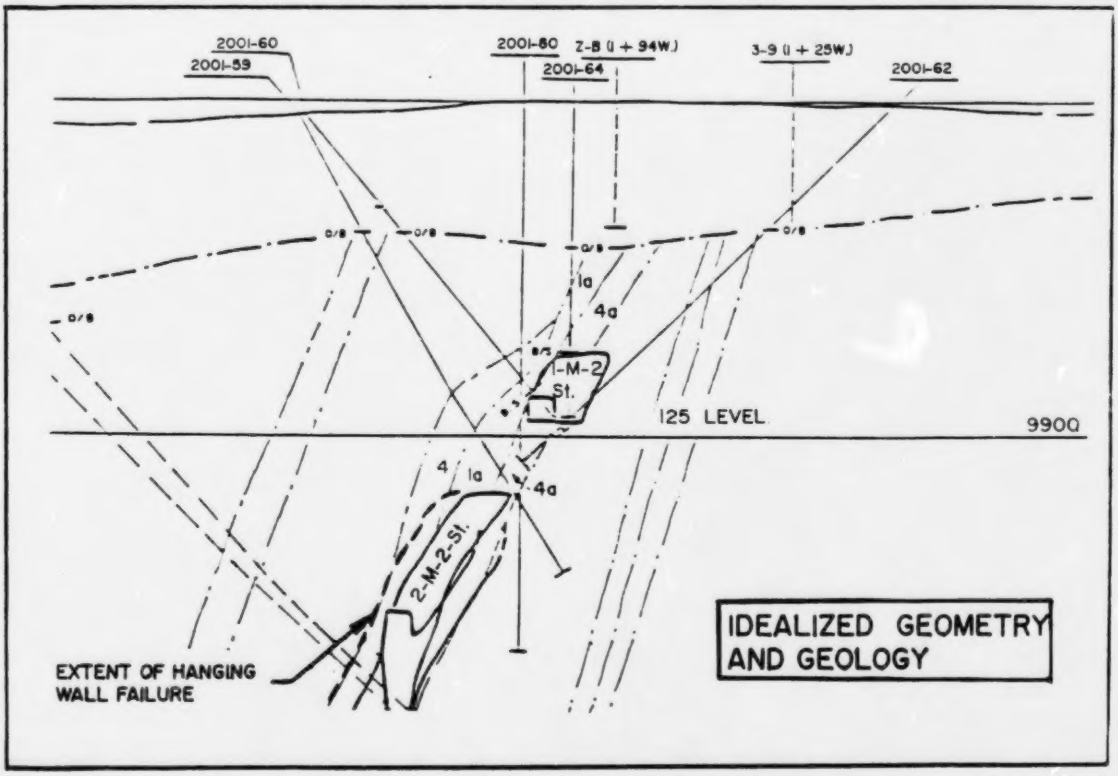

Date FEB. 13, 1990
Project 891-1739-4

Golder Associates

Drawn TDR.
Chkd. TGL

Part 3
Empirical Development of Design Procedure

Golder Associates

Section 6
Empirical Evaluation of Crown Pillar Stability

Golder Associates

6.0 EMPIRICAL EVALUATION OF CROWN PILLAR STABILITY

All of the case records collected during the course of the study are summarized on Table 2.2 and tabulated in Appendix A. As discussed in Sections 4 and 5, this information has provided the basis for the various numerical and analytical assessments carried out for this research project. When combined with information from rock mass characterization of the various pillar cases, these assessments also suggest some basic controls that allow grouping of crown pillar failure behaviour by geometry and by geological environment.

6.1 Review of Controlling Parameters

Within the crown pillar database in Appendix A the following information is tabulated:

- dimensions of individual stopes and surface crown pillars;
- rock types and condition of the hangingwall, footwall and ore-zone; and
- geometry (dip) of the ore zone or mining block which usually reflects the orientation of the prevailing / controlling discontinuity suite (namely the overall schistosity, foliation or major jointing).

In addition, where possible, data on other jointing trends and on the surface condition of joints is presented on some of the drawings included in Section 3 of this report. Information on geomechanical properties of the various rock materials and on discontinuity surfaces and infillings is also included.

Although detailed geotechnical data for many cases is missing, almost always, sufficient descriptive geological data has been reviewed to allow a global CSIR Rock Mass Rating or NGI-Q index to be estimated, based on the generic classification descriptions given on Table 2.4. Caution, however needs to be utilized when assigning such global values in order to ensure adequate definition of the rock mass quality of the critical zone likely to have initiated failure or to control possible failure if the crown pillar is currently stable.

6.2 Stability Graph Development

As a first approach to empirically evaluate whether there were any apparent trends of stability control with rock quality, the data from the 237 individual crown pillar case records compiled in Appendix A were plotted with respect to thickness to span ratios, Figure 6.1. On the Y axis, the thickness to span (width) ratios has been plotted, while on the X axis, the CSIR Rock Mass Rating and the NGI-Q values are presented. Although this graph includes all the basic essentials for use as a design chart, as the relationship is not scale-dependent, use of the chart for design under certain circumstances (for example, for small openings in weak rock) could be erroneous. This is because the chart includes several cases of crown pillar collapse in weak rock which involve collapse of several tens to hundreds of metres thick crown pillars. The scale of the opening with respect to the controlling rock mass block size, is therefore critical to defining the problem. This scale problem is also not adequately addressed by extension of the civil engineering based span versus rock quality graphs, (eg. Figure 4.3). Several other concepts were therefore examined.

Review of the principles, inherent in the analyses, presented in Sections 4 and 5, including appraisal of the empirical relationships proposed for caving assessments by Deiring and Laubscher, (1987) and those first suggested by Terzaghi in 1946 for inferring rock loads, suggests that certain groupings of geometrically important parameters could be developed to better characterize crown pillar geometry.

The ratio of crown pillar cross-sectional area (as representative of volume) to a controlling block size dimension was explored as a possible means for scaling the geometry. However, as block size is already integrated into the rock mass quality (Q) ratings for the various rock masses considered, incorporating block size into a geometry term would make it a dependant variable. Attempts at incorporating joint spacing as part of the geometrical parameter grouping were also discounted, as such an approach would also tend to double count the same parameter influence.

In consequence, the equilibrium analytical solutions discussed in Section 4 were examined as a means for deriving appropriate parametric groupings, assuming a controlling indicator such as the thrust on the hangingwall or footwall due to self weight of the pillar. Neglecting in situ, "clamping" stress effects, for stability, the thrust acting through the pillar must be less than the compressive strength of the rock mass within the crown yet sufficient to provide enough restraint at the abutments to resist sliding at the hangingwall or footwall. Thus calculation simply of the thrust for various pillar geometries, was hoped to provide a scaled measure (for any specific rock mass quality) of the likelihood of compression or shear failure.

In developing the empirical assessments for deep open stopes and caving problems, [eg. Potvin, et al (1987), and earlier by Laubscher, (1976) and Golder Associates (Mathews et. al 1981)], adjustments or modifiers were formulated to account for the dip of joints with respect to the stope layout, stress state, groundwater conditions and attitude of the stope with respect to preferred geological weakness trends. These were then incorporated into a stability number which modified a Q or RMR value for the rock mass. This approach, while effective as a means for categorizing rock mass behaviour for a given stope geometry tends to mix geomechanical variables with geometrical parameters. Although strictly there will always be some dependence inherent in stope layout on geological structure, for categorizing crown pillars, it is important to separate as much as possible the geometric dependent variables from those related to rock mass conditions.

As stability of a given crown pillar is principally related to its span, its thickness, and the weight of the rock mass comprising the pillar these parameters were considered key components for incorporating into any stability assessment. The stope geometry dominated by the dip angle of the schistosity or overall foliation was also considered a key parameter. In addition, as stability also seems to depend on mode of failure to some extent, this was also examined, particularly for the low quality rock masses where the transition between chimneying and progressive ravelling is not as well defined as the change from beam behaviour to shear failure mechanisms at the other end of the spectrum. Lastly, as for each examined failure case, stability seems dependent on block size the absolute scale of the geometry of excavation with respect to rock mass quality was reviewed.

6.3 Assessment of Crown Pillar Stability Scaling Factors

Apart from variations in rock mass quality, several geometrical factors were identified as important controls for incorporation into a stability relationship.

Some clarification of the role of each main geometrical parameter on overall crown pillar stability can be achieved using dimensional analysis procedures. If each, in turn, is evaluated with respect to its particular influence on crown stability, the various parameters can be ranked and scaled, as follows:

Parameter		Influence of increase of Parameter on Global Stability of Surface Crown Pillar
Thickness of crown,	(T)	Increases Stability
Span(width) of stope,	(S)	Decreases Stability
Strike Length of stope,	(L)	Decreases Stability
Dip of Orebody,	(θ)	From 0°, flat, to 45° - Decreases Stability From 45°, to vertical, 90° - Increases Stability
Water Pressure on abutments,	(u)	Decreases Stability
Horizontal "clamping" stress	(σ_h)	Increases Stability
Unit weight of crown ore-zone,	(γ)	Decreases Stability

From the above tabulation it can be readily appreciated that, irrespective of rock mass quality or block size, the stability of a given crown pillar can be related to the various geometrical and environmental parameters as follows:

$$\text{Crown Stability} = f\left(\frac{T\,\sigma_h\,\theta}{S\,L\,\gamma\,u}\right) \tag{6.1}$$

All the parameters except σ_h and u in the above expression are related to the geometry of the crown pillar. In the context of correlating rock mass conditions with the geometry of the pillar, the terms σ_h and u can best be incorporated in the rock mass quality evaluation so that a crown pillar geometry number can be developed that is only geometry and weight dependent. For current purposes this is expedient, as both the CSIR-RMR and NGI-Q systems of rock mass classification take into consideration the effects of in situ stresses and groundwater conditions. With refinement of the proposed empirical procedure, however, these factors may ultimately need to be considered separately and explicity.

In most crown pillar situations, because of drainage to deeper levels, groundwater is not usually of major concern. In some rocks which deteriorate with time, it can be a consideration where the action of water may bring about changes in rock properties. However, based on work, for example by Cording et al. (1972) and others, for most practical purposes it is not of major significance to underground stability.

The influence of high in situ horizontal clamping stress on crown pillar stability is also not currently clearly defined. Intuitively, it is likely to play a major role in enhancing the stability of a given crown, particularly where rock block size is small and interlock effects are not well developed. Thus, providing the span doesn't exceed the critical widths indicating by caving hypotheses, natural arching capabilities of the rock mass can be exploited (Terzaghi, 1946, Rose 1982, Coates 1981). A stable condition, therefore, may exist for a given rock mass fragment size, dependant on the magnitude of external clamping stress effects. Currently this is not quantifiable as there have been virtually no measurements of in situ stresses taken in crown pillar areas. Clamping stress effects on intermediate to good quality rock masses are also unknown. They may play a significant part in controlling the stability of strong, very thin rock crowns where potential buckling can occur due to overstress effects, but intuitively, in such situations, they are not considered to be as important to stability as they might be for weak, intensely broken and blocky rock masses.

6.4 Development of Crown Pillar Geometry Number

The following sections discuss the rationale for deriving an empirical relationship which relates all the geometric factors controlling pillar geometry; span (S), thickness (T), strike length (L) foliation/ore zone dip attitude,(Θ) and crown pillar rock mass unit weight (γ).

6.4.1 Crown Pillar Weight Factor (F_w)

In order to provide a better insight into correctly scaling the unit weight term, it is instructive to review the original rock load concept of Terzaghi (1946) with the numerous modifications by Deere, Cording and others as combined into the curve shown on Figure 6.2 (modified from Rose, 1982). The graph shown on the figure relates rock quality expressed in terms of RQD and Terzaghi's 1946 descriptive nomenclature to inferred rock loads imposed on an excavation, for various rock quality conditions (see also Table 2.4). If the rock load factor equation is rearranged and the mean to the relationship shown on Figure 6.2 is used as a representative scaling factor for all rock qualities, a rock load scaling factor can be postulated as:

$$F_w = 0.6 \times \gamma \times S \tag{6.2}$$

Even though the use of an average value of 0.6 can be justified as representative for most fair quality rock massess (CSIR-RMR = 44, NGI-Q = 1), it is difficult to rationalize the use of a single factor. As dependence of crown stability on the weight of the rock in the pillar is difficult to precisely define for the purpose of scaling, it is appropriate to scale F_w directly with respect to the unit weight of the rock mass composing the pillar. Hence, the weight factor is defined as:

$$F_w = \gamma \tag{6.3}$$

6.4.2 Span to Thickness Ratio (F_{ST})

The span to thickness ratio (or its reciprocal) has been frequently used for correlating crown pillar stability conditions and as a basis for *rule of thumb* approaches in crown pillar design. The span to thickness ratio is defined as:

$$F_{ST} = \frac{S}{T} \tag{6.4}$$

where: S = span of crown pillar, and
T = thickness of crown pillar

6.4.3 Stope span to strike length ratio (F_{SR})

The dimensional arrangement of the geometry of the stope back is of importance to determination of critical span. For stopes which are longer than four times the short span, the behaviour of the crown is essentially one-way spanning controlled by the short span. For less elongate geometries the crown acts as a plate, i.e., its stability is controlled by two-way spanning. A convenient means of scaling this effect was proposed by Laubscher, (1976). Simply, the concept of an equivalent hydraulic radius is defined, which as stope length moves to infinity, the hydraulic radius becomes asymptotic to one half of the short span.

As the expressions given previously relate to span directly, a modified scale ratio, based on the hydraulic radius concept can be developed, as follows:

$$F_{SR} = 2 \times H_R = \frac{(L \times S)}{(L + S)} = \frac{S}{1 + (S_R)} \qquad (6.5)$$

where the Span Ratio, (S_R), is defined as $S_R = (S/L)$ and the Hydraulic Radius $H_R = \frac{L \times S}{2(L+S)}$

It is important to note that although this factor does not account explicity for cross-sectional roof shape, variations in shape can be considered by careful selection of the appropriate controlling span dimension.

6.4.4 Influence of foliation dip (F_Θ)

Inspection of the failure behaviour of many crown pillars, particularly in schistose or poor quality rock masses, suggests that because of hangingwall slabbing effects, inclined stope openings paralleling foliation planes are intrinsically less stable overall, than vertical or near-vertically oriented stopes also parallel to dominant foliation attitude. This suggests that some form of derating for unfavourable orientation of the stope geometry and the primarily parallel incipient (foliation) weaknesses, such as proposed by Laubscher (1987) for caving considerations, or by Bieniawski (1976) for tunnelling geometries is needed to account for such variations. The approaches taken by Laubscher, Bieniawski and others has been to incorporate such a derating term as a modifier to the Rock Mass Rating. This can be criticized as it mixes an essentially geometrically controlled factor with the terms describing rock mass quality characteristics. As it is essentially a factor that relates to excavation shape, it can be readily incorporated into a geometric parameter grouping as:

$$F_\Theta = (1 - 0.4 \cos\Theta) \quad \text{(for } \Theta \text{ ranging between } 90^\circ \text{ and approx } 45^\circ \text{ dip)} \qquad (6.6)$$

where the constant 0.4 is based on averaging the deratings proposed by Bieniawski,1976 for tunnels, and by Laubscher 1987, for caving stopes, (see Figure 6.3).

It should also be appreciated in use of this factor that as the dip of the foliation and likely also the stope sidewalls shallows from 90° to past 45° the effective span of the stope should be no longer considered as the ore zone width but rather as the hangingwall length.

6.4.5 Crown Geometry Number

From the above discussion, the overall crown geometry number can be expressed in terms of the following functional relationships; where each is given equal ranking; ie.,

$$C_g = f\,(F_{ST} \times F_{SR} \times F_W + F_\Theta)$$

where F_{ST} = span / thickness ratio = S/T
F_Θ = stope inclination factor = $(1 - 0.4 \cos\Theta)$
F_{SR} = span ratio factor = $\dfrac{S}{(1+S_R)}$
and F_W = weight factor = γ

By regrouping the parameters in the following manner, C_g can be expressed as:

$$C_g = \frac{F_W \times F_{ST} \times F_{SR}}{F_\Theta} = \frac{\gamma S^2}{T} \times \frac{1}{(1 + S_R)} \times \frac{1}{(1 - 0.4\cos\Theta\ )} \qquad (6.7)$$

It is of interest to note that this equation is of the same form as the expression for induced bending stress for a crown pillar considered as a simply supported beam under self weight, which is as follows;

M, the bending moment, $= k_1 \times S^2 \times \gamma T$
Z, the section modulus, $= k_2 \times T^2$

and thus σ_B the induced bending stress, $= \dfrac{M}{Z} = \dfrac{\gamma k_1}{k_2} \times \dfrac{S^2}{T}$

where k_1 and k_2 are constants related to the non-dimensionalized shape of the beam and S and T are as defined previously.

6.5 Proposed Scaled Span and Critical Span Expressions

Noting that the bending stress scales approximately with the square of the span, a final empirical expression, (C_s) termed the scaled span for a particular crown pillar can be defined by taking the square root of C_g, as follows:

$$C_s = S\,[\,\gamma\,/[\,T(\,1 + S_R)(1 - 0.4\cos\Theta)\,]\,]^{0.5} \quad \text{(metres)} \qquad (6.8)$$

This factor has been calculated for each of the case records included in Appendix A and the results are plotted against the RMR/Q scale as shown in Figure 6.4.

It is of interest to note from Figure 2.4 that if the "unsupported span" line originally plotted by Barton in 1974 is plotted directly on this graph, all the case records from the current crown pillar study can be divided appropriately between failed and stable cases in much the same way as the plot for the case records from Barton's original data (Figure 4.2)

Both the empirical fit proposed by Barton in 1974 (Critial span = $2Q^{0.66}$, see Figure 2.4) and the average fit to the civil engineering and deep stope classifications shown on Figure 4.3 (Critical span = $4.4Q^{0.32}$) are also plotted on Figure 6.4. However, Barton's 1974 non-linear critical dividing line as shown on Figure 4.2, appears to provide a better fit to the currently available case records. In consequence, the following expression has been developed to match Barton's 1974 line

$$\text{Critical Span} = 3.3Q^{0.43} \times [\sinh^{0.0016}(Q)] \qquad (6.9)$$

The hyperbolic sinh term in the above expression accounts for the non-linear trend to increasing stability at the very good quality rock mass end of the Q/RMR Scale (Figure 6.4). If this term is ommitted, the expression describes the straight line portion of the trend line and has the same form as that proposed by Barton in 1974 and that shown on Figure 4.3. In this truncated form the expression obviously describes most conditions adequately, but it tends to under-estimate maximum possible spans at the good quality end of the spectrum.

In combination with the use of the C_S relationship to quantify different crown geometries (refer to equation 6.8) use of these critical span expressions provides a significant improvement on the currently available safe span versus rock quality relationships for crown pillar use. This is because these "scaled span" relationships take into account all of the relevant geometric parameters for a surface crown pillar, *including* crown thickness and thus the relationships provide a base for empirical evaluation of safe crown thickness for a required stope span.

6.6 Example Application of the Scaled Crown Span Plot to Derive Required Crown Pillar Thicknesses

Simple application of the linear relationships on Figure 6.4 for crown pillar dimensioning demonstrates the use of these concepts for empirical crown pillar sizing.

Assuming for a particular situation that a 15 m wide crown stope is required in schistose rock of poor quality i.e. about 30 on the RMR scale, (Q = 0.2), use of Figure 6.4 allows a ready first approximation to be made for necessary crown pillar thickness. Firstly though, it should be appreciated from inspection of any of the critical span lines on Figure 6.4, that in this rock mass, it is almost certain that a stope of 15 m. span will cave. However, if it is still decided that it is necessary to mine it, then combined use of Figures 6.4 and 4.14 can provide some assessment of the thickness of crown that should be left in place above the stope. From Figure 6.4, for this rock, the critical scaled crown span is about 1.65 m. (Table 6.1) ie., much less than the proposed excavated span of 15 m., thus caving will definitely occur. An estimate of the required crown thickness however can still be made. As for this example, the stope is assumed vertical and of long strike length, several terms in the crown span, C_S relationship, drop out and the thickness of the crown pillar can be deduced from:

$$T = \frac{\gamma S^2}{C_S{}^2} \tag{6.10}$$

Using this relationship, a crown pillar thickness can be established and a critical thickness to span ratio can be calculated for use in dimensioning a minimum "stable" crown pillar (Table 6.1). For this case a ratio of 16.5 is calculated commensurate with limitations on maximum crown collapses based on precedent practise. Significant support measures are obviously needed, though, if stoping to full 15 m. width is intended in this rock mass. If however, only a 3 m wide drift is required in the same rock mass, again as the span is larger than the critical span of 1.65 m. some support will still be required.

Conversely, if one wishes to make similar excavations in good quality rock, say of the same width, 15 m.; but for rock with an RMR of about 75 ($Q = 30$), the critical scaled crown span is 14.2 m. As this is reasonably close to the desired excavation span of 15 m. it is likely that the stope, if blasted carefully, will stand without support, with minimum crown thicknesses and thickness to span ratios as given in Table 6.1. For a drift of 3 m. span in the same rock, theoretically the required minimum crown thickness would be only 0.1 m. Obviously, this is impracticable to achieve, solely on blasting considerations alone, but as illustrated by several old narrow vein stopes in hard rock environments with 0.3 m. thick crowns over 3.5 to 4 m. spans, this calculated stable crown thickness is of the correct magnitude.

TABLE 6.1 - Required Crown Pillar Thicknesses and Thickness:Span Ratios for Two Spans in Two Rock Masses

Q (RMR)	Rock Quality	γ [T/m^3]	Critical Crown Span, C_s [m] $Cs = 3.3\ Q^{0.43}$	Desired Design Span [m] S	Required Crown Pillar Thickness [m] $T = \frac{\gamma S^2}{C_s^2}$	T/S
0.2 (30)	Poor	3.0	1.65	15	248	16.5
				3	9.9	3.3
30 (75)	Good	2.5	14.2	15	2.8	0.19
				3	0.1	0.04

SUMMARY OF CROWN PILLAR CASE RECORDS
(THICKNESS TO SPAN RATIOS Vs ROCK QUALITY)

FIGURE 6.1

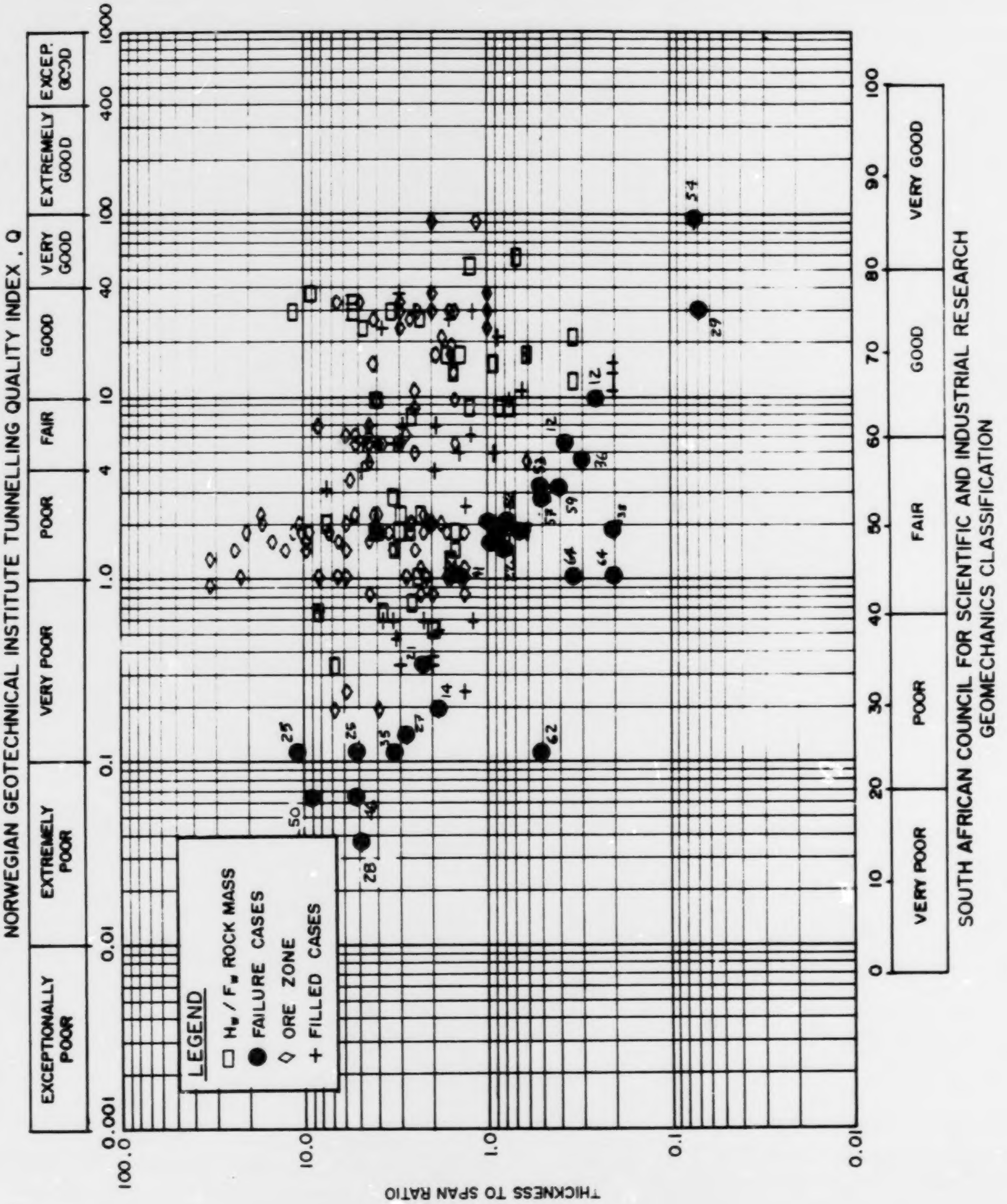

Date FEBRUARY 12, 1990.
Project 881-1739-3

Golder Associates

Drawn R.B.C.
Chkd. Tav

TERZAGHI ROCK LOAD CONCEPT USED FOR DIMENSIONALLY SCALING EFFECTIVE INDUCED LOADING/CROWN PILLAR WEIGHT EFFECTS

FIGURE 6.2

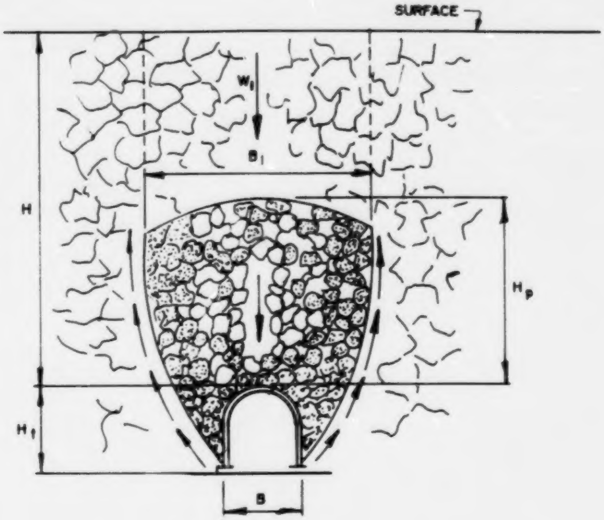

TERZAGHI (1946)
CONCEPT FOR
ROCK LOADING ON TUNNEL LININGS

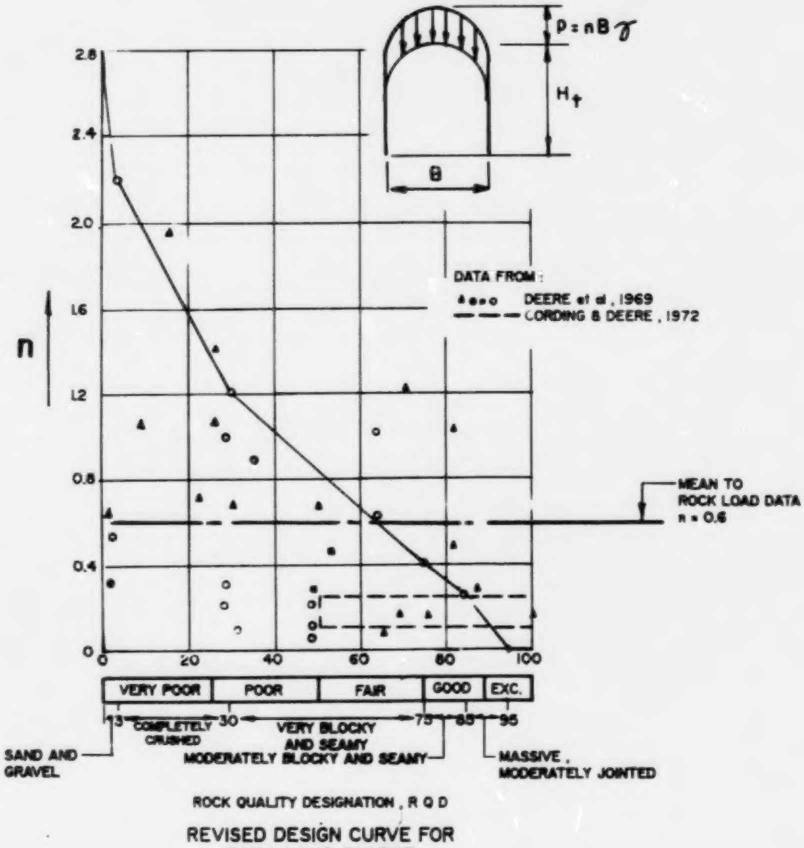

REVISED DESIGN CURVE FOR
ROCK LOAD FACTOR
(AFTER ROSE, 1982)

Date FEBRUARY 6, 1990.
Project 881-1739-3

Golder Associates

Drawn R.B.C.
Chkd. Tgl

VARIOUS DERATING FACTORS PROPOSED TO ACCOUNT FOR DIP OF GEOLOGICAL STRUCTURE WITH RESPECT TO EXCAVATION GEOMETRY

FIGURE 6.3

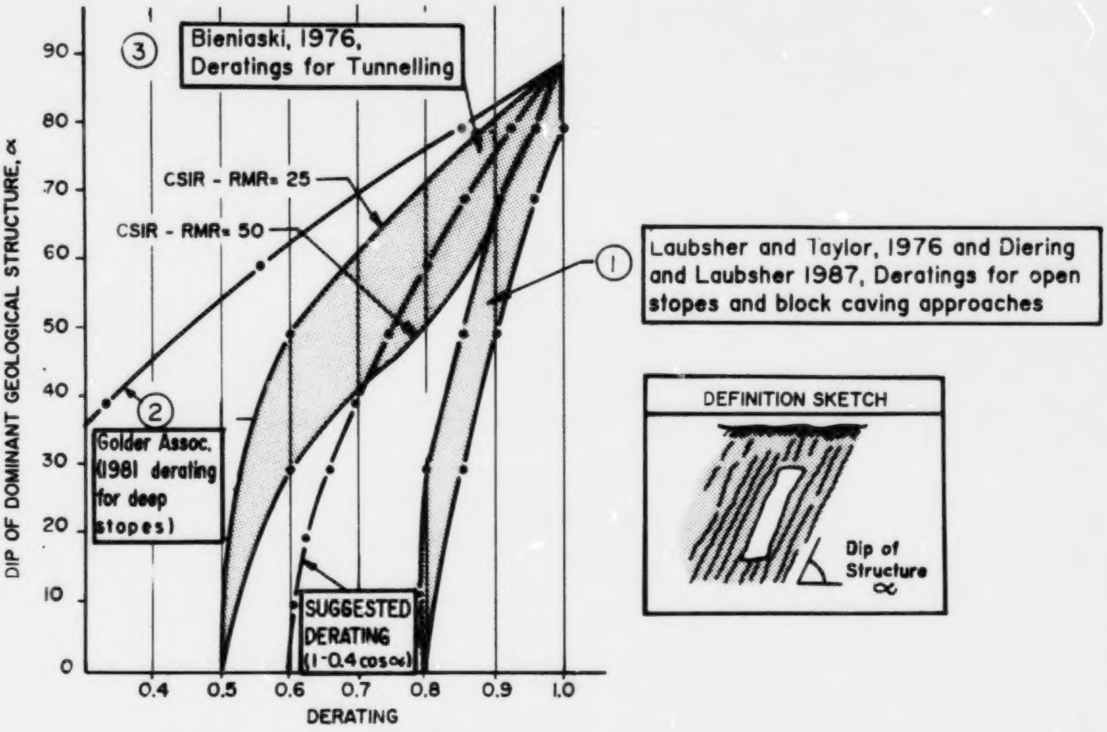

ADJUSTMENTS TO RMR FOR VARIOUS DIP ATTITUDES (after Diering and Laubsher , 1987)

①					
Dip of Structure	0 - 30°	30-50°	50-70°	70-80°	80-90°
RMR Adjustment	0.80	0.85	0.90	0.95	1.00

INCLINATION DERATING FOR SLABBING AND GRAVITY FAILURE (Golder Assoc. 1981,Potvin 1988)

②							
Dip of Structure	0	20	40	60	80	90	(1 - 7/8 cos∝)
Modified Derating Factor	—	0.18	0.33	0.56	0.85	1	

THE EFFECT OF JOINT STRIKE AND DIP ORIENTATIONS IN TUNNELLING From Bieniawski, 1976

③ THE EFFECT OF JOINT STRIKE AND DIP ORIENTATIONS IN TUNNELLING from Bieniawski, 1976	STRIKE PERPENDICULAR TO TUNNEL AXIS				STRIKE PARALLEL TO TUNNEL AXIS		Dip 0°-20° irrespective of strike
	DRIVE WITH DIP		DRIVE AGAINST DIP				
	Dip 45°-90°	Dip 20°-45	Dip 45°-90°	Dip 20°-45	Dip 45°-90°	Dip 20°-45	
	Very Favourable	Favourable	Fair	Unfavourable	Very unfavourable	Fair	Unfavourable
Recommended Derating	0	-2	-5	-10	-12	-5	-10

Date FEB. 13, 1990
Project 891-1739-4

Golder Associates

Drawn TDR
Chkd. TGL

SUMMARY OF CROWN PILLAR CASE RECORDS
(SCALED CRITICAL CROWN SPAN [Cs] Vs ROCK QUALITY)

FIGURE 6 . 4

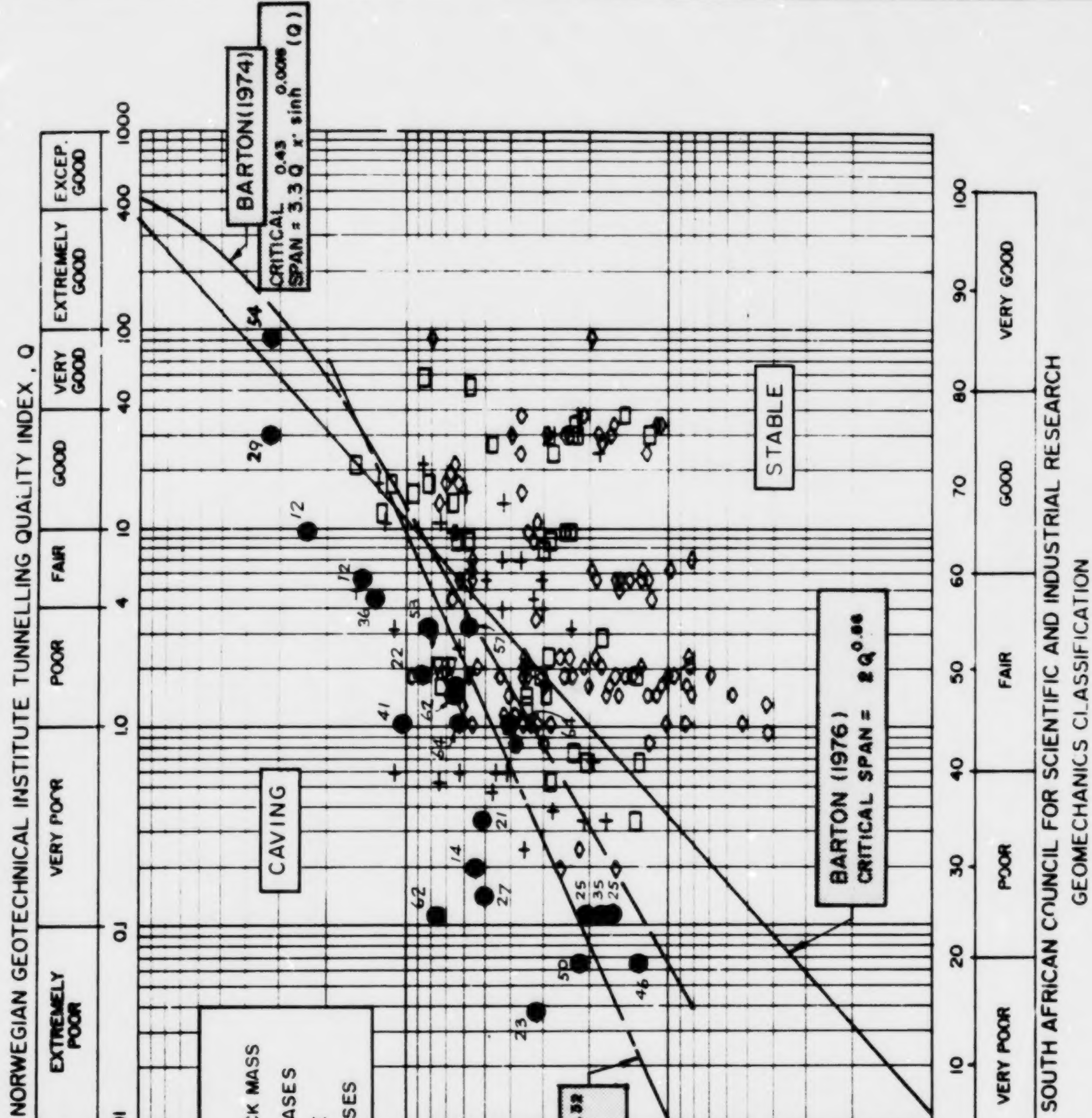

Date FEBRUARY 14 , 1990.

Project 881-1739-3

Golder Associates

Drawn R.B.C.

Chkd. TGC

Section 7
Conclusions and Recommendations

Golder Associates

7.0 CONCLUSIONS AND RECOMMENDATIONS

The data obtained from review of the information collected on old failures has often been found lacking in detail, particularly with respect to geomechanical properties of the various rock mass conditions at the sites. In particular, data on absolute characteristics of controlling weakness planes is virtually non-existant. Nevertheless, sufficient information has been gleaned to allow five basic types of crown pillar geometry to be recognized:

A - tabular, narrow vein ore zone situations
B - complex, blocky rock mass conditions
C - foliated rock environments
D - disseminated ore zones in slabby, competent rock, and
E - fault controlled situations

Representative crown pillar failures within each environment type have been found and analyses have been undertaken to characterize failure modes in each category.

Quantitative, empirically based approaches using the NGI-Q system and/or the CSIR-RMR system have been examined and extended to develop a crown pillar scaled span concept that may have application as a new design approach. The span and crown thickness charts developed on the basis of application of rock mass classification systems, together with the use of the non-linear Hoek-Brown failure criterion holds promise for development of generic crown pillar stability design guidelines. However, because of uncertainties in defining representative rock mass Q and RMR values for characterizing potential failure zones in crown pillars, there is a need to extend these approaches on a more quantifiable probabilistic basis.

The various evaluations undertaken using analytical solutions as well as numerical approaches suggest that for most of the analysable crown pillar failures, mechanisms of failure are heavily geometry and rock property dependent. Several different mechanisms are recognizeable:

- in blocky interlocked rock masses, where pillars are thin, tensile failure or gravity fall out of key central areas within the rock crown leads to kinematic destabilization,

- in schistose rock conditions, or where pillars are thick, but significant weakness zones exist transecting the pillar, shearing and large scale strain deformation of the hangingwall seems to control failure initiation. Once failure has developed, it often leads to progressive caving or to chimney or block sliding of the central section of the pillar.

Back-Analysis of the various case records has also shown that correct selection of appropriate parameters for use in analytical calculations or numerical modelling is essential as they exert considerable influence on interpreted conclusions. For instance:

- The ability of a rock mass to sustain tensile stresses, particularly normal to hangingwall or footwall surfaces can control overall stability behaviour.

- Development of any apparent cohesion in the rock mass or along joint surfaces has significant positive influence on stability by increasing both global rock mass and local joint shear strength.

- The presence of in situ compressive "clamping" stresses acting onto the surface crown pillar significantly enhances its stability by reducing the likelihood of tensile stresses developing while also increasing mobilized shear strength on adversely oriented weaknesses. Determination of representative field values of in situ stress is therefore seen as an important factor still requiring research.

Choice of analytical technique is also critical if realistic results are required for design purposes. Not all techniques are valid. Some have very specific limitations:

- Beam theory seems to be applicable only for thin crown pillars within competent rock masses and for analysing a surface pillar as a discrete structural element. For homogeneous beams with low thickness to span ratios, the stability of the pillar is likely to be governed by tensile failure of the beam at the point of maximum bending moment. For the case of thicker beams with higher thickness to span ratios, shear failure is the controlling failure mechanism especially where the interface between the pillar and the abutments is dominated by weak foliation or schistosity planes that strike parallel to the long axis of the stope.

- The application of plate theory for evaluation of pillar stability seems to be of limited usefulness because the strike length to span ratios for most stope crown pillars generally exceed 2.

- Methods involving analysis by Voussoir cracking or block caving analogies have application in certain circumstances. Their use however should be decided on the basis of presumed rock mass behaviour.

- Considerable care should be exercised in utilizing numerical modelling approaches where adequate calibration to known conditions is impracticable.

- For deep and narrow stopes, numerical analyses using elastic boundary element or finite difference codes generally suggest that large tensile zones develop around the stopes. When this is examined using FLAC with a Mohr-Coulomb model assuming a "no-tension" elastic-perfectly plastic material, any excess stresses that exist once an element goes into tension will be transferred to an adjacent element. This next element may then become overstressed and likely behave as if in a perfectly plastic state.

  In this condition, these elements can undergo substantial displacement in any subsequent process of stress redistribution so long as they remain overstressed. For this reason, very large displacements can be computed between elements, and interface displacements can become numerically very large, perhaps unrealistically so. Even when ubiquitous joint models are used the intrinisic assumption of continuum mechanics does not allow separation on joints. Thus, the resulting zone of large displacements generally extends for considerable distances. As the true displacement configuration probably lies between those of the elastic and elastic-perfectly plastic cases, some calibration of such FLAC models is necesssary. Once done, it has been found that the use of a finite value of tension cut-off to represent tensile strength in the rock mass can produces rational results.

- The MUDEC code allows separation of blocks at the defined joint contacts and thus provides more realistic displacement patterns as one approaches failure than FLAC analyses. However, it is noteworthy that for similar geometry, and discontinuity characteristics, the elastic displacements obtained from continuum analyses using FLAC are less than those from the distinct element code because MUDEC allows separation at individual joints.

It would appear, therefore, that for the purposes of detailed crown pillar design or for undertaking generic parametric analysis of crown pillar geometries discrete block codes such as MUDEC as well as many of the limit equilibrium models can have useful application. In fact, modelling, using such methods, allows significant insight to be gained into failure mechanisms. This suggests that development of rational analytical and design procedures for crown pillar layout may well be feasible within a framework of empirical controls reflecting realistic crown pillar behaviours. The use of semi-empirical calibrations provided by means of the proposed scaled crown span relationship outlined in Section 6 of this report may provide this necessary framework for development of improved design approaches. Probabilistic assessment of realistic controlling parameters, however, is an area that requires additional research before such approaches can be applied generically.

GOLDER ASSOCIATES LTD.

T. G. CARTER

T.G. Carter, P.Eng.

for J.S. Wong, P. Eng.

C.M.K. Yuen, P.Eng.

TGC/JSW/CMKY/se

Bibliography

BIBLIOGRAPHY

Amadei, B. and Savage, W.Z. (1985): "Gravitational Stresses in Regularly Jointed Rock Masses - A Keynote Lecture", Proceedings of the International Symposium on Fundamentals of Rock Joints, Bjorkliden, 15-20 September, pp.463-473.

Anderson, C. (1984): "Arching Action in Transverse Laterally Loaded Masonry Walls Panels", The Structural Engineer 26B, pp.12-23.

Anon (1916): "More Mine Cave-Ins Threaten Parts of Scranton", Engineering News, Vol. 76, pp.280-282.

Anon (1970): "The Logging of Rock Cores for Engineering Purposes", Q. Journal, Engng. Geol. 3, pp. 1-214.

Anon (1972): "The Preparation of Maps and Plans in Terms of Engineering Geology", Q. Journal. Engng. Geol. 5, pp. 293-382.

Anon (1977): "The Description of Rock Masses for Engineering Purposes", Q. Journal. Engng. Geol. 10,
pp. 355-389.

Anon (1978): "Suggested Methods for the Quantitative Description of Discontinuities in Rock Masses", ISRM Commission on Standardisation of field and laboratory tests, Int. Journ. Rock Mech. Min. Sci. 15, pp. 319-368.

Arjang, B. (1984): "Rock Mass Characterization Around the Crown Pillar at Selbaie Mine, Quebec", Minerals Research Program, Mining Research Laboratories Division Report MRP/MRL 84-53 (TR), CANMET.

Aughenbaugh, N.B. and Elifrits, C.D. (1986): "Subsidence and Time", Mining Engineering, pp.834-836.

Baldwin, M.J. and Newton, M.A. (1988): "Basal Permian Sand Mines and Associated Surface Movements in the Castleford and Pontefract Area of West Yorkshire", In: Bell, F.G., Culshaw, M.G., Cripps, J.C., and Lovell, M.A. (eds) Engineering Geology of Underground Movements, Geological Society Engineering Geology Special Publication No. 5, pp.351-357.

Bandis, S.C., Lumsden, A.C., Barton, N.R. (1983): "Fundamentals of Rock Joint Deformation", Int. J. Rock Mech. Min. Sci and Geomech. Abstr. 20, pp.249-268.
Barton, N.R. (1972): "A Model Study of Rock Joint Deformation", Int. J. Rock Mech. Min. Sci. 9, pp.579-602.

Barton, N.R. (1973): "Review of a new Shear Strength Criterion for Rock Joints", Engineering Geology, Vol.7, pp 287-332.

Barton, N.R. (1976): "Recent Experiences with the Q-System of Tunnel Support Design", Proceedings of the Symposium on Exploration for Rock Engineering, Johannesburg, pp.107-117.

Barton, N.R. (1976): "The Shear Strength of Rock and Rock Joints", Intnl. J. Rock Mech. Min. Sci., Vol. 13, No. 10, pp. 1-24.

Barton, N.R. (1981): "Estimation of In Situ Joint Properties, Nasliden Mine", Preceedings of the Conference on Application of Rock Mechanics to Cut and Fill Mining, Institute of Mining and Metallurgy, London, England, pp. 186-192.

Barton, N.R. and Bandis, S. (1982): "Effects of Block Size on the Shear Behaviour of Jointed Rock", Issues in Rock Mechanics, 23rd Symposium on Rock Mechanics, pp.739-759.

Barton, N.R. and Choubey, V. (1977): "The Shear Strength of Rock Joints in Theory and Practice", Rock Mechanics,
Vol. 10, pp.1-54.

Barton, N.R., Lien, R. and Lunde, J. (1974): "Engineering Classification of Rock masses for the Design of Tunnel Support", Rock Mechanics Vol. 6, pp.189-236.

BS 5930 (1981): "Code of Pracatice for Site investigations", British Standards Institution, London.

Beer, G. and Meek, J.L. (1982): "Design Curves for Roofs and Hangingwalls in Bedded Rock based on 'Voussoir' Beam and Plate Solutions", Trans. Instn. Min. Metall. (Section A: Min. industry), 91, pp.18-22.

Bell, F.G. (1975): "Salt and Subsidence in Cheshire, England", Engineering Geology, Vol. 9, pp.237-247.

Bell, F.G., Cripps, J.C., Culshaw, M.G. and Lovell, M.A. (1988): "Ground Movements Due to Engineering Operations", Engineering Geology of Underground Movements, Geological Society Engineering Geology Special Publication No. 5,
pp.17-21.

Bétournay, M.C. (1986A): "A Design Process for Surface Crown Pillars of Hard Rock Mines", 38th Annual C.I.M. General Meeting, Montreal, Quebec.

Bétournay, M.C. (1986B): "Preliminary Geomechanical Assessment of the Mantauban Mine", Mining Research Laboratories Divisional report MRL 86-119 (TR).

Bétournay, M.C. (1987A): "A Design Philosophy for Surface Crown Pillars of Hard Rock Mines", CIM Bulletin, Vol 80, No. 903, pp.45-61.

Bétournay, M.C. (1987B): "Preliminary Geomechanical Assessment of the Eldrich-Flavel Mine", Mining Research Laboratories Divisional Report MRL 87-91 (TR).

Bétournay, M.C., Nantel, S., and Lessard, D. (1987): "Summary of 24 Surface Crown Pillar Case Studies", Mining Research Laboratories Division Report MRL 87-10E (OP), CANMET.

Bétournay, M.C., (1988A):"Holt-McDermott Mine Visit: Stability Assessment of Shallow Underground Openings", Mining Research laboratories division Report MRL 88-72 (TR), CANMET.

Bétournay, M.C., (1988B): "Application of 2-D Finite Element Modelling to the 0997 Near-Surface Stope, Holt-McDermott Mine, Mining Research Laboratories Division Report MRL 88-82 (TR).

Bétournay, M.C., (1988C): "CANMET's in situ research in surface crown pillar stability", Proceedings CANMET Seminar, Timmins, pp.162-195.

Bétournay, M.C. et Labrie, D. (1988) "la Stabilite des Chantiers Superieurs et leurs Piliers de Surface, Mine Eldrich : Methodes Analytiques", Divisional Report 88-17 (TR), CANMET, Energy, Mines and Resources, Canada.

Bieniawski, Z.T. (1973): "Engineering Classification of Jointed Rock Masses", Transactions, South African Institution of Civil Engineers, Vol. 15, No.12, pp.335-344.

Bieniawski, Z.T. (1974): "Geomechanics Classification of Rock Masses and Its Application in Tunnelling", Proc. 3rd International Congress on Rock Mechanics, ISRM, Denver, Volume 11A, pp.27-32.

Bieniawski, Z.T. (1976): "Rock Mass Classification in Rock Engineering", Proceedings of the Symposium on Exploration for Rock Engineering, Johannesburg, pp.97-106.
Bieniawski, Z.T. (1984): Rock Mechanics Design in Mining and Tunnelling, A.A. Balkema, Boston, 271pp.

Bieniawski, Z.T., Rafia, F. and Newman, D.A. (1980): "Ground Control Investigations and Assessment of Roof Conditions in Coal Mines", Proc. 21st Symp. on Rock Mechanics, University of Missouri, Rolla, pp.691-700.

Brady, B.H.G. and Brown, E.T. (1985): Rock Mechanics for Underground Mining, Allen & Unwin (Publishers) Ltd., London, UK., 527 pp.

Braithwaite, P.A. and Seago, K.L. (1988): "Regional Study of the West Midlands Area to Locate Old Limestone Mine Workings", In: Bell, F.G., Culshaw, M.G., Cripps, J.C. and Lovell, M.A. (eds) Engineering Geology of Underground Movements, Geological Society Engineering Special Publication No. 5, pp.279-285.

Brebbia, C.A.: "The Boundary Element Methods in Geomechanics", Computational Mechanics Institute Southampton, UK, pp.1-13.

Brekke, T.L. (1968): "Blocky and Seamy Rock in Tunneling", Bull., Association of Engineering Geologists, Vol. V., Number 1.

Brekke, T.L. and Howard, T. (1972): "Stability Problems Caused by Seams and Faults", Proc. First North American Rapid Excavation and Tunnelling Conference, AIME, New York, pp.25-41.

Brown, E.T. (1987): Analytical and Computational Methods in Engineering Rock Mechanics, Allen & Unwin (Publishers) Ltd., London, UK.

Brumleve, C.B. (1988): "Rock Reinforcement of a Caving Block in Variable Ground Conditions, Kings Mine, Zimbabwe", Mining Industry, Transactions of the Institution of Mining and Metallurgy, Vol. 97, Section A, pp.77-84.

C.I.M., Jubilee Volume (1948): "Structural Geology of Canadian Ore Deposits."

Burman, B.C. (1974): "Development of a Numerical Model for Discontinua", Australian Geomechanics Journal.

Canadian Geotechnical Society (1985): "Canadian Foundation Engineering Manual", 2nd Edition.

CANMET (1984): "Surface Pillars", Contract Report 26SQ23440-3-9005, Roche Associates.

CANMET (1985): "Eighteen Surface Crown Pillar Case Studies (in 2 Volumes)", Contract Report 26SQ23440-5-9014.

Carter, T.G. (1989): "Design Lessons from Evaluation of Old Crown Pilller Failures", Proc. Int. Conf. on Surface Crown Pillars for Active and Abandoned Metal Mines, pp. 177-187.

Carter, T.G., Busbridge, J.R., Mackassey, W.O., and Annan, A.P. (1988): "Investigations and Remedial Measures for Reinstatement of Highway Collapse over Old Mine Workings", Proc. 2nd Int. Conf. on construction in Areas of Abandoned Mineworkings, Edinburgh, pp. 289-297.

Centre de Research Minérais. (Service de Technologie Minière) (1986): "Guide d'Ingénierie pour la Conception des Piliers de Surface", Dossier 5187, Roche Ltée.

Chen, J.Y. (1982): "Stability Analysis of the Sublevel Caving Method", Proc. First International Conference on Stability in Underground Mining, pp.450-483.

Closset, L. (1988) "Numerical modelling and surface crown pillar design", CANMET Seminar, Timmins, pp.198-209.

Coates, D.F. (1981): Rock Mechanics Principles, (2) 31-45.

Coffman, B.S. (1960): "Estimating the Relative Density of Sands, Civil Engineering, October.

Cooke, N. (1988): "Instability of Masonry Arches", Proc. Instr. Civ. Engrs., Part 2, Vol. 85, pp.373-387.

Cording, E.J., and Deere, D. U. (1972): "Rock Tunnel Supports and Field Measurements", Proceedings, Rapid Excavation and Tunnelling Conference, American Institution of Mining Engineers, New York, pp. 601-622.

Cundall, P.A. (1971): "A Computer Model for Simulating Progressive Large Scale Movements in Blocky Rock Systems", Proc. Int. Symp. Rock Fract., Nancy Paper, pp. 2-8.

Cundall, P.A. (1976): "Explicit Finite Difference Methods in Geomechanics", Proc. Conf. on Numerical Methods in Geomech., Vol. 1, pp. 132-150.
Cundall, P.A. (1988): "Formulation of a Three-dimensional Distinct Element Model - Part I. A Scheme to Detect and Represent Contacts in a System Composed of Many Polyhedral Blocks", Int. J. Rock. Mech. Min. Sci. & Geomech. Abstr., Vol. 25, No. 3, pp.107-116.

Curran, J.H. and Corkum, B.T. (1989): "EXAMINE: Excavation Analysis for Mines", A 2-D boundary element program. University of Toronto, MTD, Noranda.

D'Appolonia, E. (1970): "Dynamic Loadings", Journ. SMFE, ASCE 96, No. SM1, January.

Davidson, S. (1948): "The Beattie Mine: In Structural Geology of Canadian Ore Deposits", Can. Inst. Min. Met., Jubilee Volume, pp. 692-701.

Dean, J.W. (1967): "Old Mine Shafts and Their Hazards", Mining Engineer, 126, pp.368-380.

Deere, D.U. (1964): "Technical Description of Rock Cores for Engineering Purposes, Rock Mechanics and Engineering Geology", Vol. 1, pp.17-22.

Deere, D.U., Hendron, Jr., A.J., Patton, F.D. and Cording, E.J. (1966): "Design of Surface and Near-Surface Construction in Rock", Symposium Rock Mech., 8th Minnesota, (Proc. published IME, 1967).

Deere, D.U. and Miller, R.P. (1966): "Engineering Classification and Index Properties for Intact Rock, Tech. Report No. AFNL-TR-65-116, Air Force Weapons Laboratory, New Mexico.

Dileo, D., Morrison, D.M. and Girard, N.A. (1987): "Case History of a Groundfall at Falconbridge's East Mine", Underground Support Systems, Canadian Institute of Mining and Metallurgy, Special Volume 35, pp.51-57.

Diering J.A.C. and Laubscher D.H. (1987): "Practical Approach to the Numerical Stress Analysis of Mass Mining Operations", Trans. Instn. Min. Metallurgy,Vol.96,Section A pp A179-A188.

Eden, W.J. (1964): "Earthflows at the Beattie Mine, Quebec, Canada", Can. Geotech. Journal, Vol. 1, No. 2, pp. 104-114.

Edmonds, C.N. (1988): "Induced Subsurface Movements Associated with the Presence of Natural and Artificial Underground Openings in Areas Underlain by Cretaceous Chalk", In: Bell, F.G., Culshaw, M.G., Cripps, J.C. and Lovell, M.A. (eds), Engineering Geology of

Underground Movements, Geological Society Engineering Geology Special Publication No. 5, pp.205-214.

Evans, W.H. (1941): "The Strength of Undermined Strata", Trans. Inst. Mining and Metallurgy 50, pp.475-500.

Franklin, J.A. (1975): "Safety and Economy of Tunnelling", Proc. Tenth Canadian Rock Mechanics Symposium, Kingston.

Free, G.D., (1970): "Mathematical and model studies of the flow of material in the sublevel caving mining method" Unpublished M.Engng. thesis University of Queensland, Australia, 295 pp.

Geis, H.P. (1973): "Cave-in and Subsidence at the Rodsand Mine, Western Norway, "SME Mining Engineering Handbook, pp.645-648.

Gen-hua Shi and Goodman, R.E. (1981): "A New Concept for Support of Underground and Surface Excavations in Discontinuous Rocks Based on a Keystone Principle", Proc. 22nd U.S. Symposium on Rock Mechanics, Mass. Inst. Technology, pp.290-296.

Ghaboussi, J. (1988): "Fully Deformable Discrete Element Analysis using a Finite Element Approach", Computers and Geotechnics 5.

Goel, S.C. and Page, C.H. (1982): "An Empirical Method for Predicting the Probability of Chimney Cave Occurrence over a Mining Area", Int. J. Rock Mech. Min. Sci and Geomech. Abstr., Vol. 19, pp.325-337.

Golder Associates (1981): Report 802-1571 to CANMET on "Prediction of Stable Excavation Spans for Mining at Depths Below 1000 Meters in Hard Rock", Canmet Contract No. 17SQ.23440-0-9020.

Goodman, R.E. (1989): "Introduction to Rock Mechanics)", John Wiley and Sons, Second Edition.

Goodman, R.E., Gen-hua Shi and Boyle, W. (1982): "Calculation of Support for Hard, Jointed Rock Using the Keyblock Principle", Issues in Rock Mechanics, Proc. 23rd Symposium on Rock Mechanics, pp.883-898.
Government of Quebec, Executive Council (1981): "Commission d'enquête sur la tragédie de la mine Belmoral et les conditions de sécurité dans les mines sonterraines (in 3 volumes)".

Hanson, D.S.G. (1989): "Geotechnical Assessment of the
No. 5 Shaft Crown Pillar: Falconbridge Mine", Proc. Int. Conference on Surface Crown Pillars, Timmins, pp.37-46.

Hart, R., Cundall, P.A. and Lemos, J. (1988): "Formulation of a Three-dimensional Distinct Element Model - Part II. Mechanical Calculations for Motion and Interaction of a System Composed of Many Polyhedral Blocks", Int. J. Rock. Mech. Min. Sci & Geomech. Abstr., Vol. 25,No. 3,pp.117-125.

Herget, G. (1980): "Regional Stress Measurements in the Canadian Shield", Underground Rock Engineering, C.I.M. Special Vol. 22, pp.9-16.

Heuze, F.E., Goodman, R.E. (1970): "The Design of Room and Pillar Structures in Competent Jointed Rock, Example: The Crestmore Mine, California", Proc. 2nd Congress ISRM, Belgrade, topic 4, paper 41.

Heyman, J. (1980): "The Estimation of the Strength of Masonry Arches", Proc. Instn. Civ. Engrs, Part 2, 69, Dec., pp.921-937.

Heyman, J. (1969): "The Safety of Masonry Arches", Int. J. Mech. Sci., Vol 11, pp.363-385.

Heyman, J., Hobbs, N.B. and Jermy, B.S (1980): "The Rehabilitation of Teston Bridge", Proc. Instr. Civ. Engrs., Part 1, Vol. 68, pp.489-497.

Hoek, E. (1982): "Geotechnical Considerations in Tunnel Design and Contract Preparation", Transaction Inst. Min. Metall., Vol. 91, Section A (Mining Industry), A101-109.

Hoek, E. (1983): " Strength of Jointed Rock Masses", 23rd Rankine Lecture. Géotechnique, Vol 33. No 3, pp.187-223

Hoek, E. (1989): "A Limited Equilibrium Analysis of Surface Crown Pillar Stability", Proc. Int. Conf. on Surface Crown Pillars for Active and Abandoned Metal Mines, Timmins, pp. 3-13.

Hoek, E. and Brown, E.T. (1980): Underground Excavations in Rock, IMM, London, U.K., Stephen Austin and Sons.
Hoek, E. & Brown, E.T. (1988): "The Hoek-Brown Failure Criterion -A 1988 Update", Proc. 15th Canadian Rock Mech. Symp., Toronto, pp. 31-38.

Hoek, E. and Wood, D.F. (1987): "Support in Underground Hard Rock Mines", Underground Support Systems, ed. J. Udd. (Montreal: Canadian Inst. Min. Metall.), Special Vol. 35, pp. 1-16.

Hunt, W.G. (1989): "Geomechanics Methods Employed to Evaluate Near-Surface Crown Pillar Stability at the Old Moneta Mine, Timmins, Ontario", Proc. Int. Conference on Surface Crown Pillars, CANMET, Timmins, pp.143-154.

ISRM (1981): "Rock Characterization Testing and Monitoring - ISRM Suggested Methods", Pergamon Press, Osgood, U.K.

Itasca Consulting Group, Inc. (1986): "MUDEC: Micro Distinct Element Code - Version 1.00", Minneapolis, Minnesota.

Itasca Consulting Group, Inc. (1987): "FLAC: Fast Lagrangian Analysis of Continua - Version 2.0", Minneapolis, Minnesota.

Janelid, I. and Kvapil, R. (1966): "Sublevel Caving", International J. Rock Mech. Sci., Vol. 3, pp. 129-153.

Jennings, J.E., Brink, A.B.A., Louw, A. and Gowan, G.D. (1965): "Sinkholes and Subsidences in the Transvaal Dolomite of South Africa", Proc. 6th Int. Conf. Soil Mech. Foundn. Engng., Montreal, Vol. 1, pp.51-54.

Just, G.D. and Free, G.D., (1971): "The gravity flow of material in the sublevel caving mining system" Proc. of the First Australian-New Zealand Conference on Geomechanics, Melbourne, P. 88-97.

Karfakis, M.G. (1987): "Chimney Subsidence Over Abandoned Coal Mines", International Journal of Mining and Geological Engineering, Vol. 5, pp.131-141.

Kelly, J.G., Magijc I.D. and Rispin M.P. (1988): "Surface Crown Pillar blast at Sherrit's Fox Mine', C.I.M. 88th Annual Gerard Meeting, Montreal, paper 175.

Kendorski, F.S. (1978): "The Cavability of Ore Deposits", Min. Engng., Vol. 30, No. 6, pp. 628-631.
Kendorski, F.S., Cummings, R.A., Bieniawski, Z.T. and Skinner, E.H. (1983): "Rock Mass Classification for Block Caving Mine Drift Support", Proc. Int. Cong. Rock Mech., Melbourne, Australia, Vol. B., pp.51-63.

Kirsten, R.W.O. (1984): "The Design of Pillars in the Shrinkage Stoping of a South African Gold Mine", J.S. Afr. Inst. Min. Metall., Vol. 84, No. 11, pp.365-368.

Knight, C.W. (1915): "The North Shore of Lake Huron", Ontario Dept. of Mines Annual Report, Vol. 24, pp. 216-241.

Krstulovic, G. (1979): "Influence of Tectonic Stresses on the Caving Process - Mining by Block Caving Methods", Proc. 4th Congr. Int. Soc. Rock Mech., Montreaux, Vol. 1, pp.459-466.

Kulhawy, F.H. (1978): "Geomechanical Model for Rock Foundation Settlement", J. Geotech. Eng., pp. 104, 211-227.

Kvapil, R., Baeza, L., Rosenthal, J. and Flores, G. (1989): "Block Caving at El Teniente Mine, Chile", Transactions of the Institution of Mining and Metallurgy, Vol. 98, Section A (Mining Industry), pp.A43-56.

Lambe, T.W. & Whitman, R.V. (1969): Soil Mechanics.

Lang, T.A. and Bischoff, J.A. (1982): "Stabilization of Rock Excavations Using Rock Reinforcement", Issues in Rock Mechanics, 23rd Symposium on Rock Mechanics, pp.935-944.

Laubscher, D.H. (1975): "Class Distiction in Rock Masses", Coal, Gold and Base Minerals of S.A., vol. 23, no. 6, pp. 37-50.

Laubscher, D.H. (1981): "Selection of Mass Underground Mining Methods", Design and Operation of Caving and Sublevel Stoping Mines, Society of Mining Engineers of the American Institute of Mining, Metallurgical and Petroleum Engineers, Inc., pp.32-33.

Laubscher, D.H. (1984): "Design Aspects and Effectiveness of Support Systems in Different Mining Conditions", Transactions of the Institution of Mining and Metallurgy, Vol. 93, Section A (Mining Industry), pp.A70-81.

Laubscher, D.H. and Taylor, H.W. (1976): "The Importance of Geomechanics Classification of Jointed Rock Masses in Mining Operations", Proceedings of the Symposium on Exploration for Rock Engineering,Johannesburg,pp.119-128.

Lauffer, H. (1958): "Gebirgsklassiziziering fur den Stollendau", Geologie und Bauwesen, Vol. 24,No.1 pp.46-51

Lee, A.J. (1966): "The Effect of Faulting on Mining Subsidence", Mining Engineering, 125, pp.735-745.

Lorig, L.J. (1988): "Rock Reinforcement: Mechanical Representations and Use in Finite Difference Schemes" International Symposium on Underground Engineering, New Delhi.

Lorig, L.J. and Brady, B.G.H. (1984): " A Hybrid Computational Scheme for Excavation and Support Design in Jointed Rock Media". Proc. ISRM Conf. on Design and Performance of Underground Excavations, Cambridge, England, pp.105-112.

Mathews, K.E. (1975): "Fracture Measurements and Analysis of Data for Excavation Design", Proc. 10th Canadian Rock Mechanics Symposium, Queens University, Kingston, Ontario.

Mathews, K.E. (1978): "Design of Underground Mining Layouts", Underground Space, Vol. 2, pp.195-209.

Maury, V. (1979): "Effondrements spontanes: Synthese d'observations et possibilite de mechanisme initiateur par mise en charge hydraulique", Chef du Service, Géotechnique - Geostock, pp.511-522.

Mirza, C., Lau, K.C., Bétournay, M.C., and Crawford, A.M. (1989): "Complete Recovery of Surface Crown Pillars without Removal of Overburden", Proc. Int. Conference on Surface Crown Pillars, Timmins, pp.113-122.

Nicholas, D.E. (1981): "Method Selection - A Numerical Approach", Design and Operation of Caving and Sublevel Stoping Mines, Society of Mining Engineers of the American Institute of Mining, Metallurgical and Petroleum Engineers, Inc., 49 and 51.

Page, C.H. and Brenner, R.G. (1982): "Stability of Large Open Stopes in Weak Rock", First International Conference on Stability in Underground Mining, pp.336-356.

Patching, T.H. and Coates, D.F. (1968): "A Recommended Rock Classification for Rock Mechanics Purposes", C.I.M. Bulletin.

Peck, R.B. (1969): "Deep Excavations and Tunnelling in Soft Ground", Proceedings, 7th International Conference SMFE, State of the Art Vol., Mexico City, Mexico.
Pender, M.J. (1985): "Prefailure Joint Dilatancy and the Behaviour of a Beam with Vertical Joints", Rock Mechanics and Rock Engineering 18, pp.253-266.

Piciacchia, L., Bétournay, M.C. and Labrie, D. (1989): "Rock Mechanics Investigation and Assessment of Near Surface Crown Pillar Stability at Four Ontario and Quebec Mines", Proc. Int. Conference on Surface Crown Pillars, CANMET, Timmins, pp.47-56.

Pijaudier-Cabot, G., Bazant, Z.P. and Tabbara, M. (1988): "Comparison of Various Models for Strain-Softening", Eng. Comput., Vol. 5.

Pippard, A.J.S. (1948): "The Approximate Estimation of Safe Loads on Masonry Bridges", Civil Engineer in War, Vol 1, pp.365-372.

Pippard, A.J.S. Tranter, E. and Chitty, L. (1936): "The Mechanics of the Voussoir Arch", J. Instn. Civ. Engrs. 4, pp.281-306.

Potts, E.L.J., Szecki, A., Watson, S.H., Mottahed, P. (1979): "The Evaluation of the Design Criteria for an Underground Roof Strata Considered as a Linear Arch Structure", Proc. 11th Congress ISRM, Montreux, Vol. 2, pp.531-538.

Potvin et al (1988): "Summary Papers - Integrated Mine Design Project", Vol. 3, NSERC Project #CRD-8612

Priest, S.D. and Hudson, J.A. (1981): "Estimation of Discontinuity Spacing and Trace Length Using Scanline Surveys", Int. J. Rock Mech. Min. Sci. 18.

Rajala, L.H. (1989): "The Recovery of No. 1 Shaft Crown Pillar at Falconbridge Mine", Ninth Underground Operator's Conference, Sudbury, Ontario.

Roark, R.J. (1965): Formaulas for Stress and Strain, 4th Edition, McGraw-Hill, Inc.

Rose, D. (1982): "Revising Terzaghi's Tunnel Rock Load Coefficients", Issues in Rock Mechanics, 23rd Symposium on Rock Mechanics, pp.953-960.

Rosenbleuth, E. (1972): Point Estimates for Probability Moments, Proc. Nat. Acad. Sci., USA, Vol. 10, pp 3812-3814.

Rutledge, J.C. and Preston, R.L. (1978): "Experience with Engineering Classifications of Rock for the Prediction of Tunnel Support", Proceedings, International Tunnelling Symposium, Tokyo, A-3-1:7.

Salas, J.A.J. (1973): "Two Cases of Subsidence in Spain", SME Mining Engineering (in Spanish), pp.375-382.

Schneider, H.J. (1976): "Friction and Deformation Behaviour of Rock Joints", Rock Mechanics 8, pp.169-184.

Serafim, J.L. and Pereira, J.P. (1983): "Considerations on the Geomechanical Classification of Bieniawski", Proceedings from the International Symposium on Engineering Geology and Underground Construction, Lisbon, Portugal,
pp.33-42.

Sheorey, P.R. (1984): "Use of Rock Classification to Estimate Roof Caving Span in Oblong Workings", International Journal of Mining Engineering, Vol. 2, pp.133-140.

Spooner, J. (ed), (1971): "Mufulira Interim Report", Min. Journal, Vol. 276, p. 122.

Softek Services Ltd. (1988): "P-FRAME: An Engineering Analysis Program for Two Dimensional Structural Systems - Release 1.05", Vancouver, B.C.

Stacey, T.R. (1986): "Interaction of Underground Mining and Surface Development in a Central City Environment", Transactions of the Institution of Mining and Metallurgy, Vol. 95, Section A), pp.A176-180.

Starfield, A.M. and Cundall, P.A. (1988): "Towards a Methodology of Rock Mechanics Modelling", Int. J. Rock. Mech. Min. Sci & Geomech. Abstr., Vol. 25, No. 3, pp.99-106.

Stephans, D.E. (1974): "It Happened at Moose River", Lancelot Press, N.S., 99 pp.

Stephansson, O. (1971): "Stability of Single Openings in Horizontally Bedded Rock", Engineering Geology, Vol. 5, pp.5-71.

Strata Engineering Corp. (1987): "Report to Energy, Mines and Resources Canada (CANMET), Weak Rock Mass Model for Support of Surface Crown Pillars at Les Mines Selbaie - Phase II Model Development and Calibration, Joutel, Quebec, DSS File No. 015SQ 23440-5-9017.

Strata Engineering Corp. (1988): "Report to Energy, Mines and Resources Canada (CANMET), Recovery of the surface crown pillar through the Control Caving Method at Les Mines Selbaie, Joutel, Quebec, DSS File No. 035Q 23440-7-9195.

Terzaghi, K. (1943): "Theoretical Soil Mechanics", John Wiley & Sons, New York.

Terzaghi, K. (1946): "Introduction to Tunnel Geology", and "Rock Defects and Loads on Tunnel Support", Rock Tunnelling with Steel Supports, eds. R.V. Proctor and T. L. White, Commercial Shearing and Stamping Co., Youngstown, Ohio, pp.15-99.

Thomas, G.G. (1988): "A Cost-Benefit Analysis for Stabilizing Shallow Bath Stone Mine Workings at Corsham, Wiltshire", In: Bell, F.G., Culshaw, M.G., Cripps, J.C., and Lovell, M.A. (eds) Engineering Geology of Underground Movements, Geological Society Engineering Geology Special Publication No. 5, pp.167-174.

Touseull, J. and Rich, C. (Jr.) (1980): "Documentation and Analysis of a Massive Rock Failure at the Bautsch Mine, Galena, Ill.", Report of Investigation 8453, United States Department of the Interior, pp.1-49.

Tse, R. and Curden, D.M. (1979): "Estimating Joint Roughness Coefficients", Int. J. Rock Mech. Min. Sci. & Geomech. Abstr., Pergamon Press Ltd., Vol. 16 pp. 303 - 307.

Unal, E. (1983): "Design Guidelines and Roof Control Standards for Coal Mine Roofs, Ph. D. Thesis, Pennsylvania State University.

Vera, S.G. (1981): "Caving at Climax", Design and Operation of Caving and Sublevel Stoping Mines, Society of Mining Engineers of the American Institute of Mining, Metallurgical and Petroleum Engineers, Inc., 166.

Voegele, M., Fairhurst, C. and Cundall, P.A. (1978): "Analysis of Tunnel Support Loads Using a Large Displacement, Distinct Block Model". In Storage in Excavated Rock Caverns, ed. M. Bergman, Oxford: Pergammon Press. Vol.2 pp.247-252.

Voegele, M.D. and Fairhurst, C. (1982): "A Numerical Study on Excavation Support Loads in Jointed Rock Masses", Issues in Rock Mechanics, Proc. 23rd Symposium on Rock Mechanics, pp.673-683.

Wallwork, K.L. (1960): "Some Problems of Subsidence and Land Use in the Mid-Cheshire Industrial Area", Geog. Journal 126, pp.191-199.

Warburton, P.M. (1983): "Application of a New Computer Model for Reconstructing Blocky Geometry - Analysing Single Block Stability and Identifying Keystones". Proc. 5th. Congr. Intnl. Soc. Rock Mechanics, Melbourne, pp.225-229.

Wickham, G.E., Tiedemann, H.R. and Skinner, E.H. (1972): "Support Determination Based on Geologic Predictions". Proceedings, Rapid Excavation and Tunnelling Conference, AIME, New York, pp.43-64.

Yenge, L.I. (1980): "Analysis of Bulk Flow of Materials Under Gravity Caving Process, Part 1: Sublevel Caving in Relation to Flow in Bins and Bunkers", Colorado School of Mines, Quarterly, Vol. 75, No. 4.

Yenge, L.I. (1981): "Analysis of Bulk Flow of Materials Under Gravity Caving Process, Part 2: Theoretical and Physical Modelling of Gravity Flow of Broken Rock", Colorado School of Mines, Quarterly, Vol. 76, No. 3.

Yu, T.R. and Counter,D.B. (1989): "Geophysical Delineation of a Surface Crown Pillar at the Hoyle Pond Mine", Proc. Int. Conference on Surface Crown Pillar, CANMET, Timmins, pp.67-76.

Appendix A
Crown Pillar Database

Golder Associates

Crown Pillar Data Base

Mine	Mine	Rock				o/b	Dimensions			Stope	Fill	Gamma	RMR		T/S	Cs
Number	Type	HW	Ore	FW	DIP (Degrees)	thickness (m)	t (m)	w (m)	l (m)	Height (m)	Height (m)	Rock (T/m3)	Hw/Fw	Ore		
#1	A	Gneiss (qtz, mica, sericite and amphibole) and schistose sediments/slates	Massive and disseminated sulphides	Gneiss (qtz, mica, sericite and amphibole) gabbro and diorite dykes	70	0	37	9	30	82	70	2.7	65	75	4.1	2.3
					70	0	21	8	58	91	73	2.7	65	75	2.6	3.0
					70	0	12	14	46	100	82	2.7	65	75	0.9	6.4
					70	0	9	12	58	104	104	2.7	65	75	0.8	6.6
					70	0	9	14	49	104	104	2.7	65	75	0.6	7.4
					70	0	9	27	37	104	85	2.7	65	75	0.3	12.3
					70	0	9	12	46	104	104	2.7	65	75	0.8	6.4
					70	0	9	12	21	104	85	2.7	65	75	0.8	5.8
#2	D	Volcaniclastic sediments Chlorite Schist	Massive sulphides	Chlorite/biotite schist and quartzitic rocks	70	0	15	30	50	110	110	2.7	55	70	0.5	11.0
					70	0	30	23	50	110	110	2.7	55	70	1.3	6.3
					70	0	27	14	50	110	110	2.7	55	70	1.9	4.3
#3	C	Biotite schist, peridotite, leached skarn	Massive sulphides	Biotite schist and peridotite	65	18	70	21	238	183	183	2.8	40	60	3.3	4.5
					65	21	67	21	274	183	183	2.8	40	60	3.2	4.6
					65	27	76	9	244	183	183	2.8	40	60	8.4	1.9
					65	33	61	27	366	183	183	2.8	40	60	2.3	6.3
					65	18	79	43	91	183	183	2.8	40	60	1.8	7.5
					65	27	73	61	128	183	183	2.8	40	60	1.2	11.0
					65	21	79	21	137	183	183	2.8	40	60	3.8	4.1

* Indicates Crown Pillar Failure

Mine Number	Mine Type	Rock			DIP (Degrees)	o/b thickness (m)	Dimensions			Stope Height (m)	Fill Height (m)	Gamma Rock (T/m3)	RMR		T/S	Cs
		HW	Ore	FW			l (m)	w (m)	l (m)				Hw/Fw	Ore		
#4	D	Sericite, quartz biotite and andesite gneiss schists & tuffs	Sulphides with a carbonate gangue sphalerite	Metasediments, chlorite gneiss, schist and gabbros	45	43	24	40	40	55	30	2.7	70	75	0.6	11.3
					45	43	30	90	27	43	30	2.7	70	75	0.3	15.5
					45	43	37	40	46	61	49	2.7	70	75	0.9	9.4
					45	34	46	30	41	79	67	2.7	70	75	1.5	6.6
					45	18	49	35	79	61	52	2.7	70	75	1.4	8.2
#5	D	Fragmental rhyolite and altered dacite	Massive sulphides	Fragmental rhyolite and andesite	75	4	34	14	88	--	--	2.8	45	65	2.4	4.0
#6	A	Andesite and chlorite schist rhyolite	Carbonates, andesite and chloritic schist	Andesite rhyolite	80	21	46	2	271	116	0	2.8	70	45	23.0	0.5
					80	18	68	2	27	152	0	2.8	70	45	34.0	0.4
					80	18	68	2	41	152	0	2.8	70	45	34.0	0.4
					80	13	18	11	67	34	0	2.8	70	45	1.6	4.2
					80	0	12	2	104	101	0	2.8	70	45	6.0	1.0
					80	0	9	2	407	137	0	2.8	70	45	4.5	1.2
					80	0	17	2	207	70	0	2.8	70	45	8.5	0.8
					80	0	8	6	61	183	0	2.8	70	45	1.3	3.6
					80	0	13	6	66	21	0	2.8	70	45	2.2	2.8
					80	0	12	6	105	104	0	2.8	70	45	2.0	3.0

* Indicates Crown Pillar Failure

Mine Number	Mine Type	Rock HW	Rock Ore	Rock FW	DIP (Degrees)	o/b thickness (m)	Dimensions t (m)	Dimensions w (m)	Dimensions l (m)	Stope Height (m)	Fill Height (m)	Gamma Rock (T/m3)	RMR Hw/Fw	RMR Ore	T/S	Cs
#7	A	Andesite and diorite	Veins of qtz and auriferous carbonates	Andesite and diorite	80	2	6	2	50	30	0	2.7	85	60	3.0	1.4
					80	6	8	2	24	24	0	2.7	85	60	4.0	1.2
					80	9	9	2	268	34	0	2.7	85	60	4.5	1.1
					80	5	12	2	37	37	0	2.7	85	60	6.0	1.0
					80	6	5	2	61	43	0	2.7	85	60	2.5	1.5
					80	5	14	5	12	9	0	2.7	85	60	2.8	1.9
					80	5	15	4	14	9	0	2.7	85	60	3.8	1.6
					80	5	17	2	27	8	0	2.7	85	60	8.5	0.8
#8	C	Peridotite with large granitic porphyry inclusions	Massive and brecciated sulphides	Peridotite with inclusions of sub-volcanic or granitic porphyry (often sheared)	80	34	116	15	210	76	76	2.7	55	60	7.7	2.3
					80	34	73	15	542	43	43	2.7	55	60	4.9	3.0
#9	B	Norite and Peridotite	Granite breccia brec'd sulphides	Granite gneiss and metaseds.	43	14	34	11	15	128	128	3.0	80	60	3.1	3.0
					43	14	21	11	31	137	137	3.0	80	60	1.9	4.3
					43	14	20	14	43	134	134	3.0	80	60	1.4	5.6
Density		3			43	14	17	14	24	140	140	3.0	80	60	1.2	5.6
UCS (MPa)		190			43	14	53	18	18	110	110	3.0	80	60	2.9	3.6
E (GPa)		48 - 62			43	18	82	18	29	76	76	3.0	80	60	4.6	3.2
					43	20	87	18	24	104	104	3.0	80	60	4.8	3.0
					43	23	67	73	159	131	131	3.0	80	60	0.9	15.3
					43	21	102	31	46	95	95	3.0	80	60	3.3	4.9

* Indicates Crown Pillar Failure

Mine Number	Mine Type	Rock			DIP (Degrees)	o/b thickness (m)	Dimensions			Stope Height (m)	Fill Height (m)	Gamma Rock (T/m3)	RMR		T/S	Cs
		HW	Ore	FW			t (m)	w (m)	l (m)				Hw/Fw	Ore		
#10	B	Metadiorite and Tuff, porphyritic rhyolite	Siderite and Quartz veining	Chert - banded Siderite	70	7	46	15	18	101	0	2.9	50	85	3.1	3.1
					70	7	46	14	18	101	0	2.9	50	85	3.3	2.9
					70	24	46	67	18	107	0	2.9	80	85	0.7	8.5
					70	24	37	30	18	76	0	2.9	80	85	1.2	5.6
Density		2.9	3.56	2.93												
UCS (MPa)		145 - 195	265	274												
E (GPa)		34 - 76	62 - 117	48 - 96												
#11	A	Syenite porphyry Diabase & Tuff	Quartz veins sericite/chlor schists	Conglomerate a Red syenite porphyry	80	12	12	6	30	24	24	2.7	55	35	2.0	2.7
					80	18	6	3	104	24	24	2.7	55	35	2.0	2.1
					80	12	9	3	91	24	24	2.7	55	35	3.0	1.7
					80	18	8	6	70	24	24	2.7	55	35	1.3	3.5
Density		2.7	2.7	2.7												
Point Load (MP		4.7 - 7.4		4.7 - 5.3												
RQD		< 25	< 25	< 25												
NGI(Q)				0.05 - 1.5												
#12	B*	Andesite and peridotite	Finely bedded massive sulphide rhyolites	Peridotite, volcanics, gabbro	85	15	34	91	40	116	116	2.7	60	80	0.4	14.5 *
					85	15	55	91	55	79	79	2.7	70	80	0.6	12.7
					85	15	79	91	30	152	152	2.7	70	80	0.9	8.6
					85	15	20	80	125	155	120	2.7	65	80	0.3	23.5 *

* Indicates Crown Pillar Failure

Mine Number	Mine Type	Rock HW	Rock Ore	Rock FW	DIP (Degrees)	o/b thickness (m)	Dimensions t (m)	Dimensions w (m)	Dimensions l (m)	Stope Height (m)	Fill Height (m)	Gamma Rock (T/m3)	RMR Hw/Fw	RMR Ore	T/S	Cs
#13	C	Anorthosite	Sericitized Schist Zone	Anorthosite	45	3	23	6	94			2.9	75	50	3.8	2.5
					45	3	23	11	15			2.9	75	50	2.1	3.5
					45	3	24	6	55			2.9	75	50	4.0	2.4
Density		3	2.9	3	45	3	49	2	27			2.9	75	50	24.5	0.6
UCS (MPa)		80	65	80	45	3	37	5	43			2.9	75	50	7.4	1.6
CSIR		68	53	68	45	3	24	9	56			2.9	75	50	2.7	3.5
NGI(Q)		90	3	90	45	3	30	3	24			2.9	75	50	10.0	1.0
					45	3	27	12	15			2.9	75	50	2.3	3.5
					45	3	21	6	18			2.9	75	50	3.5	2.3
					45	3	46	3	21			2.9	75	50	15.3	0.8
					45	3	30	5	27			2.9	75	50	6.0	1.7
					45	3	21	8	77			2.9	75	50	2.6	3.4
					45	3	53	5	101			2.9	75	50	10.6	1.4
					45	3	23	6	107			2.9	75	50	3.8	2.5
					45	3	53	3	101			2.9	75	50	17.7	0.8
					45	3	30	3	67			2.9	75	50	10.0	1.1
					45	3	52	3	49			2.9	75	50	17.3	0.8
					45	3	27	5	64			2.9	75	50	5.4	1.9
					45	3	24	6	37			2.9	75	50	4.0	2.3
					45	3	24	9	46			2.9	75	50	2.7	3.4
					45	3	27	12	71			2.9	75	50	2.3	4.3
					45	3	27	6	15			2.9	75	50	4.5	2.0
					45	3	27	15	70			2.9	75	50	1.8	5.3
					45	3	30	4	82			2.9	75	50	7.5	1.4
					45	3	30	12	55			2.9	75	50	2.5	4.0
					45	3	64	3	12			2.9	75	50	21.3	0.7

* Indicates Crown Pillar Failure

Mine Number	Mine Type	Rock			DIP (Degrees)	o/b thickness (m)	Dimensions			Stope Height (m)	Fill Height (m)	Gamma Rock (T/m3)	RMH		T/S	Cs
		HW	Ore	FW			t (m)	w (m)	l (m)				Hw/Fw	Ore		
#13 Continued					45	3	35	3	37			2.9	75	50	11.7	1.0
					45	3	30	5	61			2.9	75	50	6.0	1.8
					45	3	27	30	55			2.9	75	50	0.9	9.4
					45	3	24	9	55			2.9	75	50	2.7	3.5
					45	3	33	5	40			2.9	75	50	6.6	1.7
					45	3	30	3	143			2.9	75	50	10.0	1.1
#14	C*	Pyroclastic rocks greywackes	Intermediate tuff, schists	Schistose mafic to sericitic tuff	85	5	43	23	100	113	113	2.8	30	45	1.9	5.4 *
					85	15	43	5	100	40	0	2.8	41	45	8.6	1.3
Density		2.77	3.04	2.77												
UCS (MPa)		7 - 10	13-62	21 - 59												
RQD		0	0-20	50 - 70												
#15	C	Sheared andesite, tuff, graphite horizon	Graphitic schist and smoky quartz	Andesite & tuff graphite horizon	75	30		4		40	0	2.9	65	45		
E lab (GPa)		87.28 - 107.50														
E emp (GPa)		17.78 - 35.50														

* Indicates Crown Pillar Failure

Mine Number	Mine Type	Rock			DIP (Degrees)	o/b thickness (m)	Dimensions			Stope Height (m)	Fill Height (m)	Gamma Rock (T/m3)	RMR		T/S	Cs
		HW	Ore	FW			t (m)	w (m)	l (m)				Hw/Fw	Ore		
#16	D	Metasediments	Massive Sulphide	Metasediments	75	0	15	6	67	137	137	2.9	75	85	2.5	2.7
		(Argillitic)	Gosson Fe-form'	qtz-schist,Fe-fr	75	9	15	4	49	137	137	2.9	75	85	3.8	1.8
					75	9	15	5	32	137	137	2.9	75	85	3.0	2.2
Density		2.9-3.0	4.3	2.9-3.0												
UCS (MPa)		34-69	138-345	62-103												
E (GPa)		30-69	103-207	28-83												
NGI			180													
#17	C	Greywacke,sericit biotite schist	Vein of quartz and stibnite	Greywacke,seric biotite schist	33	1	21	3	70	229	0	2.8	35	70	7.0	1.3
#18	D	Massive rhyolite serpentinized	Brecciform massive sulphide carbonated horizons,	Andesite-diorite rhyolite	68		30	18				2.7	70	80	1.7	
#19	A	Anorthosite	Sulphides	Altered	56	3	59	5	61	46		2.6	75	80	11.8	1.2
		porphyry dykes	porphyry	anorthosite	56	5	49	21	46	46		2.6	75	80	2.3	4.6
					56	6	49	9	61	46		2.6	75	80	5.4	2.2
					56	6	49	9	107	43		2.6	75	80	5.4	2.3
					56	5	58	12	76	40		2.6	75	80	4.8	2.7
					56	7	17	5	84	55		2.6	75	80	3.4	2.2
					56	3	56	6	79	50		2.6	75	80	9.3	1.4

* Indicates Crown Pillar Failu

Mine	Mine	Rock				o/b	Dimensions			Stope	Fill	Gamma	RMR		T/S	Cs
Number	Type	HW	Ore	FW	DIP (Degrees)	thickness (m)	t (m)	w (m)	l (m)	Height (m)	Height (m)	Rock (T/m3)	Hw/Fw	Ore		
#20	A	Epidiorite & Shear Zones	Chalcopyrite-bearing quartz veins in gabbro and pyroxenite	Altered gabbro and porphyry	63	14	8	2	38	46		2.8	50	70	4.0	1.3
					63	3	12	15	61	91		2.8	50	70	0.8	7.3
					63	4	9	6	30	107		2.8	50	70	1.5	3.4
					63	4	14	6	43			2.8	50	70	2.3	2.8
					63	0	6	4				2.8	50	70	1.5	
					63	0	8	3				2.8	50	70	2.7	
					63	0	9	3				2.8	50	70	3.0	
					63	0	21	5				2.8	50	70	4.2	
					63	0	23	3				2.8	50	70	7.7	
#21	E	Tuffs, Breccia	Carbonized, kaolinized shears	Chloritic and Pyritic Volcanics	50	45	35	22	30	20		2.8	75	45	1.6	5.6
					50	45	35	22	48	20		2.8	75	45	1.6	6.1
					50	45	35	15	22	20		2.8	75	45	2.3	3.9
Gamma (T/m3)		2.7	2.9	2.7	50	45	35	15	22	20		2.8	75	45	2.3	3.9
Point Load (MP		197	25.6	197	50	40	50	22	50	20		2.8	75	35	2.3	5.1 *
E (GPa)		28	18	28												
#22	C*	Volcanics and Conglomerates	Conglomerate and greywackes	Greywackes and Slates	75	8	14	17	50	37		2.8	75	50	0.8	7.1 *
					75	8	14	18	56	37		2.8	75	50	0.8	7.5 *
					75	14	14	15	58	37		2.8	75	50	0.9	6.4 *
E lab (GPa)		59.66 - 142.9			75	8	18	18	58	37		2.8	75	50	1.0	6.7 *
E emp (GPa)		14.96 - 70.8			75	8	38	17	59	37		2.8	75	50	2.2	4.4
					75	8	14	21	58	37		2.8	75	50	0.7	8.6 *

* Indicates Crown Pillar Failure

Crown Pillar Data Base

Mine Number	Mine Type	Rock			DIP (Degrees)	o/b thickness (m)	Dimensions			Stope Height (m)	Fill Height (m)	Gamma Rock (T/m3)	RMR		T/S	Cs
		HW	Ore	FW			t (m)	w (m)	l (m)				Hw/Fw	Ore		
#23	D	Andesite and altered peridotite	Brecciated peridotite	Basalt and altered massive peridotite	35	19	179	40	250	24		2.7	80	60	4.5	5.6
					35	19	179	40	250	24		2.7	80	60	4.5	5.6
					35	19	179	45	250	24		2.7	80	60	4.0	6.2
					35	19	179	40	250	24		2.7	80	60	4.5	5.6
#24	C	Peridotite	Serpentinized peridotite	Peridotite & Sheared zones								2.9	55	25		
#25	C	Porphyry	Qtz-carbonate shears	Greywacke	85	6	42	6	113	24	0	2.9	45	30	7.0	1.6
					85	6	42	8	65	57	0	2.9	45	25	5.3	2.0 *
					85	13	44	11	41	52	0	2.9	45	30	4.0	2.6
					85	8	60	10	113	102	0	2.9	45	30	6.0	2.2
					85	86	122	11	65	146	0	2.9	45	25	11.1	1.6 *
#26	A*	Sheared greywacke	Schist, greywacke	Quartzite, greywacke	55	3	12	13	23			2.7	80	50	0.9	5.7 *
#27	E*	Porphyry/schist	Foliated Porphyry	Talc chlorite schist	75	2	65	23	260	146	0	2.9	27	55	2.8	5.0 *
#28	E*	Sheared porphyry peridotite	Schist, porphyry	Talc chlorite schist, peridotite	70	2	97	19	65	21	0	2.9	60	15	5.0	3.2 *

* Indicates Crown Pillar Failure

Mine Number	Mine Type	Rock			DIP (Degrees)	o/b thickness (m)	Dimensions			Stope Height (m)	Fill Height (m)	Gamma Rock (T/m3)	RMR		T/S	Cs
		HW	Ore	FW			t (m)	w (m)	l (m)				Hw/Fw	Ore		
#29	B*	Conglomerate	Sheared Conglomerate	Conglomerate	65	3	2	30	70	40	0	2.7	90	75	0.1	32.7 *
#30	A	Porphyry + volcanics	Qtz-carb-chalcopyrite	Porphyrys	80		68	16	64	55	0	2.7	75	50	4.3	3.0
					80		68	16	23	55	0	2.7	75	50	4.3	2.6
#31	A	Gabbro + volcanics	Qtz-infilled shears	Volcanics + Gabbro	85		16	3	133	32	0	2.7	85	60	5.3	1.3
					85		16	3	58	32	0	2.7	85	60	5.3	1.2
#32	A	Gabbro, foliated	Altered chalcopyrite	Gabbro, blocky	70		8	6	39	52	0	2.7	75	50	1.3	3.6
					70		65	6	42	49	0	2.7	75	50	10.8	1.3
					70		78	6	81	19	0	2.7	75	50	13.0	1.2
#33	A	Basalt+Greenston Porphyry	Qtz viens porphyry	Porphyry	80		3	3	26	446	316	2.8		75	1.0	2.9
					80		6	3	39			2.8		75	2.0	2.1
					80		8	3	26			2.8		75	2.7	1.8
#34	A	Granodiorite	Silicified grandiorite	Granodiorite	80	6	39	3	32			2.8	75	50	13.0	0.8
					80	3	6	3	39			2.8	75	50	2.0	2.1
					80	6	29	3	36			2.8	75	50	9.7	0.9

* Indicates Crown Pillar Failure

Mine Number	Mine Type	Rock			DIP (Degrees)	o/b thickness (m)	Dimensions			Stope Height (m)	Fill Height (m)	Gamma Rock (T/m3)	RMR		T/S	Cs	
		HW	Ore	FW			t (m)	w (m)	l (m)				Hw/Fw	Ore			
#35	C*	Sheared granodiorite	Sheared,foliated granodiorite	Foliated granodiorite	70	10	10	3	450	65	15	2.9	54	25	3.3	1.8	*
					70	6	10	3	450	46	0	2.9	54	25	3.3	1.8	
E lab (GPa)		68.90 - 76.03															
E field (GPa)		1.35 - 3.95															
E emp (GPa)		12.6 - 15.8															
#36	A*	Syenite + Porphyry	Splay fault + dykes	Syenite Porphyry	87		6	3	40	35	0	2.6	90	85	2.0	1.9	
					87		6	20	200	300	0	2.7	85	58	0.3	13.0	*
					87		6	10	200	300	0	2.7	85	58	0.6	6.6	
#37	A	Argillite, conglomerate	Qtz-carb shears	Conglomerates	85	5	3	2	30			2.6	60		1.5	1.8	
					85	3	9	3	15			2.6	60		3.0	1.5	
#38	A*	Conglomerate + argillite	Qtz-carb shears	Conglomerates	85	10	1	6	40	60	0	2.7	50		0.2		*
#39	B*	Gabbro + volcanics	Qtz x-cr shears	Mafic volcanics	60		20	65				2.8		50	0.6		*

* Indicates Crown Pillar Failure

Mine Number	Mine Type	Rock			DIP (Degrees)	o/b thickness (m)	Dimensions			Stope Height (m)	Fill Height (m)	Gamma Rock (T/m3)	RMR		T/S	Cs
		HW	Ore	FW			t (m)	w (m)	l (m)				Hw/Fw	Ore		
#40	A	Conglomerate	Conglomerate + greywacke	Syenite Porphyry	80	10	3	2	13			2.6		75	1.5	1.8
					80		6	2	6			2.6		75	3.0	1.2
					80		10	2	65			2.6		75	5.0	1.1
					80		6	6	55			2.6		75	1.0	3.9
#41	D*	Serpentinite meta-dolomite	Dolomitic Magnesite	Limestone+ Dolomitic Magnesite	65	6	85	60	150	75	60	2.8	45	55	1.4	10.3 *
#42	A	Syenite Porphyry	Diabase+qtz carbonate	Syenite + Conglonerate	80		6	5	10	65	65	2.6	85	75	1.2	2.8
					80		8	5	52	65	65	2.6	85	75	1.6	2.9
					80		10	5	28			2.6	85	75	2.0	2.5
					80		5	5	58			2.6	85	75	1.0	3.6
					80		21	5	58			2.6	85	75	4.2	1.8
					80		12	5	75			2.6	85	75	2.4	2.4
					80		8	5	55			2.6	85	75	1.6	2.9
					80		5	5	49			2.6	85	75	1.0	3.6
#43	A	Syenites + tuffs	Qtz-carbonate fractures	Metaseds + tuff	85		9	3	97	176	0	2.6	85	75	3.0	1.6
					85		20	3	81	65	0	2.6	85	75	6.7	1.1
					85		9	3	39	19	0	2.6	85	75	3.0	1.6

* Indicates Crown Pillar Failure

Mine Number	Mine Type	Rock			DIP (Degrees)	o/b thickness (m)	Dimensions			Stope Height (m)	Fill Height (m)	Gamma Rock (T/m3)	RMR		T/S	Cs
		HW	Ore	FW			t (m)	w (m)	l (m)				Hw/Fw	Ore		
#44	A	Chlorite schist and basalt	Carbonate-qtz veins	Carbonate schist, porphry	60		16	10	12	28	0	2.7	45	60	1.6	3.5
					60		10	5	40	23	0	2.7	40	60	2.0	2.8
					60		19	5	50	13	0	2.7	40	60	3.8	2.0
					60		13	5	16	19	0	2.7	40	50	2.6	2.3
#45	C	Ultramafic + schists	Qtz-carbonate Porphyry	Mafic Volcanics	60	15	8	6	68	8	0	2.7	70	45	1.3	3.8
					60	13	28	10	36	65	0	2.7	70	45	2.8	3.1
					60	16	8	6	42	7	0	2.7	70	45	1.3	3.7
#46	A*	Volcanics + conglomerate	Greywacke + conglomerate	Greywacke + slates	80	23	5	3	91	50	50	2.7	80	50	1.7	2.3
					80	21	16	3	143	95	0	2.7	80	20	5.3	1.3 *
					80	6	3	3	97	47	47	2.7	75	50	1.0	2.9
					80	10	10	3	20	40	40	2.7	75	50	3.3	1.5
#47	D	Diorite + tonalite	Sheared + altered diorite	Diorite + Tonalite	38	10	15	20	100			2.8	80	60	0.8	9.6

* Indicates Crown Pillar Failure

Mine Number	Mine Type	Rock HW	Rock Ore	Rock FW	DIP (Degrees)	o/b thickness (m)	Dimensions t (m)	Dimensions w (m)	Dimensions l (m)	Stope Height (m)	Fill Height (m)	Gamma Rock (T/m3)	RMR Hw/Fw	RMR Ore	T/S	Cs
#48	B	Limestone	Altered carbonate	Carbonate	0		38	24	73	90	0	2.7	85	70	1.6	7.0
E (GPa)		30	40	40	0		48	27	49	90	0	2.7	85	70	1.8	6.5
Poisson's Ratio		0.25	0.25	0.25	0		50	32	34	90	0	2.7	85	70	1.6	6.8
UCS (MPa)		45	45	45	0		50	26	55	90	0	2.7	85	70	1.9	6.3
					0		41	27	73	90	0	2.7	85	70	1.5	7.5
					0		64	15	91	90	0	2.7	85	70	4.3	3.6
#49	A	Chlorite basalt and shear zone	Massive basalt	Graphitic schist	70	10	40	6		40	0	2.8	55	45	6.7	
#50	C*	Dacite/Andesite	Serpentinized Peridotite	Basalt/Andesite	80	15	140	15	150	135	0	2.9	70	20	9.3	2.2 *
#51	C	Andesites + chlorite schist	Sheared altered rhyolites	Rhyolite + basalts	45	0	10	17	80	35	0	2.8	70	41	0.6	9.7
#52	B*	Gneiss	Serpentinite	Gneiss	70	60	10	12	80	300	200	2.8	75	48	0.8	6.5 *
#53	A*	Syenite porph+ sh'd alt. porph	Brecciated Syenite Porph.	Tuff and andesites	80	33	6	12	80	80	0	2.7	85	54	0.5	7.9 *

* Indicates Crown Pillar Failure

Mine Number	Mine Type	Rock			DIP (Degrees)	o/b thickness (m)	Dimensions			Stope Height (m)	Fill Height (m)	Gamma Rock (T/m3)	RMR		T/S	Cs
		HW	Ore	FW			t (m)	w (m)	l (m)				Hw/Fw	Ore		
#54	B*	Andesite	Brecciated and Qtz-[illegible]in Andesite	Andesite Breccia	80	2	3	43	56	150	60	2.7	90	85	0.1	32.2 *
#55	C	Alt'd felsic schists + tuff	Silicified Aggl. and schist	Schistose agglomerate	60	0	60	15	100	120	0	2.7	55	45	4.0	3.4
#56	B	Altered porphyry	Monzonite porphyry	Greywacke metaseds.	55	5	150	30	100	500	0	2.7	70	50	5.0	4.1
#57	A*	Amygdaloidal andesite	Brecciated Andesite and Tuff	Leucocratic Andesite	75 75	5 5	9 3	6 6	80 40	70 100	0 0	2.7 2.7	72 70	65 55	1.5 0.5	3.4 5.7 *
#58	A	Volcanics + Metasediments	Qtz-Carbonate veins	Shrd schtse metaseds.	80 80	38 85	25 25	10 10	50 70			2.7 2.7	75 75	65 65	2.5 2.5	3.2 3.2
#59	B*	Sheared diabase	Qtz-Carbonate veins	Diabase	80	3	4	10	110	65	0	2.7	55	70	0.4	8.3 *
#60	A	Granodiorite	Aggl;tuff, qtz veins	Granod'te Porphyry	65	15	10	6	80	30	0	2.8	80	60	1.7	3.4

* Indicates Crown Pillar Failure

Mine Number	Mine Type	Rock			DIP (Degrees)	o/b thickness (m)	Dimensions			Stope Height (m)	Fill Height (m)	Gamma Rock (T/m3)	RMR		T/S	Cs
		HW	Ore	FW			t (m)	w (m)	l (m)				Hw/Fw	Ore		
#61	B	Norite	Breccia	Greenstone/ schist	75	30	10	6	• • •			2.7	80	45	1.7	3.3
#62	E*	Biotite Schists	Sheared and Brecciated Shists	Schists, Greywakes	65 50	25 25	40 5	10 10	25 25			2.7 2.9	65 25	80 80	4.0 0.5	2.5 7.6 *
#63	A	Ultramafic,	Diorite porphyry	Porphyry	70	5	10	6	80	30	0	2.8	80	60	1.7	3.4
#64	A*	Argillite, Conglomerate	Conglomerate+ Calcite Veins	Conglomerate	85 85	0 0	1 1	3 5	5 6			2.8 2.7	85 85	45 45	0.3 0.2	4.1 * 6.2 *
#65	A	Argillite, Conglomerate	Conglomerate+ Calcite Veins	Conglomerate	85	2	5	4	20	25	0	2.8	64	36	1.3	2.8
#66	A	Conglomerate, Metaseds	Quartz, Conglomerate	Conglomerate, Metaseds	35	16	24	21	146			2.6	85	85	1.1	7.9
#67	D*	Wollastonite+ Diopside Hornfels	Porcellanite, Skarn	Porcellanite Wollastonite, Hornfels	30		240	60	60		0	2.7	85	65	4.0	5.5

* Indicates Crown Pillar Failure

Mine Number	Mine Type	Rock				o/b	Dimensions			Stope	Fill	Gamma	RMR		T/S	Cs
		HW	Ore	FW	DIP (Degrees)	thickness (m)	t (m)	w (m)	l (m)	Height (m)	Height (m)	Rock (T/m3)	Hw/Fw	Ore		
#68	D	Quartz Mica Schist	Banded Schist	Quartz Mica Schist	15	15	25	45	25	3		2.7	60	56	0.6	11.1
#69	D	Sericite Schist	Massive Sulphide	Biotite Garnet Gneiss, Schists	85 85 85		137	24	107	150	0	2.8	65	56	5.7	3.2
E (GPa)			103													
Poisson's Ratio			0.31													
UCS (MPa)		28	100	52												
#70	D	Quartz Porphry	Massive Sulphide	Chloritic Tuff	85		42	19	46	55	55	2.8	68	70	0.2	4.2
							45	23	46	42	42	2.8	68	70	0.2	5.9
E (GPa)		68.7	119.3	68.7			19	32	46	55	55	2.8	68	70	0.2	11.9
Poisson's Ratio		0.19	0.24	0.25												
UCS (MPa)		84	91	177												

* Indicates Crown Pillar Failure

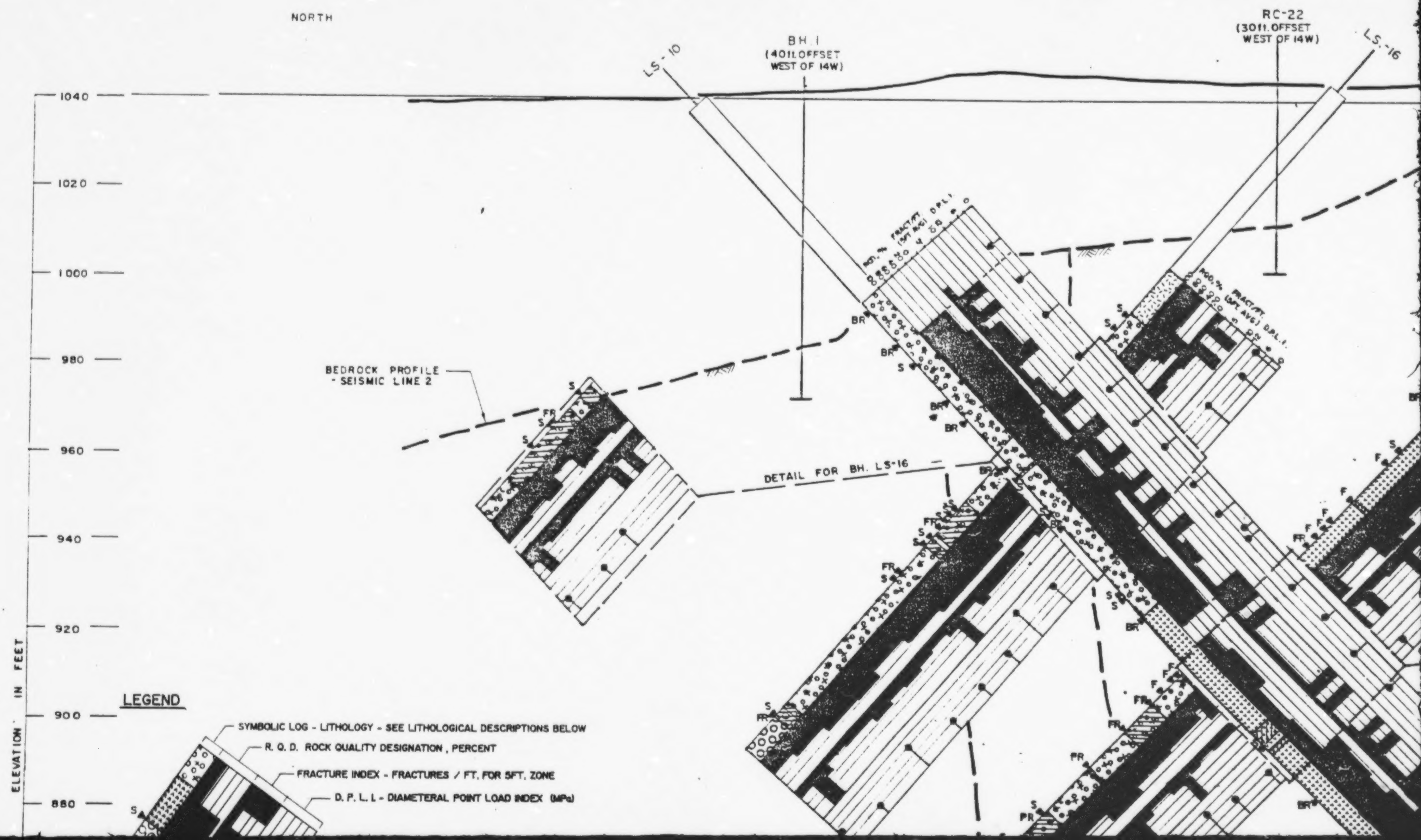
NORTH
LS-10
BH. 1
(40ft. OFFSET
WEST OF 14W)
RC-22
(30ft. OFFSET
WEST OF 14W)
LS.-16
1040
1020
1000
980
960
940
920
900
880
ELEVATION IN FEET
BEDROCK PROFILE
- SEISMIC LINE 2
DETAIL FOR BH. LS-16
RQD % FRACT/FT (5FT AVG) D.P.L.I.
S
FR
BR
F
LEGEND
SYMBOLIC LOG - LITHOLOGY - SEE LITHOLOGICAL DESCRIPTIONS BELOW
R. Q. D. ROCK QUALITY DESIGNATION , PERCENT
FRACTURE INDEX - FRACTURES / FT. FOR 5FT. ZONE
D. P. L. I. - DIAMETERAL POINT LOAD INDEX (MPa)

MINE #11 DETAILED DRILLING DATA FOR ASSESSMENT OF CROWN PILLAR CONDITIONS

FIGURE 3.3

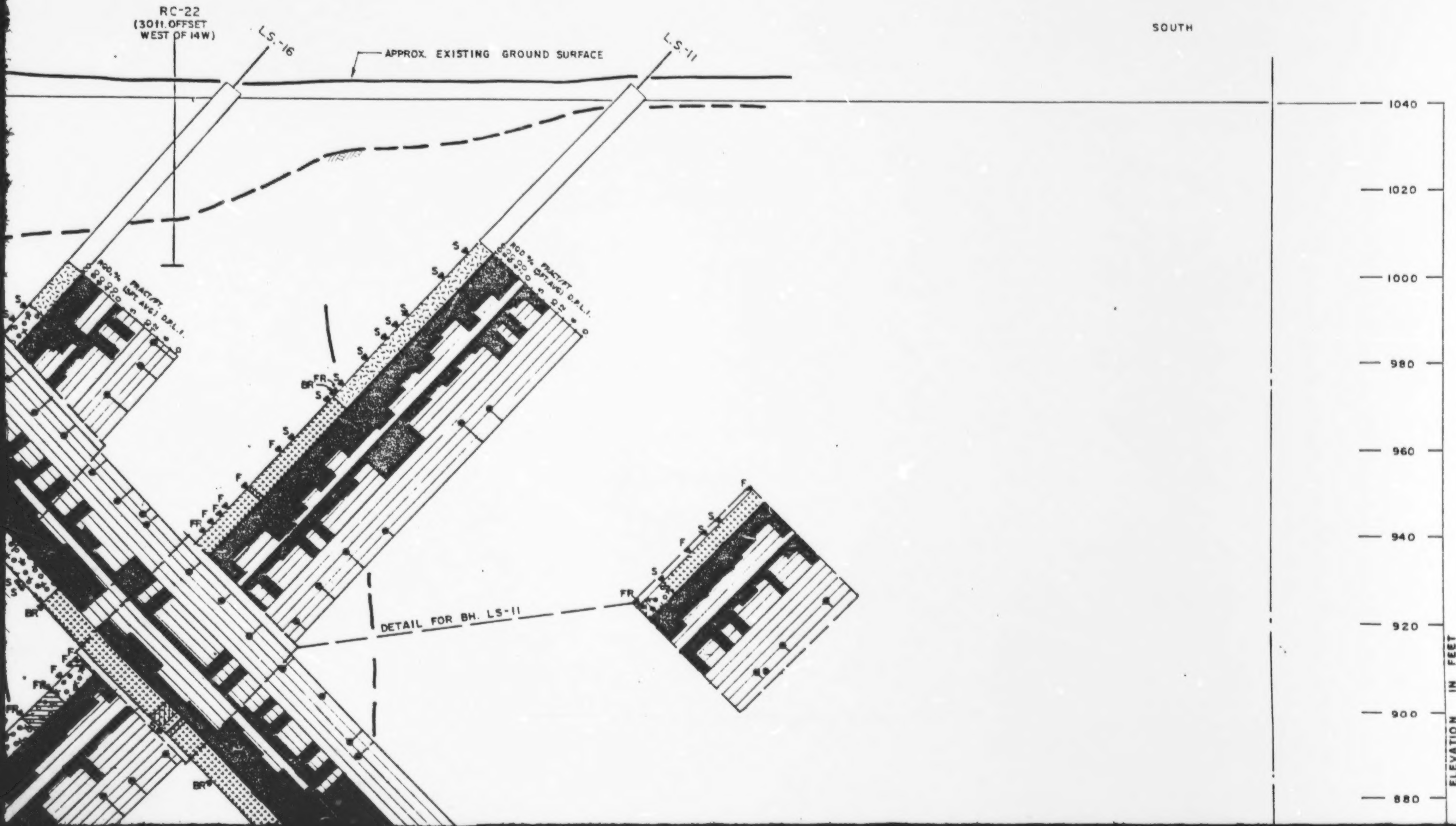

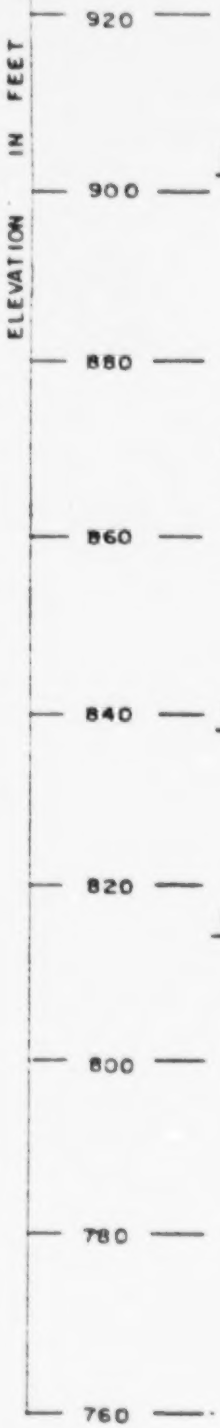

LEGEND

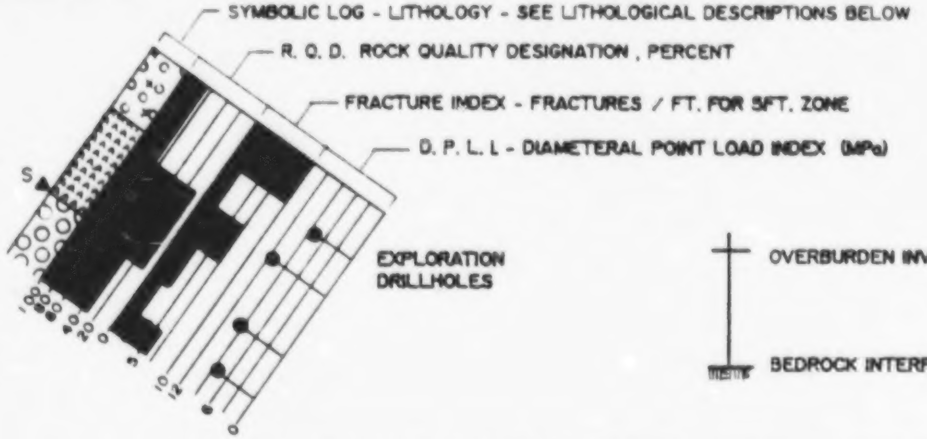
SYMBOLIC LOG - LITHOLOGY - SEE LITHOLOGICAL DESCRIPTIONS BELOW
R. Q. D. ROCK QUALITY DESIGNATION , PERCENT
FRACTURE INDEX - FRACTURES / FT. FOR 5FT. ZONE
D. P. L. I. - DIAMETERAL POINT LOAD INDEX (MPa)
S
100
50
0
30
10
0

EXPLORATION DRILLHOLES

OVERBURDEN INVESTIGATION HOLES

BEDROCK INTERFACE

BEDROCK BOUNDARY INFERRED FROM SEISMIC REFRACTION SURVEY

STRUCTURAL SYMBOLS

FR ▶	BREAK / JOINT	FR ▶	FRACTURE	* ▶	ZONE OF WATER LOSS
BR ▶	BRECCIA	SH ▶	SHEARED ZONE		
F ▶	FAULT	S ▶	SLIP (GENERALLY SLICKENSIDED)		

LITHOLOGY

○○○	TEMISKAMING CONGLOMERATE GREYISH GREEN TO BROWN AND OCCASIONALLY BLACK , THICKLY BEDDED , FINE TO MEDIUM GRAINED POLYMICTIC CONGLOMERATE WITH ROUNDED CLASTS TYPICALLY 30mm TO 40mm DIAMETER SET WITHIN A SILTY SAND MATRIX.
░	DIABASE GREENISH BLACK , MASSIVE , MEDIUM GRAINED , OPHITIC DIABASE.
▒	TUFF DARK GREY TO BLACK WITH OCCASIONAL GREENISH STREAKS , MASSIVE TO FLOW BANDED , FINE GRAINED TUFF WITH FRAGMENTAL INCLUSIONS UP TO 5mm DIAMETER.
▩	BASIC SYENITE DARK GREEN TO GREENISH BLACK , MASSIVE , MEDIUM TO COARSE GRAINED SYENITE.
▦	FELSIC SYENITE REDDISH BROWN TO BLACK , MASSIVE , FINE GRAINED FELDSPATHIC SYENITE WITH OCCASIONAL CARBONATE AND QUARTZ STRINGERS.
⁘	RED SYENITE PORPHYRY VARIABLE COLOURS BETWEEN PINK AND REDDISH BROWN TO DARK BROWN AND BROWNISH GREY , MASSIVE , MEDIUM GRAINED SYENITE PORPHYRY CONTAINING 3mm TO 5m FELSPAR PHENOCRYSTS OCCASIONAL 10mm TO 40mm DIAMETER FELDSPAR PHENOCRYSTS.
⁙	GREEN SYENITE PORPHYRY GREEN TO DARK GREENISH GREY , MASSIVE MEDIUM GRAINED , MODERATELY TO HEAVILY SILICIFIED SYENITE PORPHYRY WITH 3mm TO 5mm DIAMETER FELDSPAR PHENOCRYSTS.
▨	ZONE OF MODERATELY TO EXTENSIVELY ALTERED OR BLEACHED ROCK.
☐	CASING (ASSUMED OVERBURDEN).

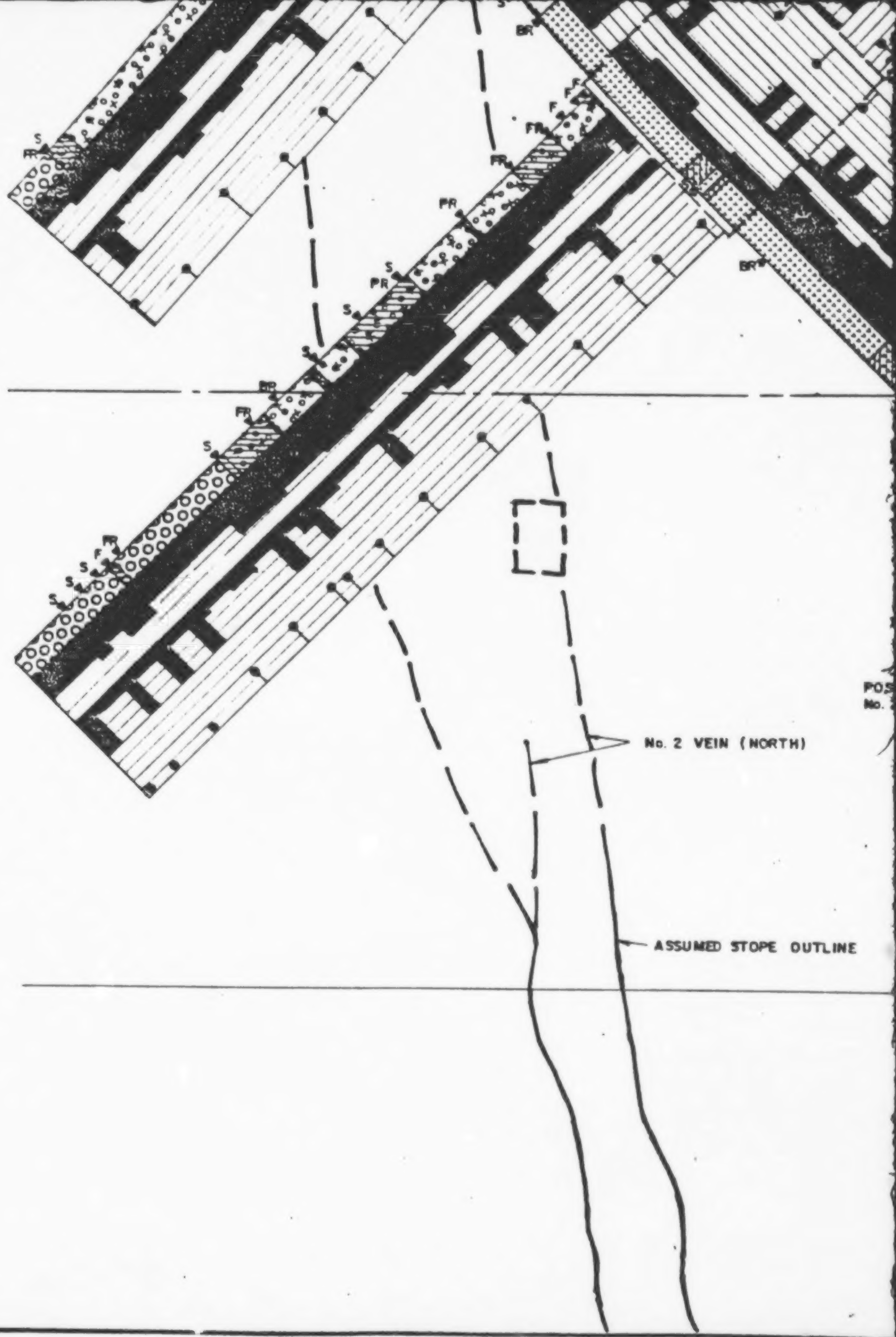

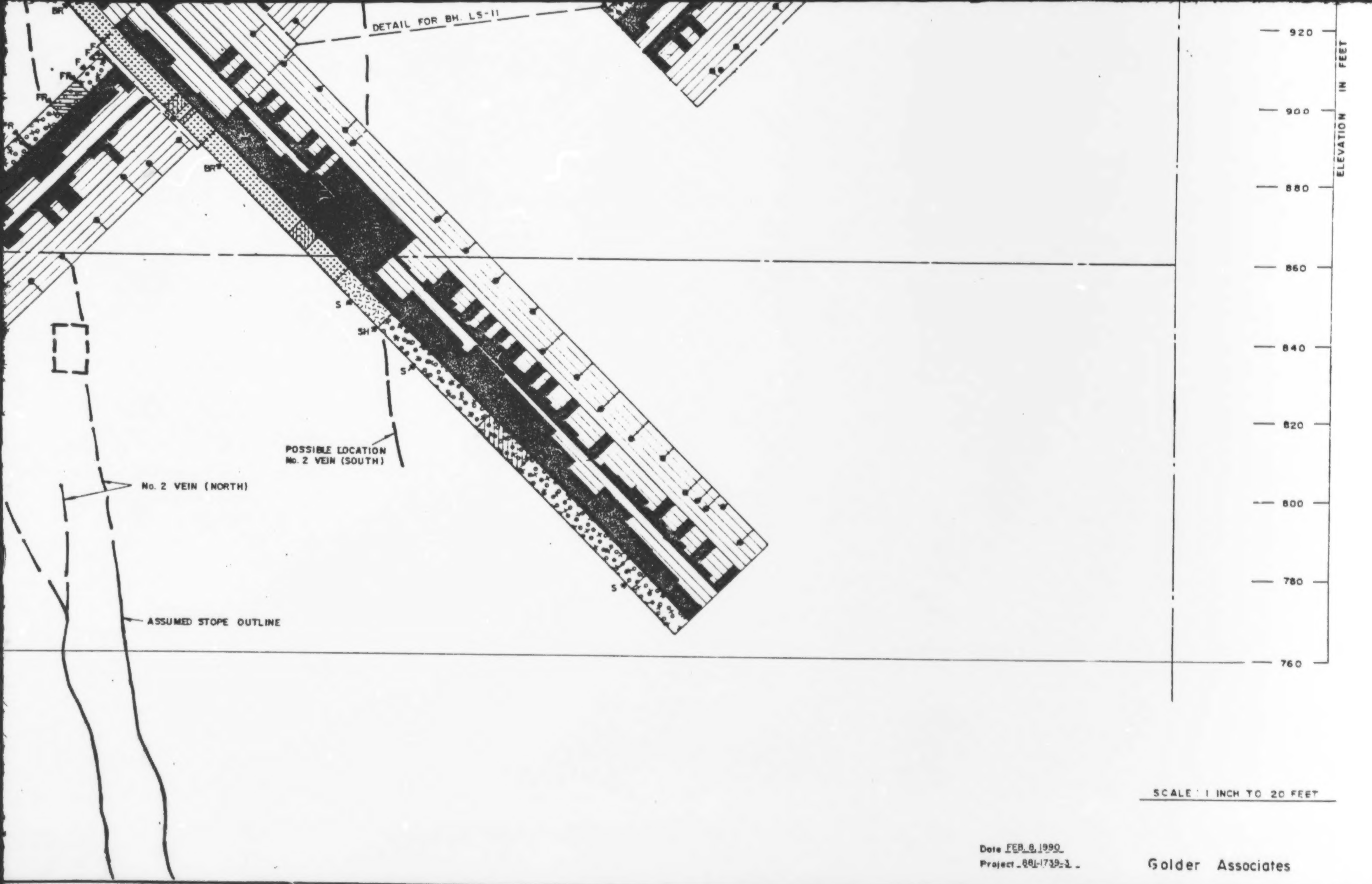

SCALE : 1 INCH TO 20 FEET

Date FEB. 8, 1990
Project 881-1739-3

Golder Associates

Drawn P.L.
Chkd